with Author's
Compliments
Cho-Teng Liu

NOAA Technical Memorandum ERL PMEL-34

ANALYSIS OF TROPICAL PACIFIC SEA SURFACE TEMPERATURES FOR 1975 TO 1980

Cho-Teng Liu

Pacific Marine Environmental Laboratory
Seattle, Washington
June 1982

UNITED STATES
DEPARTMENT OF COMMERCE
Malcolm Baldrige,
Secretary

NATIONAL OCEANIC AND
ATMOSPHERIC ADMINISTRATION
John V. Byrne,
Administrator

Environmental Research
Laboratories
George H. Ludwig
Director

CONTENTS

Analysis of Tropical Pacific Sea Surface Temperatures for 1975 to 1980

Cho-Teng Liu

ABSTRACT. This report presents contoured objective analyses made between 1975 and 1980 (inclusive) of sea surface temperature measurements taken in the Pacific from the western coastline of the Americas to 150°E, and from 25°N to 30°S. The analyses represent two-week-averaged SST fields contoured according to surface isotherms and include the time period of both the relatively weak El Niño of 1976 and the post-El Niño period, as well as the spatial domain of other climatically interesting regions of the western and central Pacific. While providing SST fields useful to study of the El Niño in terms of sea surface temperature variation, this report also draws attention to the nonseasonal SST (NSST) variation. At the onset of the 1976 El Niño, the equatorial NSST was 4σ (standard deviation) below its normal temperature for 1977-1980, while the mean NSST along 30° was 3σ above normal.

1. INTRODUCTION

Because of the relative positioning of the Earth and Sun, the Earth receives and absorbs more solar energy in the tropics than in the polar regions. This nonuniform heating and temperature distribution drives the atmosphere--the weather machine--and changes the weather and climate on both short and long time scales. The climate, the long-time average of the weather, however, is believed to be more nearly controlled by the slowly varying oceans, because of the thermal inertia of seawater. To understand climatic variations, we have to understand how the oceans vary in time and space.

Under the auspices of the Equatorial Pacific Ocean Climate Study (EPOCS) program, we have constructed semimonthly sea surface temperature (SST) fields for the tropical Pacific Ocean from January 1975 through December 1980. The method of constructing the SST field is basically Cressman's (1959) objective analysis, with some modifications to include *a priori* knowledge of the anisotropy in the spatial variation of SST fields. The SST data used in the analysis are from ships' weather reports, ships' expendable bathythermographs (XBT), aircraft XBT (AXBT), and drifter buoy reports. Most of these SST data were available in the form of radio messages and had been either transmitted to shore stations or relayed through Integrated Global Ocean Station System (IGOSS) to data distribution centers. Because these data are potentially available to users on a real-time basis, similar SST analysis may be performed in the future for studying the evolution of major oceanic variations such as forthcoming El Niño events.

2. DATA DESCRIPTION

The ideal data for construction of semimonthly SST fields should satisfy the following criteria:

1) Quality--no bias and small RMS error.
2) Quantity--extensive spatial coverage in each half-month period.
3) Availability--accessibility to user on a "real-time" basis (*i.e.*, within 24 hours).

In actuality, there is no observed SST data set that can meet all of these criteria, since the first two are mutually exclusive when cost is considered. Therefore, several types of surface-observed SST data, most of them simply "available," are blended to construct the SST field. These data are from ship reports, which give wide spatial coverage but somewhat lower accuracy, and from the drifting buoy, XBT, and bathythermograph (BATHY) data, which give higher accuracy but limited spatial coverage.

A correction (0.2°C according to Tabata, 1978; 0.7°C according to Saur, 1963) for the bias of ship data was not attempted, because the bias is not uniform among all ships, nor is it independent of ships' location or constant in time. The "intrinsic error" is approximately ±1.5°C for ship injection temperatures (as compared to bucket temperatures, which have errors less than 0.1°C), and is about ±0.2°C for buoy and XBT observations. Since all data used for deriving the semimonthly mean SST field are observations of the instantaneous SST field, rather than the mean SST field, the RMS error, defined as "apparent error" of SST data with respect to the mean SST field, is affected by both the RMS fluctuations of SST field at the locality of each SST observation and the "intrinsic error" of that SST observation. Besides these errors in SST observations, there are other sources of errors, including errors in time and location data, and errors that occur during data transmission, etc. Therefore, the apparent error of SST data is statistically considerably larger than their intrinsic accuracy.

It is likely that the apparent error of buoy, XBT, and BT data is far larger than their "intrinsic error," which is about ±0.2°C. The degradation of data accuracy, caused by unobserved fluctuations in the temperature field, reaches an extreme in regions where the temporal or spatial variations of SST are high, such as near SST frontal areas.

Data available for this analysis include the following:

1) SPOT data*: These are ship weather reports received at a teletype terminal, plus some SST reports from FGGE (First GARP Global Experiment) drifting buoys in the southern hemisphere.

2) BATHY reports*: Included are declassified XBT and AXBT data from Fleet Numerical Oceanography Center (FNOC).

3) XBT data (mostly between Dec. 1977 and Dec. 1979)*: The majority of XBT data for the period between Jan. 1975 and Feb. 1977 are from National Oceanographic Data Center (NODC).

---

* Data provided courtesy of Dr. D. McLain of NOAA/NMF

4) EPOCS drifter buoy data**: These data cover the two-year period, 1979-1980, and were located mostly in the equatorial Pacific Ocean or near the Peru coast.

3. METHOD OF ANALYSIS

A spatially interpolated and averaged field of SST can be derived either subjectively or objectively from a set of randomly located observations. In a subjective SST analysis, the rules of analysis are set subjectively by the analyst, and these rules may be modified from time to time and from one portion of the SST field to another, in order to accommodate the analyst's intuitive information on the "true" SST field. In an objective analysis, while the rules of analysis are also subjectively preset by the analyst, rules are not modified during the course of the analysis. Thus, the outcome of an SST analysis depends not only on the data fed into the analysis, but also on the method of analysis as well. Therefore, tests of data validity are an essential part of the analysis.

3.1 Data Validity Tests

Before data are blended into the SST analysis, they are subjected to validity tests for the following categories:

1. Location. Only those data in the region of 30°S-30°N, 150°E-70°W of the Pacific Ocean are accepted.

2. Temperature. Only those data giving SST's in the range from 10°C to 35°C are accepted.

3. Climatology. Fields of allowable deviation of SST data from the mean monthly SST fields (Robinson, 1976; Alexander and Mobley, 1976) are assigned for every month. Any SST datum deviating from the mean SST field by more than its allowance will be rejected. This allowable SST deviation is an approximation of the total RMS error caused by the instrument errors combined with the natural temporal fluctuations of the SST fields. As an example, the allowable SST deviations in November are 7.6°C off the coast of Peru where coastal upwelling dominates SST fluctuations, 3.9°C near the Galápagos Islands, and less than 3.5°C in most of the central and western tropical Pacific ocean.

4. Ship speed. Ship speeds are computed on the basis of the location and time of two consecutive reports from each ship and buoy. In the case of SPOT data, one or both of two consecutive reports will be rejected if the ship speed is over 14 m s^{-1}. In the case of XBT or BATHY data, a manual inspection was attempted in order to "correct" the data (*e.g.*, a sudden change from 161°E to 162°W, then to 163°E), wherever the error was obvious. In the case of AXBT reports, the maximum allowable aircraft speed is 200 m s^{-1}.

** Data provided courtesy of Dr. C. Paul of NOAA/ERL/AOML.

5. Air-Sea temperature. SST data will be accepted if they differ from air temperature by 5°C or less and are not exactly the same as the temperature of the overlying air.

6. Redundancy. Redundant data (about 5%) are removed.

3.2 Methodology

The method of objective analysis used for deriving SST fields from various and randomly distributed surface SST data is an iterative relaxation procedure. This procedure iteratively modifies an estimated SST field according to the rules preset for each iteration, so as to relax (reduce) the difference between the estimated SST field and the observed SST.

The climatological monthly mean SST field $T^{(1)}$ is taken as the first of the estimated SST fields, $T^{(n)}$, which are defined on a 1° x 1° grid over the region of 150°E - 70°W and 30°S - 25°N. At a grid point (i,j), where i,j are the longitudinal and latitudinal coordinates, a correction field $C_{ij}^{(n)}$ (Levitus and Oort, 1977) is first computed from the weighted differences between the SST field and the observed SST in the nearby region. Then a spatially smoothed SST field $M_{ij}^{(n)}$ is computed from the current estimate $T_{ij}^{(n)}$. For a bi-weekly mean SST field, the data-corrected SST field $T_{ij}^{(n)} + C_{ij}^{(n)}$ is assumed to be as accurate as the smoothed SST field $M_{ij}^{(n)}$. Then, the optimal choice of the new field $F_{ij}^{(n+1)}$ may be shown to be

$$F_{ij}^{(n+1)} = (T_{ij}^{(n)} + C_{ij}^{(n)} + M_{ij}^{(n)}) /2. \qquad (1)$$

If there is no datum existent in the vicinity of (i,j), then $F_{ij}^{(n+1)}$ is replaced by $M_{ij}^{(n)}$. This substitution is designed to allow the information on the SST field to propagate into these data-void regions in such a way that the final SST field, $T^{(8)}$, in these regions has least dependence on the initial guess, the climatological mean SST field $T^{(1)}$. After $F_{ij}^{(n+1)}$ over all grid points are computed, $F_{ij}^{(n+1)}$ is filtered through a curvature-preserving operator to arrive at a new estimate of SST field at (i,j):

$$T_{ij}^{(n+1)} = \tfrac{1}{4}\,[F_{i,j+1}^{(n+1)} + F_{i,j-1}^{(n+1)} + F_{i+1,j}^{(n+1)} + F_{i-1,j}^{(n+1)}] - \Delta T_{ij}^{(1)} \qquad (2)$$

where $\Delta T_{ij}^{(1)}$ represents the curvature of $T^{(1)}$ at grid point (i,j)

$$\Delta T_{ij}^{(1)} = \tfrac{1}{4}\,[T_{i,j+1}^{(1)} + T_{i,j-1}^{(1)} + T_{i+1,j}^{(1)} + T_{i-1,j}^{(1)}] - T_{ij}^{(1)} \qquad (3)$$

With increasing n, the SST field $T^{(1)}$ are iteratively corrected through Eq. (1)-(3) to give $T^{(2)}$, $T^{(3)}$, ... etc. At the end of the 7th iteration ($n = 7$), $T^{(8)}$ is derived from Eq. (2) and then smoothed with the Laplacian smoother, *i.e.*, replacing $T_{ij}^{(8)}$ by the average of $T^{(8)}$ on the neighboring four grid points.

3.3 Computation of Correction field, $C_{ij}^{(n)}$, and smoothed SST field, $M_{ij}^{(n)}$

A region of influence is assigned to every grid point (i,j). Any observed SST located within this region exerts "influence" on the correction of SST field at this grid point, $T_{ij}^{(n)}$. The correction field is taken as:

$$C_{ij}^{(n)} = \sum_{k=1}^{N} W_k (D_k - T_k^{(n)}) \Big/ \sum_{k=1}^{N} W_k \qquad (4)$$

where T_k is the interpolated SST field at the location of D_k, and D_k is the k^{th} observed SST in the region of influence. If $|D_k - T_k^{(n)}|$ is larger than a preset critical value (2.5°C for $n = 7$), then D_k will not be used for correcting the SST field. For W_k, the weighting function, Levitus and Oort (1977) assumed a uniform radius of influence R, and whereby any observed SST located within a distance $r = (x^2 + y^2)^{\frac{1}{2}}$ from (i,j) had an influence on $T_{ij}^{(n)}$ that was weighted by

$$W_k = \begin{cases} e^{-4r^2/R^2} & \text{if } r \leq R \\ 0 & \text{if } r > R \end{cases} \qquad (5)$$

We have modified the functional form for W_k in order to utilize *a priori* information on data accuracy, the climatological mean SST field, and the north-south and east-west gradients of that field. We take as an overall weighting function the product of three terms, that is:

$$W_k = f_a \cdot f_c \cdot f_d \qquad (6)$$

The effects of each factor are listed in Table 1; following are definitions of these factors. The factor f_a accounts for the quality of data and has a larger weight for more accurate and more spread-out data, that is,

$f_a = 1$ for SPOT data;

$f_a = 2$ for EPOCS buoy data, accurate, but with some redundancy;

$f_a = 4$ for BATHY data;

$f_a = 8$ for XBT data, which are determined more accurately than the others.

The weight f_c gives greater emphasis to those data that deviate less from the climatological mean temperature, T_c. We take as a functional form,

$$f_c = 4/(2 + |D_k - T_c|)$$

Generally, $2 \geqq f_c \geqq 0.5$.

The term f_d gives larger weight to those data that are closer to the grid point (i,j), as measured by a Gaussian distribution having bidirectional radii of influence (R_x, R_y). In order to account for the local directional SST gradient, the circular field of influence (Cressman, 1959) is modified into an elliptical shape that has R_x and R_y as major and minor axes. We take

$$f_d = \begin{cases} e^{-4\,x^2/R_x^2 - 4\,y^2/R_y^2} & \text{if } x^2/R_x^2 + y^2/R_y^2 \leqq 1 \\ 0 & \text{otherwise} \end{cases} \qquad (7)$$

where $R_x(i,j) = R/(0.5 + 2\,|T_x(i,j)|)$, and $R_y(i,j) = R/(0.5 + 2\,|T_y(i,j)|)$. Here R is an assigned scale factor for R_x and R_y, and $T_x(i,j)/T_y(i,j)$ is the maximal longitudinal/latitudinal gradient of the climatological SST field within a distance of 3° longitude/latitude from (i,j), with a value limited to 1°C per degree of longitude/latitude. We limit $2R \geqq (R_x, R_y) \geqq 0.4R$ under all conditions. R is chosen to be of four grid-lengths for the first four iterations and to be of three grid-lengths for the next (also final) three iterations. R_x, R_y have the range 120 km to 660 km depending on the local SST gradient.

The mean temperature $M_{ij}^{(n)}$ is the arithmetic average of the four SST field values at the corners of a rectangle bounded by $x = \pm R_x$ and $y = \pm R_y$. This rectangle does not extend outside of the region under study.

As required by all objective analyses, a group of subjective rules must be established before the analyses. The parameterization of f_a, f_b, f_c and the relaxation procedures are thus the subjective rules of this analysis. Although arbitrarily chosen, they mostly fall within a range of two and are not critical factors in determining the large-scale features of the SST fields, e.g., the warming and cooling stages of an El Niño event. The estimated effects of these weighting factors are summarized in Table 1. In test cases, the adoption of bidirectional radii of influence R_x, R_y is found to have more impact on the analyzed SST field than the other two modifications on f_a and f_c in the weighting factor W_k.

4. RESULTS AND COMMENTS

For the six-year period 1975-1980, there are 144 semimonthly SST fields derived from ship, buoy, XBT, and AXBT observations of SST. the analyzed SST fields are contoured into surface isotherms and are presented in the 144 figures of this report. Associated with each contoured SST field is a station plot of all SST data accepted and incorporated into the SST field. These station plots are intended as zero-order estimates of the reliability of the analyzed SST fields. The reliability is low where the SST field near the border of a map is extrapolated from a remotely located observation of SST. The reliability is high where the SST field is an average of nearby buoy, XBT, or AXBT data.

Figure 1 is a summary plot that shows all the SST data actually used for deriving the subset of 72 SST fields for February to July 1975-1980. In this figure one can easily observe general characteristics of every data set: unevenly scattered ship stations, meandering buoy tracks, and straight XBT and AXBT sections. The most important information revealed by this figure is the distribution of ship data, namely its sparseness and nonuniformity.

These 144 SST-fields are not totally independent of each other. For the month of December, there are 12 biweekly SST fields in 6 years. All these 12 fields are iteratively corrected from the same climatological mean SST, and therefore they may have slight positive correlation with the initial SST fields. To assure that the correlation is small, we have re-derived an SST field for the second half of December 1980 using a severely distorted climatological mean SST as a first guess of SST field, that is: 2°C warmer than the climatic mean SST to the east of 140°W, and 2°C colder than the climatic mean SST to the west of 140°W. As shown in Figure 2, the resulting difference is less than 0.4°C, except in a few localities where ship data are inconsistent with each other, and the differences in the final SST fields are much smaller than the differences inserted into the initial SST field. Therefore, the analyzed SST fields are nearly independent from the first-guess field.

Because of the way the SST fields were prepared, oceanic temperature fluctuations with time scales greater than one month or with space scales greater than 250 km will be well resolved by the scales. Therefore, the year-long, basinwide oceanic events such as El Niño are readily observable in the analyzed fields. On the other hand, these fields are not suitable for studying localized oceanic events like coastal upwelling, equatorial upwelling, or sharp SST fronts.

Although El Niño is the major climatic event in the tropical Pacific Ocean and has been studied by scientists of many disciplines, it is still neither fully understood nor predictable. El Niño is a complex of events, accompanied by abnormally warm water off the Peruvian coast and along the eastern equatorial Pacific Ocean, with torrential rains along the Peruvian coast and with a shift of the intertropical convergence zone and a shift of the spatial distribution of clouds and precipitation.

There are many descriptive and theoretical papers on El Niño events occurring before 1973. Most of the authors used SST's from island stations along the Equator and coastal stations of South America. Here, we would like to demonstrate the temporal evolution and the spatial extent of the 1976 El Niño using SST fields derived mostly from ship data.

Figure 3 shows time series of (a) SST along 140°W, (b) SST averaged along several latitude arcs, and (c) SST averaged basinwide. The equatorial SST for 1976 behaves similarly to the three earlier major El Niño events in 1957-58, 1965, and 1972 (Weare *et al.*, 1976; Wyrtki, 1975), namely with a year-end sudden warming that was preceded by a year or more of abnormally low SST, and which was then followed by months of continuous warming. Unlike the SST anomalies at coastal stations, SST anomalies at island stations (Hickey, 1975) and our open-ocean equatorial (140°W) SST anomalies did not peak during the first three months, but rather later in the year. The phase and amplitude of the cooling-warming episodes vary from place to place. Similar phenomena are also observed in the composite SST sections along the Equator and Peruvian coast (Rasmusson and Carpenter, 1982).

Compared to SST in the normal years, the SST (or NSST) during an El Niño shows anomalously warm SST along the Equator in the eastern Pacific and along the South American coast. Since the statistical significance of a SST anomaly depends on the amplitudes of natural fluctuations, it is informative to scale the El Niño signal in terms of the standard deviation of SST anomalies in their normal (non-El Niño) years, in this case, assumed to be 1977-80.

(Figure 4 shows the normalized SST anomalies computed from the SST time series in Figure 3 expressed in the units of standard deviations of nonseasonal SST fluctuation during 1977 to 1980.) A few interesting points are worth mentioning. First, the pre-El Niño cooling is not confined to the Equator, but is nearly basinwide in the tropics; and the normalized amplitude and the phase of both warm episodes are quite similar to each other. Second, the onset of the warm episode of an El Niño occurs at essentially the same time along the entire Equator as does the cold phase along 30°S. Although this is best shown by comparing time series of all equatorial SST anomalies, the evidence can be found by comparing the sudden warming of the equatorial SST anomaly at 140°W with its equatorial mean. Third, SST's along the 30°S latitude arc generally behave out of phase with the SST along the Equator, in that there was a warm 1975 followed by a sudden cooling at the start of the 1976 El Niño. Fourth, between 100°W and 160°W, there is a gradual delay of the onset of the warm episode as one moves from the Equator toward 15°S.

These are a few examples of the types of information that may be obtained from the data set presented here. More comprehensive and sophisticated analyses are currently underway in an attempt to understand the large-scale behavior of upper-ocean temperatures during the El Niño cycle, and these will be reported on later.

5. ACKNOWLEDGEMENTS

I am grateful to Dr. John Apel for his support in this research. I would like to thank Dr. D. McLain of Southwest Fisheries Center/Pacific Environmental Group for providing SPOT, BT, and XBT data for the Central Pacific, and the climatological mean SST fields. I am also thankful to Dr. C. Paul of NOAA/ERL/ AOML for providing SST data from EPOCS drifter buoys, and to Mr. W. Otto of CIRES for transfering the SPOT data to us. Critiques from Drs. B. Taft and R. Preisendorfer are greatly appreciated. This work was supported by grants from the Equatorial Pacific Ocean Climate Studies Program (EPOCS) of ERL/NOAA.

6. REFERENCES

Alexander, R. C. and R. I. Mobley (1976) Monthly average sea-surface temperature and ice-pace limits on a 1° global grid. *Mon. Wea. Rev. 104*, 143-148.

Barnett, T. (1981) Statistical Prediction of North American Air Temperatures from Pacific Predictors. *Mon. Wea. Rev. 109*, 1021-1040.

Bengtsson, L. (1975) 4-Dimensional Assimilation of Meteorological Observations. GARP Publication Series No. 15.

Cressman, G. (1959) An Operational Objective Analysis System. *Mon. Wea. Rev., 87*, 367-374.

Hickey, B. (1975) The relationship between fluctuations in sea level, wind stress and sea surface temperature in the equatorial Pacific. *J. Phys. Oceanogr., 5*, 460-475.

Horel, J. and J. Wallace (1981) Planetary-Scale Atmospheric Phenomena Associated with the Southern Oscillation. *Mon. Wea. Rev. 109*, 813-829.

Levitus, S. and A. Oort (1977) Global Analysis of Oceanographic Data *Bulletin American Meteorological Society, 58*, No. 12, p. 1270-1284.

Oceanographic Monthly Summary, 1981. U.S. Department of Commerce NOAA/NWS/NESS. Vol. 1.

Perlroth, I. (1979) Reliability of IGOSS Bathythermograph (BT) data. UNESCO, Intergovernmental Oceanographic Commission, Workshop report No. 17, Supplement.

Rasmusson, E. and T. Carpenter (1982) Variations in tropical sea surface temperature and surface wind fields associated with the Southern Oscillation/El Niño. *Mon. Wea. Rev.* (in press).

Robinson, M. K. (1976) Atlas of North Pacific Ocean monthly mean temperatures and mean salinities of the surface layers. NavOceano Ref. Pub. 2.

Royer, T. C. (1976) A note comparing historical sea surface temperature observations at Ocean Station P. *J. Phys. Oceanogr., 6*, 969-971.

Saur, J. F. T. (1963) A Study of the Quality of Sea Water Temperatures Reported in Logs of Ships' Weather Observations. *J. of Applied Meteorology, 2*, 417-425.

Tabata, S. (1978) Comparison of Observations of Sea Surface Temperatures at Ocean Station P and NOAA Buoy Stations and those made by Merchant Ships Traveling in their Vicinities, in the Northeast Pacific Ocean. *J. of Applied Meteorology, 17*, 374-385.

Weare, B., A. Navato and R. Newell (1976) Empirical Orthogonal Analysis of Pacific Sea Surface Temperatures. *J. of Phys. Oceanogr. 6*, 671-678.

Wyrtki, K. (1975) El Niño - The Dynamic Response of the Equatorial Pacific Ocean to Atmospheric Forcing. *J. of Phys. Oceanogr., 5*, 572-584.

Table 1.--Effects of weighting factors f_a, f_c and f_d on the objective analysis, relative to the case $f_a = f_c = 1$ and $R_x = R_y = R$. N/E means little or no effects, P/I means possible improvements (see text for definition of symbols).

Condition	f_a	f_c	f_d
region of no data	N/E	N/E	N/E
region of sparse data	N/E	N/E	P/I, isotherms tend to be parallel to the isotherms of the climatological mean SST
region of conflicting data	P/I, high quality data dominate over others	P/I, "wild" data are given less weight	P/I, larger tolerance on data in high SST gradient region
region where all SST data are higher (or lower) than the climatology	P/I, as above	the analyzed SST field differs less from the climatology	P/I, as above
overall SST-field	better accuracy	less "wild" spots of questionable SST anomaly, and more resistant to deviation from the climatology	the pattern of isotherms conforms better with the climatology; no effect on the oceanwide mean SST; more permissible to the formation of SST front parallel to the mean isotherms, but less to the formation of eddies.

GLOSSARY

AXBT	Airborne Expendable Bathythermograph
BATHY, BT	BATHY/TESAC data, temperature/salinity data transmitted through Global Telecommunication System
EPOCS	Equatorial Pacific Ocean Climate Study
FGGE	First GARP Global Experiment
FNOC	Fleet Numerical Oceanography Center
GARP	Global Atmospheric Research Program
SPOT	Ship and buoy data from FNOC
SST	Sea Surface Temperature
XBT	Expendable Bathythermograph

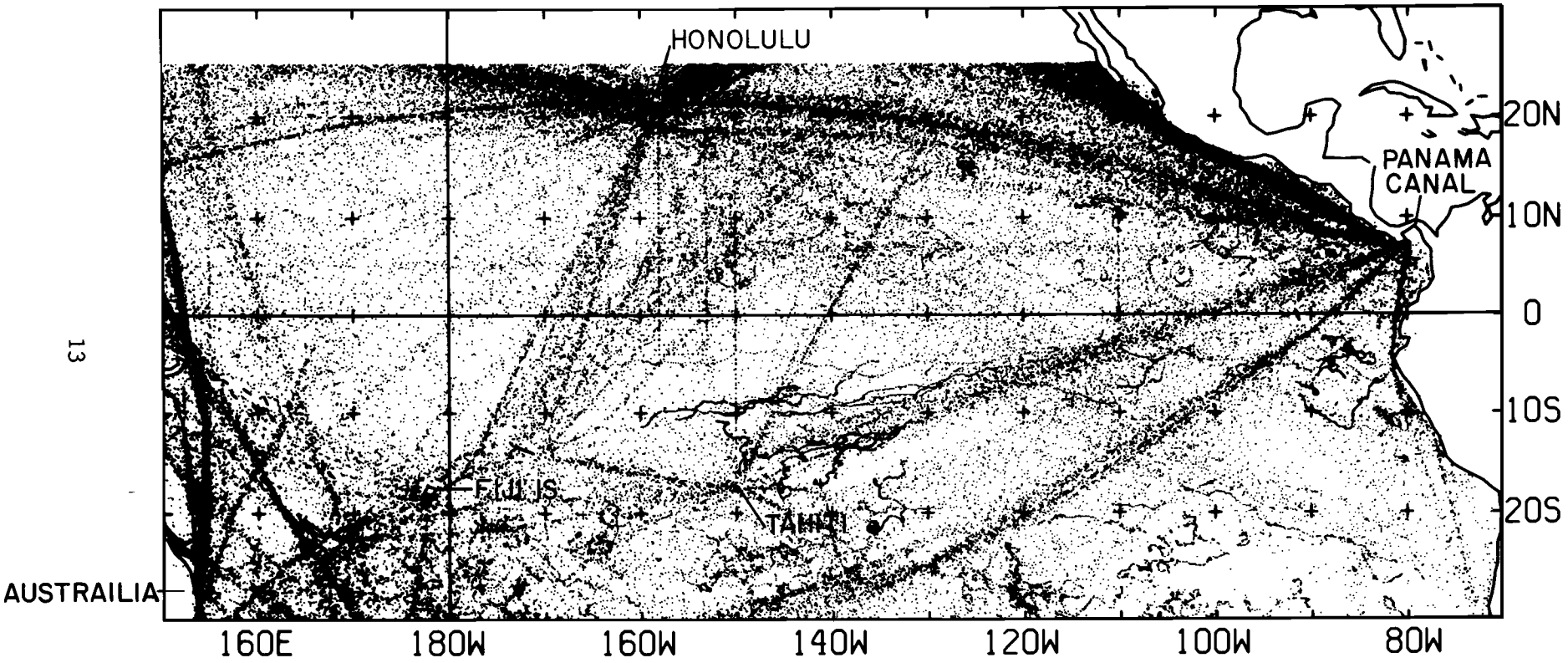

Figure 1. Composite of station data used for the analysis of semimonthly SST's in the period of February-July, 1975-1980. Small dots indicate the location of ship reports, with shipping lanes defined by thousands of these small dots. Curvy, dotted lines are buoy tracks. Lines of larger dots indicate XBT and AXBT sections, e.g., Hawaii-to-Tahiti Shuttle cruises. (Copyright, *J. Geophysical Research* (Green), Seasat II, 1982).

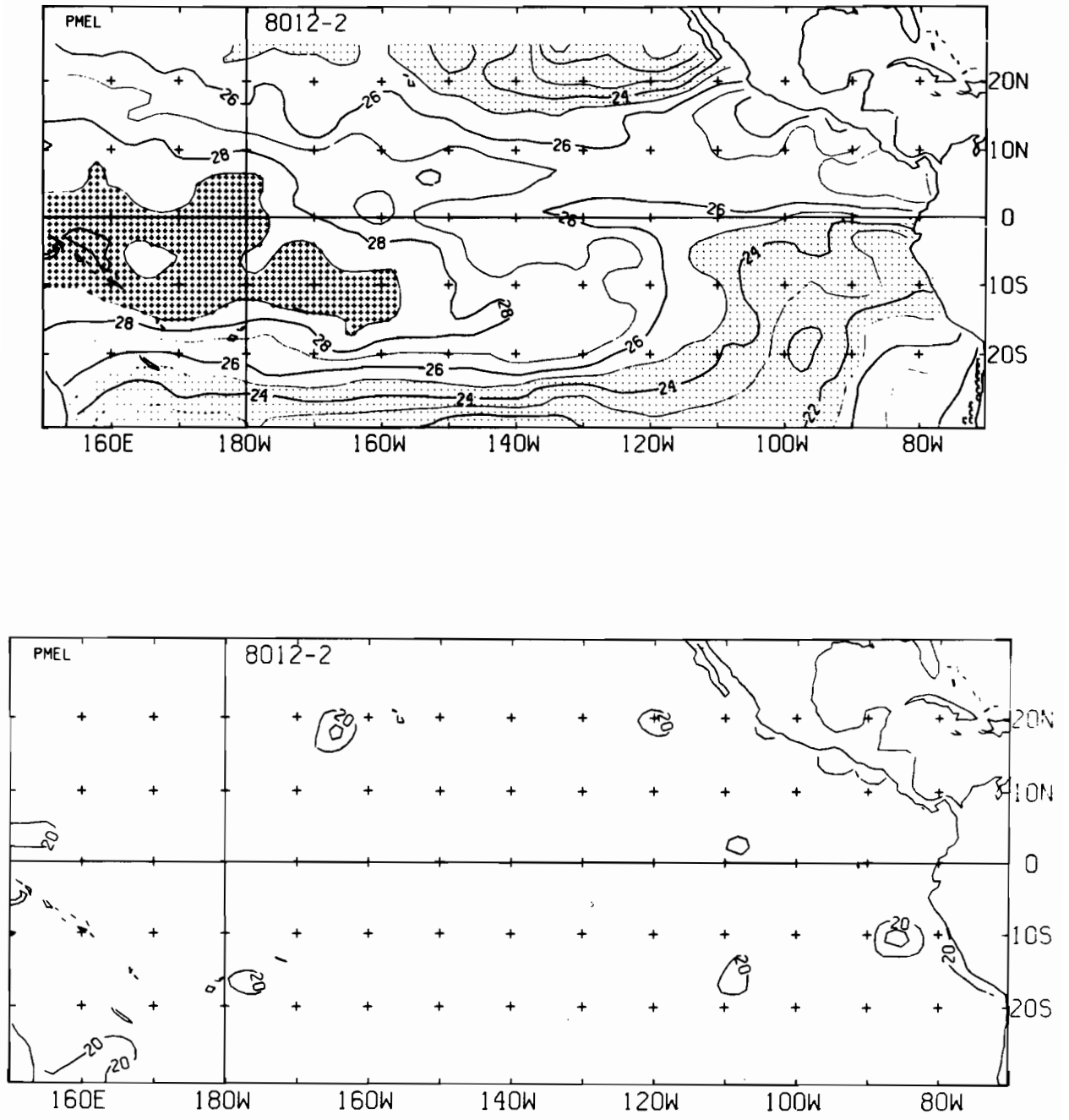

Figure 2. Top: The final SST field for the second half of December 1980, as derived from a modified initial field that is 2°C warmer than the climatic mean SST to the east of 140°W, and 2°C colder to the west of 140°W. Bottom: Residuals (in percentage) in the analyzed SST field due to 2°C distortion on the initial SST field. A 20% residual amounts to 0.4°C change in the analyzed SST field.

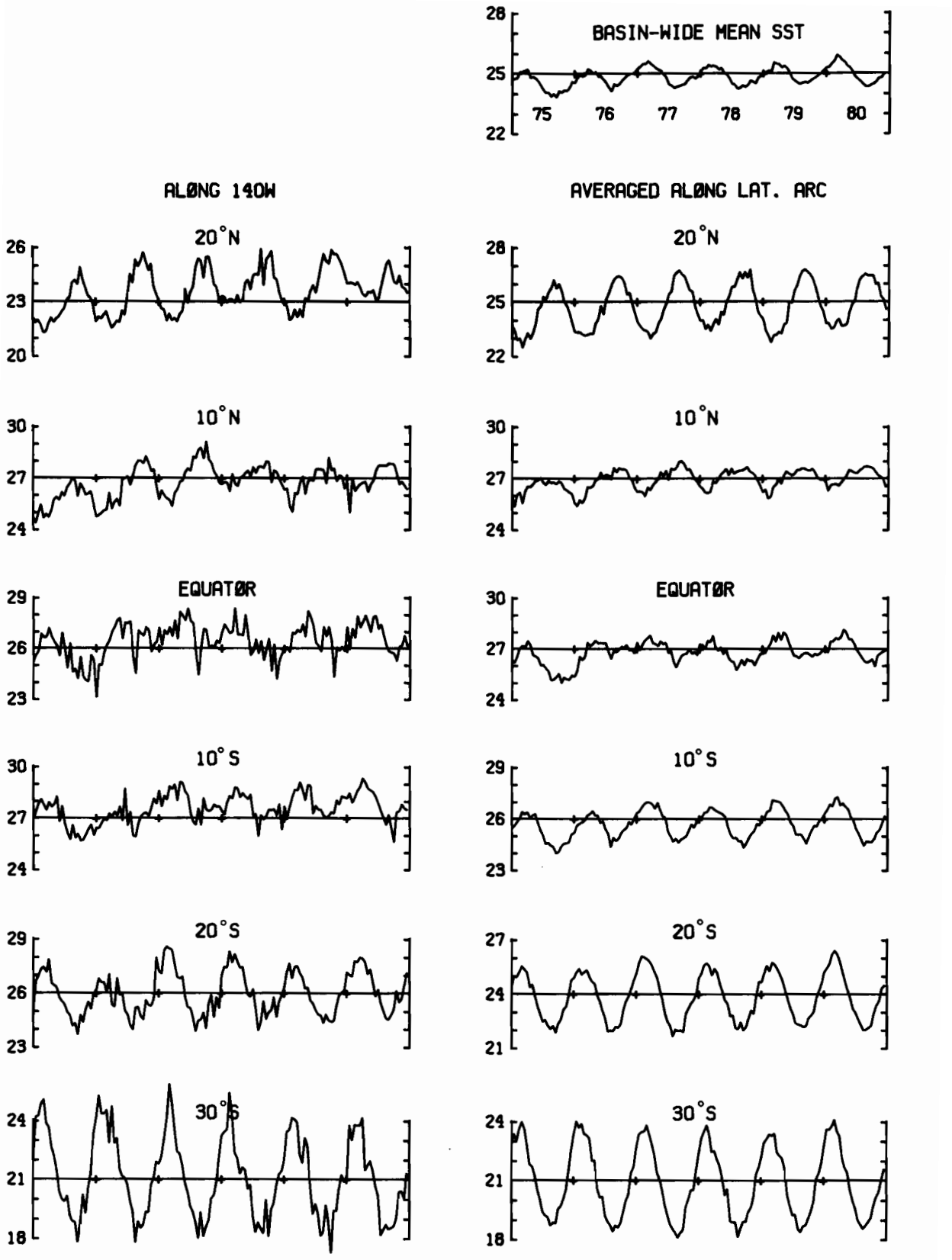

Figure 3. Left: A time series of SST along 140°W. Right: SST field averaged along several latitude arcs. Upper right: SST averaged basinwide (30°S-25°N, 150°E-70°W), all for the period 1975-1980.

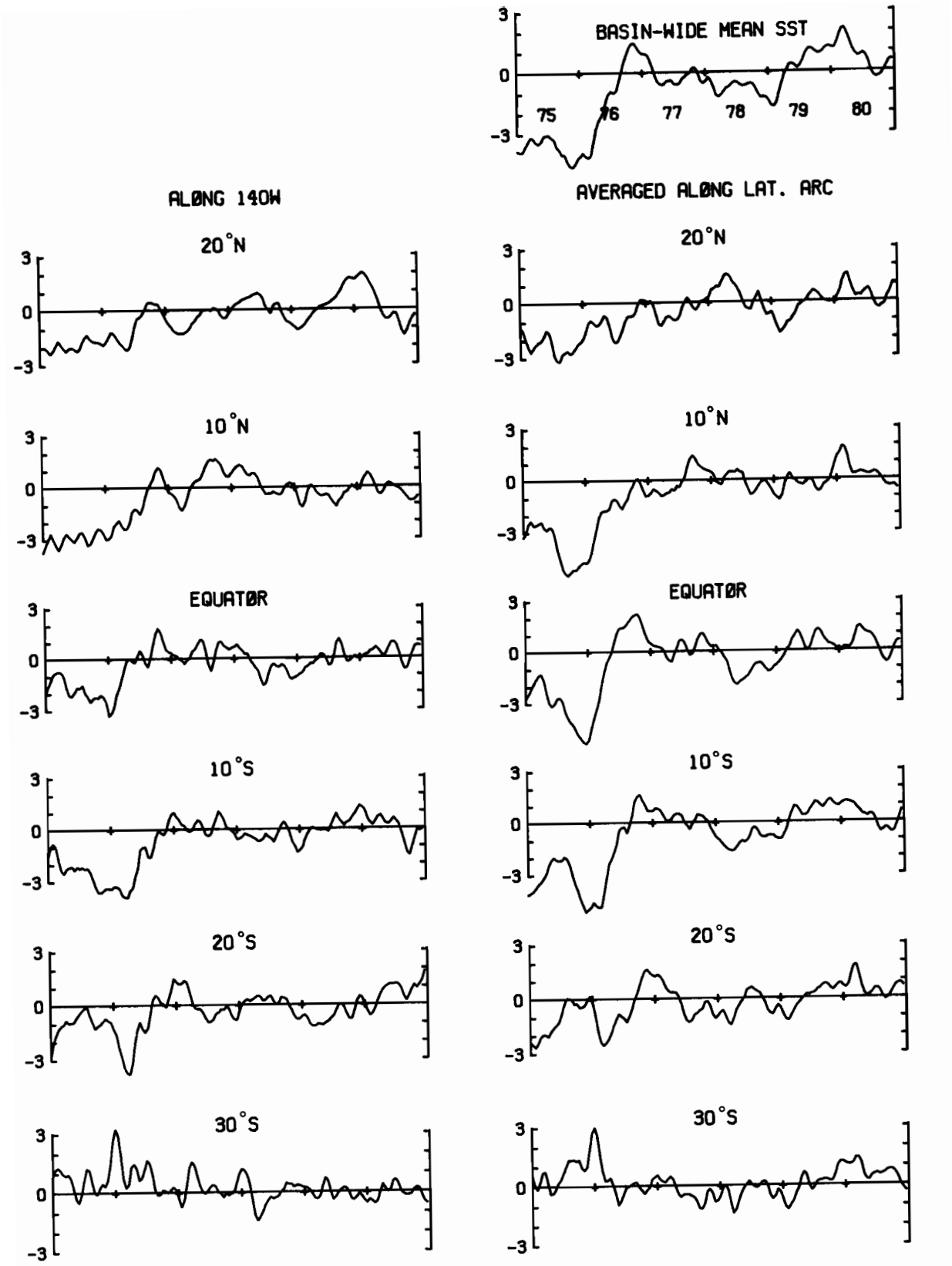

Figure 4. Similar to Figure 3, except for the nonseasonal SST, which are normalized by their standard deviations in the post-El Niño years, 1977-1980.

Figures 5-148.

Figures 5 through 148 are station locations and analyzed fields for 1975-1980. The 144 semimonthly SST analyses are indexed by their dates, e.g., the SST analysis for the 2nd half of January 1975 is indexed as 7501-2. As described in the figure caption, this particular field is derived from 1568 SPOT (ship of FGGE buoy) data and 102 XBT data. No BT (BATHY/TESAC) or E-BUOY (EPOCS buoy) data were available for this half month. (Because of the gaps in SPOT data, the SST-fields for 7503-1, 8008-1, and 8009-2 are linearly interpolated between the two closest SST fields. All upper panels show the location of accepted SST data. Different types of data are differentiated by the size and intensity of the letters: small ones for SPOT data, large and heavy ones for BT and XBT data, and large but faint ones for the EPOCS buoy data.

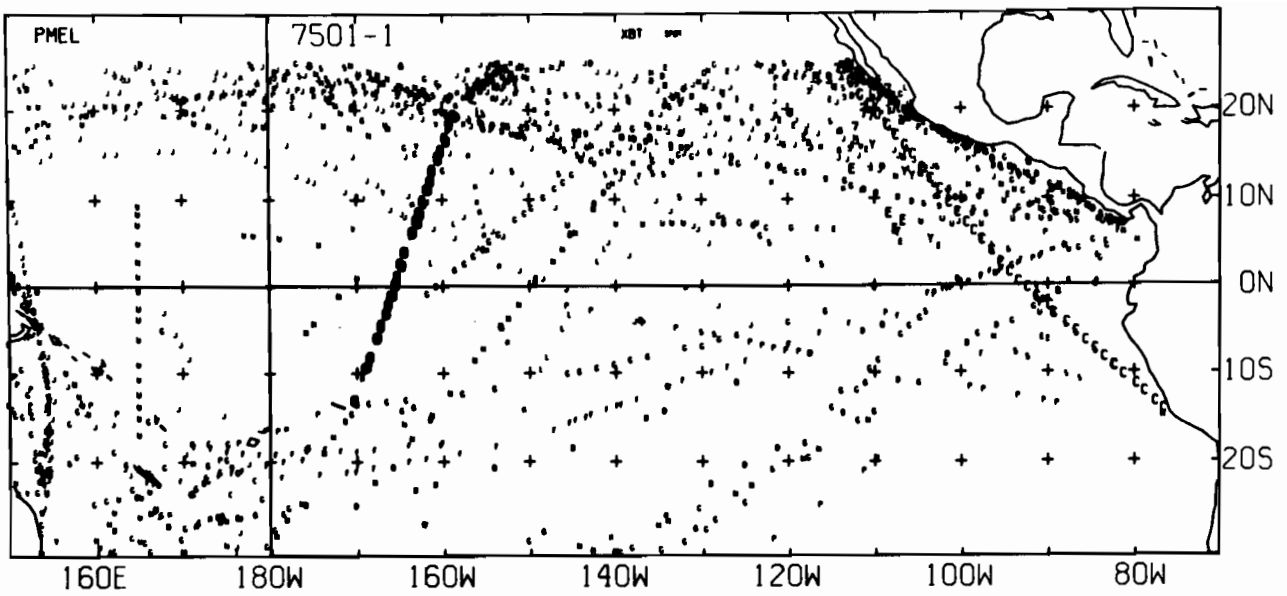

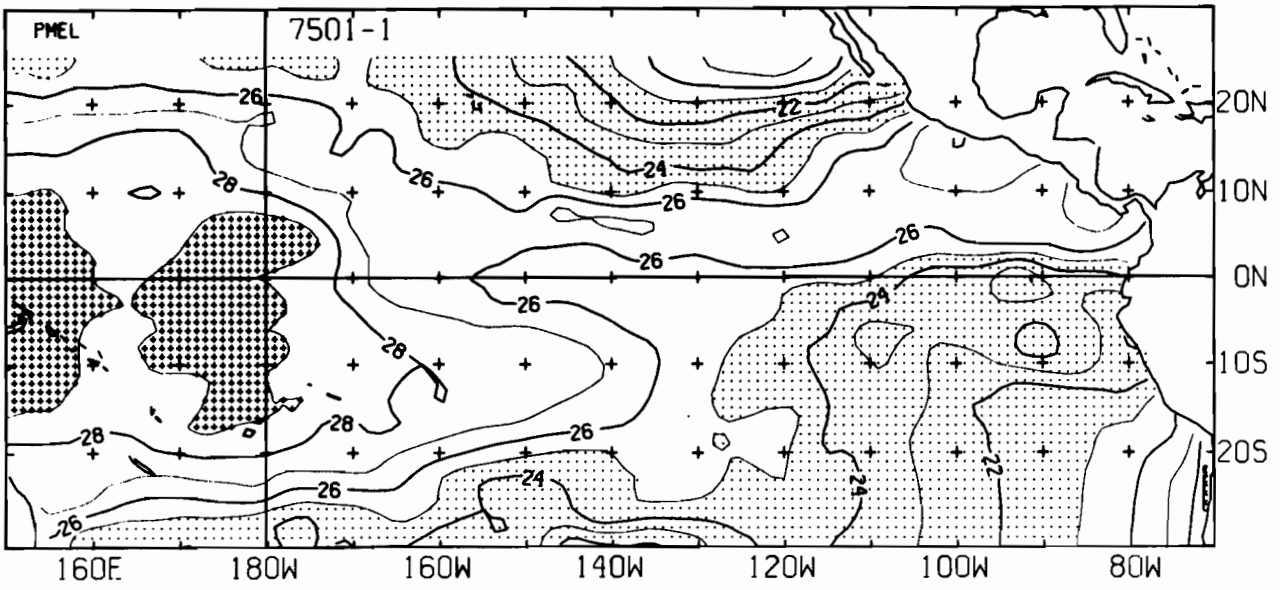

7501-1 SST. 0 E-BUØY. 0 BT. 102 XBT. 1568 SPØT DATA

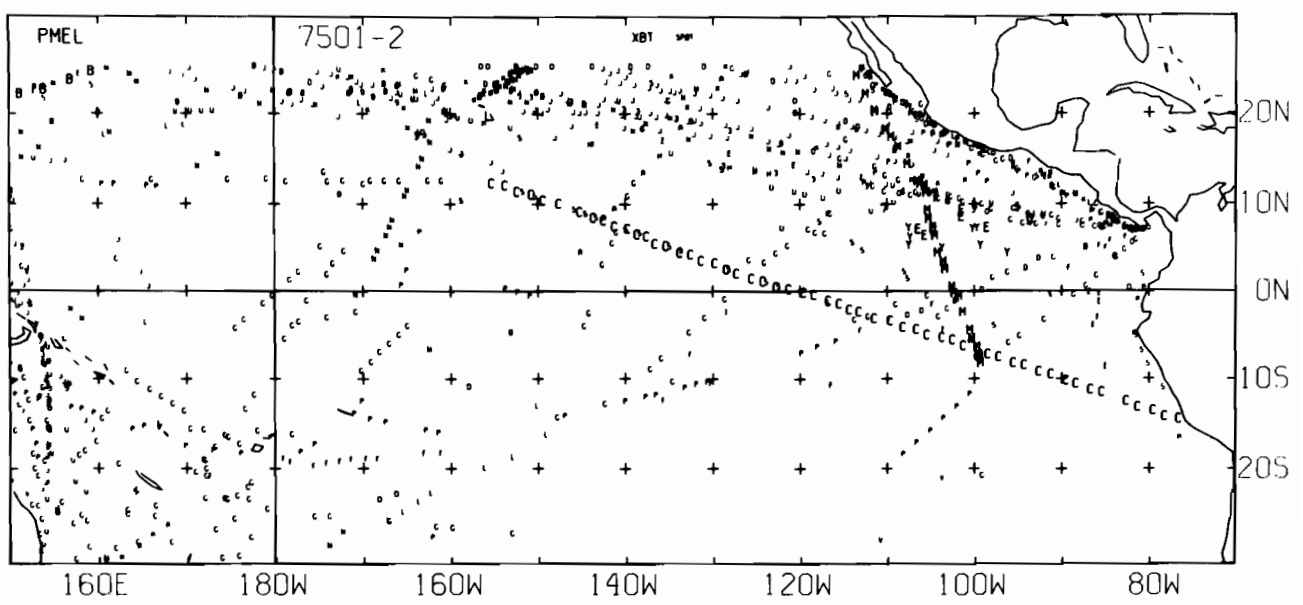

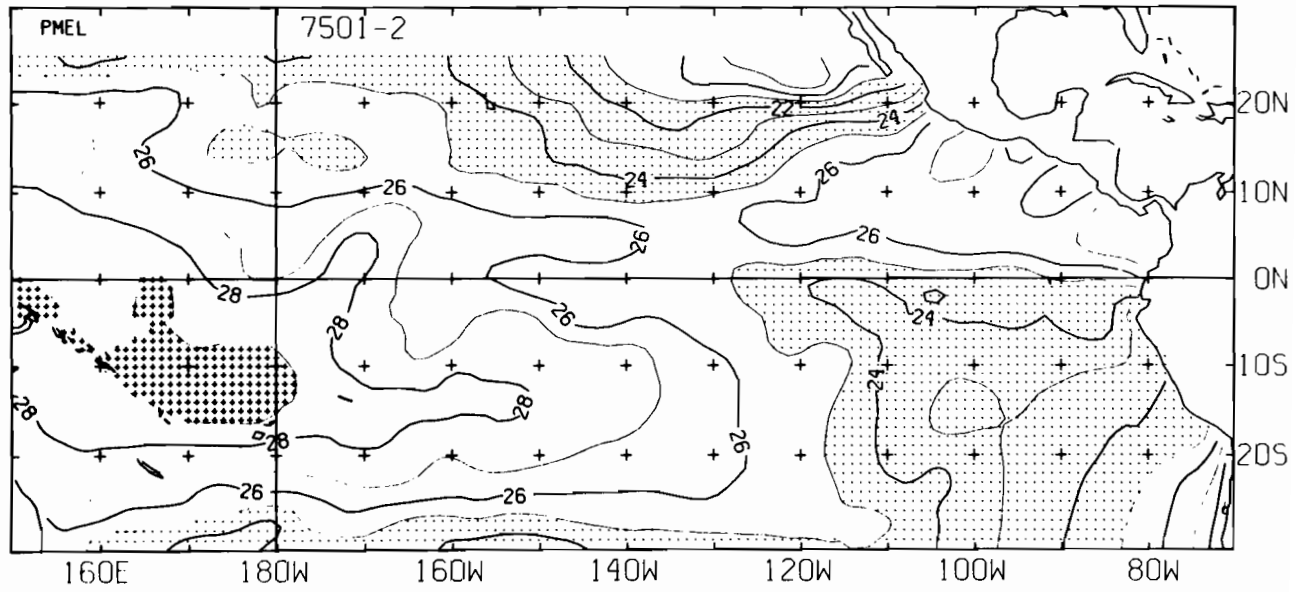

7501-2 SST. 0 E-BUØY. 0 BT. 105 XBT. 995 SPØT DATA

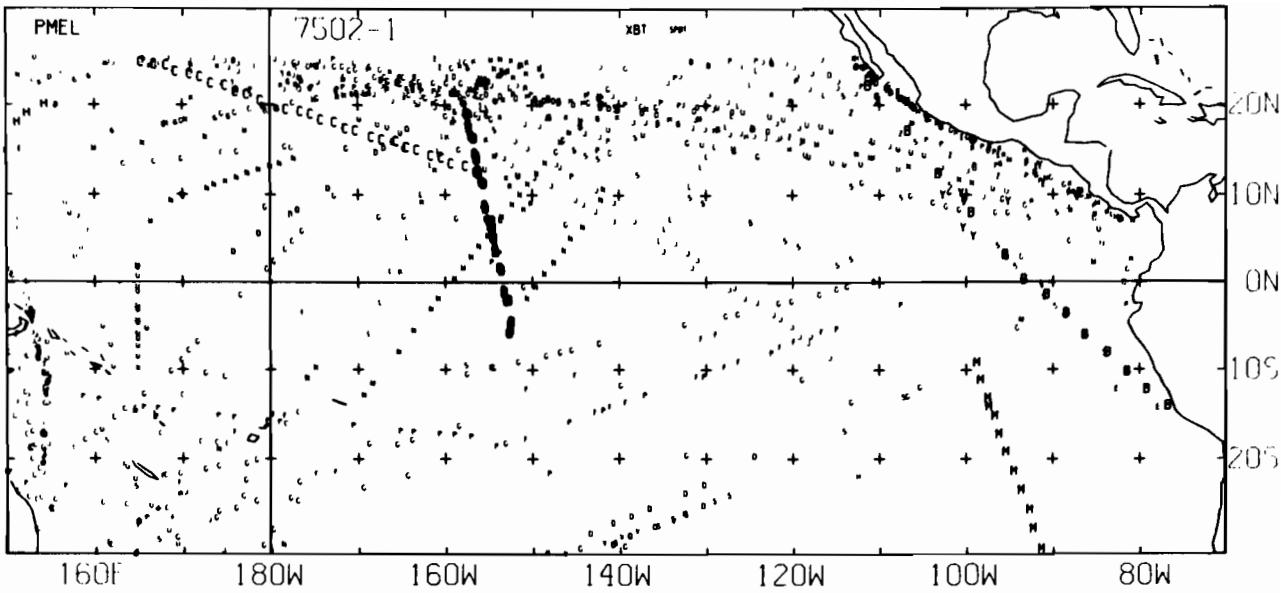

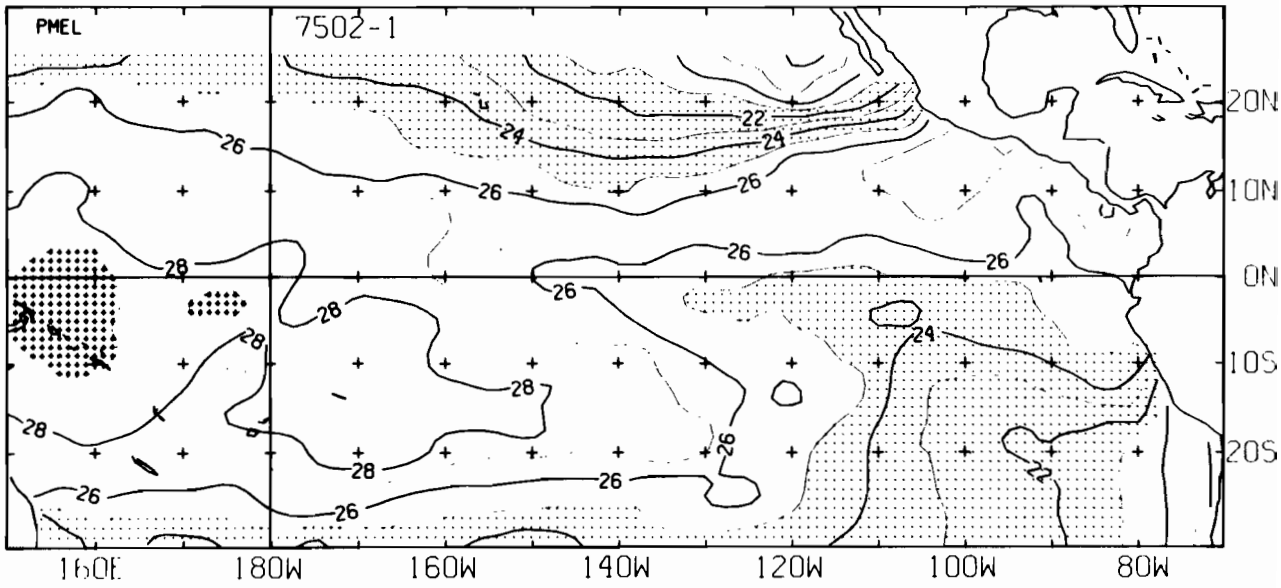

7502-1 SST. 0 E-BUØY. 0 BT. 98 XBT. 1028 SPØT DATA

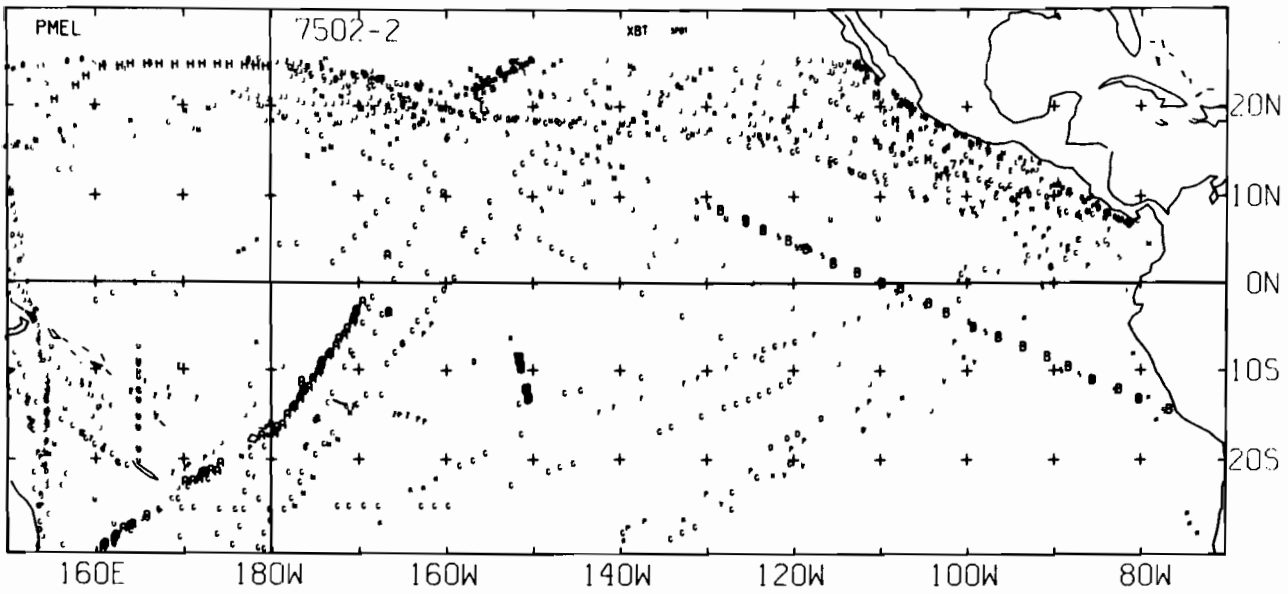

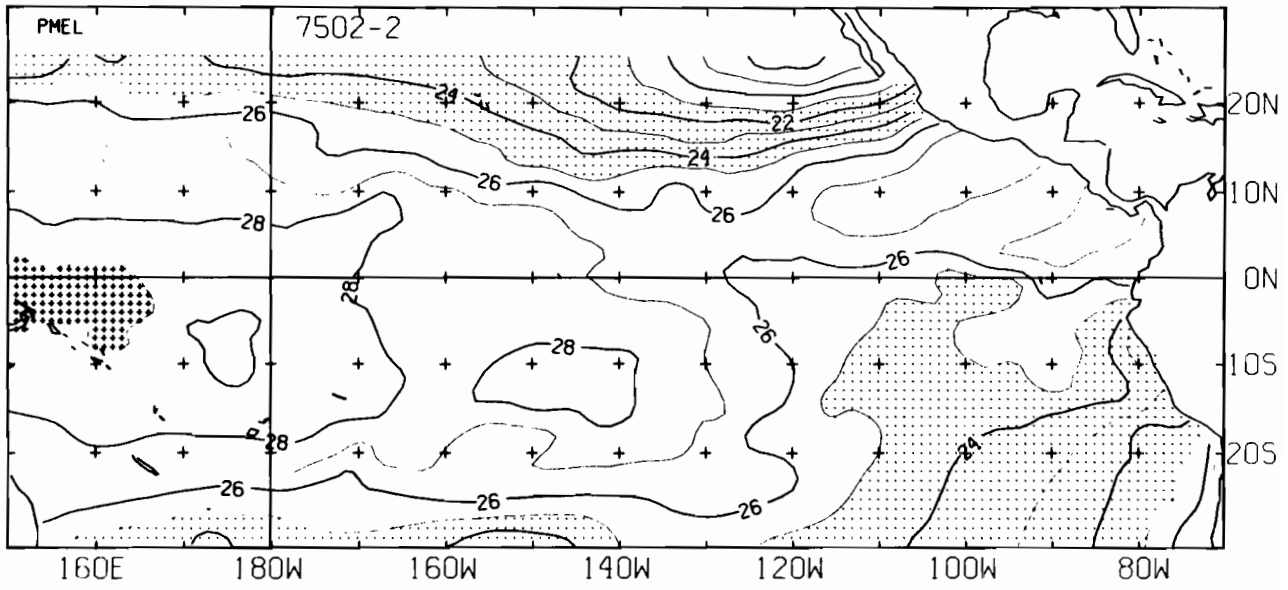

7502-2 SST. 0 E-BUØY. 0 BT. 104 XBT. 1151 SPØT DATA

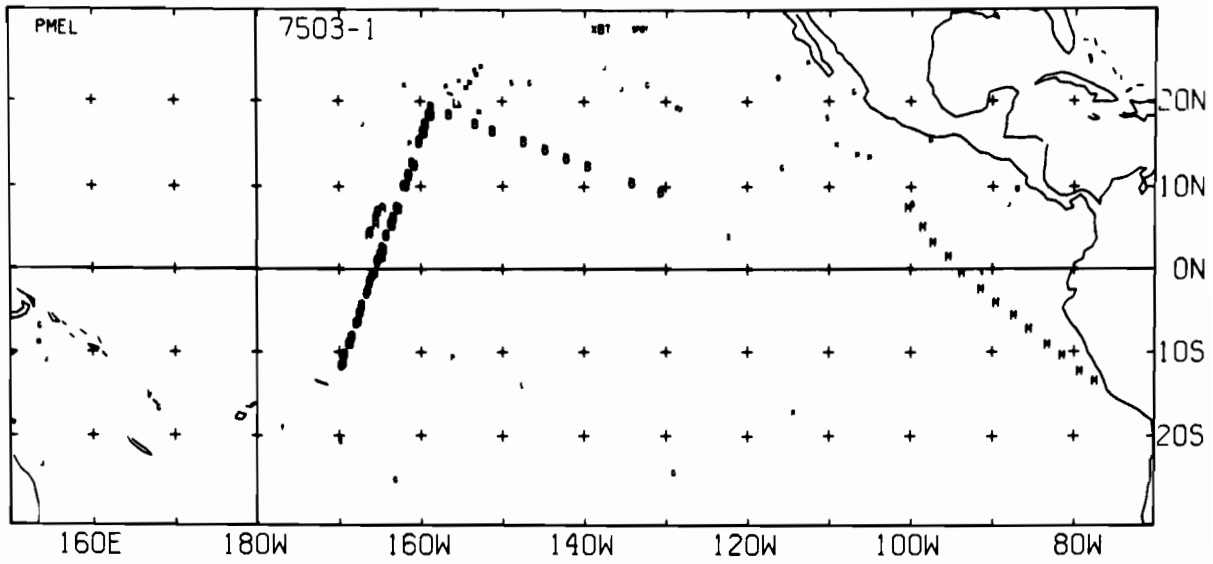

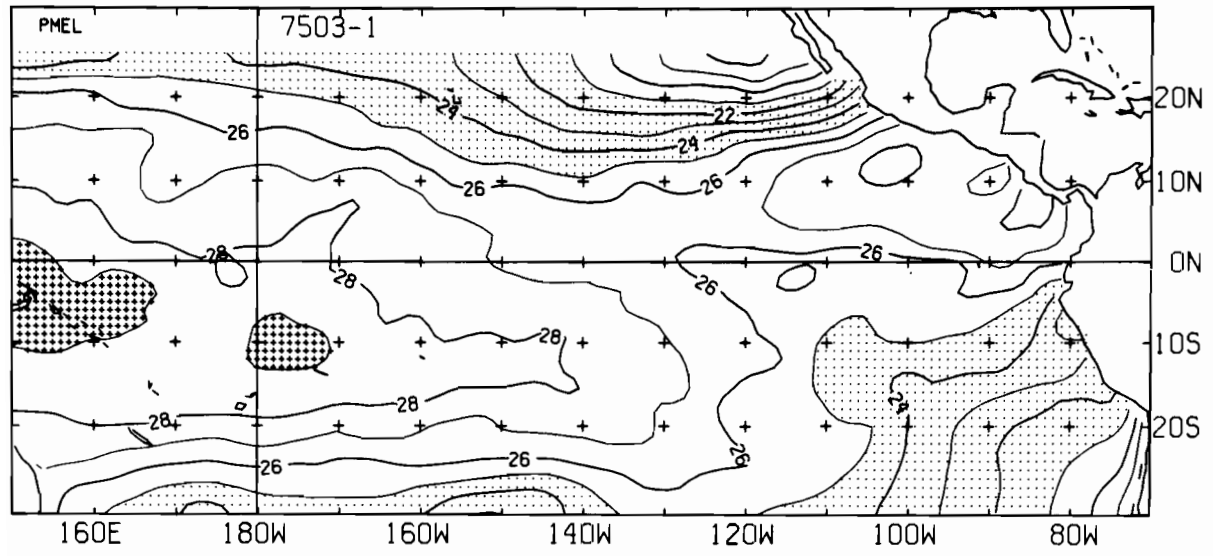

7503-1 SST. 0 E-BUØY. 0 BT. 77 XBT. 77 SPØT DATA

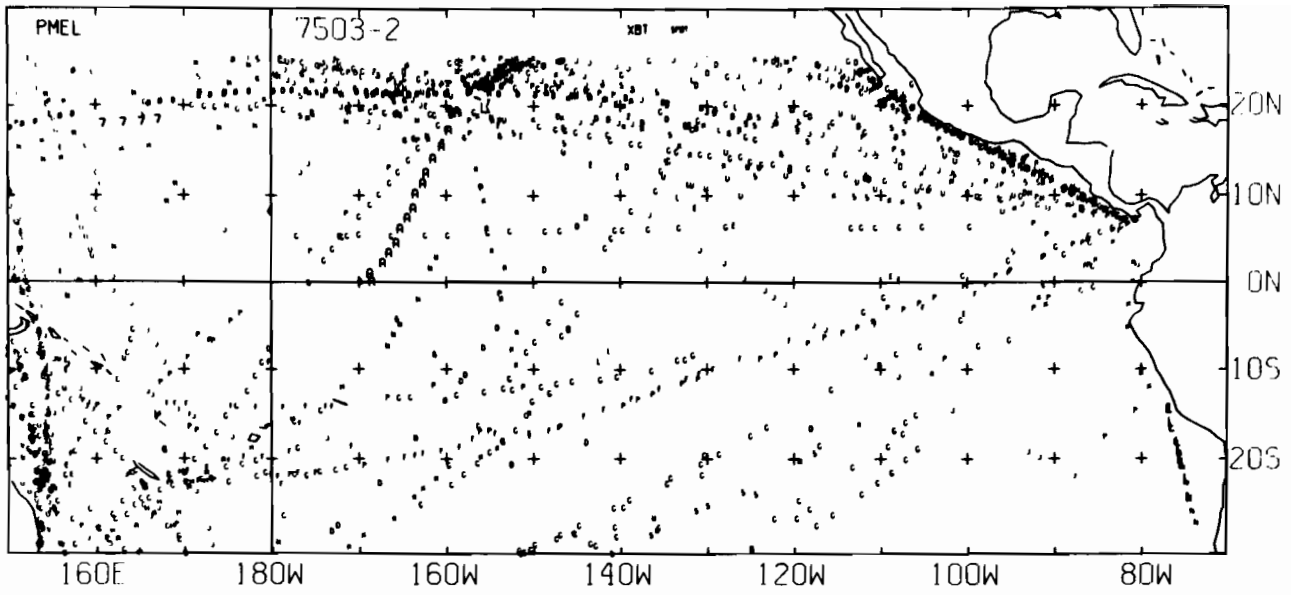

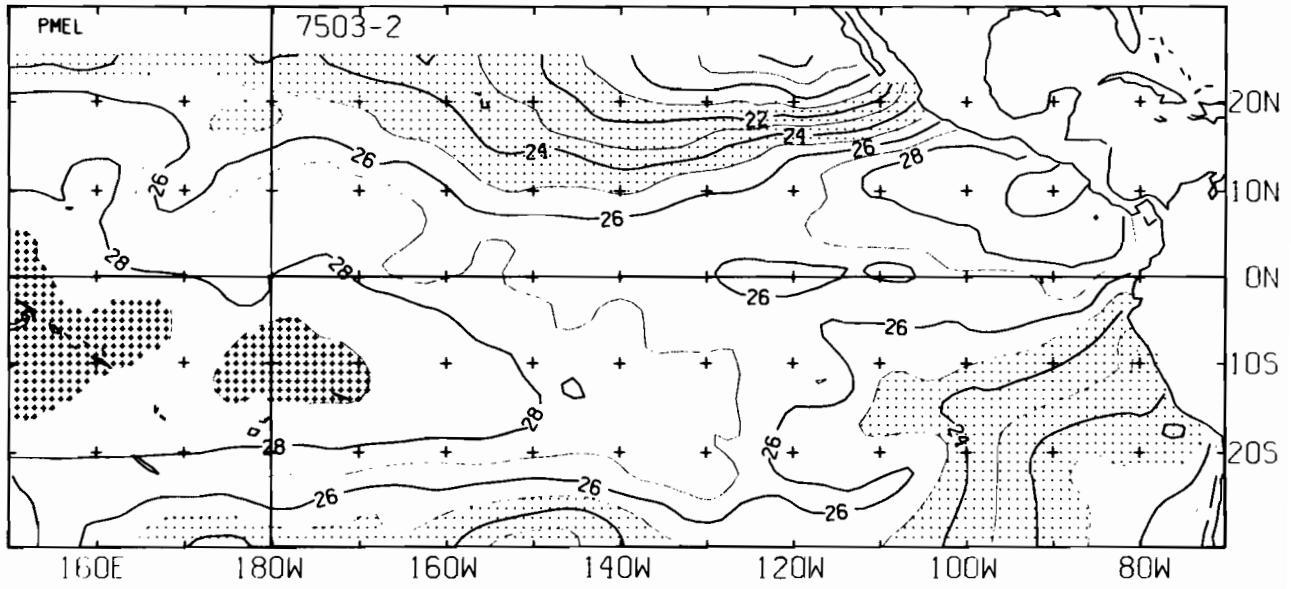

7503-2 SST. 0 E-BUØY. 0 BT. 28 XBT. 1507 SPØT DATA

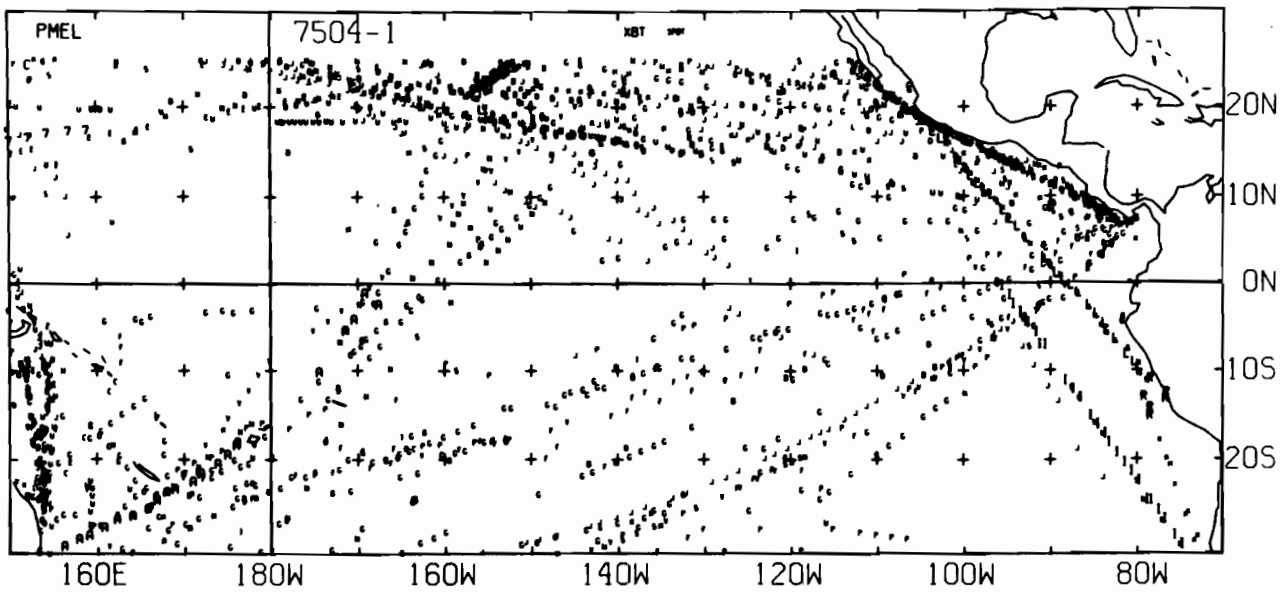

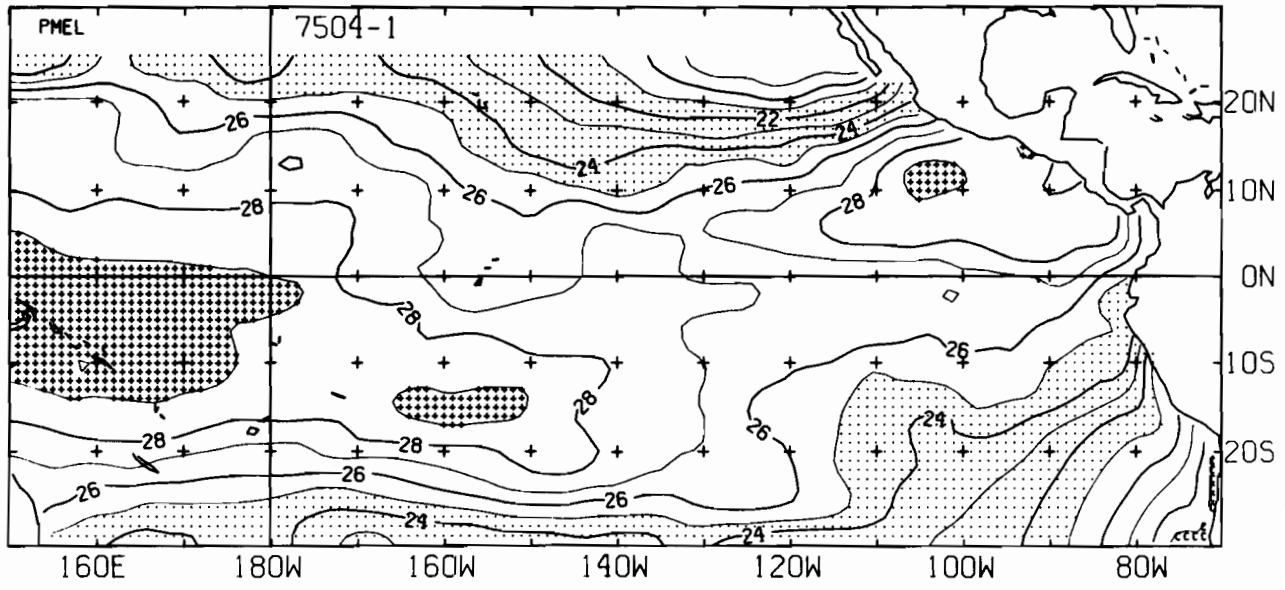

7504-1 SST. 0 E-BUØY. 0 BT. 86 XBT. 1789 SPØT DATA

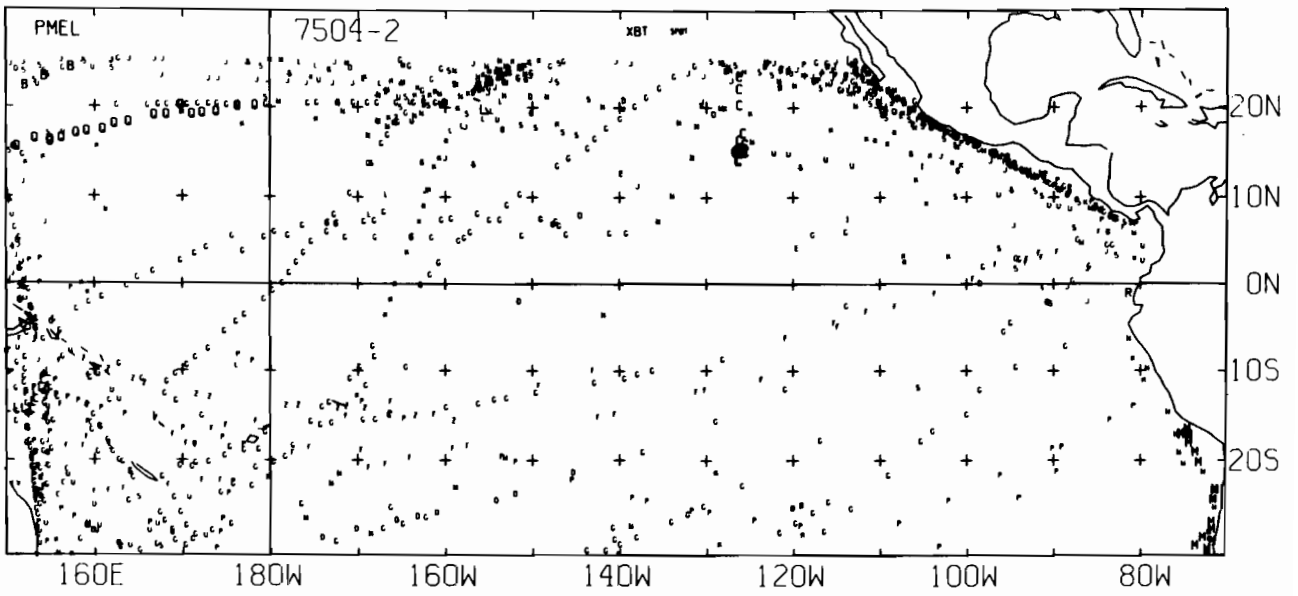

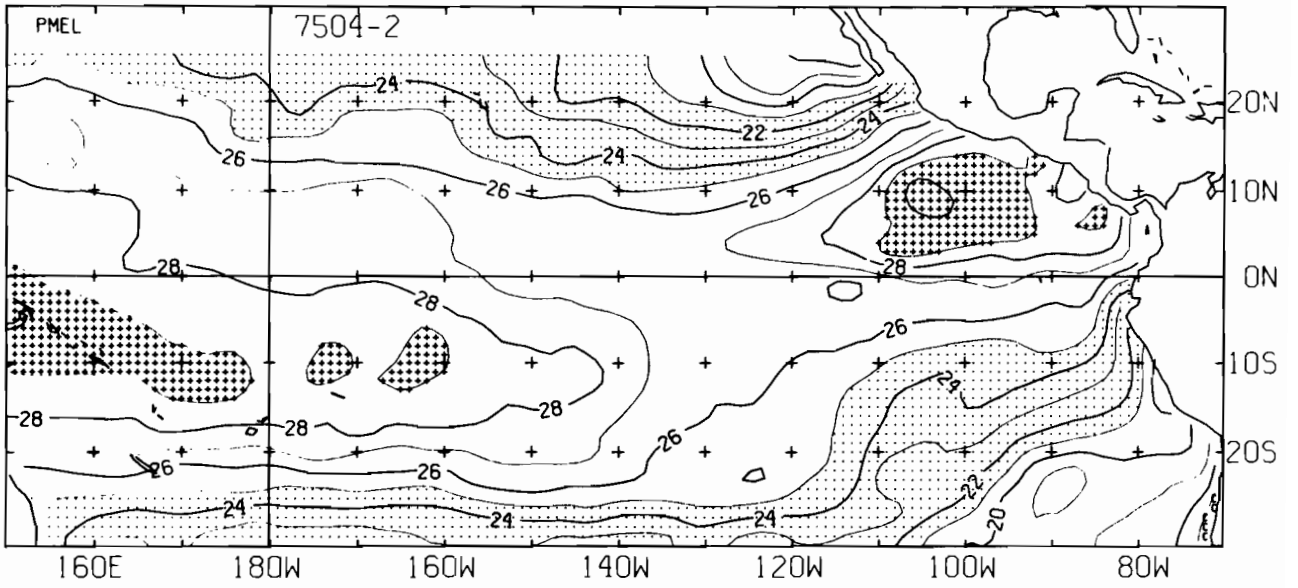

7504-2 SST. 0 E-BUØY. 0 BT. 89 XBT. 1158 SPØT DATA

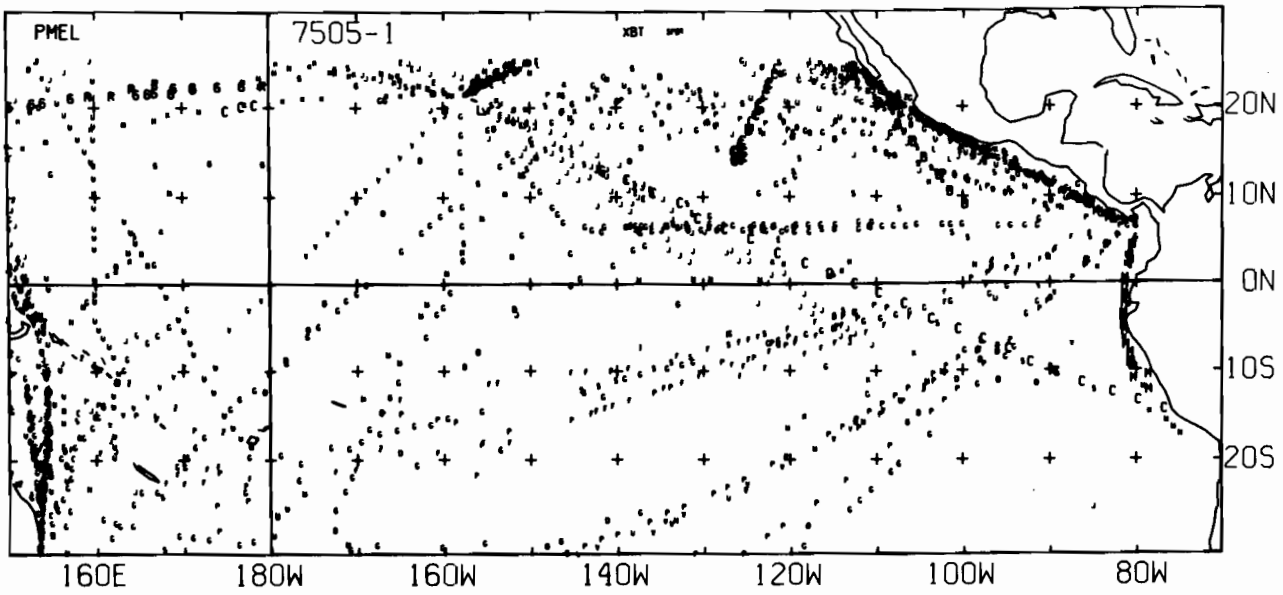

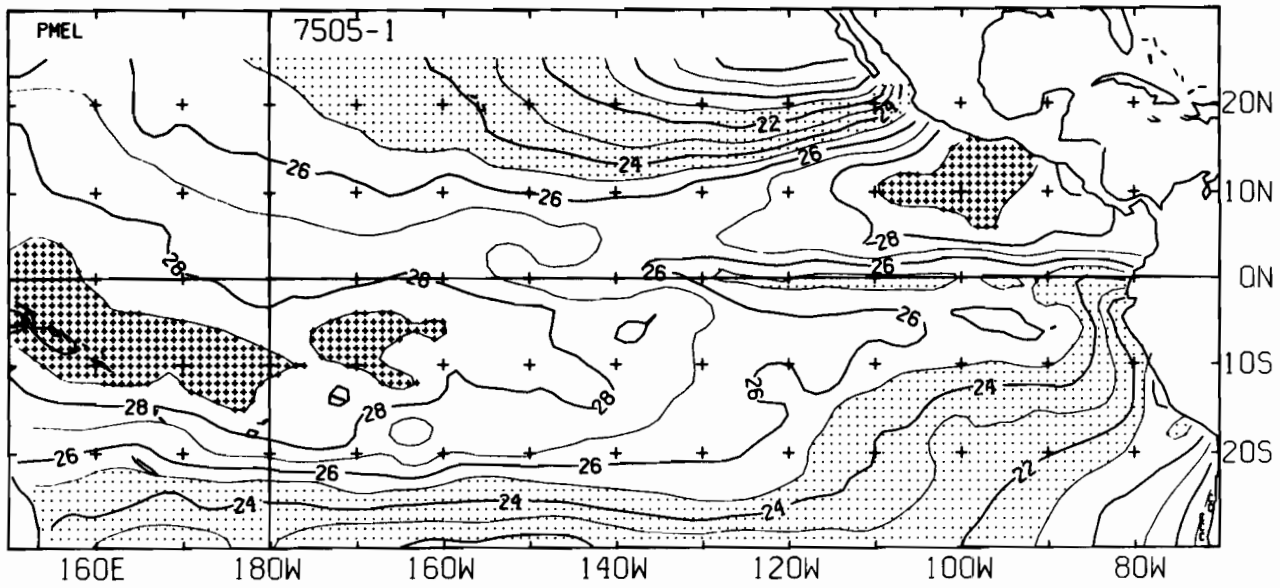

7505-1 SST, 0 E-BUØY, 0 BT, 95 XBT, 1622 SPØT DATA

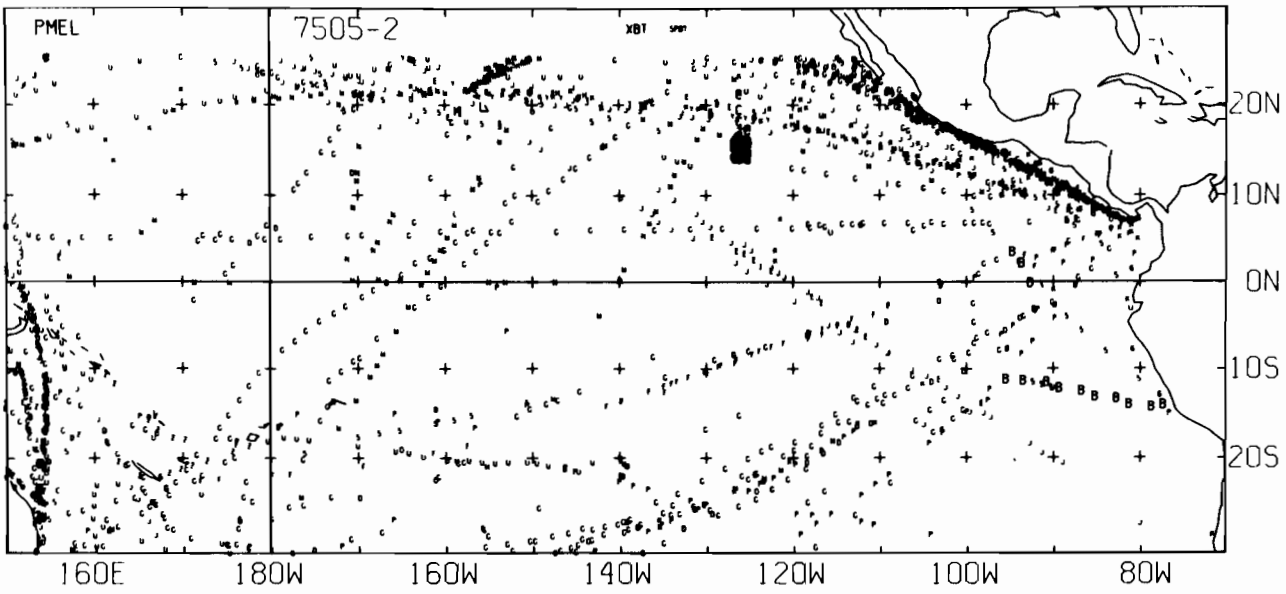

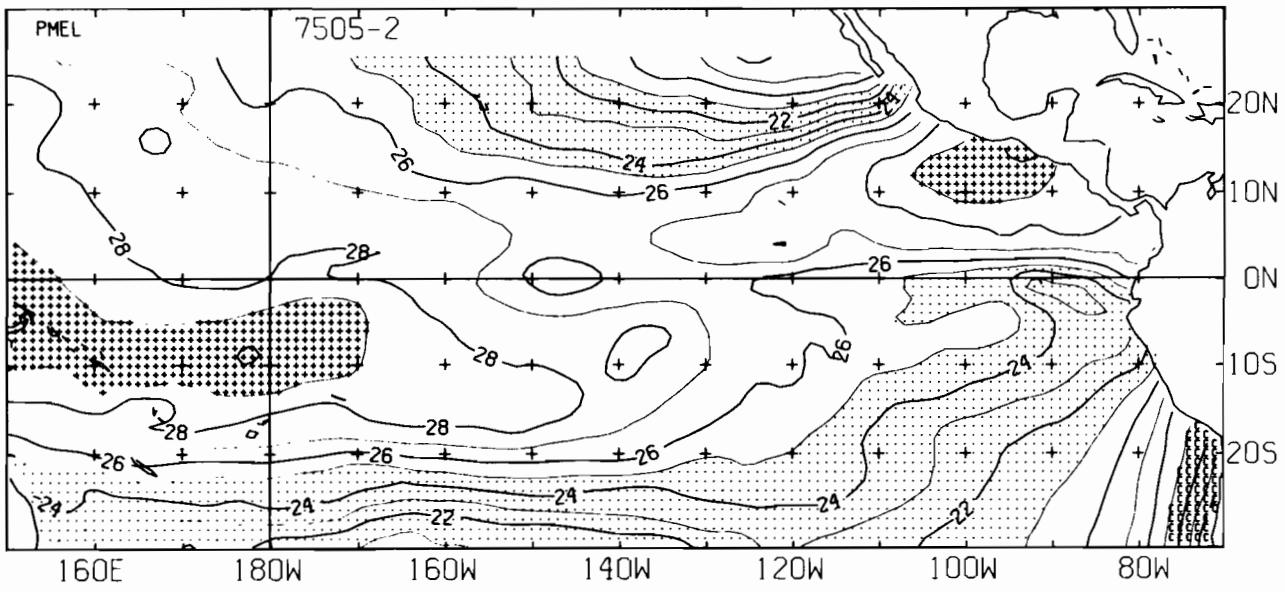

7505-2 SST. 0 E-BUØY. 0 BT. 144 XBT. 1724 SPØT DATA

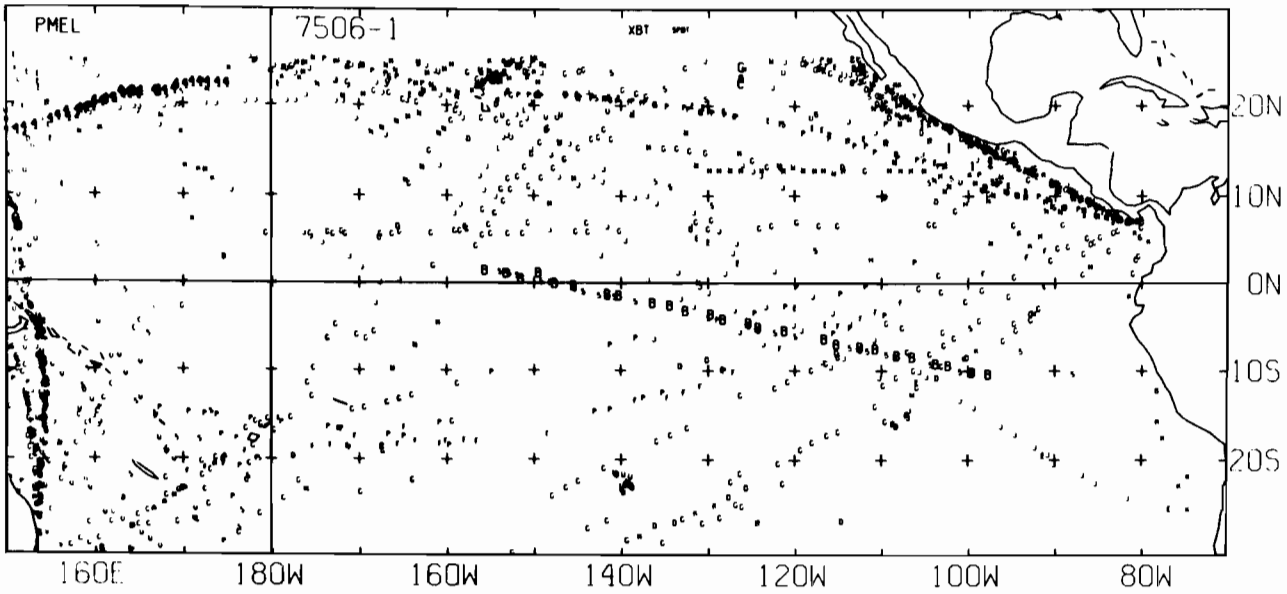

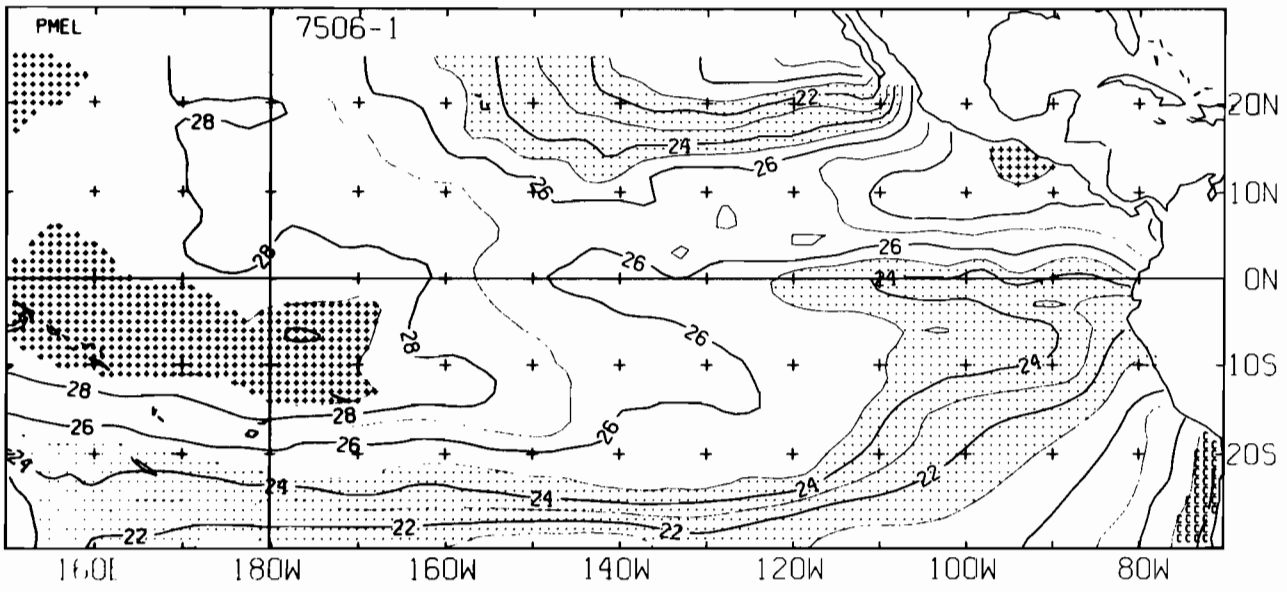

7506-1 SST. 0 E-BUØY. 0 BT. 100 XBT. 1366 SPØT DATA

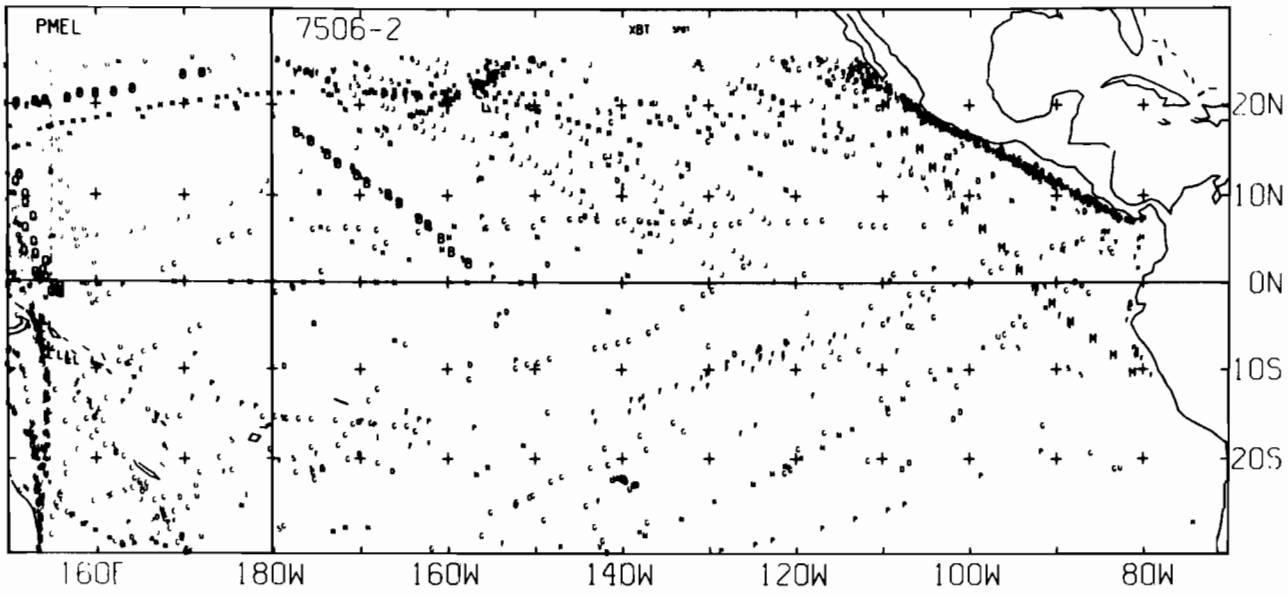

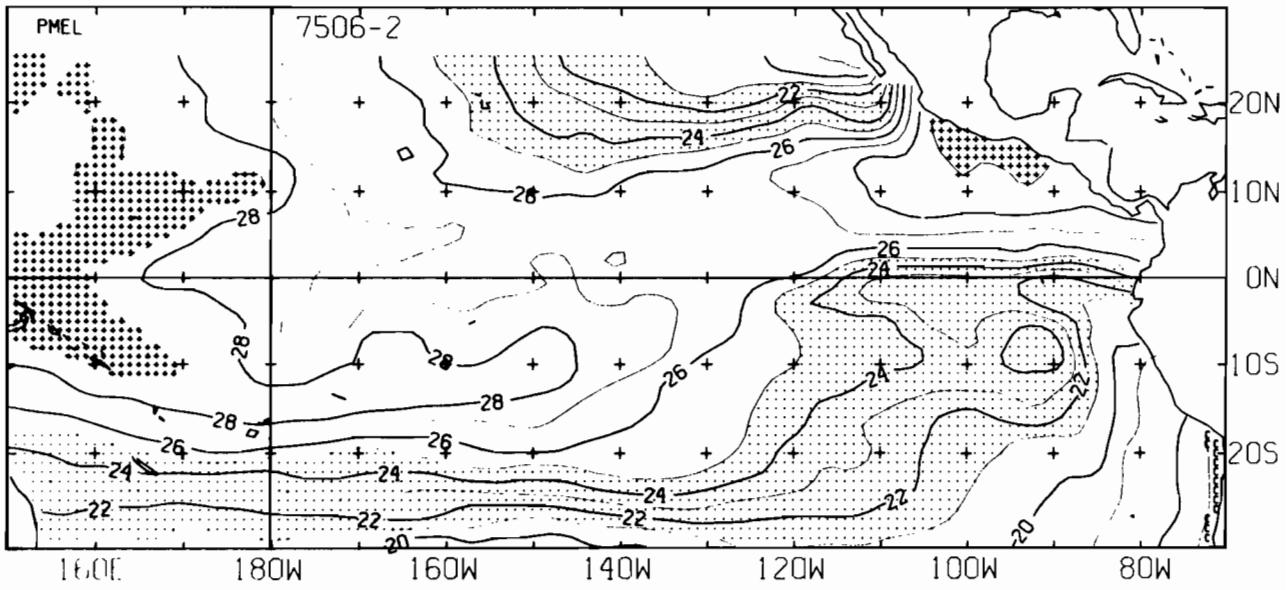

7506-2 SST. 0 E-BUØY. 0 BT. 86 XBT. 1468 SPØT DATA

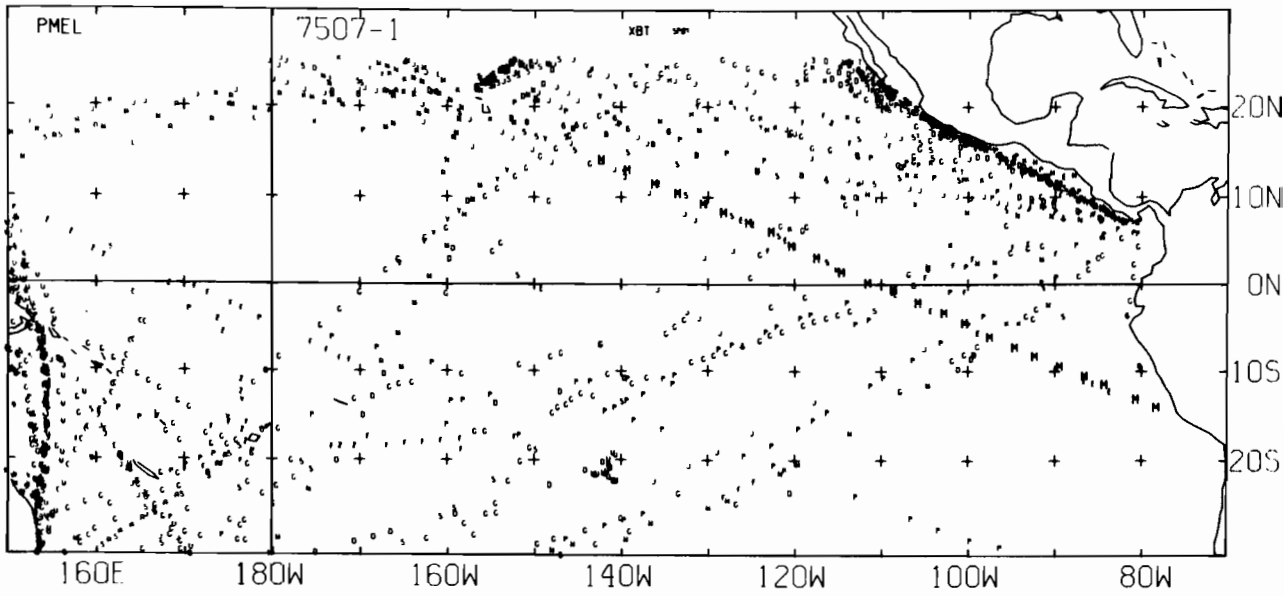

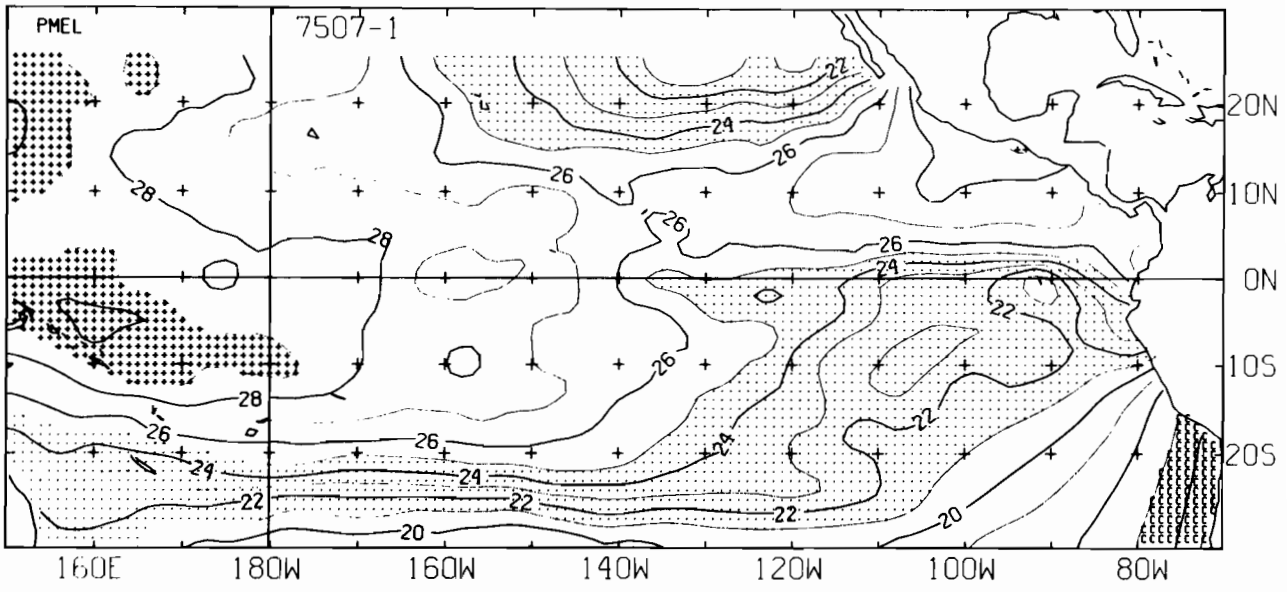

7507-1 SST. 0 E-BUØY. 0 BT. 24 XBT. 1387 SPØT DATA

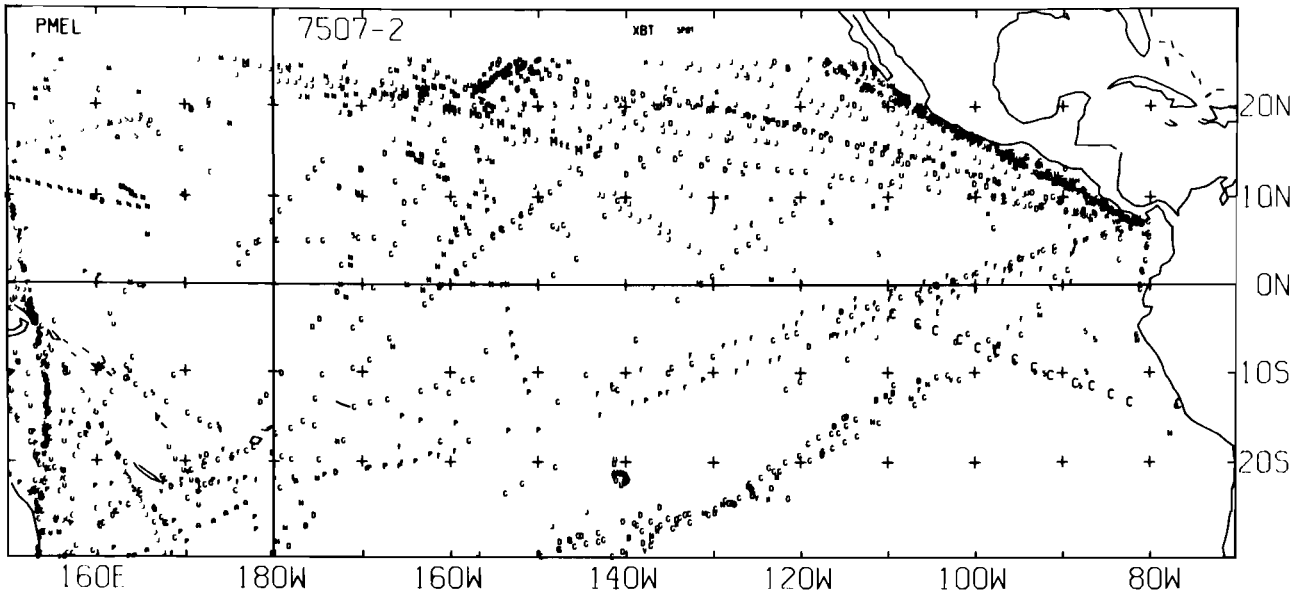

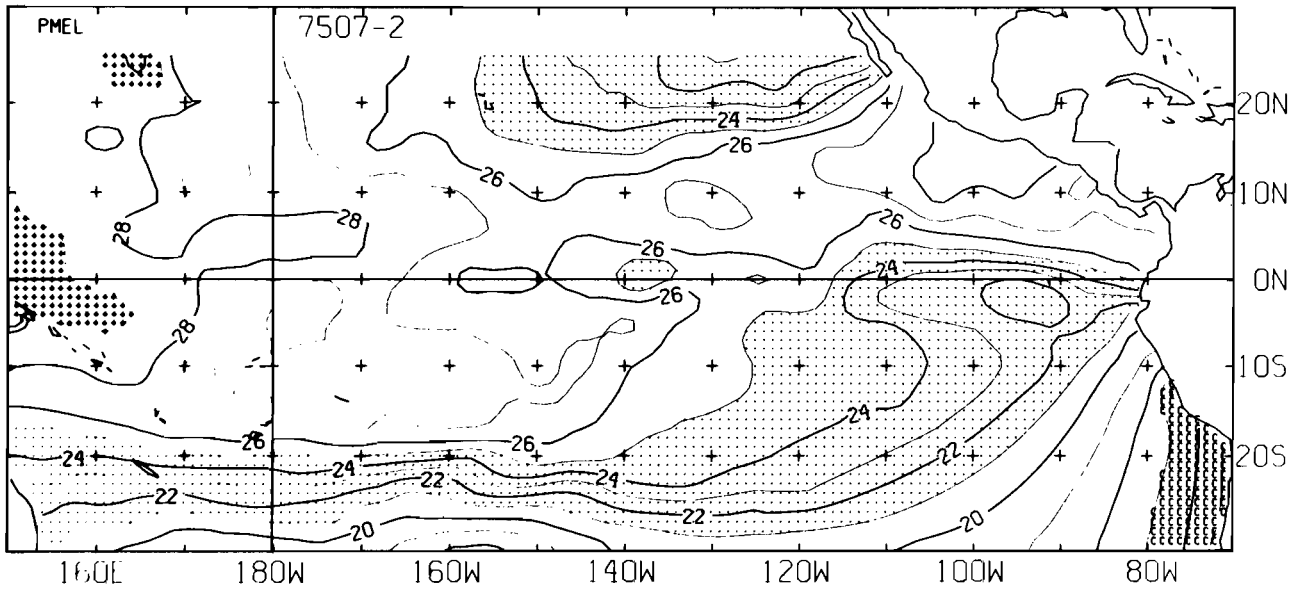

7507-2 SST. 0 E-BUØY. 0 BT. 21 XBT. 1670 SPØT DATA

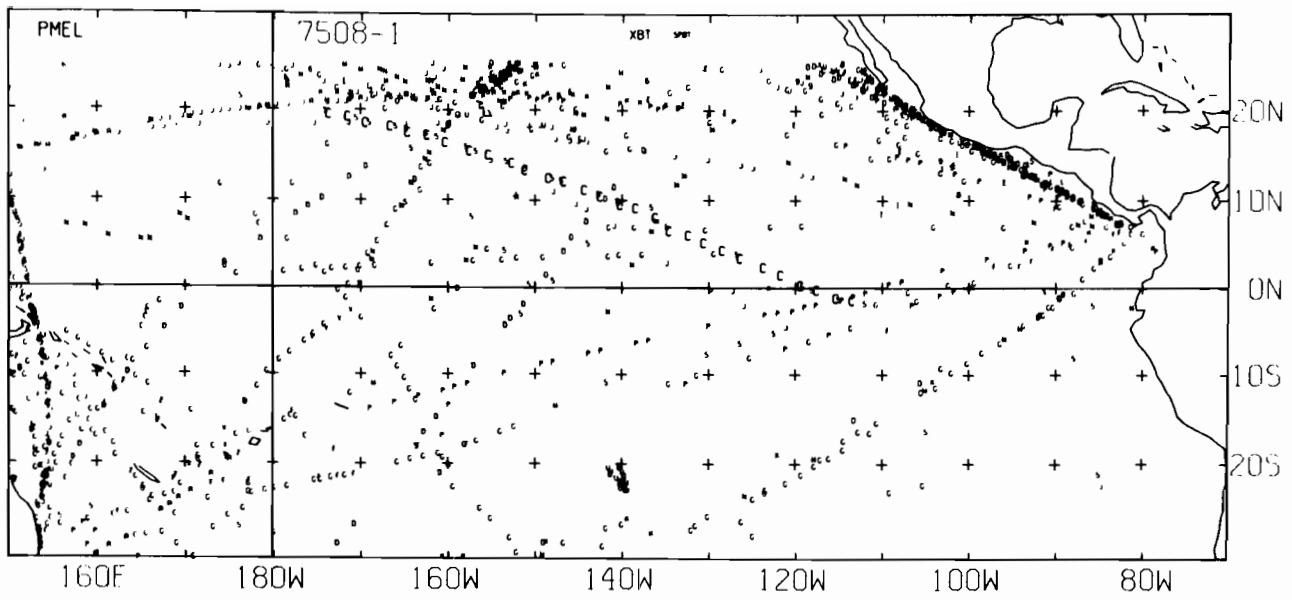

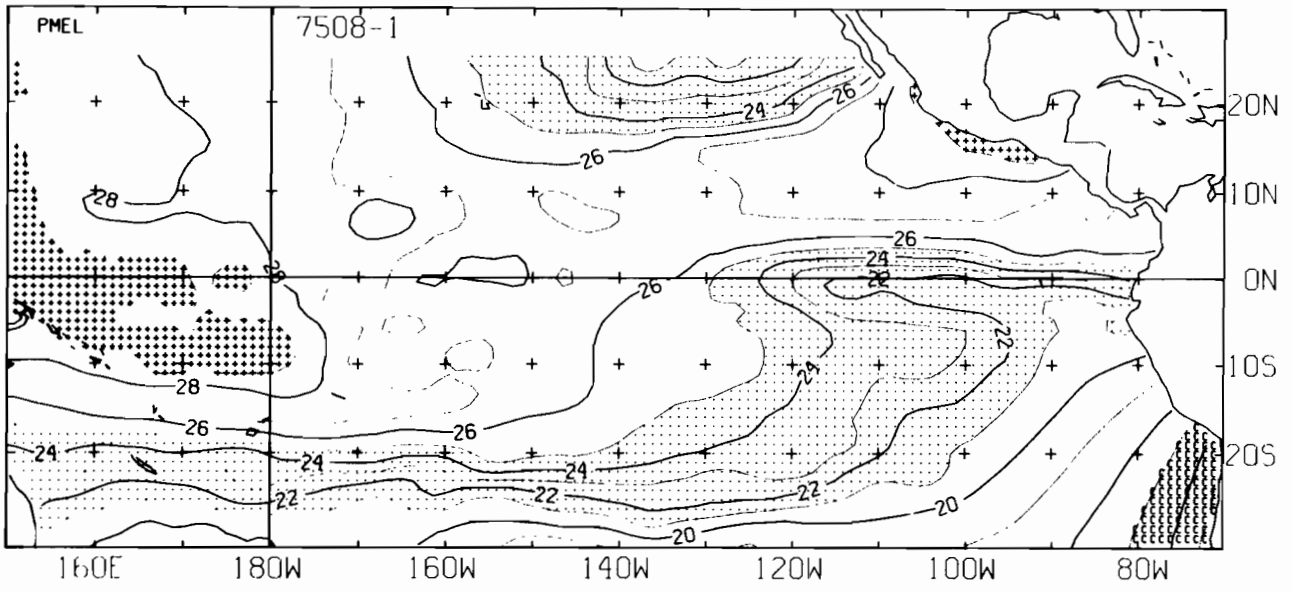

7508-1 SST. 0 E-BUØY. 0 BT. 29 XBT. 1195 SPØT DATA

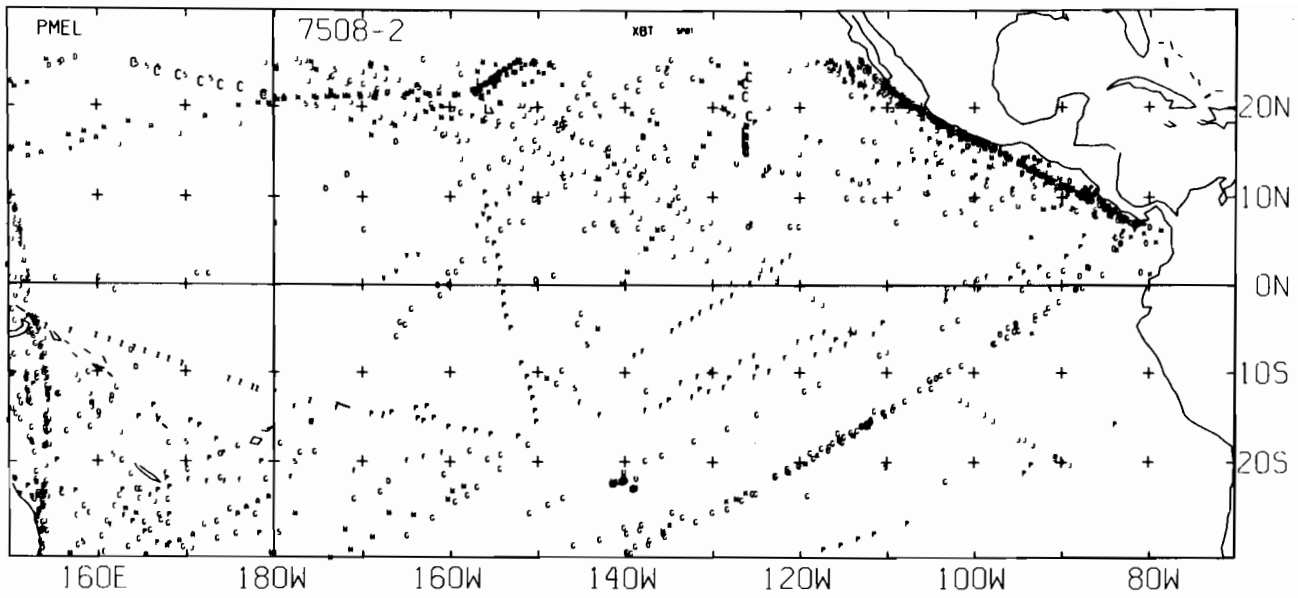

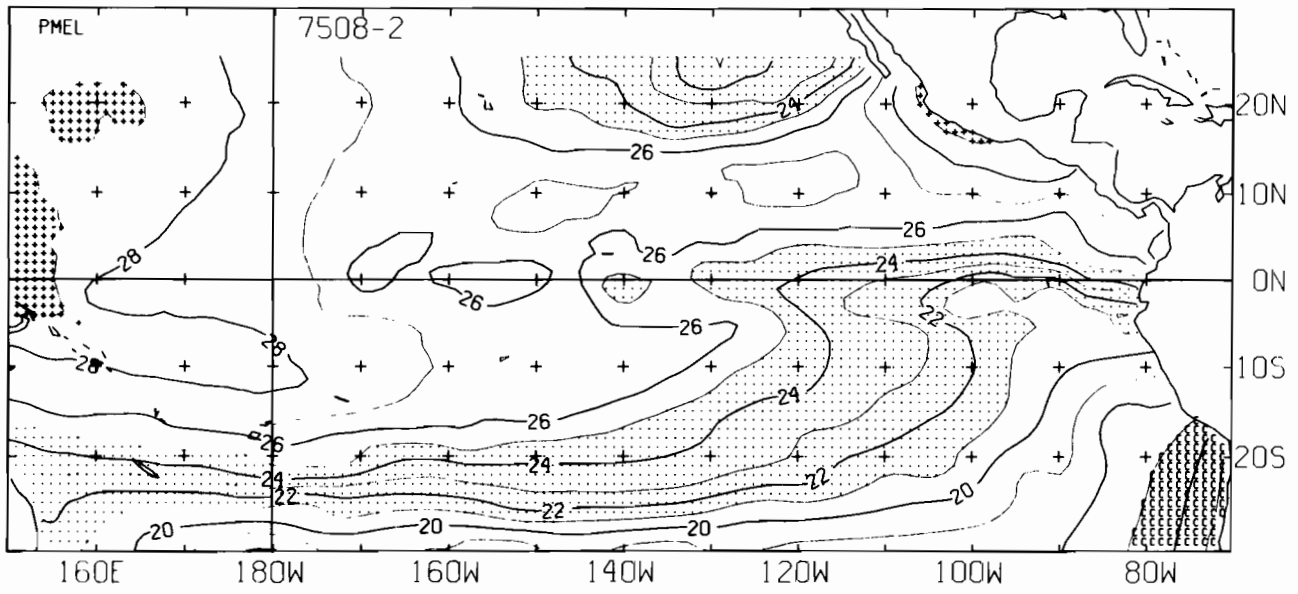

7508-2 SST. 0 E-BUØY. 0 BT. 16 XBT. 1352 SPØT DATA

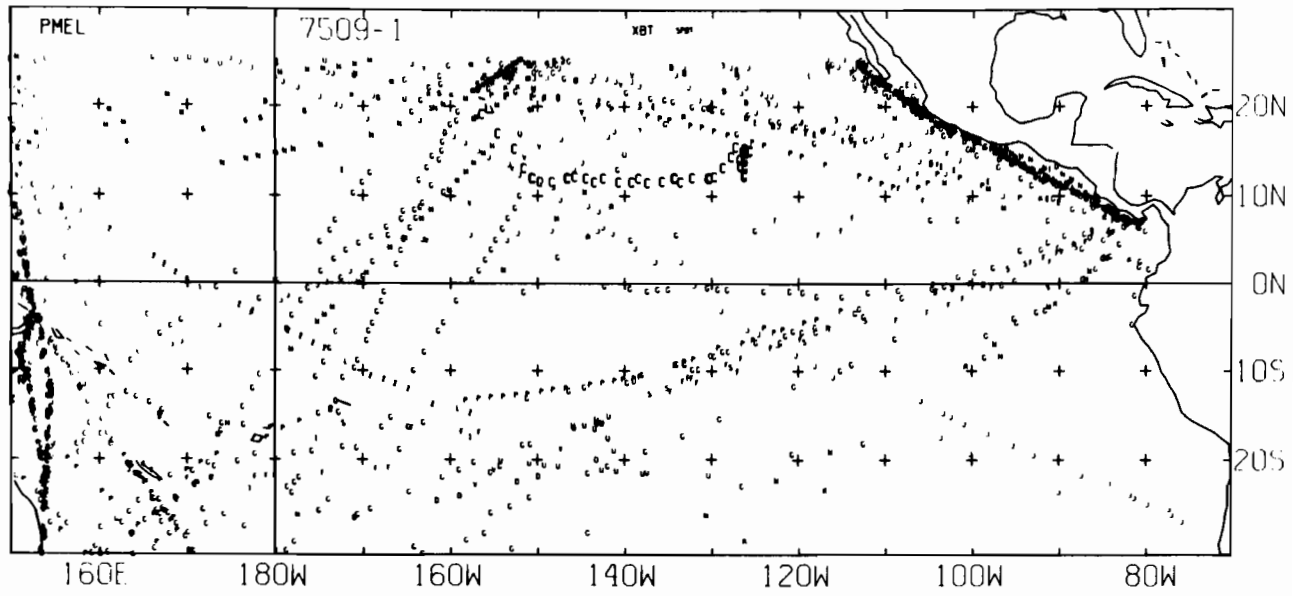

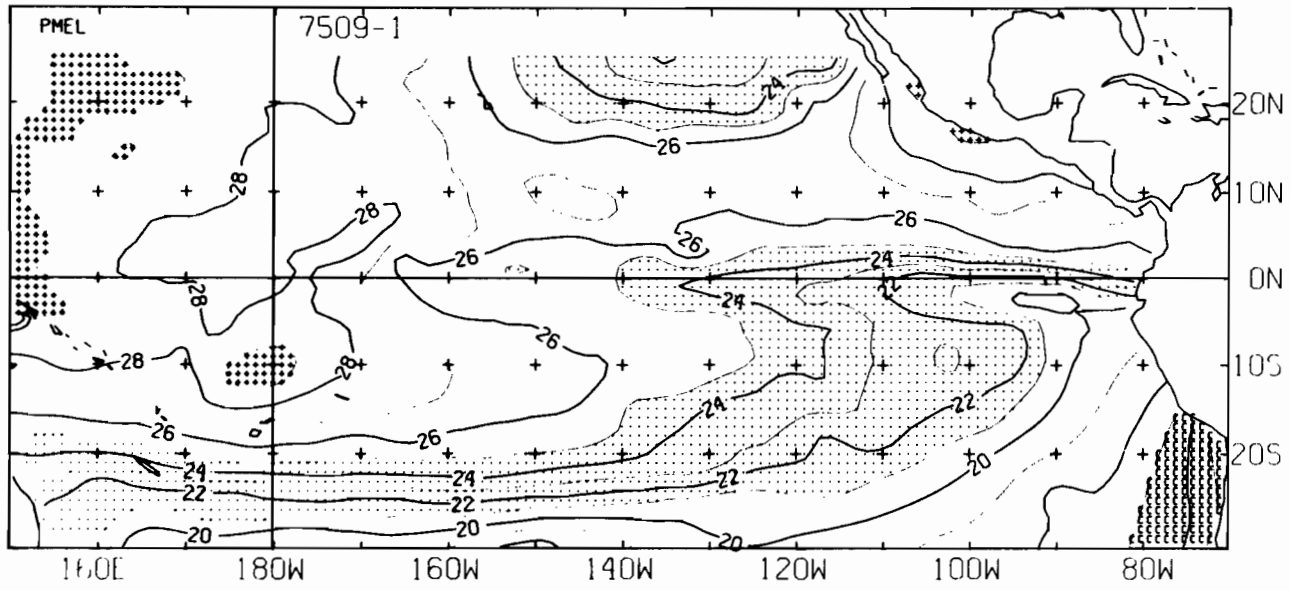

7509-1 SST. 0 E-BUØY. 0 BT. 52 XBT. 1399 SPØT DATA

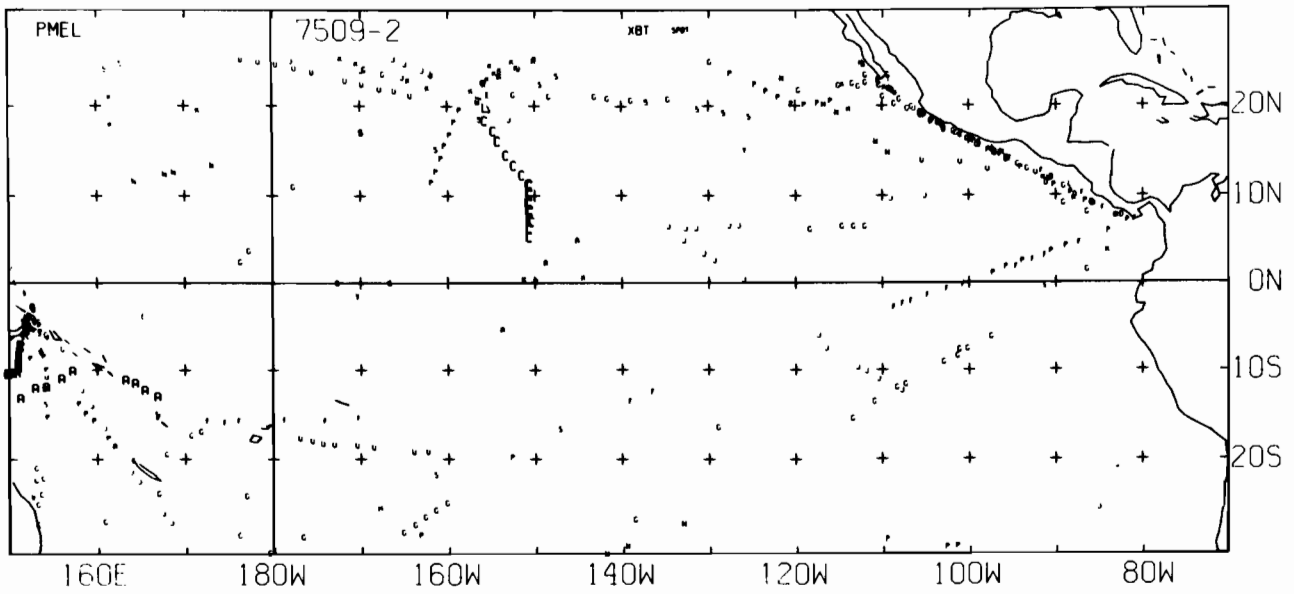

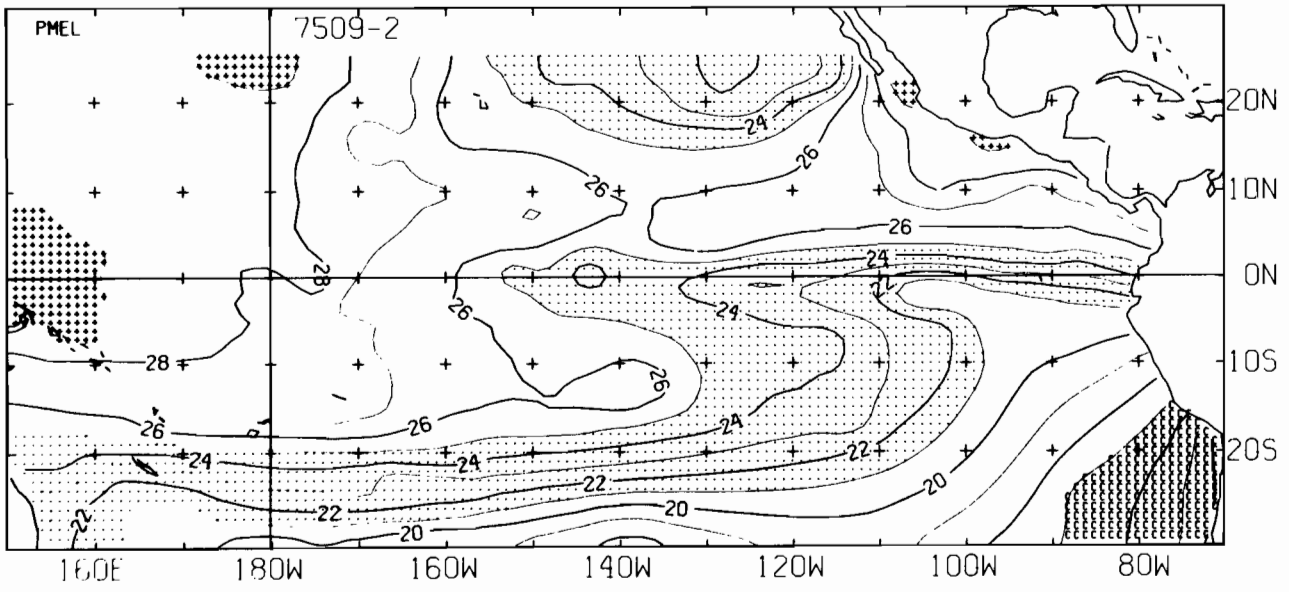

7509-2 SST. 0 E-BUØY. 0 BT. 52 XBT. 349 SPØT DATA

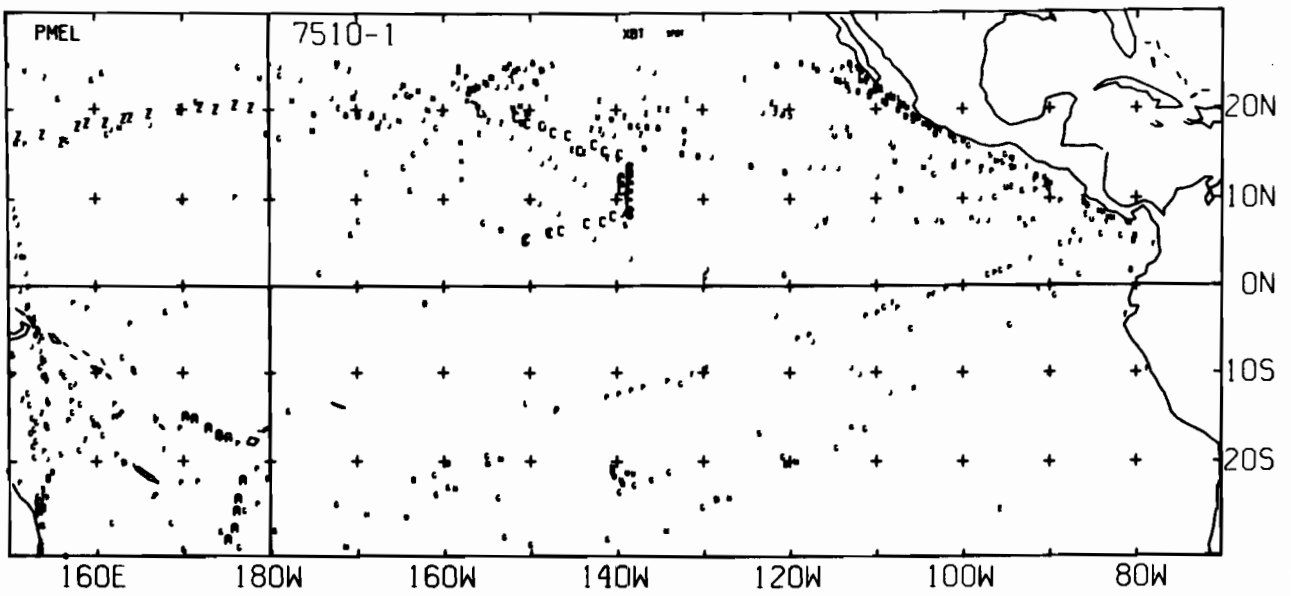

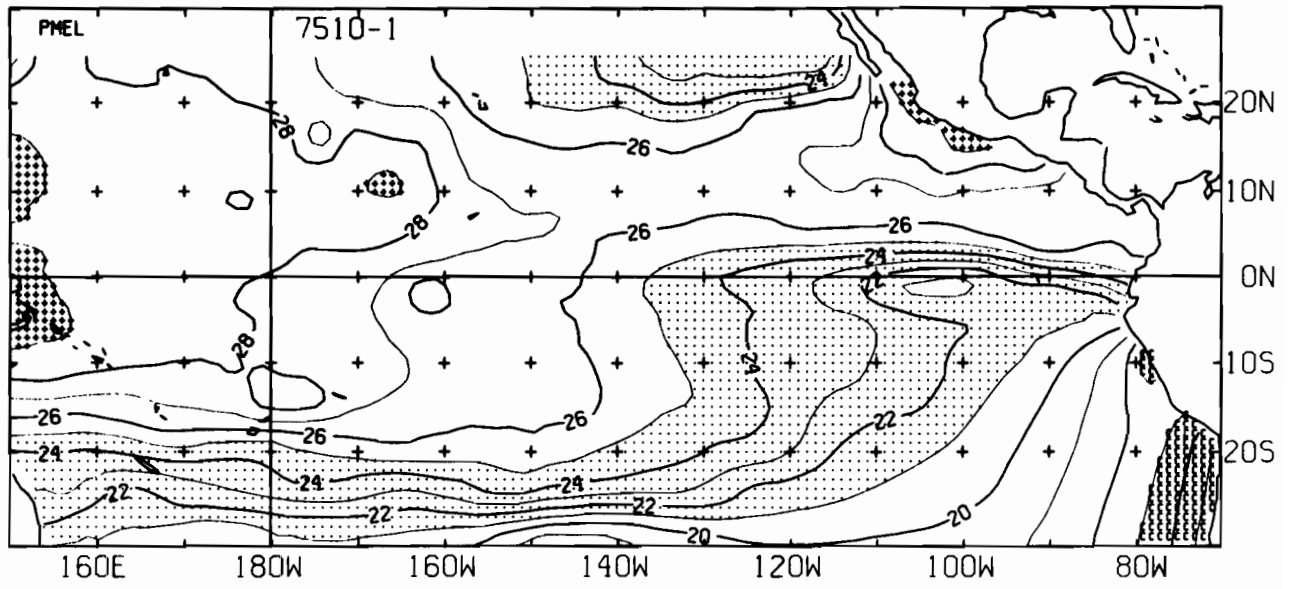

7510-1 SST. 0 E-BUØY. 0 BT. 60 XBT. 529 SPØT DATA

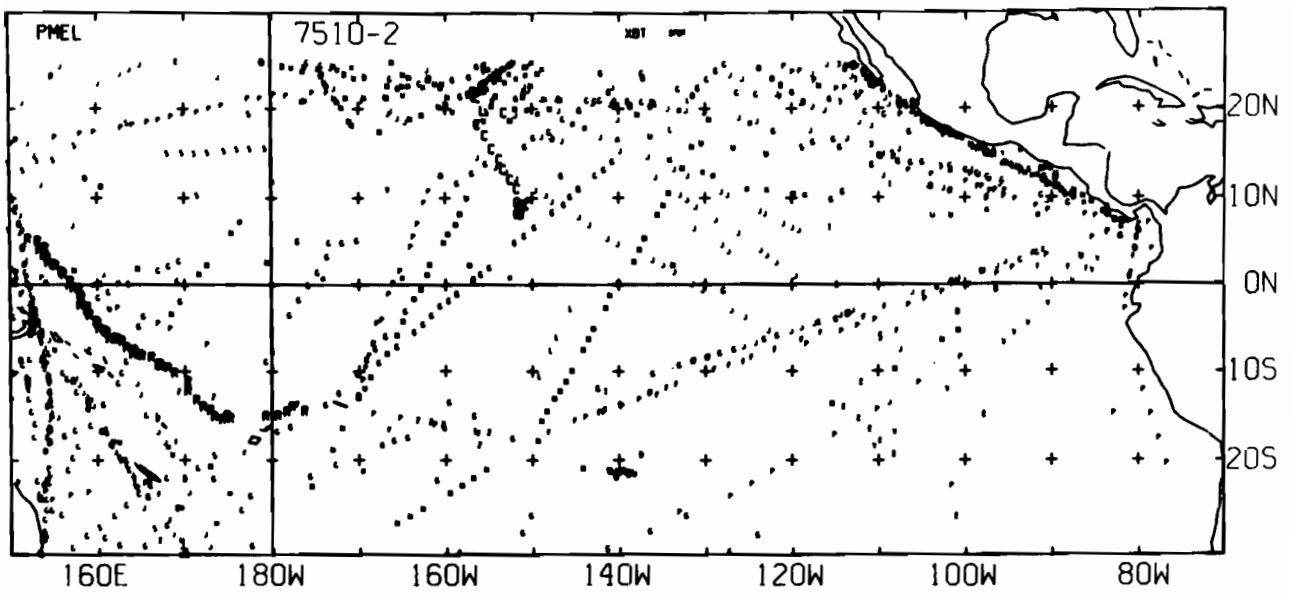

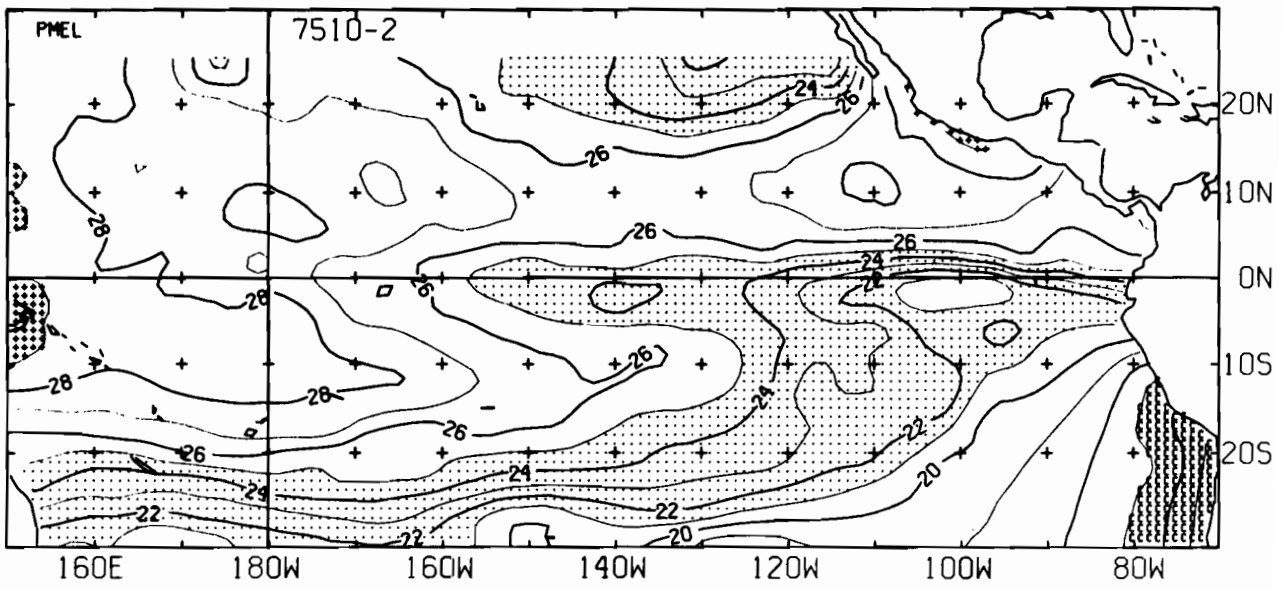

7510-2 SST. 0 E-BUØY. 0 BT. 72 XBT. 1104 SPØT DATA

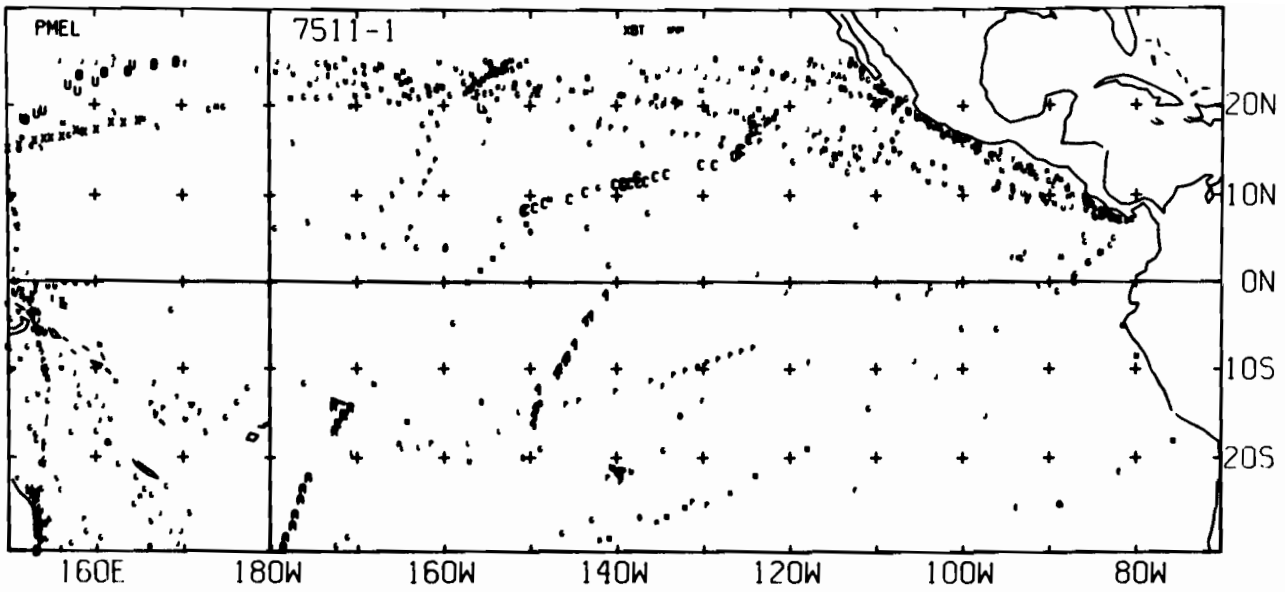

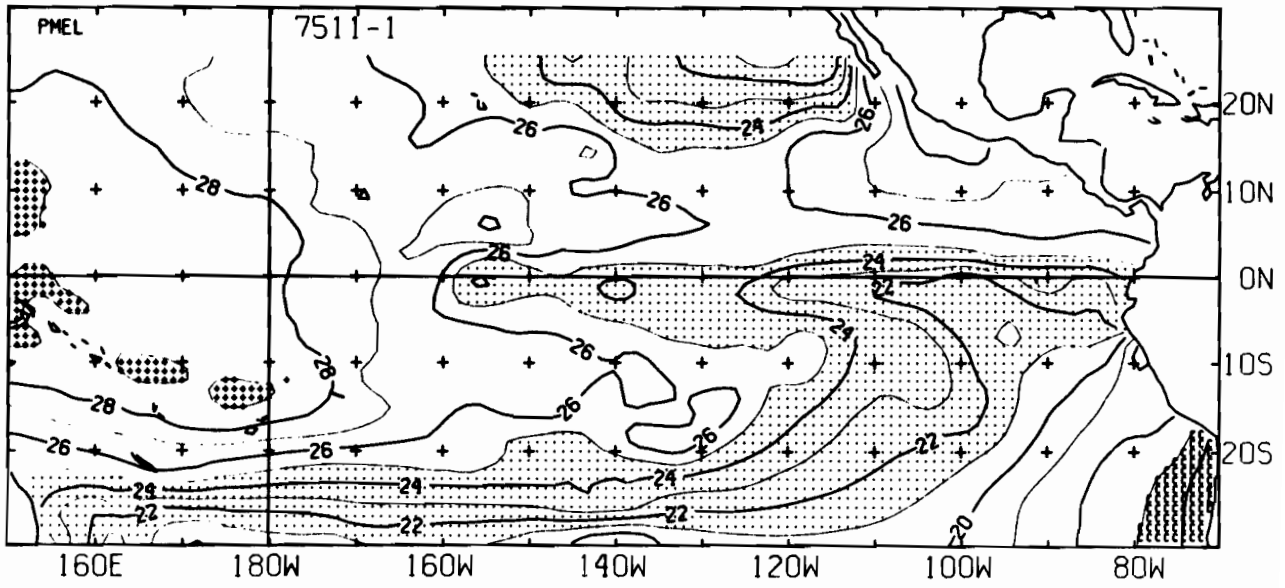

7511-1 SST. 0 E-BUØY. 0 BT. 92 XBT. 684 SPØT DATA

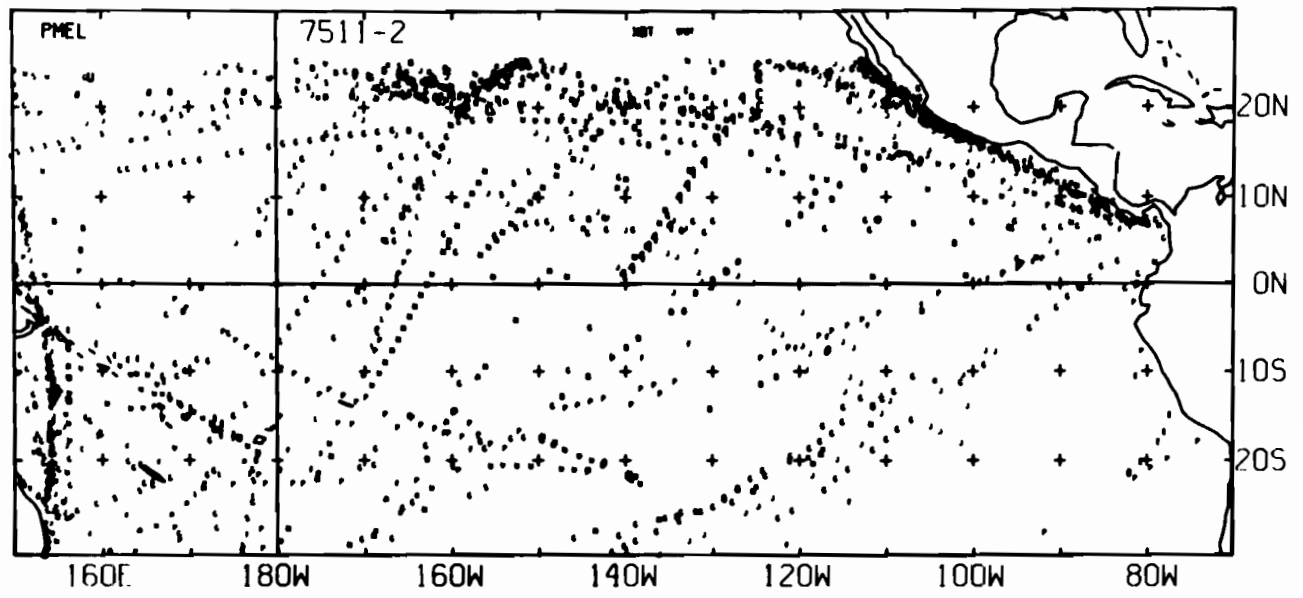

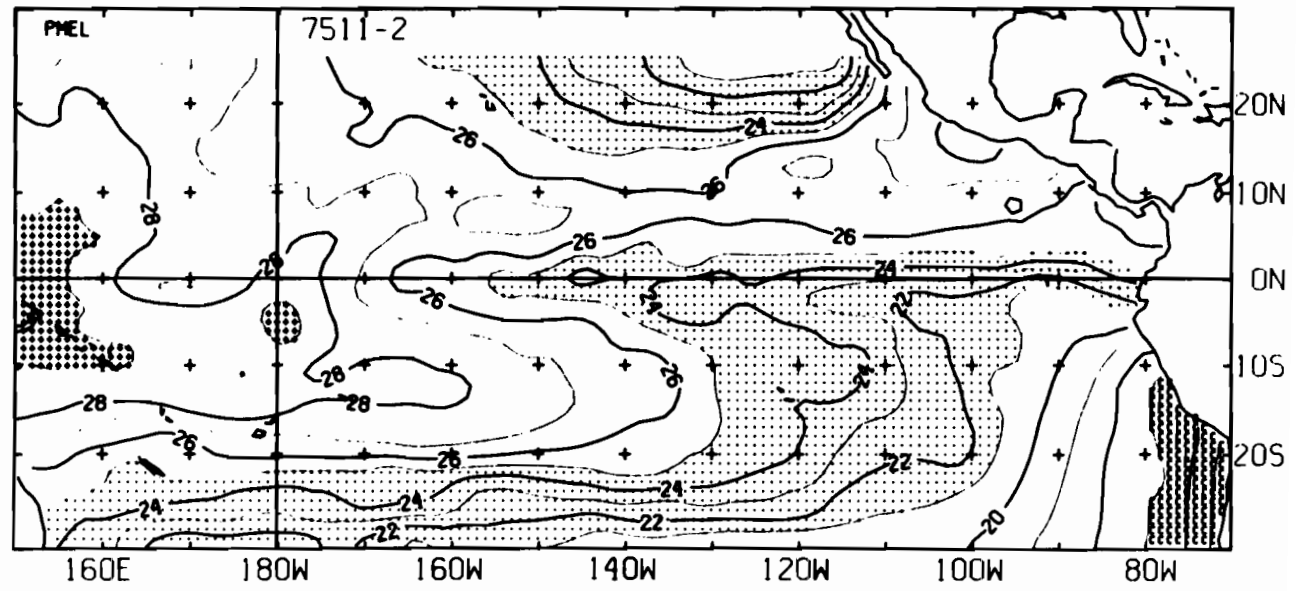

7511-2 SST. 0 E-BUØY. 0 BT. 24 XBT. 1567 SPØT DATA

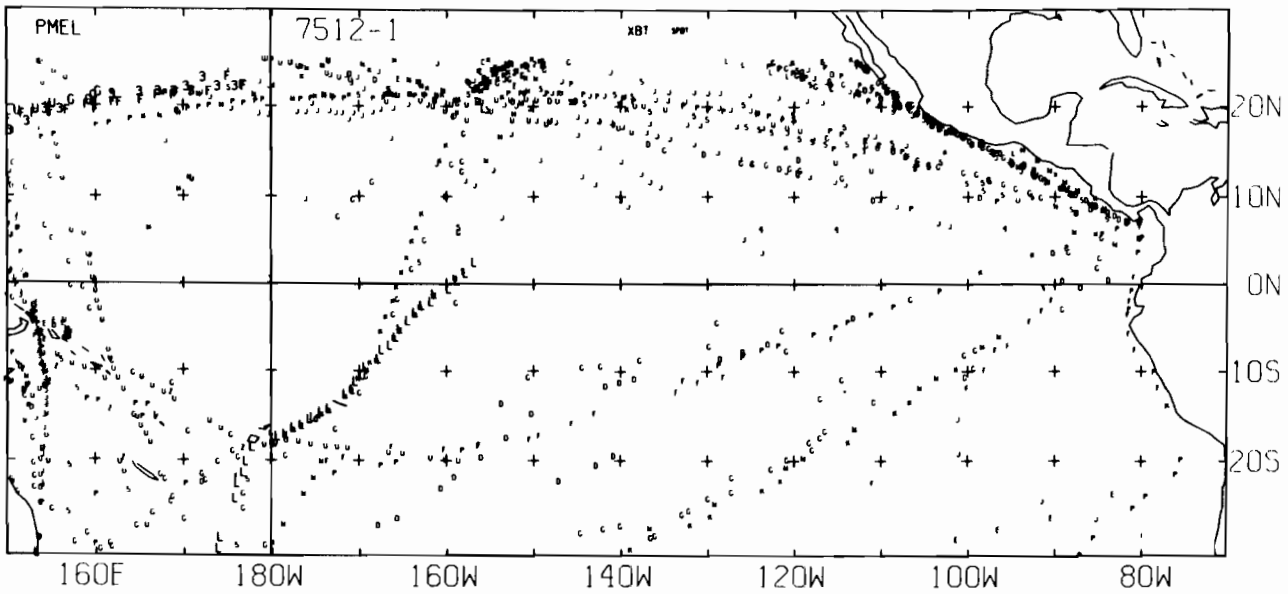

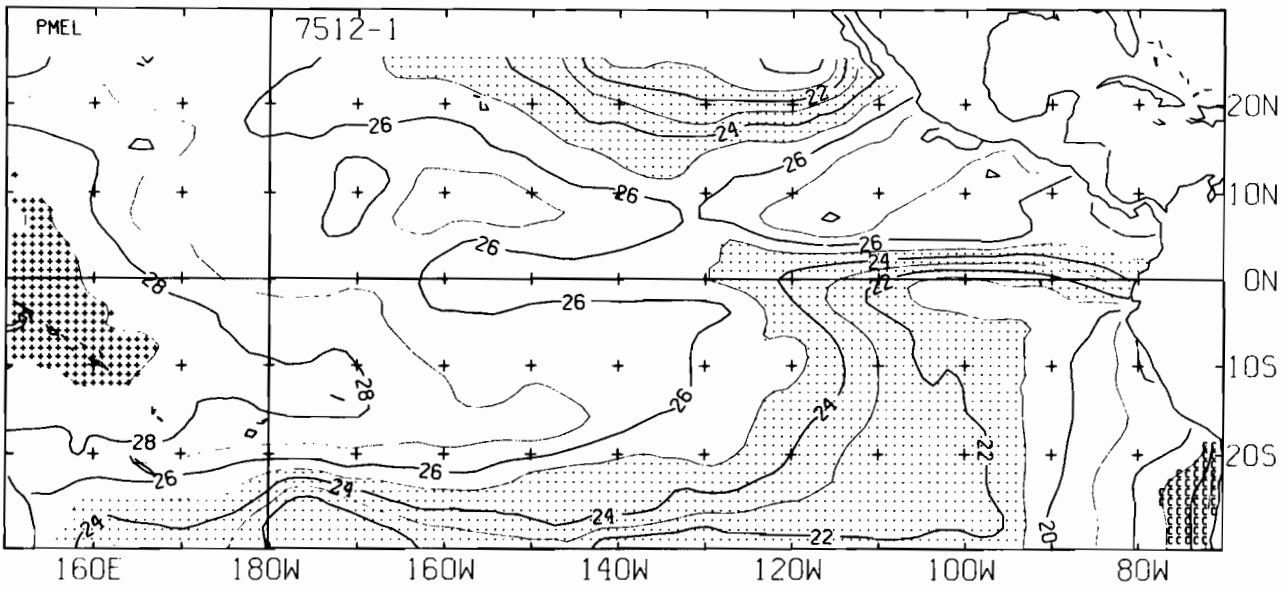

7512-1 SST. 0 E-BUØY. 0 BT. 74 XBT. 1079 SPØT DATA

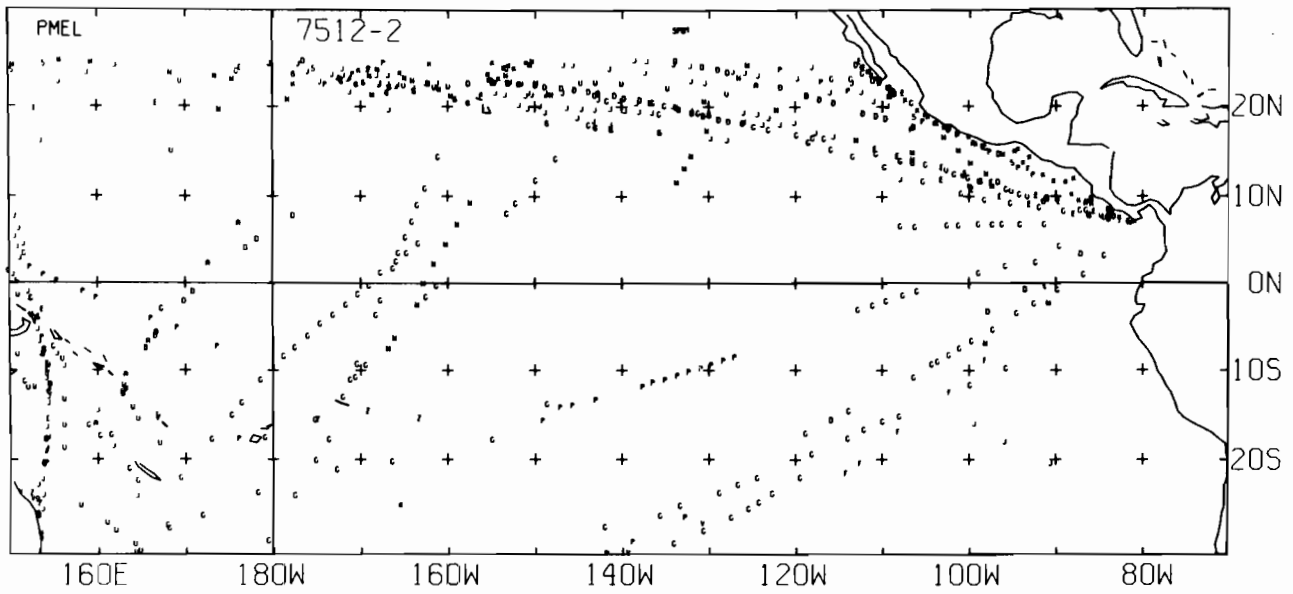

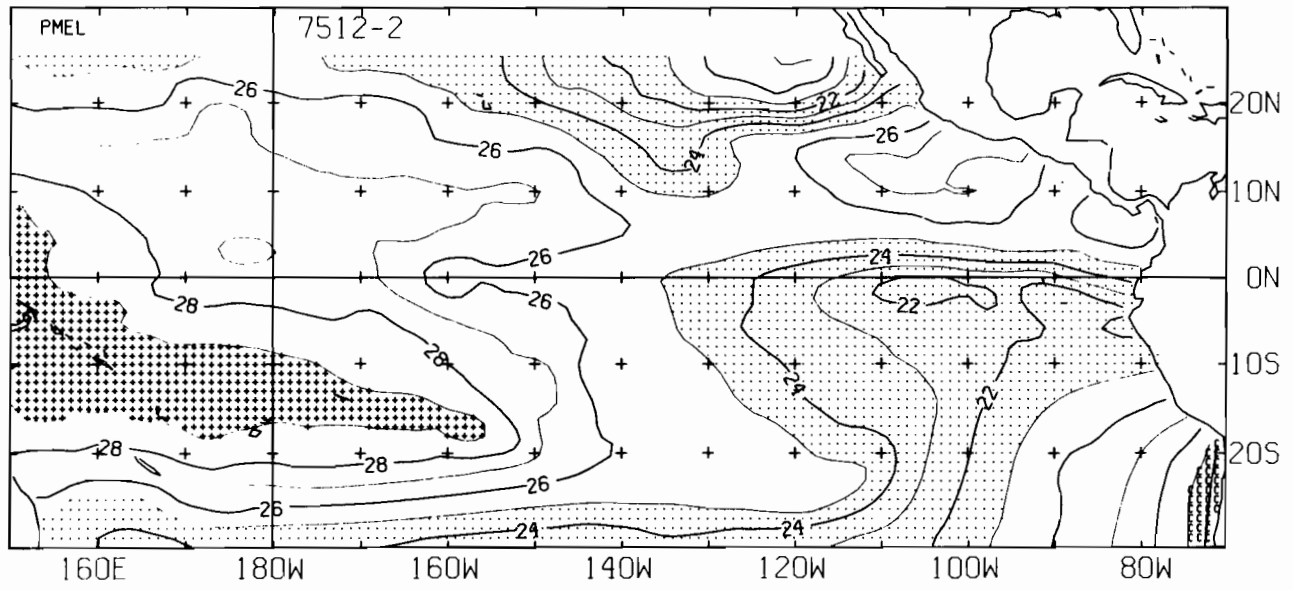

7512-2 SST. 0 E-BUØY. 0 BT. 0 XBT. 623 SPØT DATA

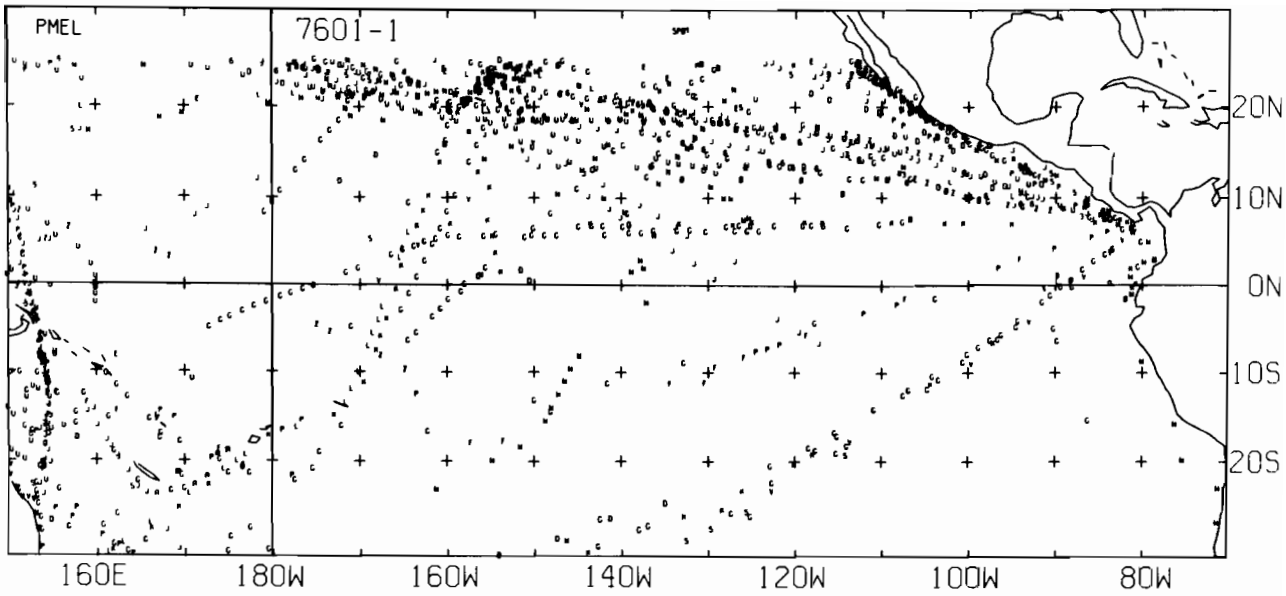

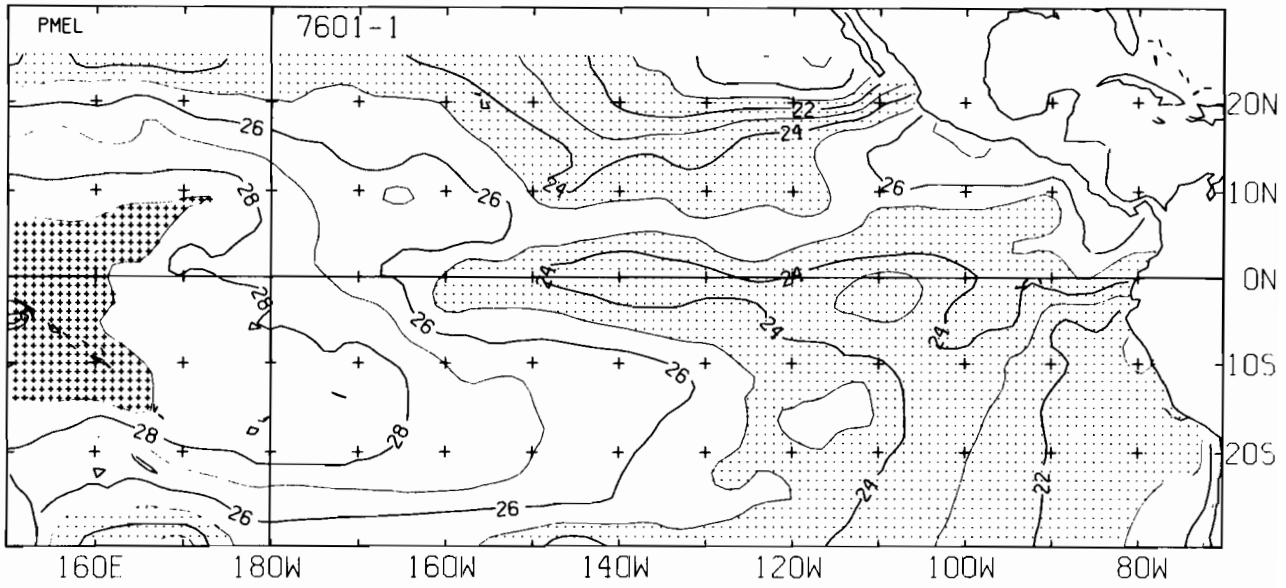

7601-1 SST. 0 E-BUØY. 0 BT. 0 XBT. 1298 SPØT DATA

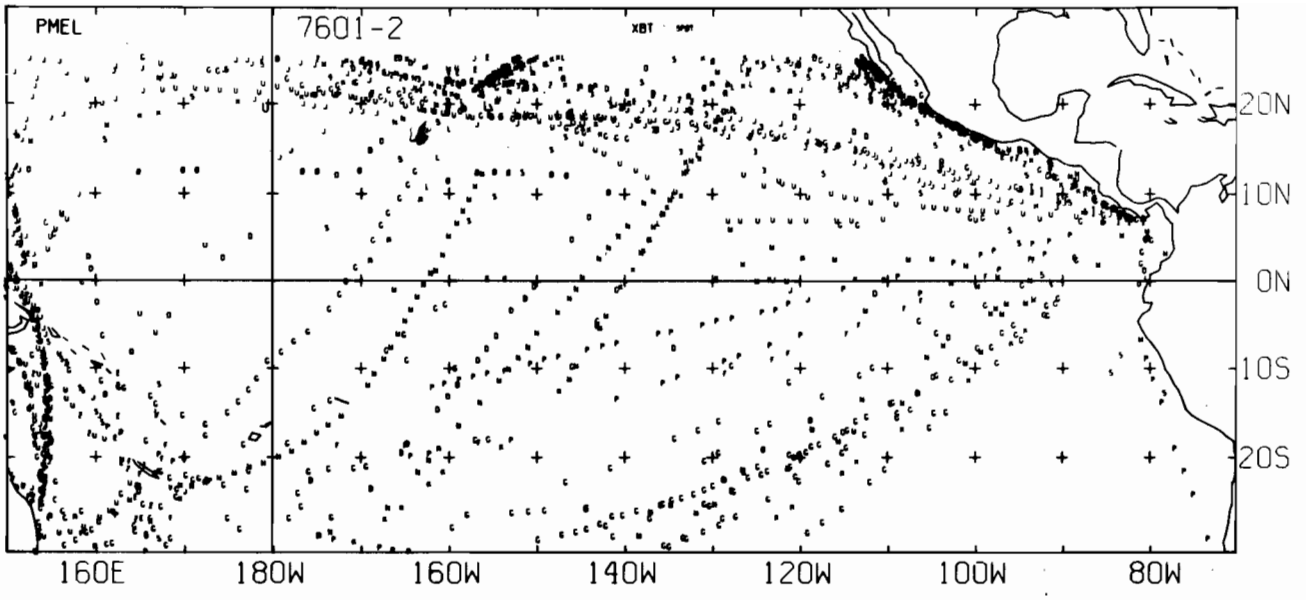

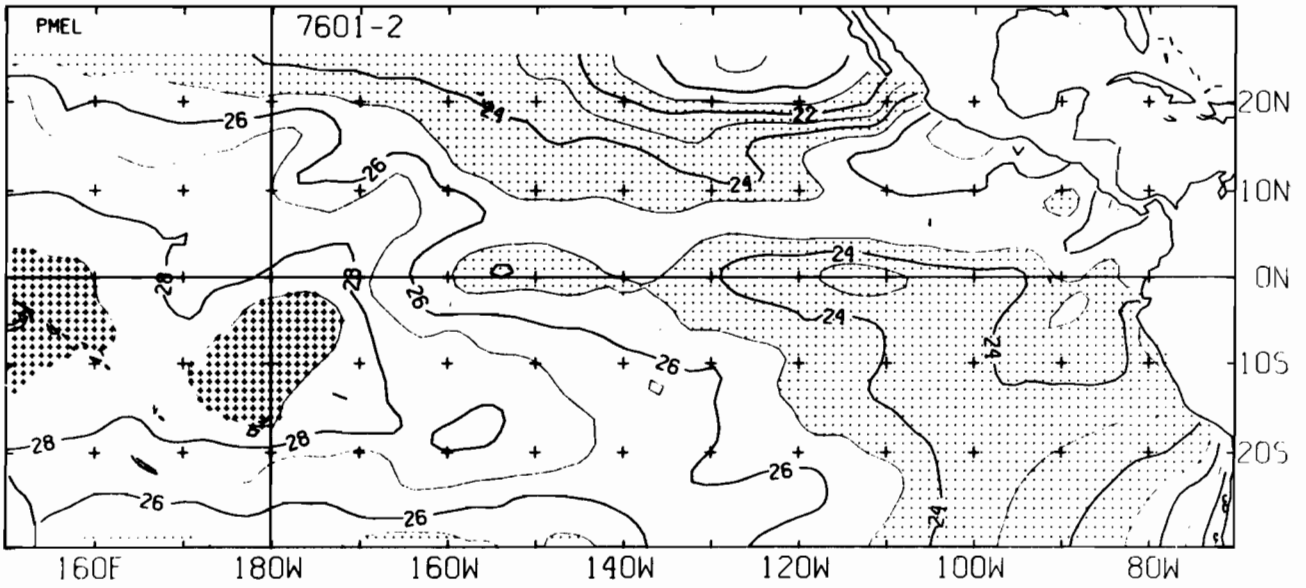

7601-2 SST. 0 E-BUØY. 0 BT. 15 XBT. 1644 SPØT DATA

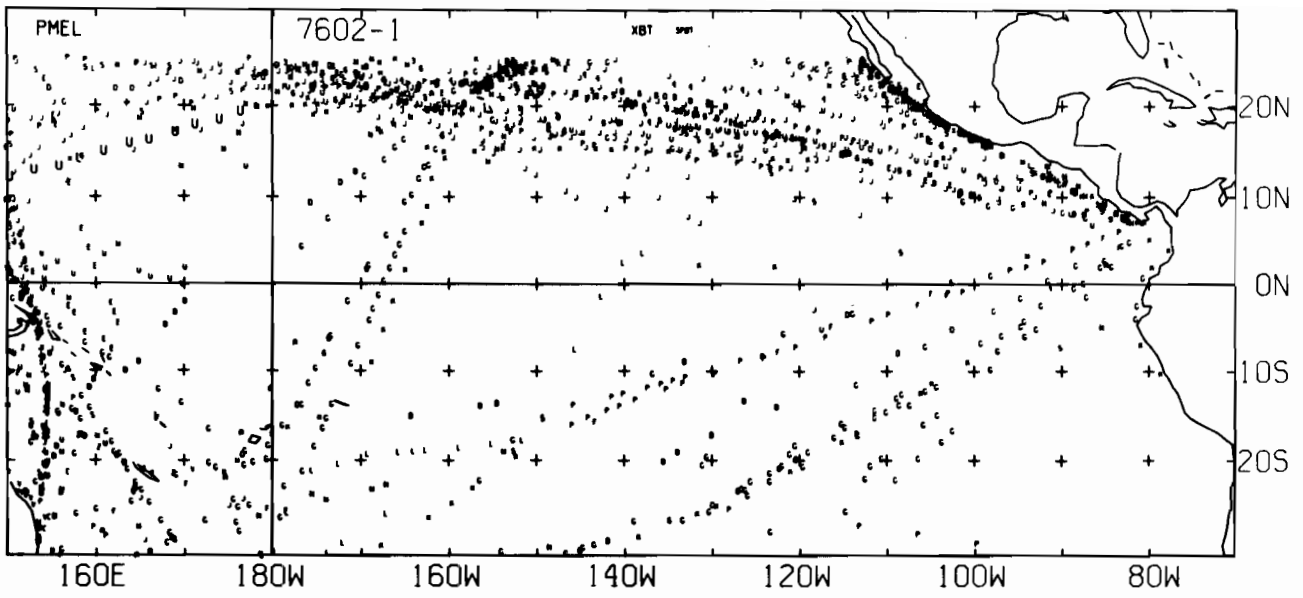

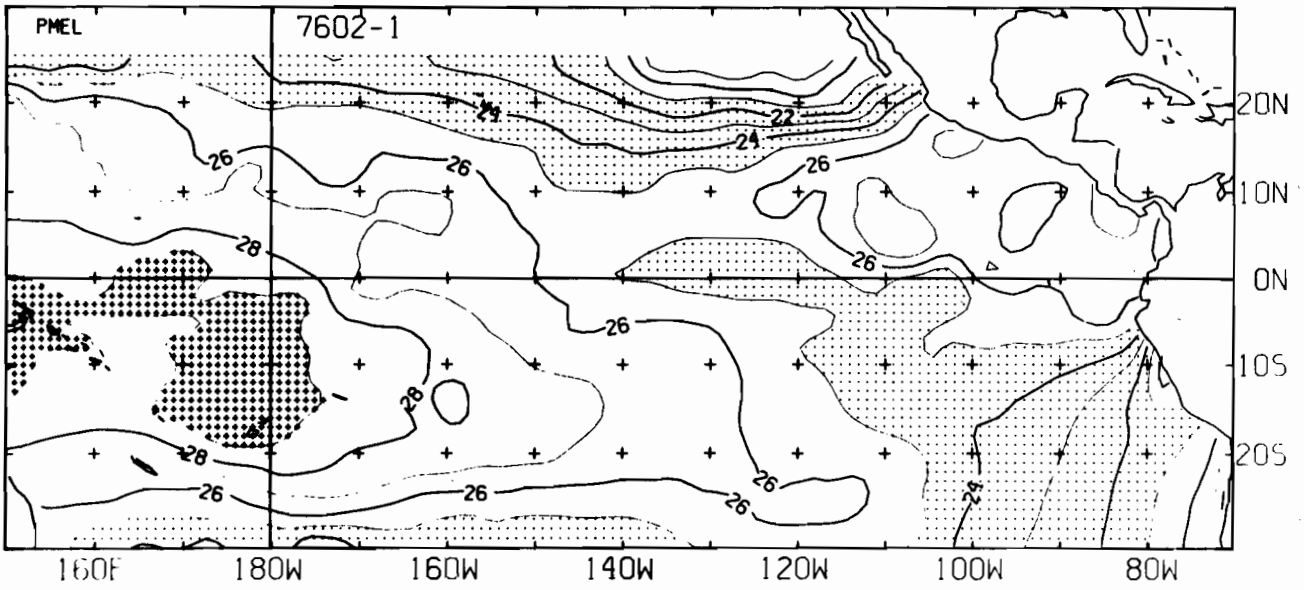

7602-1 SST. 0 E-BUØY. 0 BT. 11 XBT. 1516 SPØT DATA

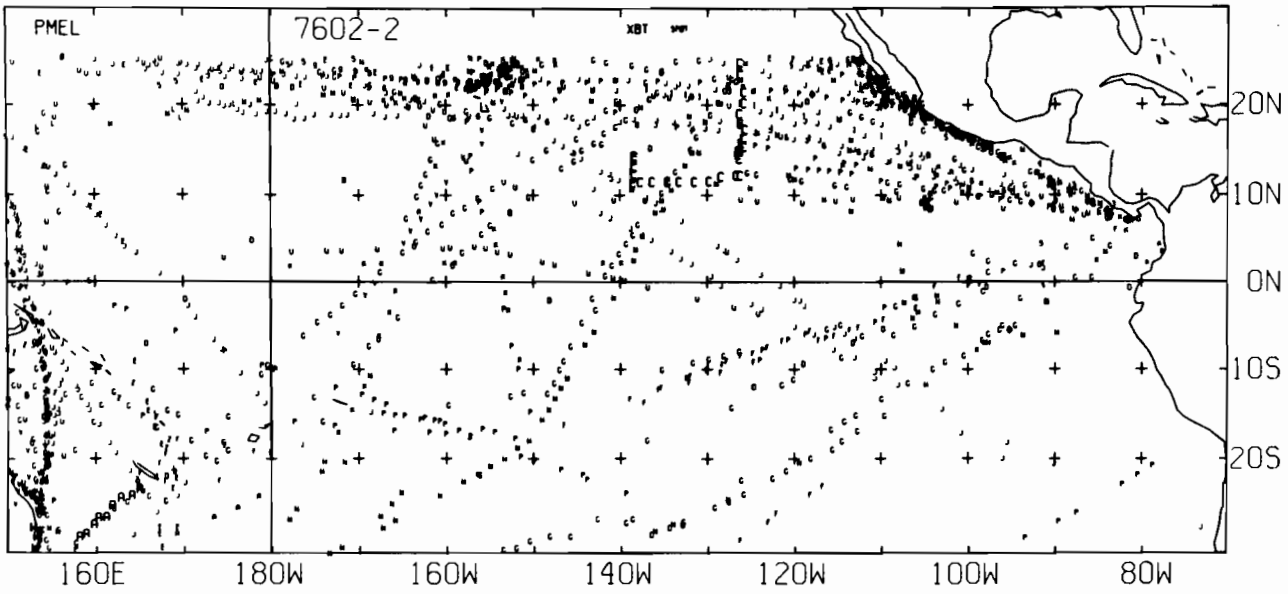

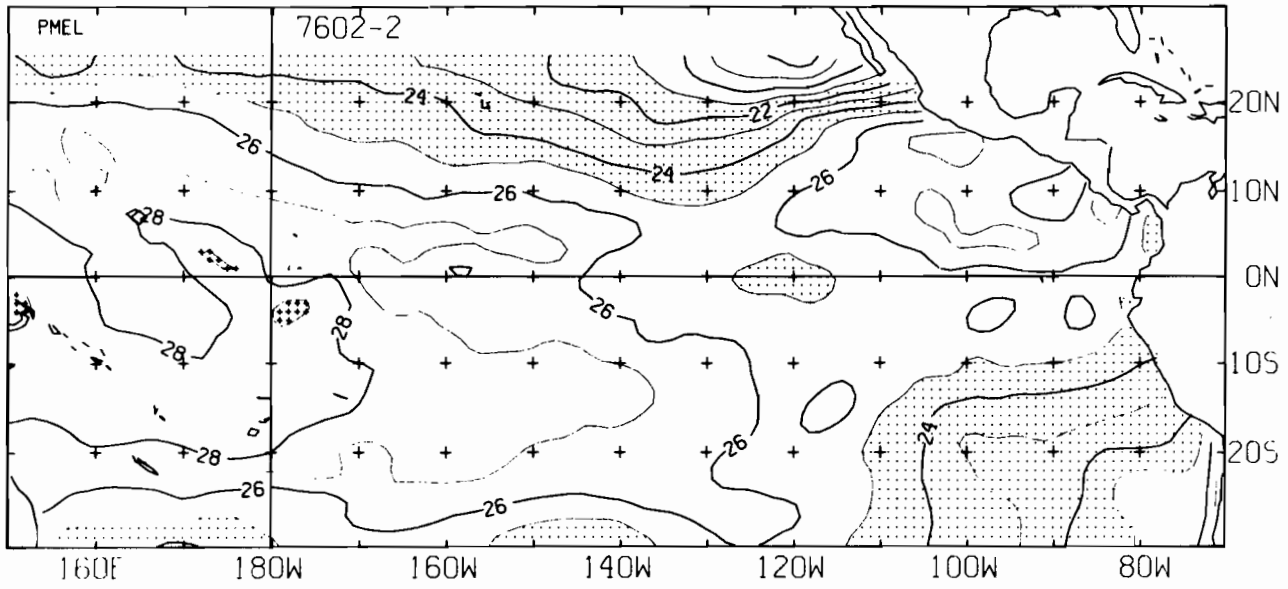

7602-2 SST. 0 E-BUØY. 0 BT. 41 XBT. 1589 SPØT DATA

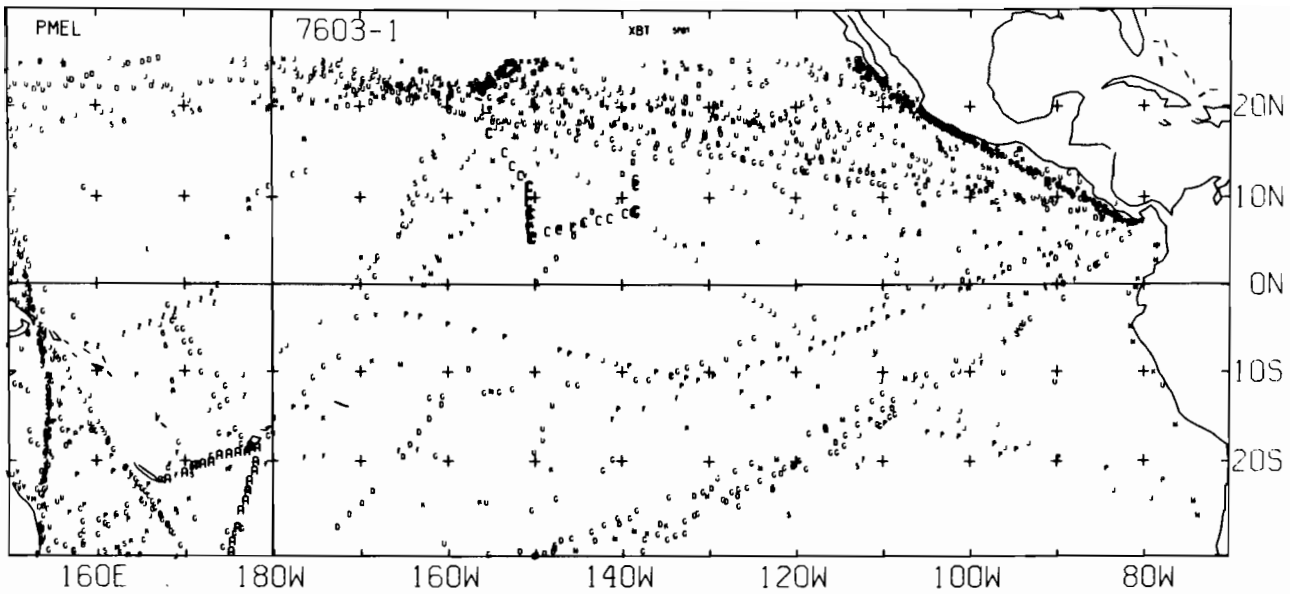

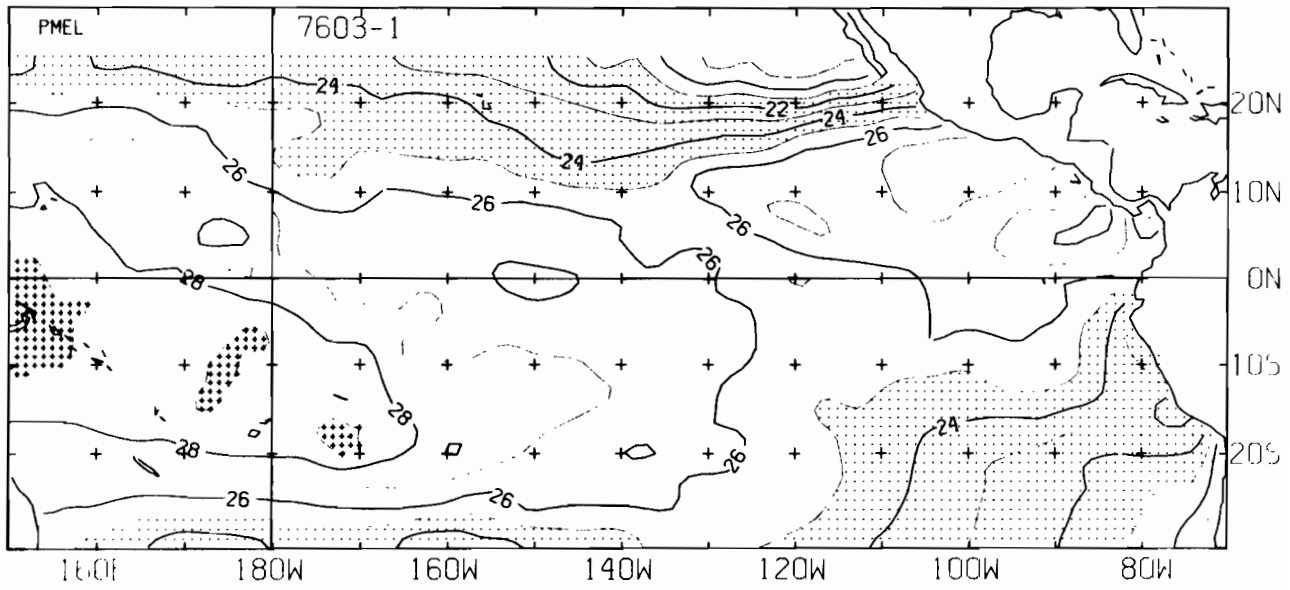

7603-1 SST. 0 E-BUØY. 0 BT. 64 XBT. 1659 SPØT DATA

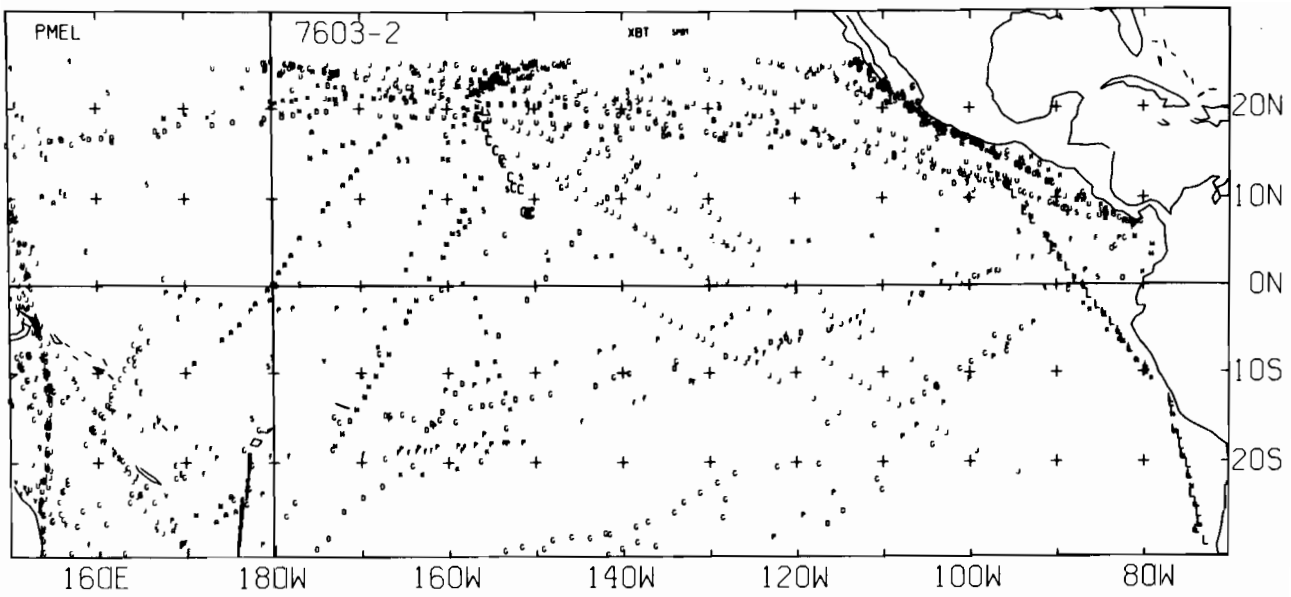

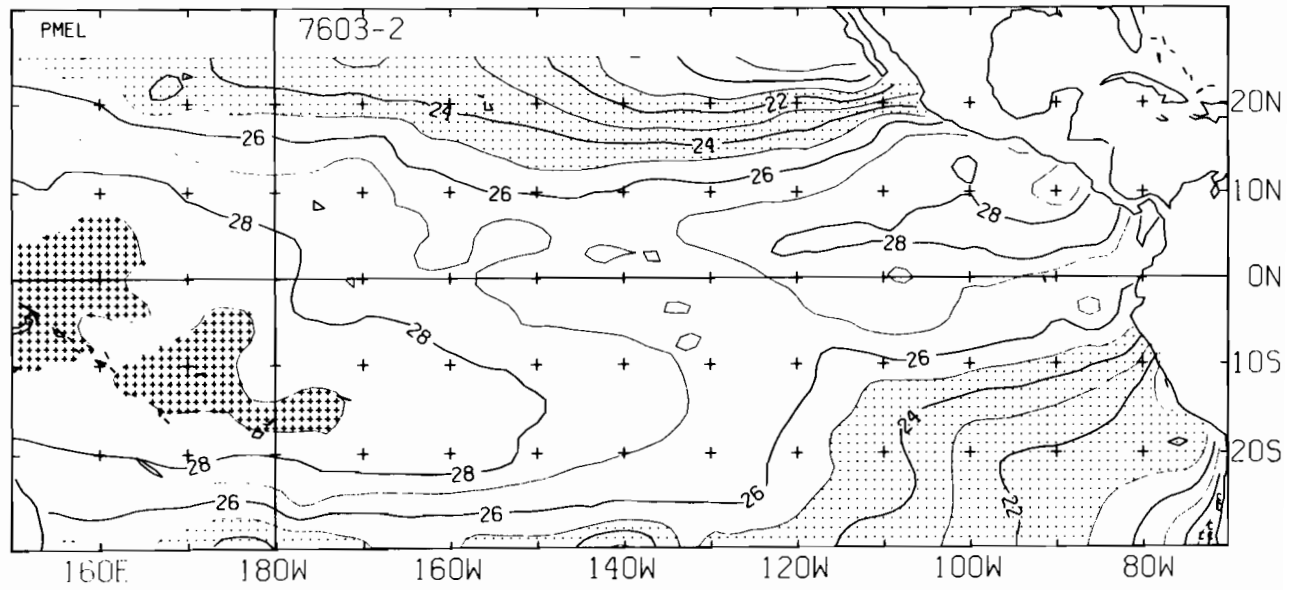

7603-2 SST. 0 E-BUØY. 0 BT. 118 XBT. 1361 SPØT DATA

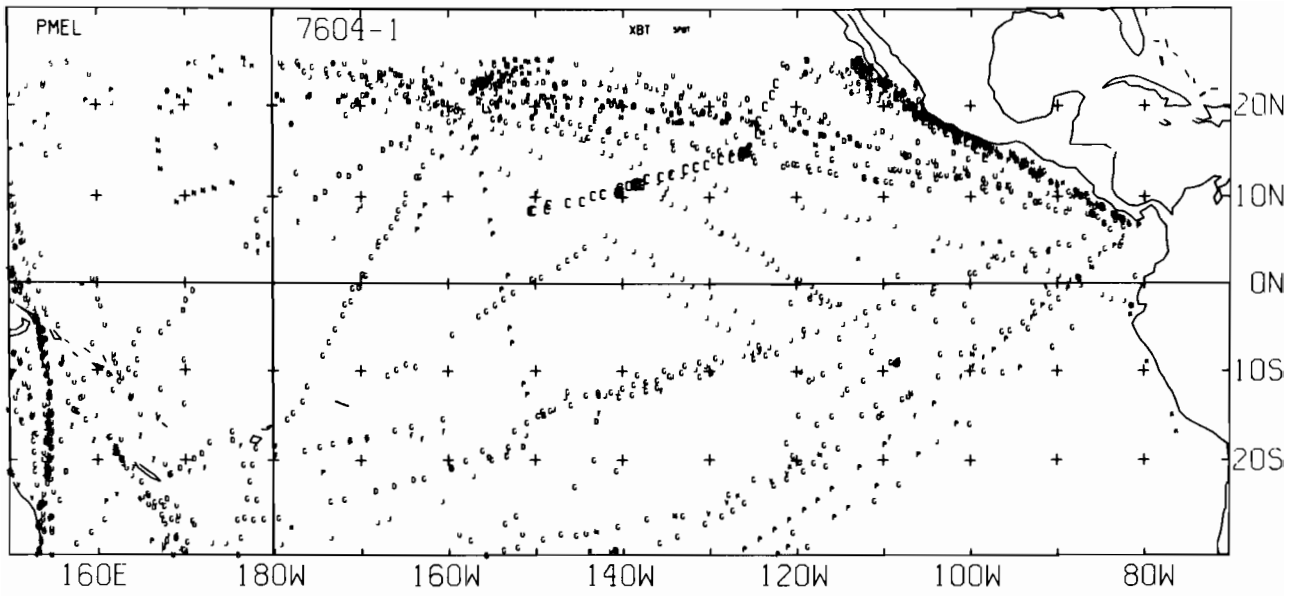

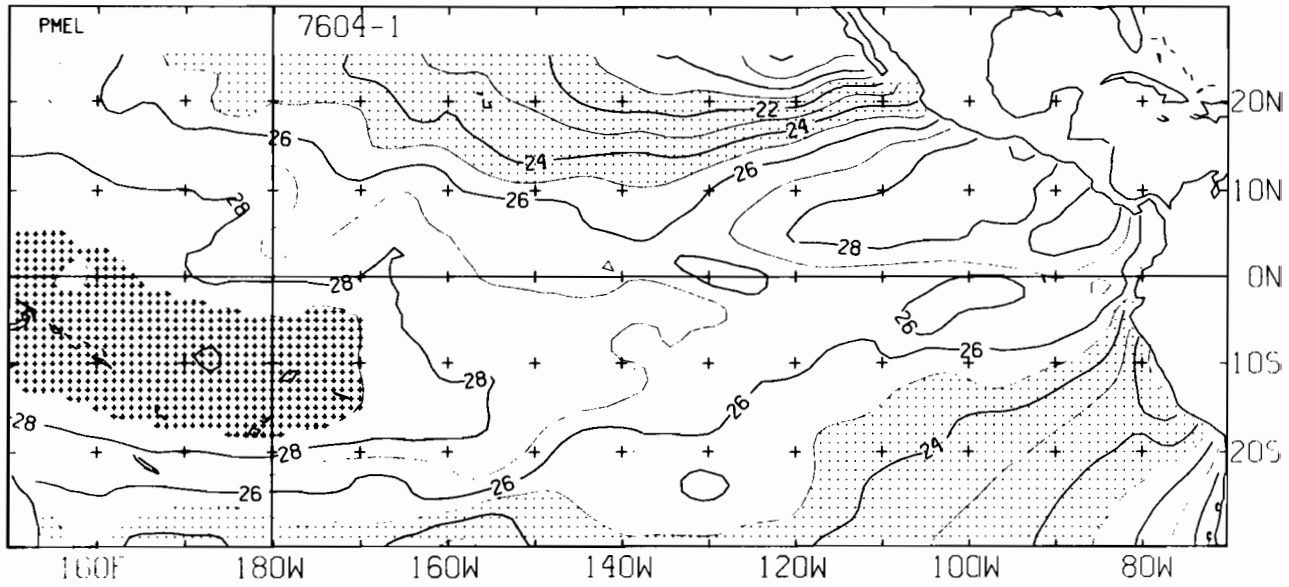

7604-1 SST. 0 E-BUØY. 0 BT. 60 XBT. 1491 SPØT DATA

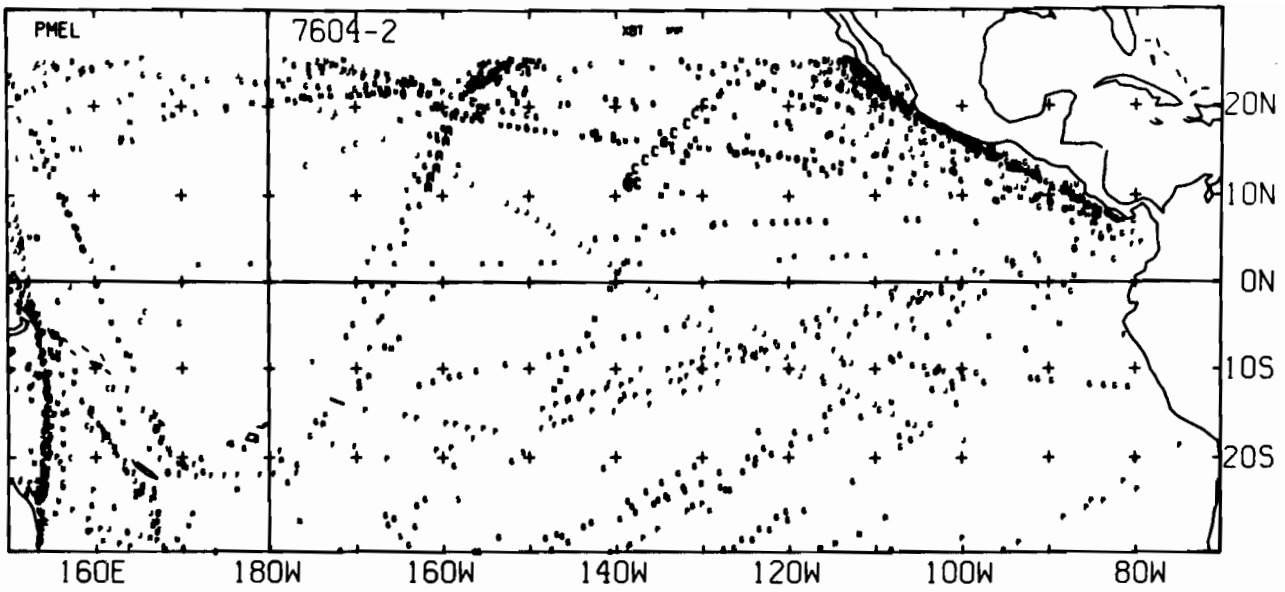

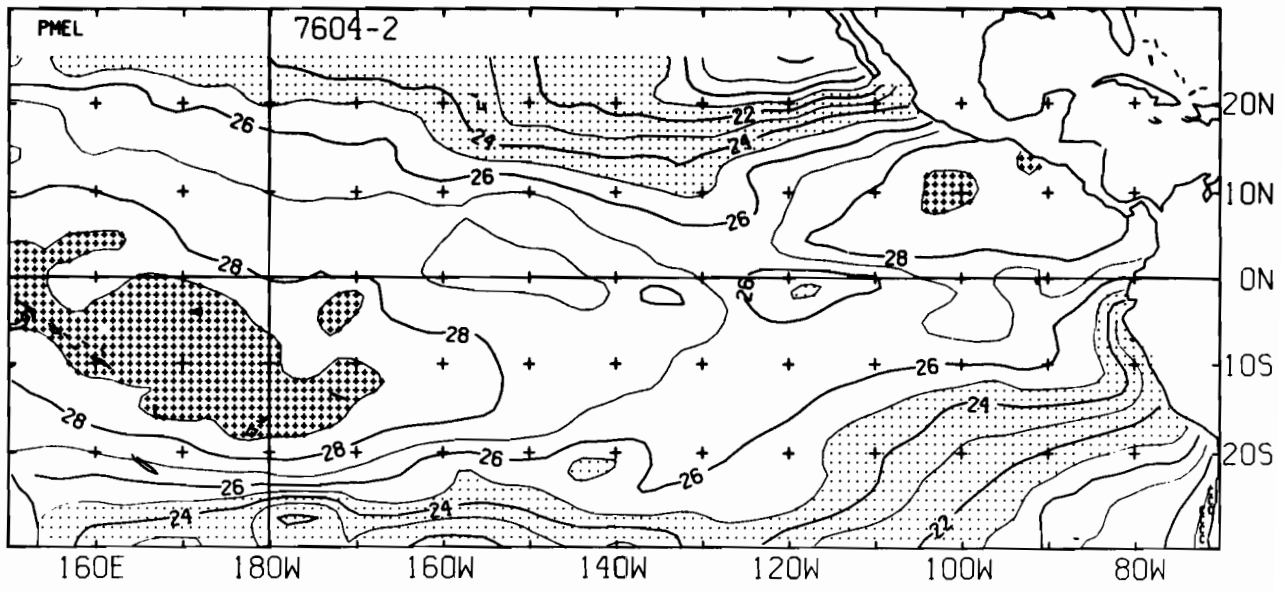

7604-2 SST. 0 E-BUØY. 0 BT. 23 XBT. 1484 SPØT DATA

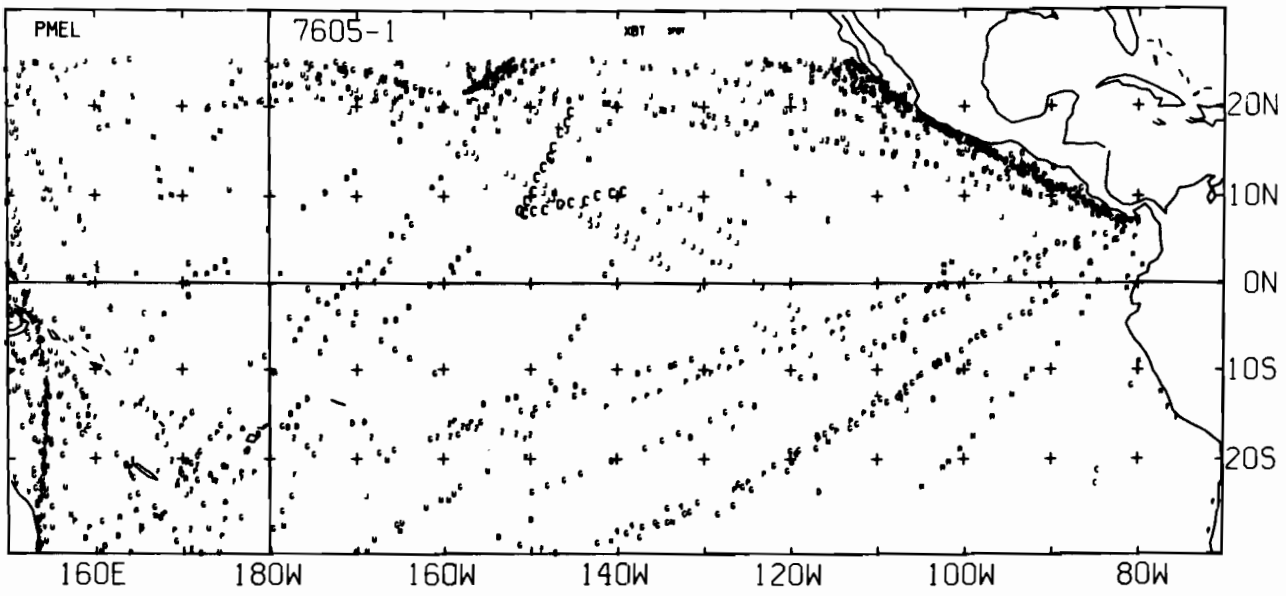

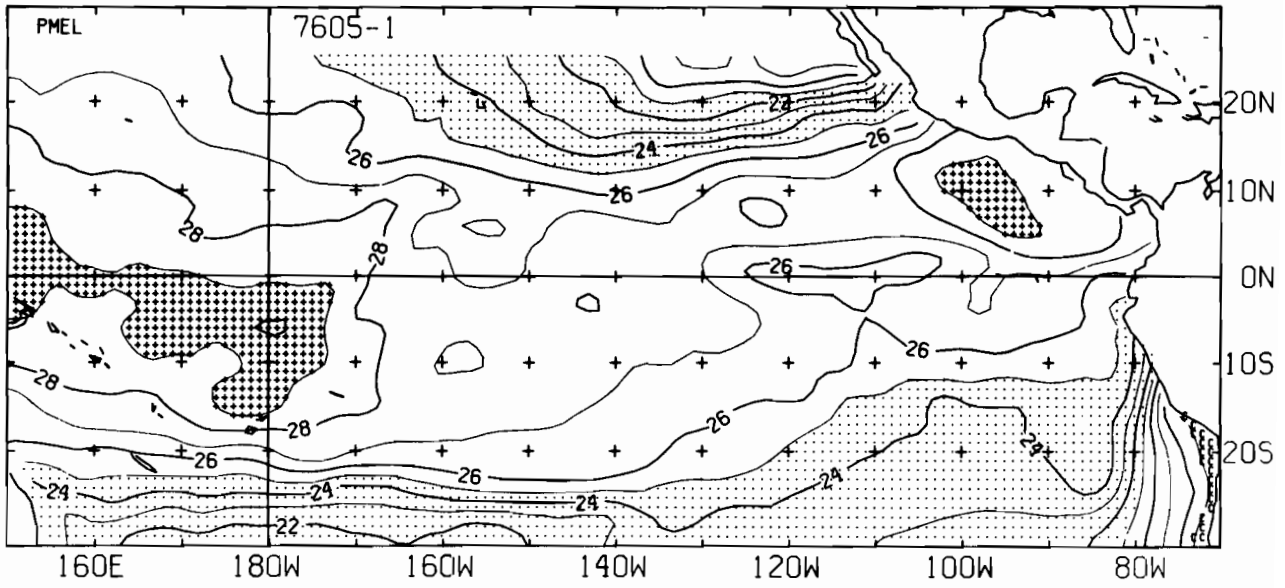

7605-1 SST. 0 E-BUØY. 0 BT. 23 XBT. 1352 SPØT DATA

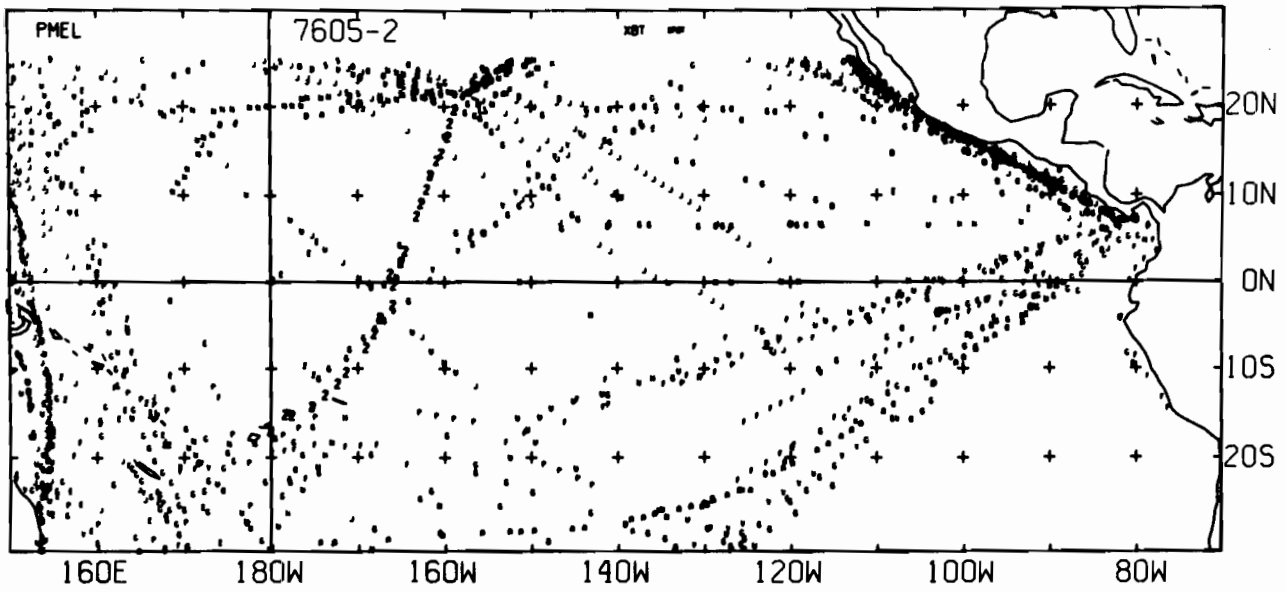

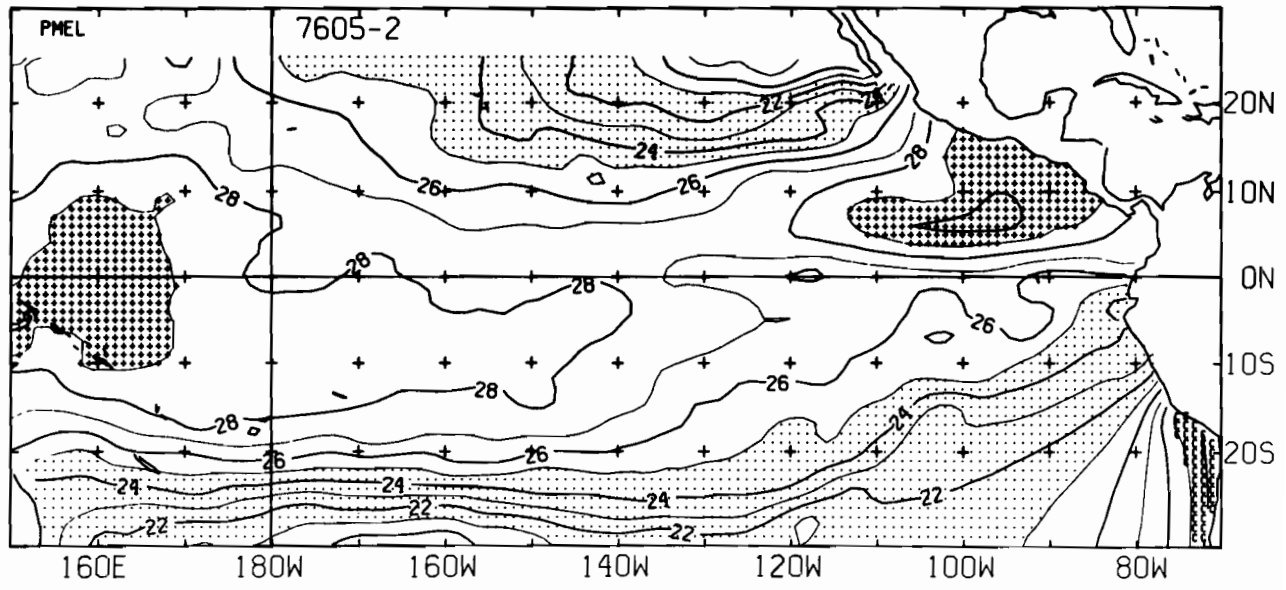

7605-2 SST. 0 E-BUØY. 0 BT. 28 XBT. 1541 SPØT DATA

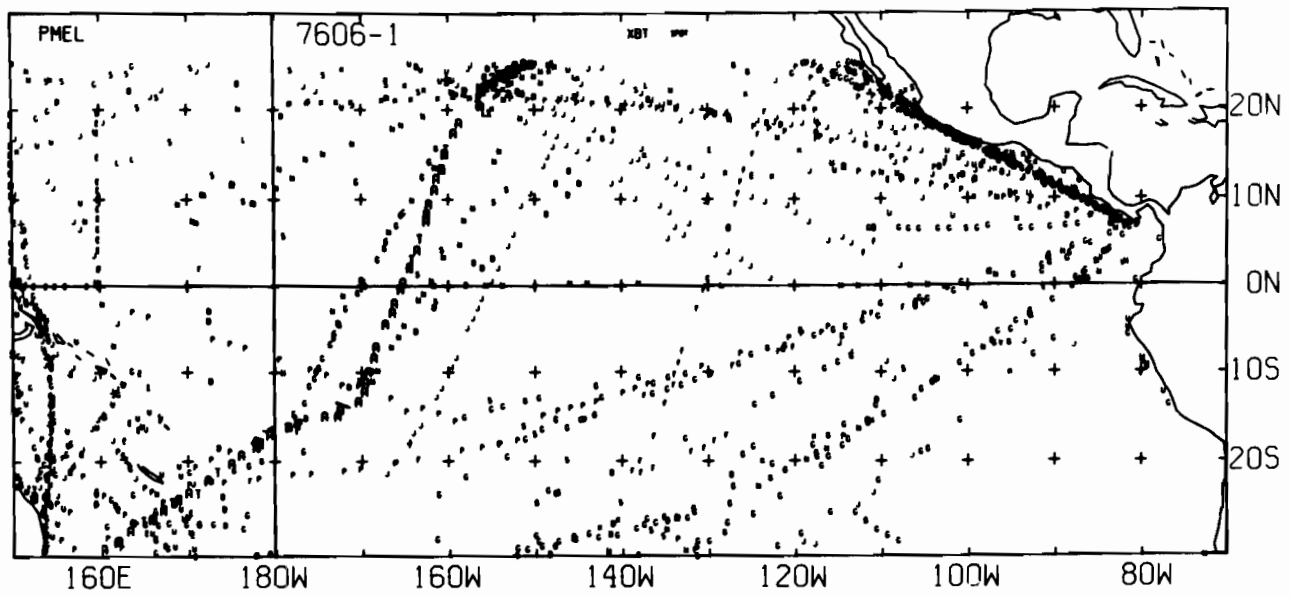

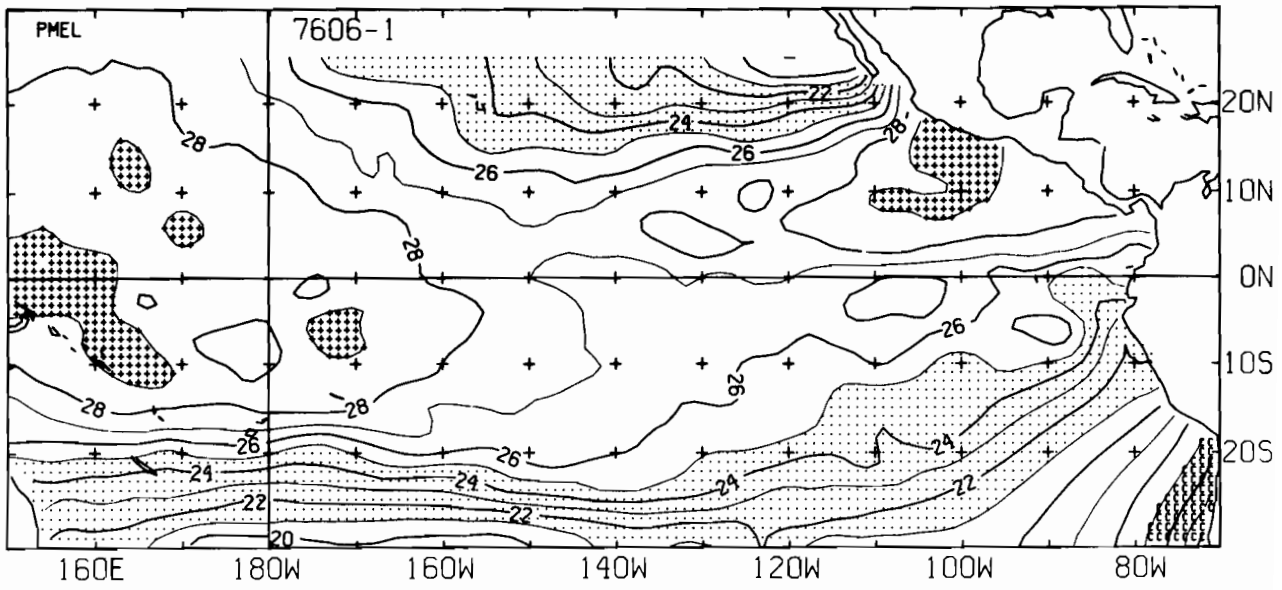

7606-1 SST. 0 E-BUØY. 0 BT. 63 XBT. 1511 SPØT DATA

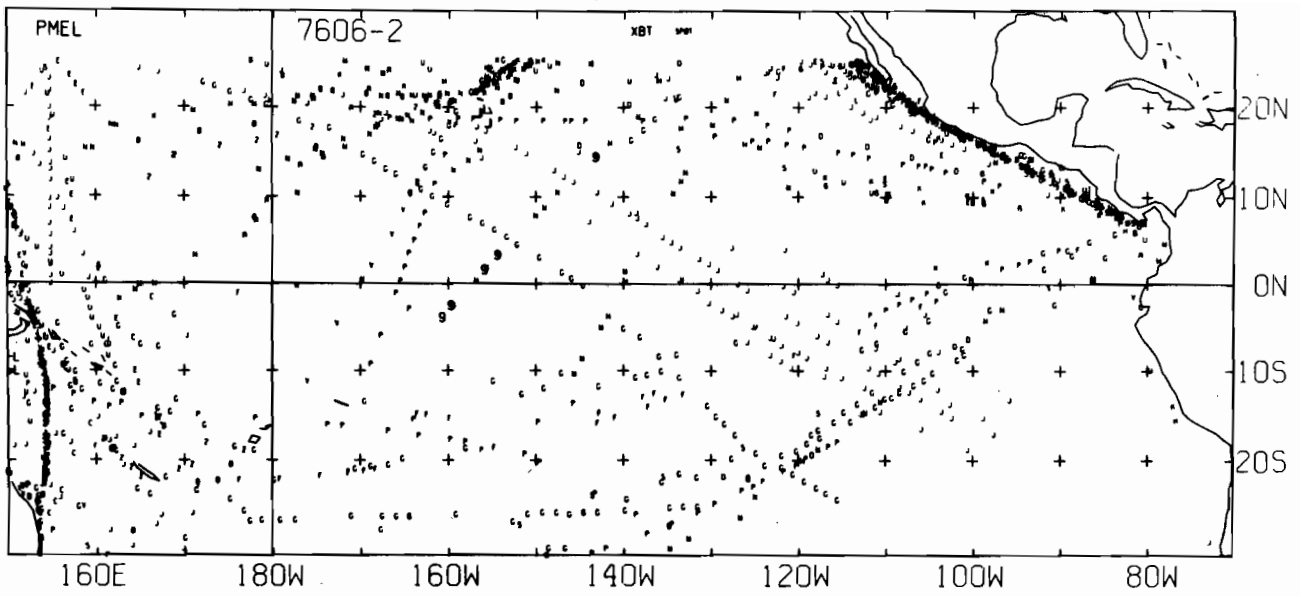

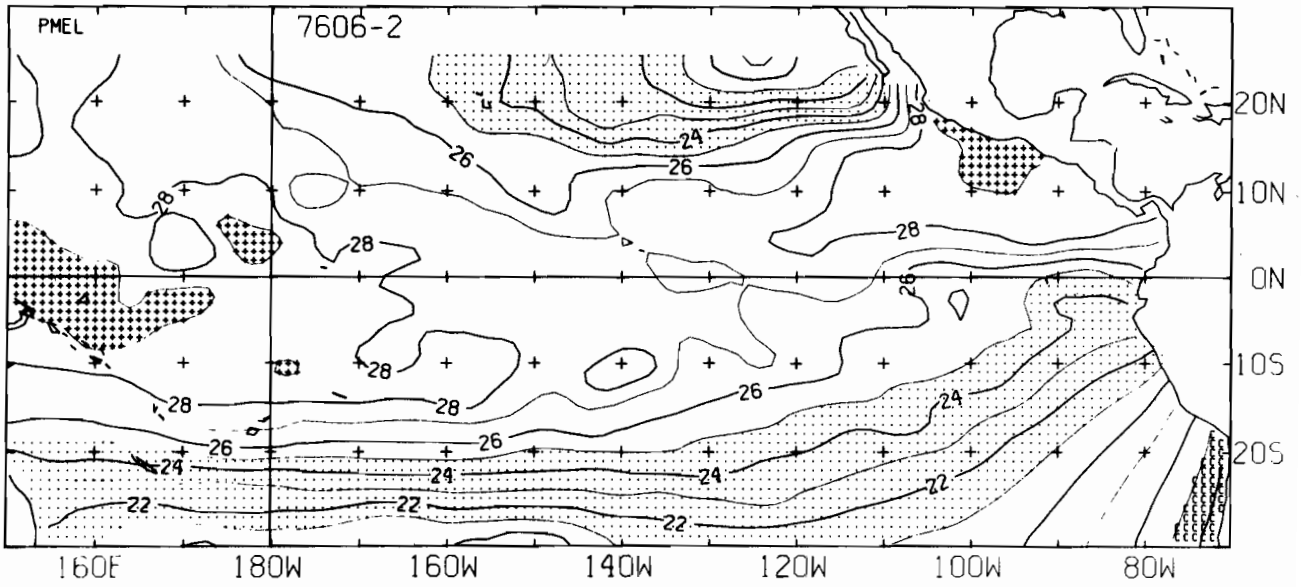

7606-2 SST. 0 E-BUØY. 0 BT. 12 XBT. 1261 SPØT DATA

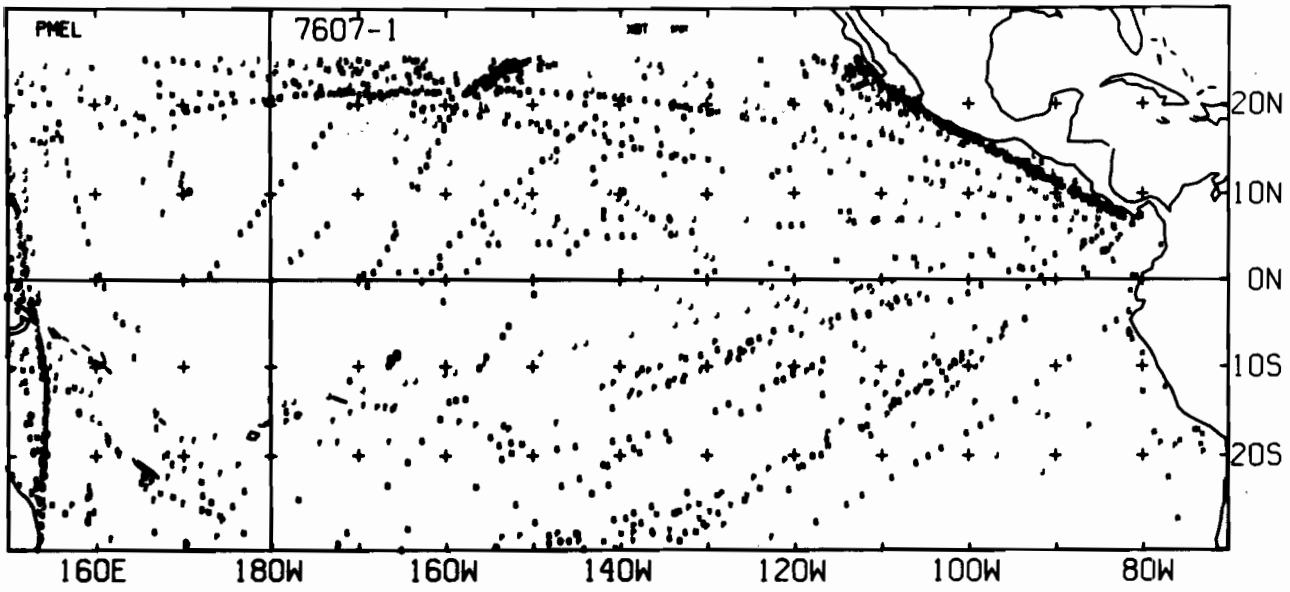

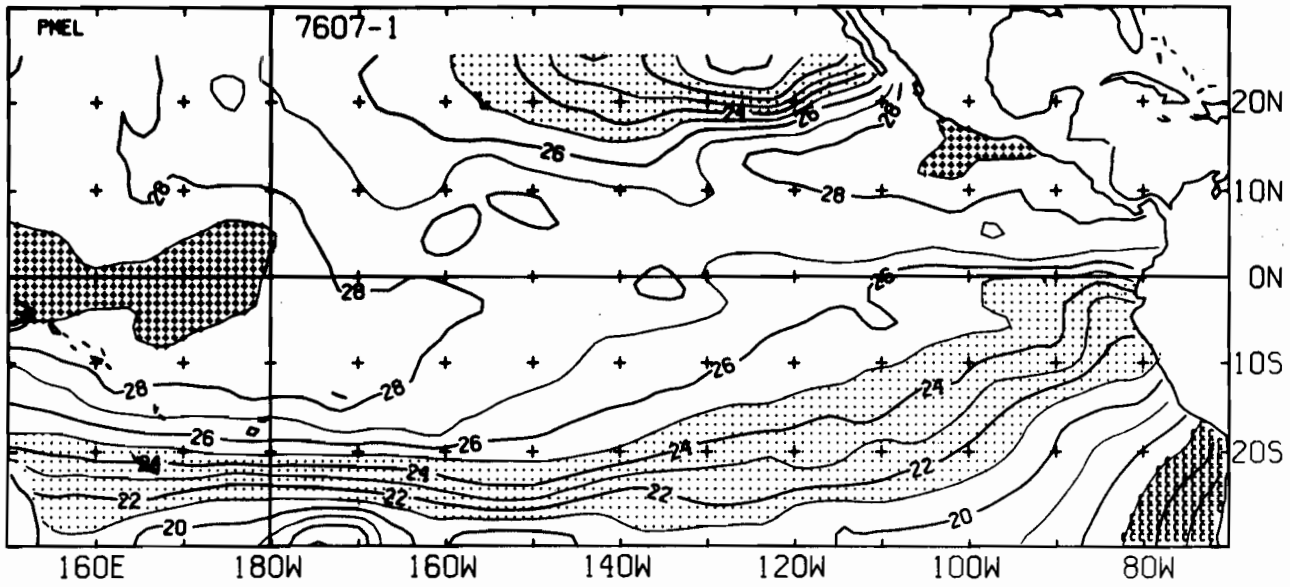

7607-1 SST. 0 E-BUØY. 0 BT. 2 XBT. 1477 SPØT DATA

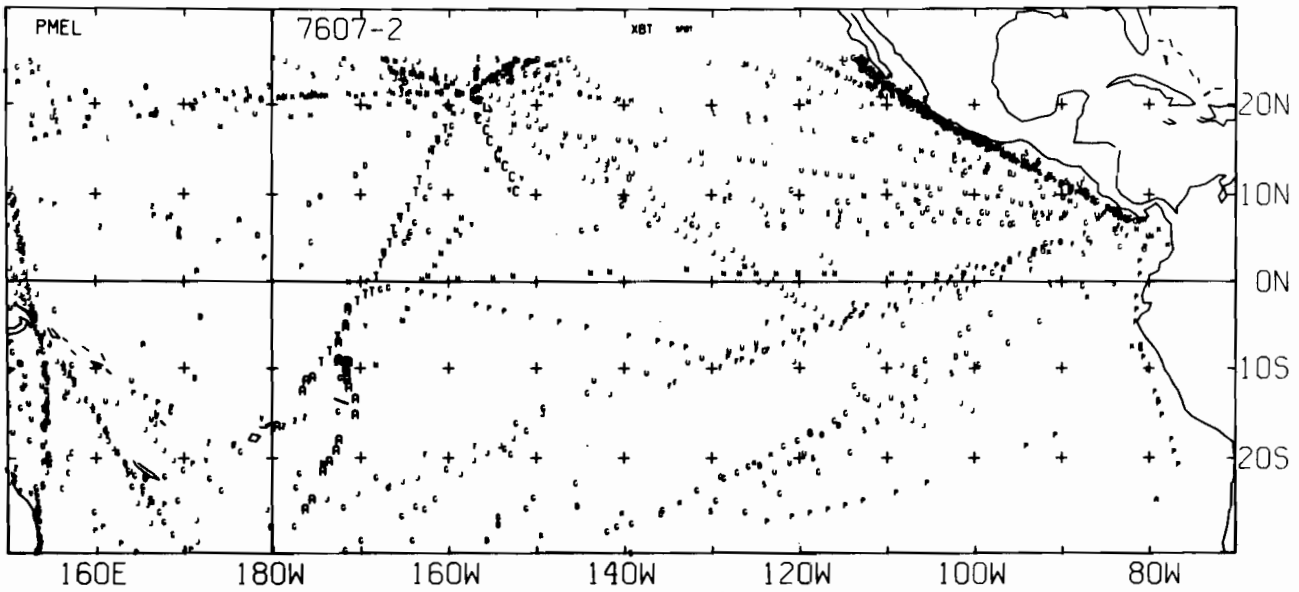

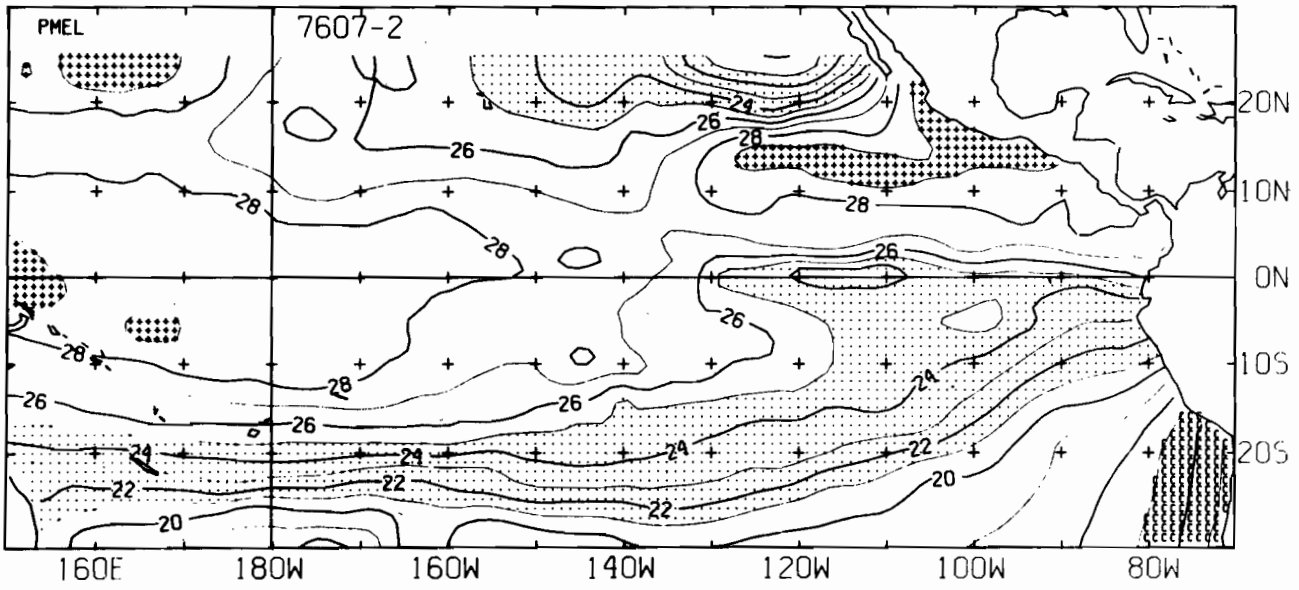

7607-2 SST. 0 E-BUØY. 0 BT. 53 XBT. 1294 SPØT DATA

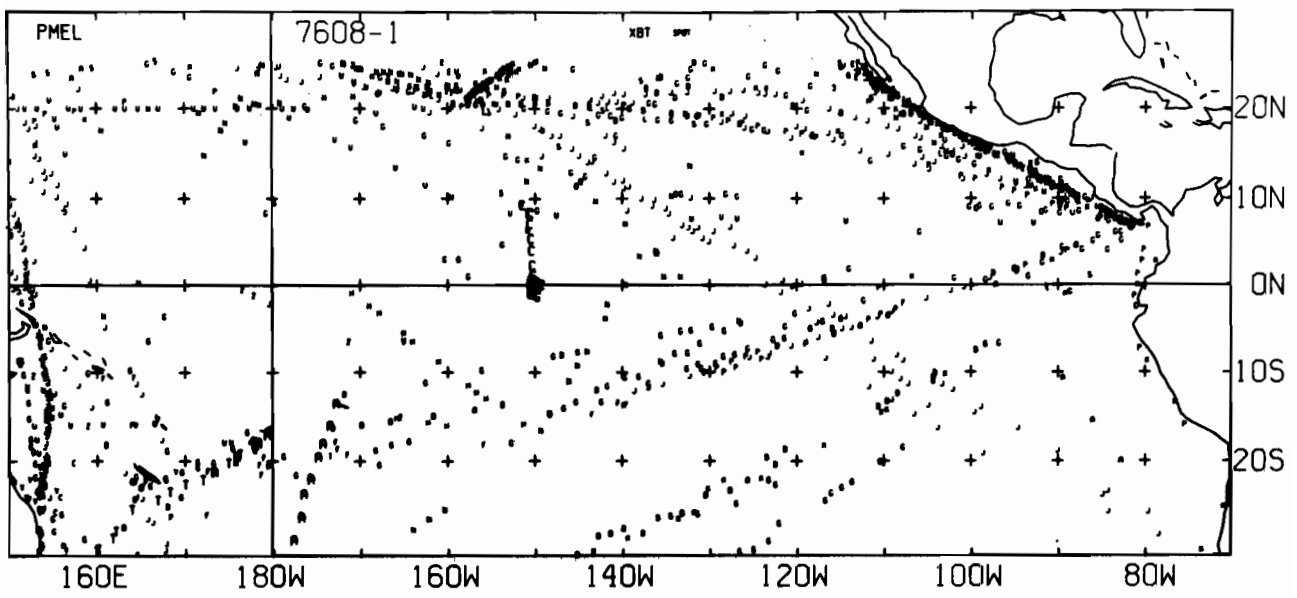

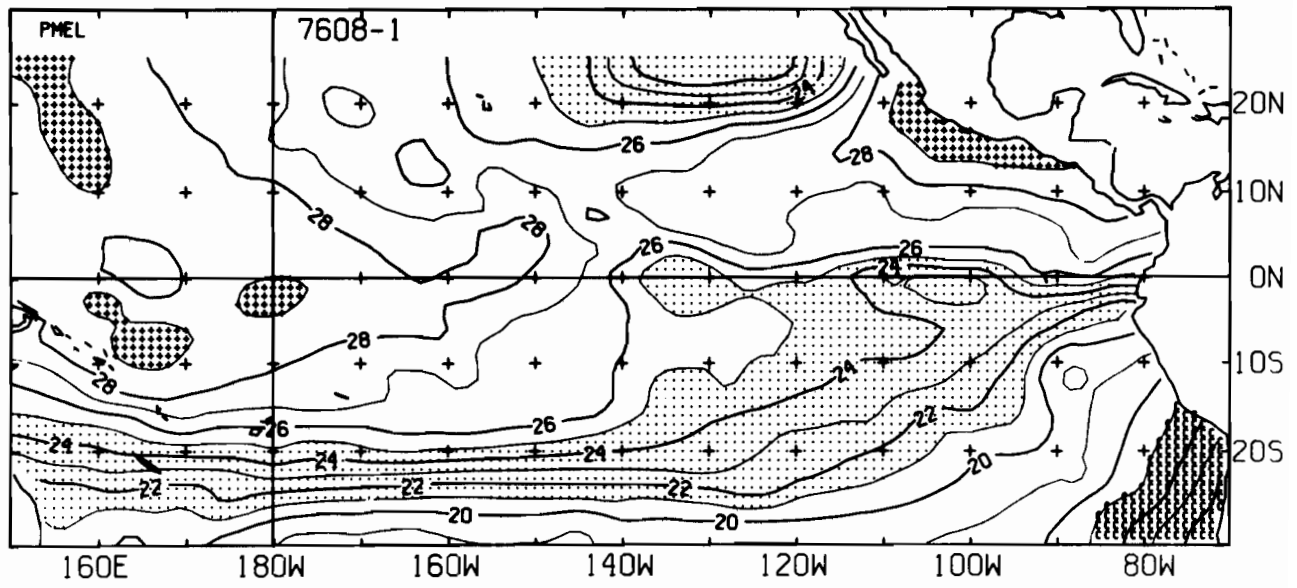

7608-1 SST. 0 E-BUØY. 0 BT. 56 XBT. 1198 SPØT DATA

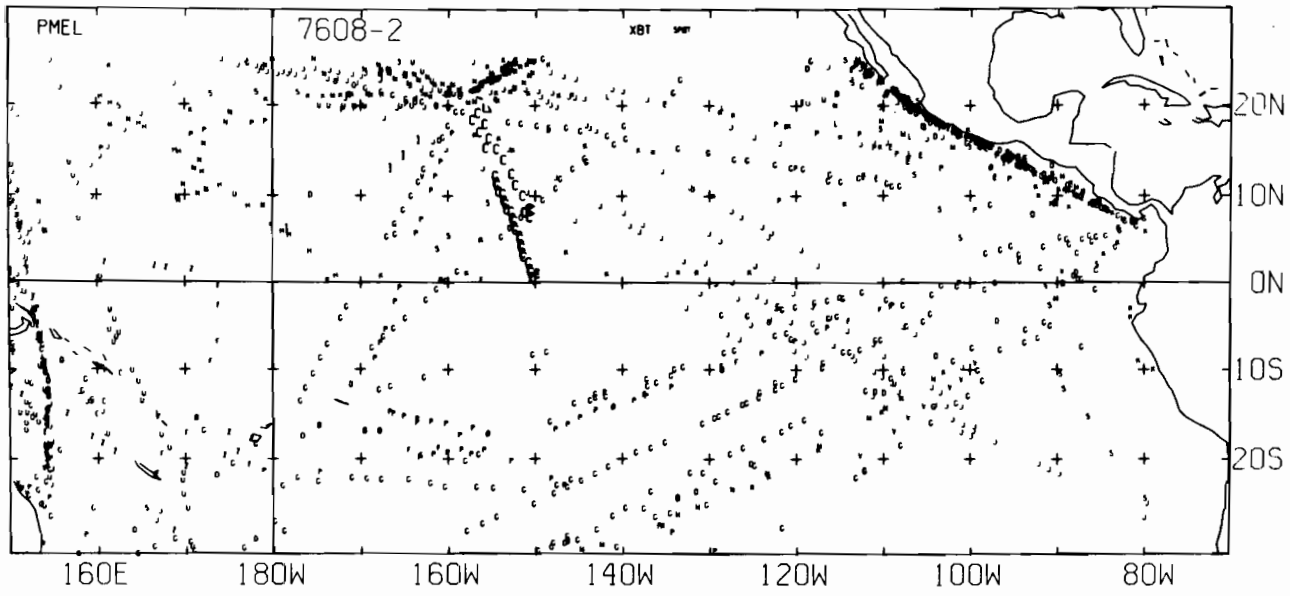

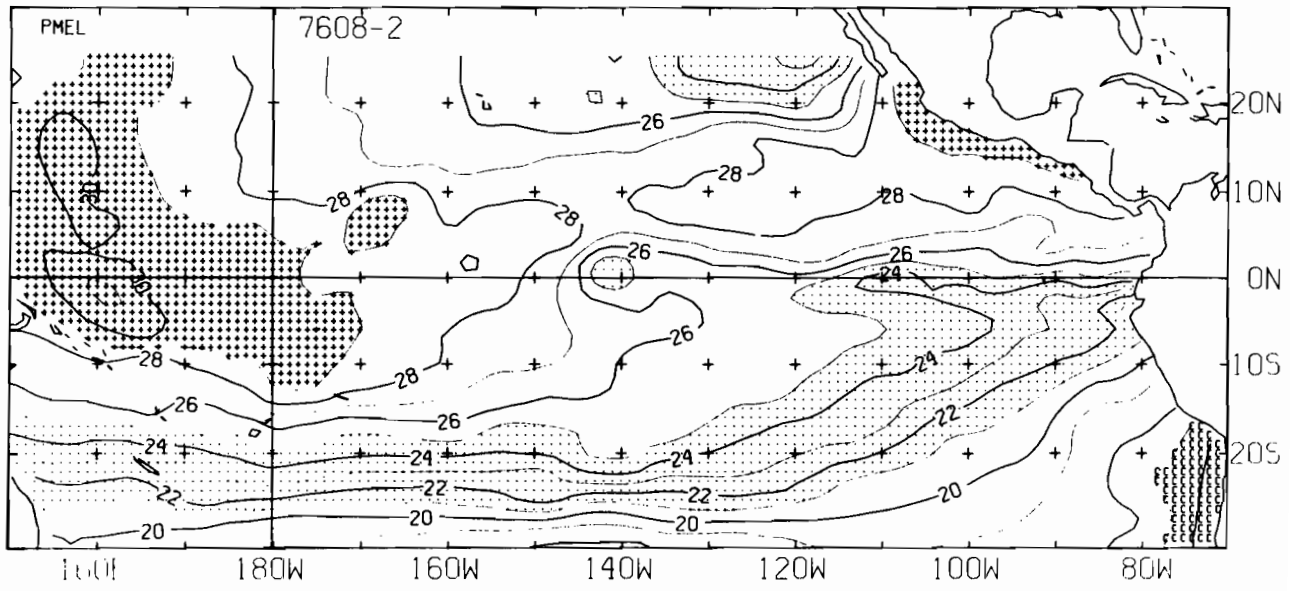

7608-2 SST. 0 E-BUØY. 0 BT. 50 XBT. 1211 SPØT DATA

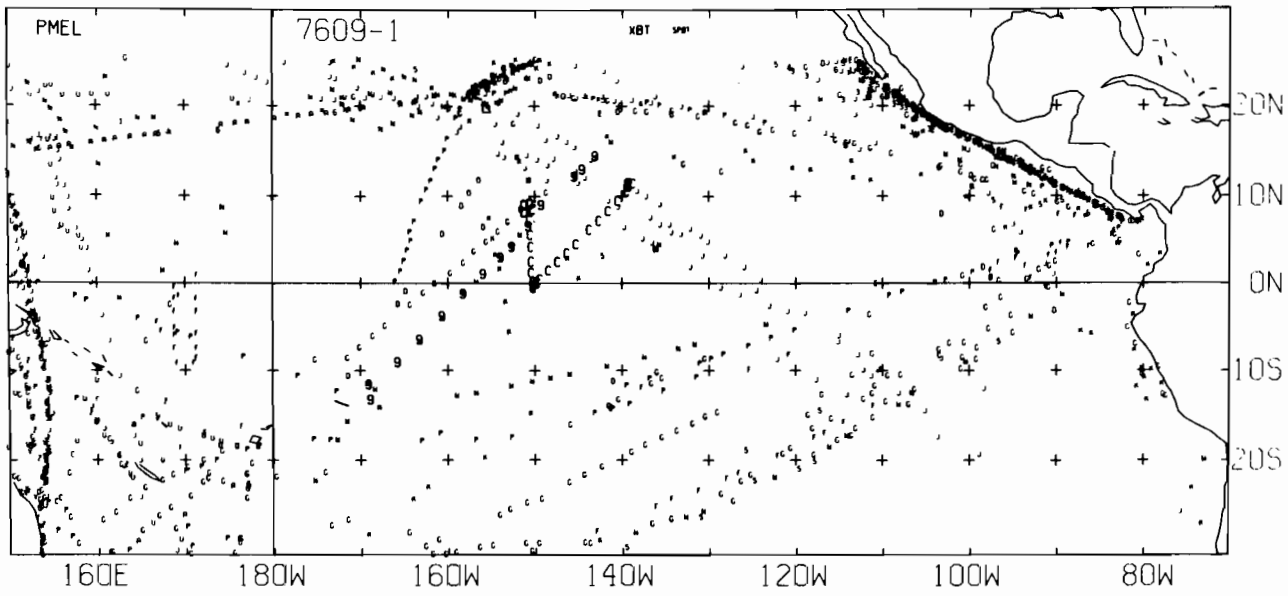

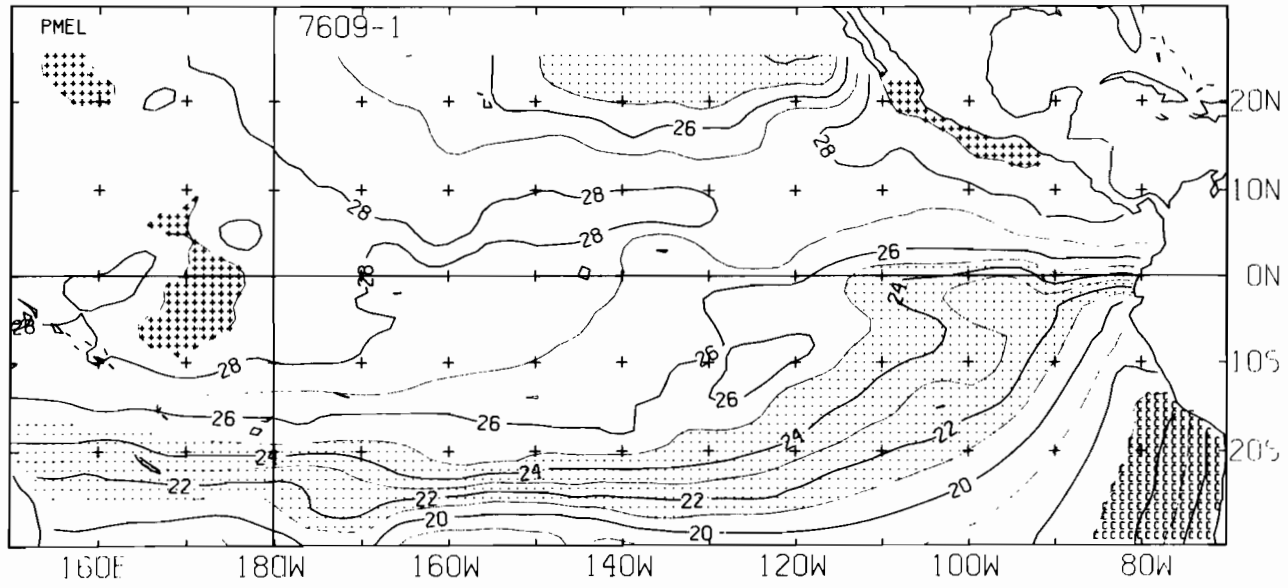

7609-1 SST. 0 E-BUØY. 0 BT. 54 XBT. 1286 SPØT DATA

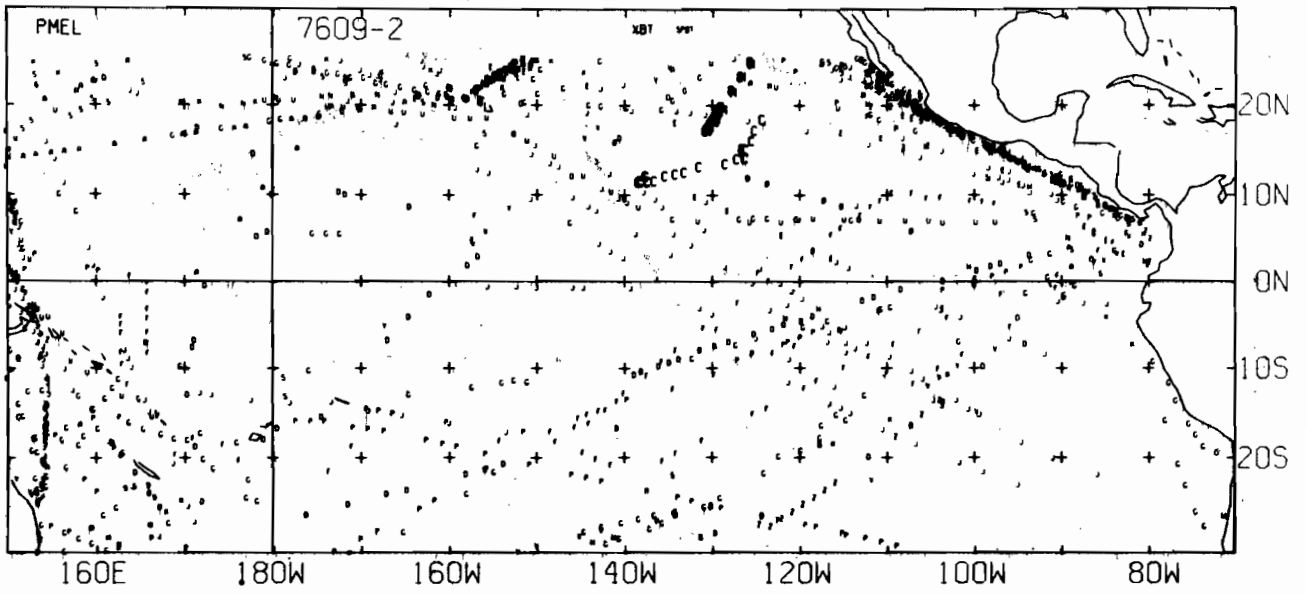

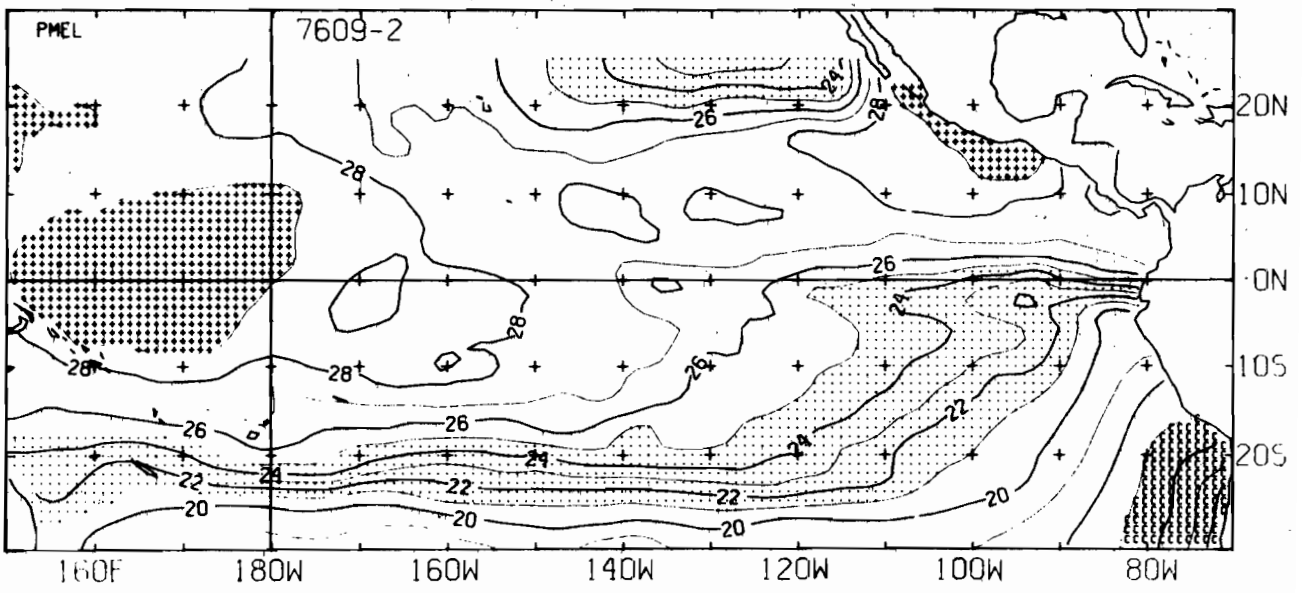

7609-2 SST. 0 E-BUØY. 0 BT. 58 XBT. 1234 SPØT DATA

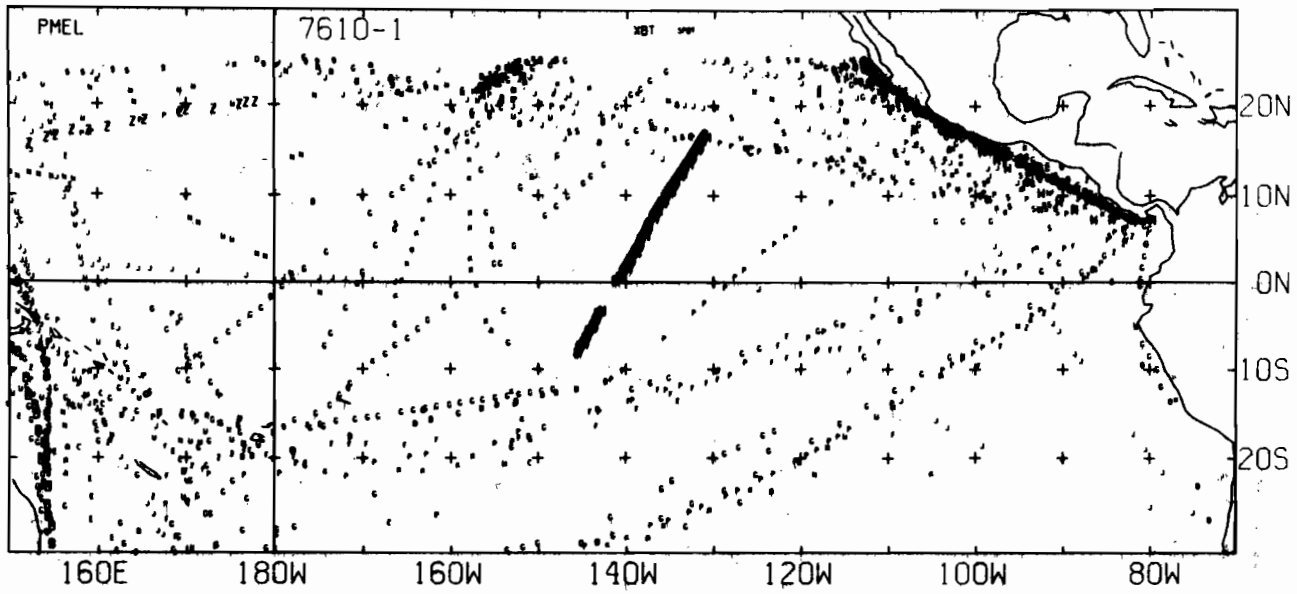

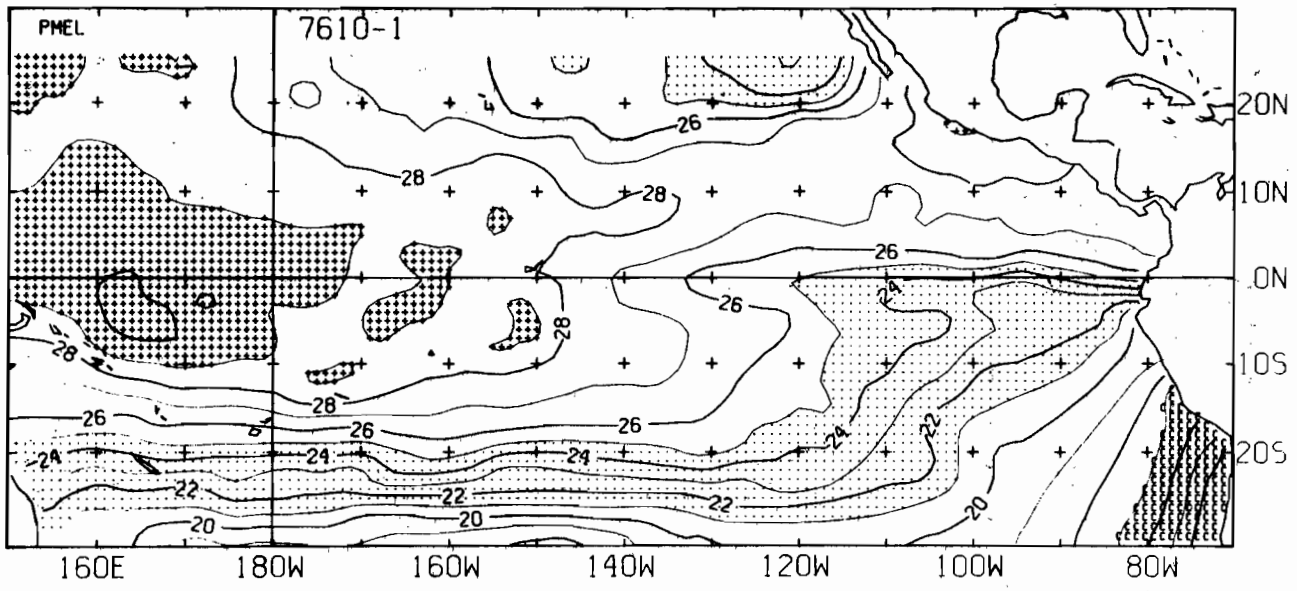

7610-1 SST. 0 E-BUØY. 0 BT. 207 XBT. 1561 SPØT DATA

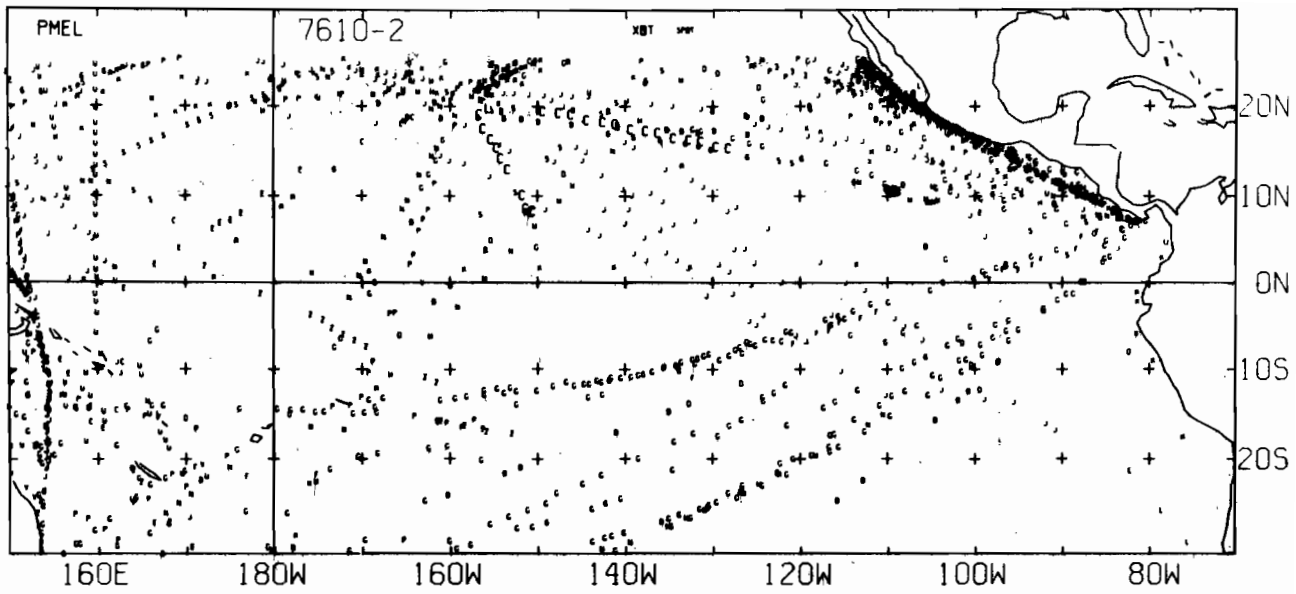

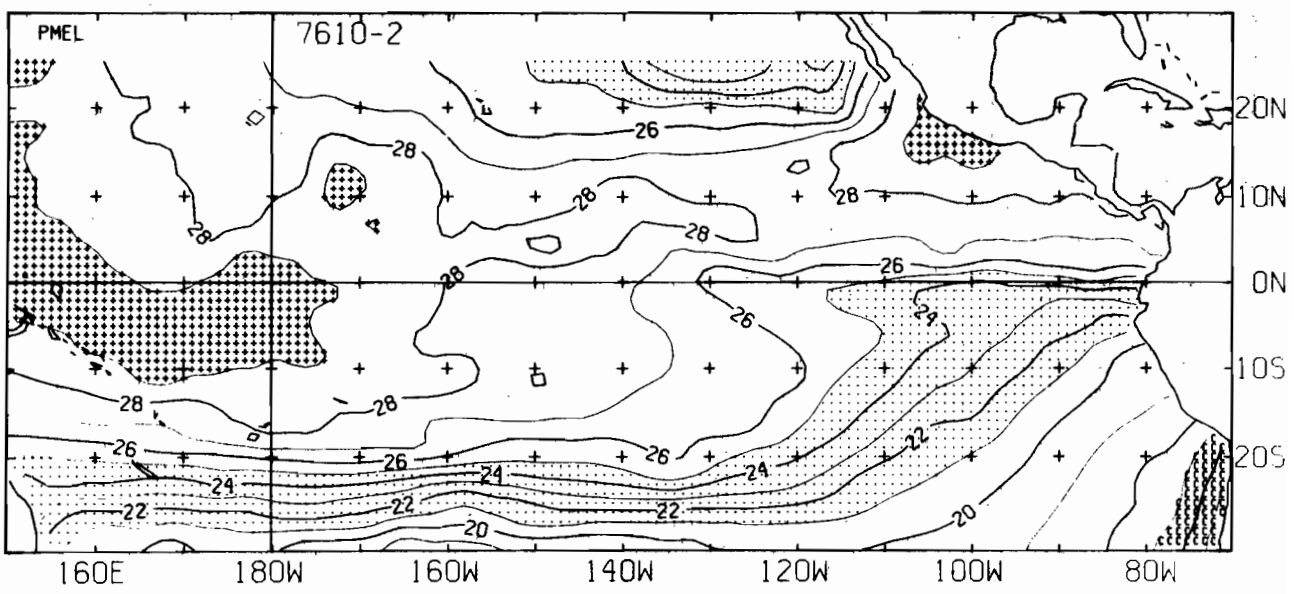

7610-2 SST. 0 E-BUØY. 0 BT. 25 XBT. 1484 SPØT DATA

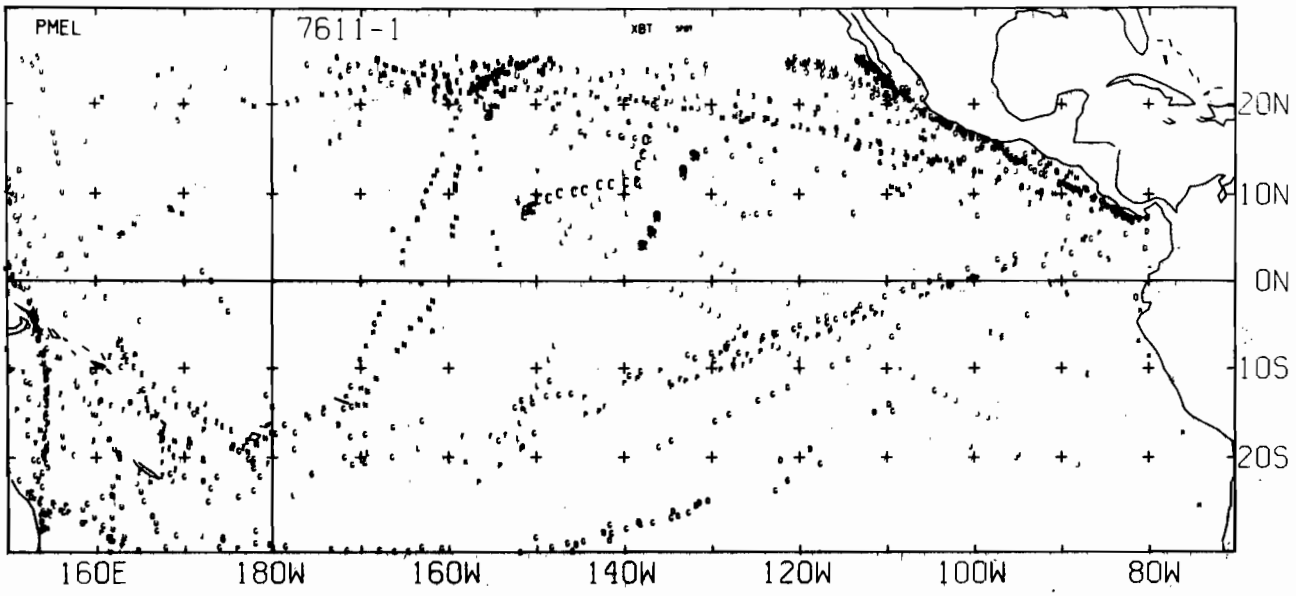

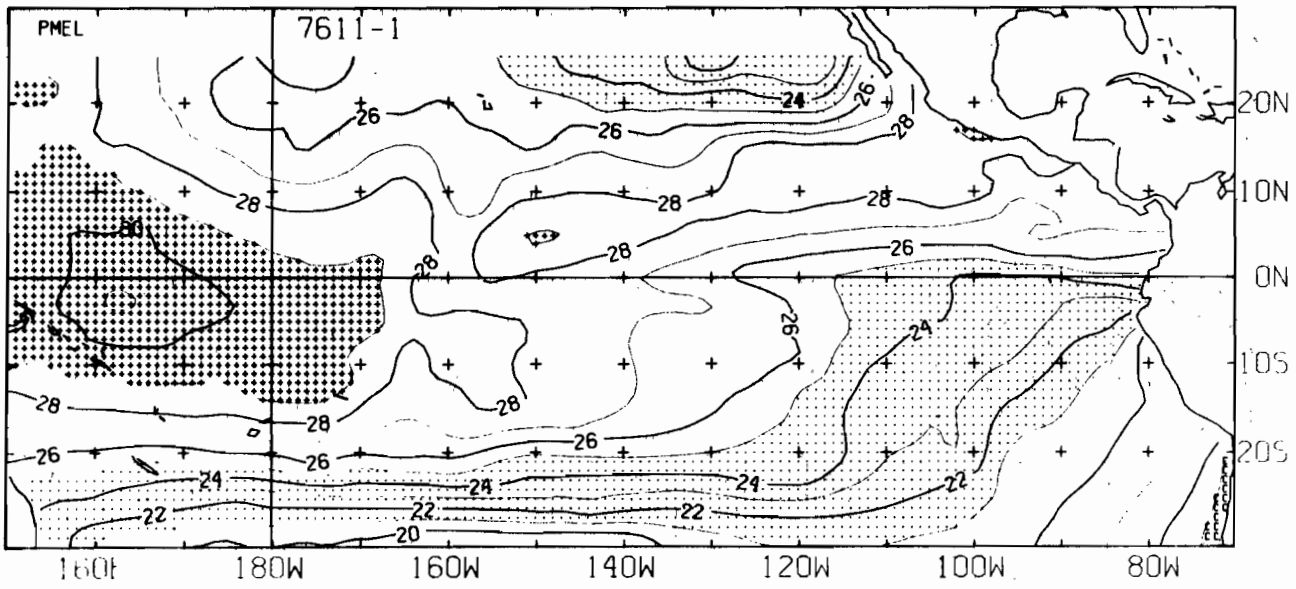

7611 1 SST. 0 E-BUØY. 0 BT. 29 XBT. 1173 SPØT DATA

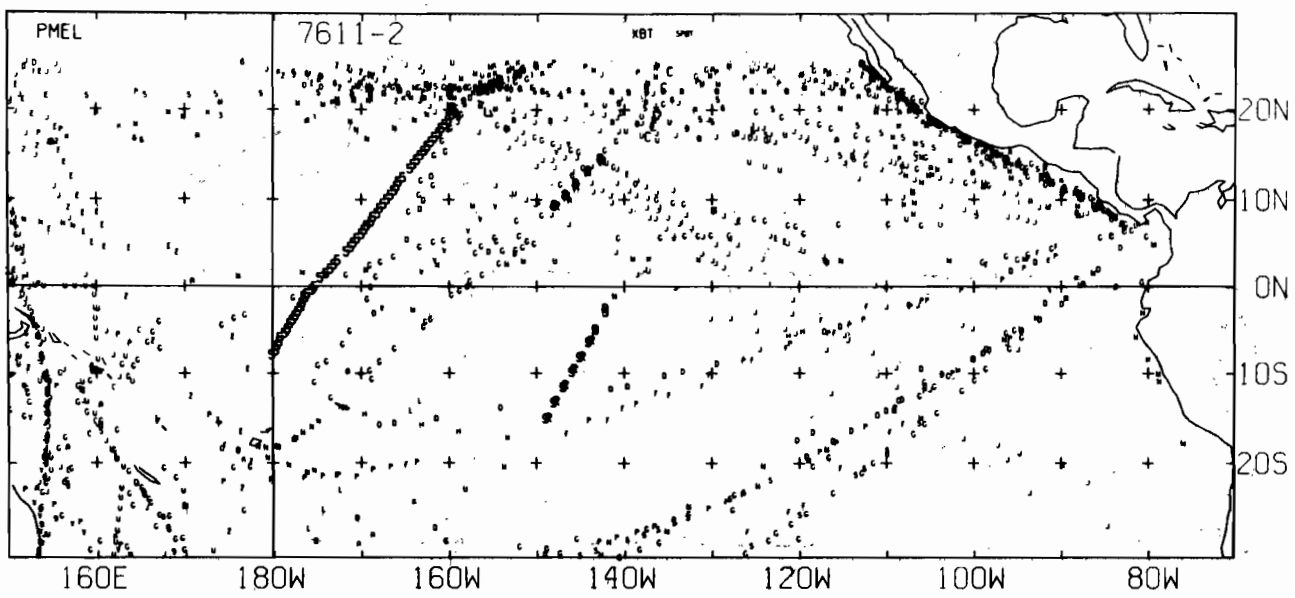

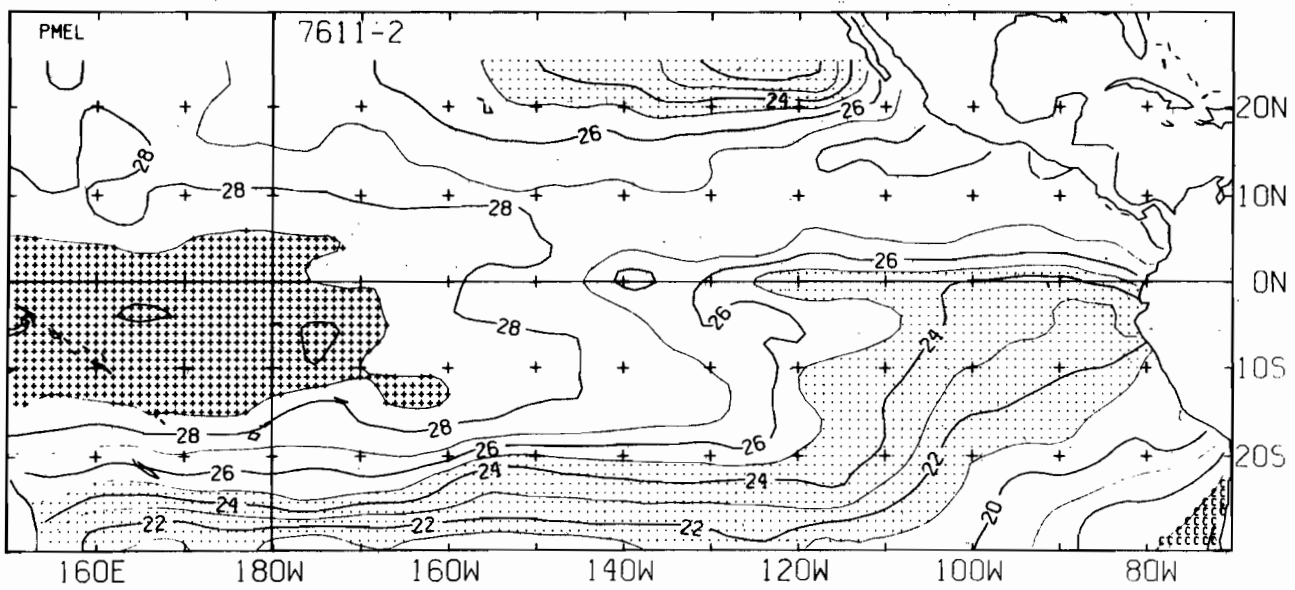

7611-2 SST. 0 E-BUØY. 0 BT. 86 XBT. 1460 SPØT DATA

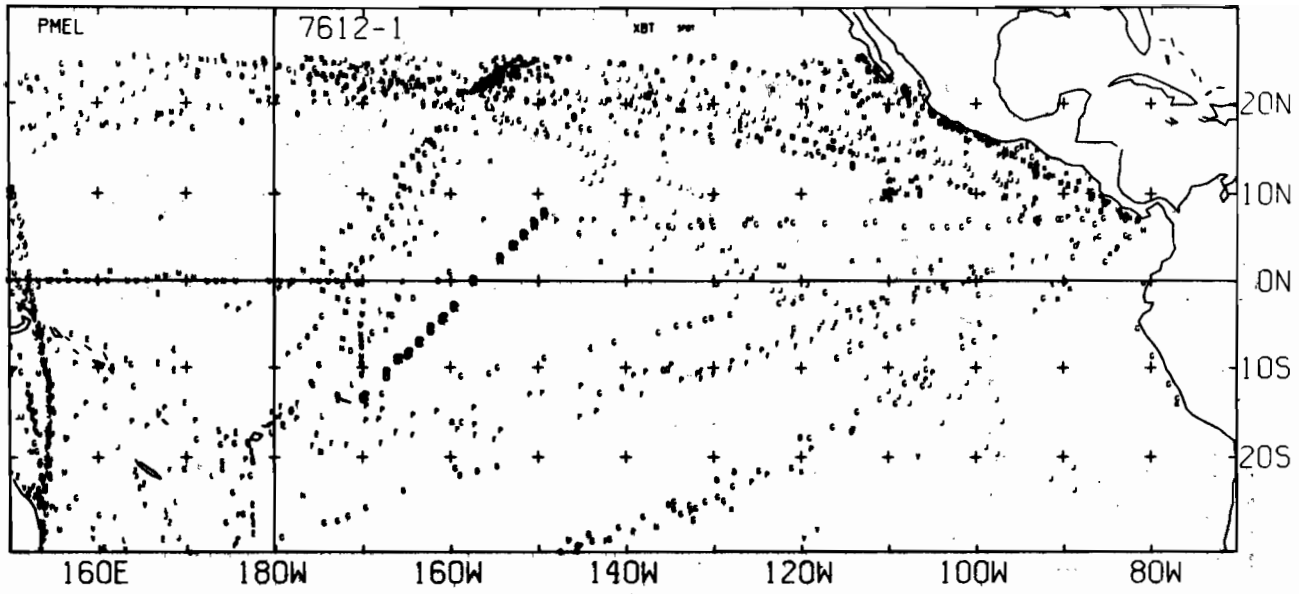

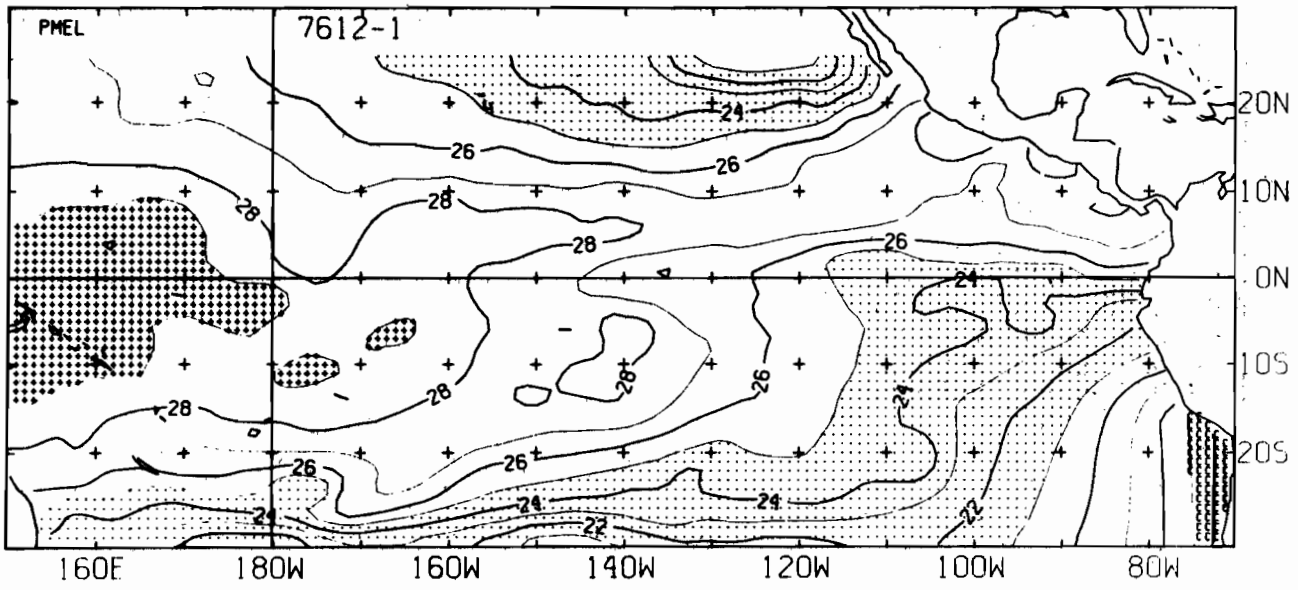

7612-1 SST. 0 E-BUØY. 0 BT. 28 XBT. 1451 SPØT DATA

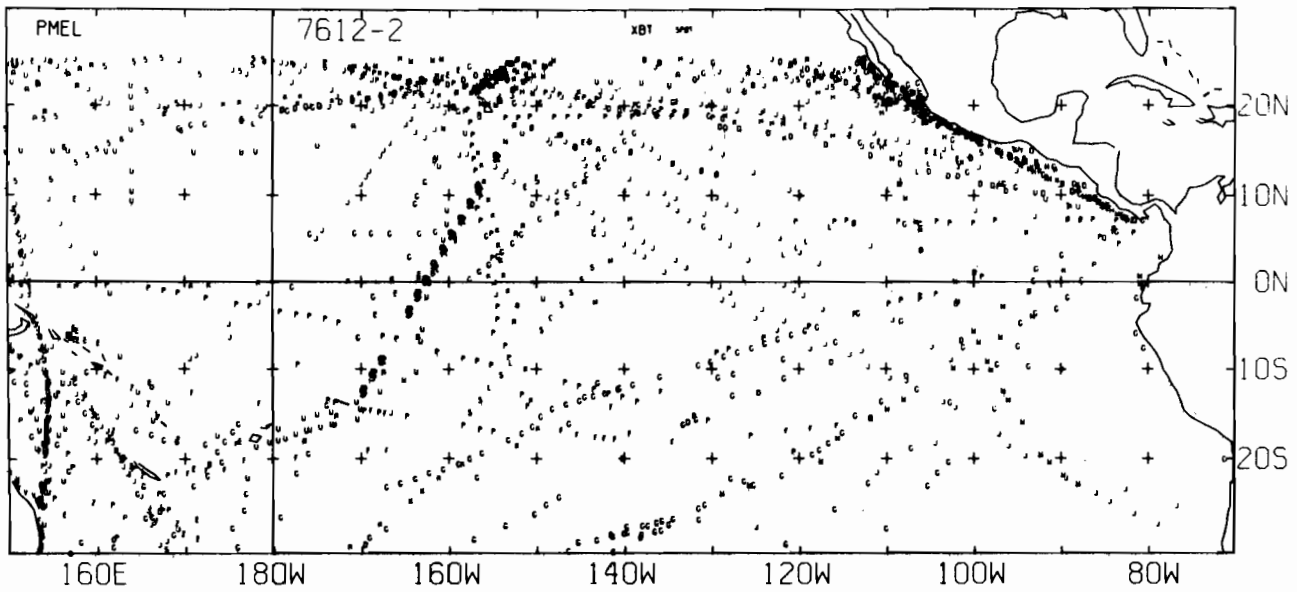

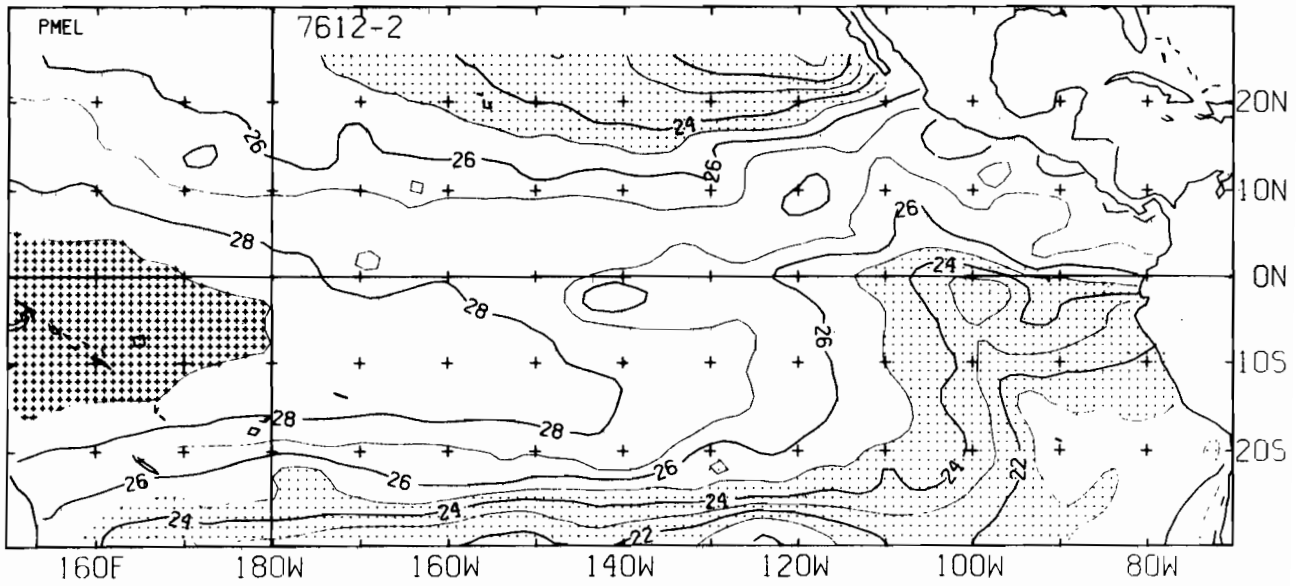

7612-2 SST. 0 E-BUØY. 0 BT. 28 XBT. 1583 SPØT DATA

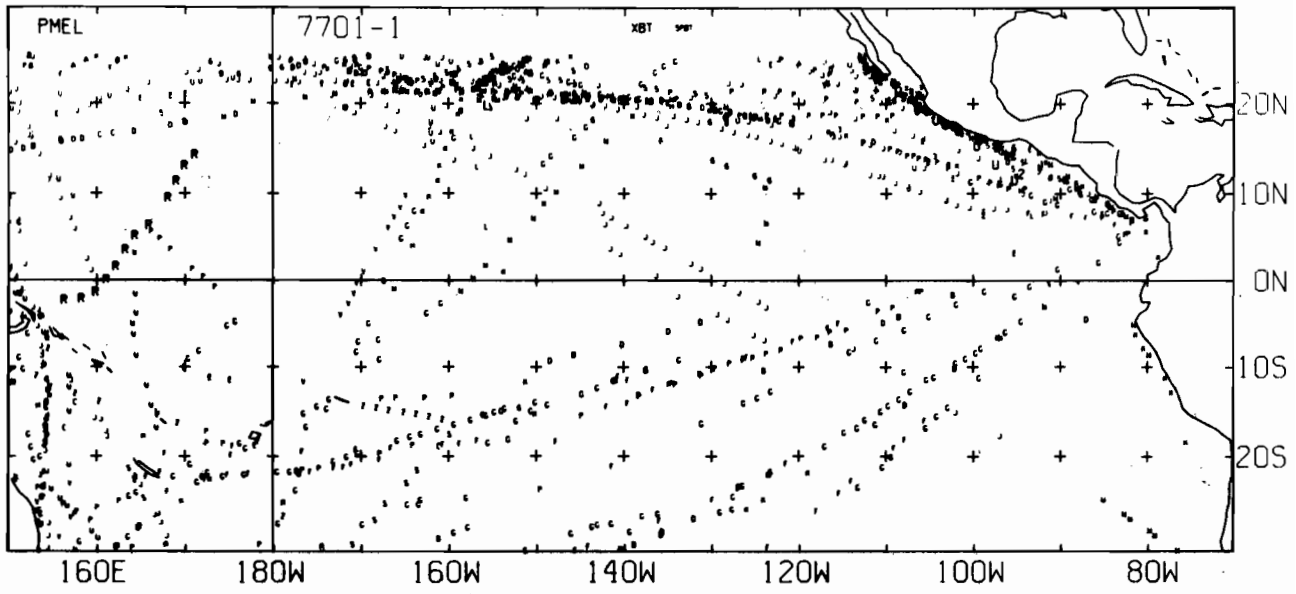

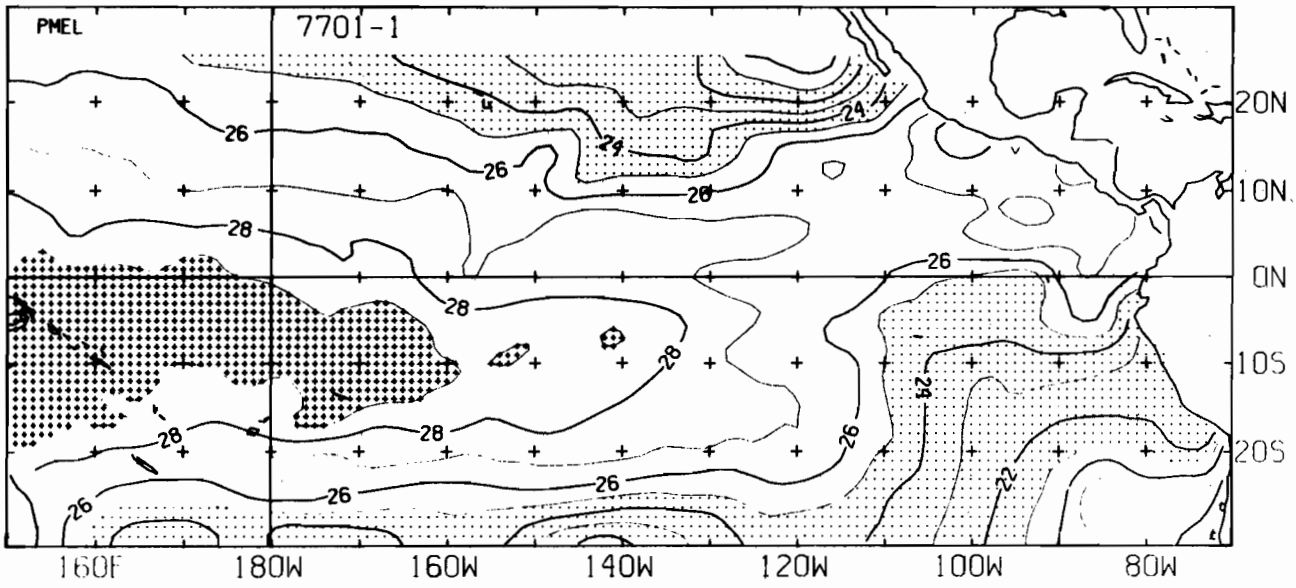

7701-1 SST. 0 E-BUØY. 0 BT. 22 XBT. 1201 SPØT DATA

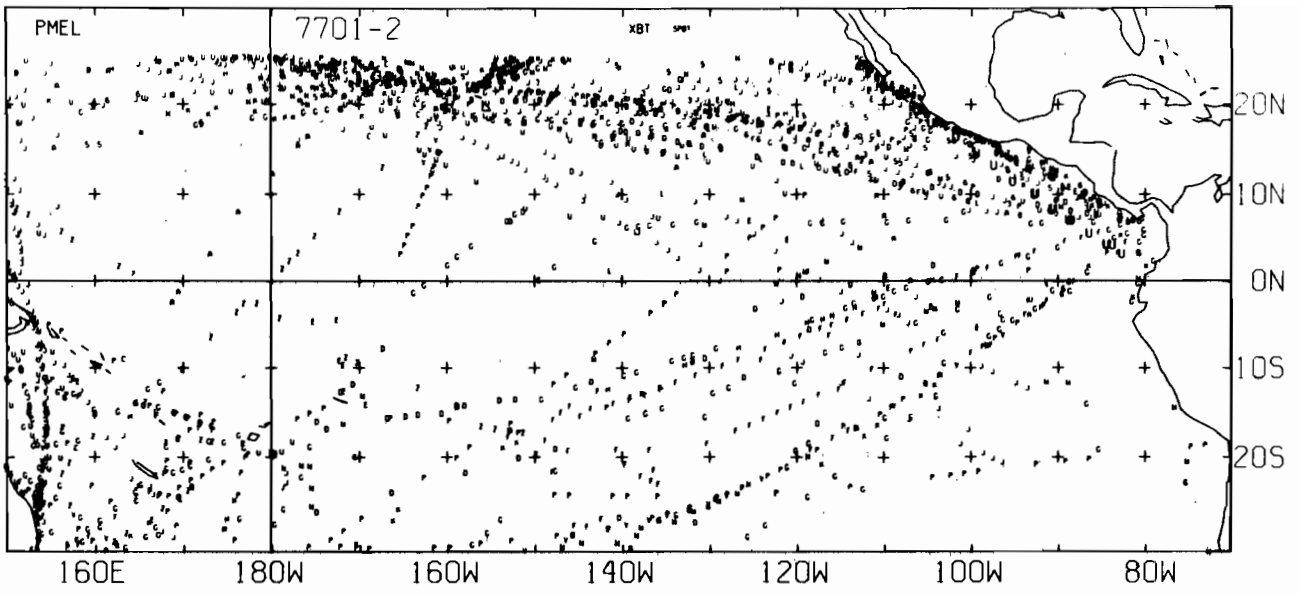

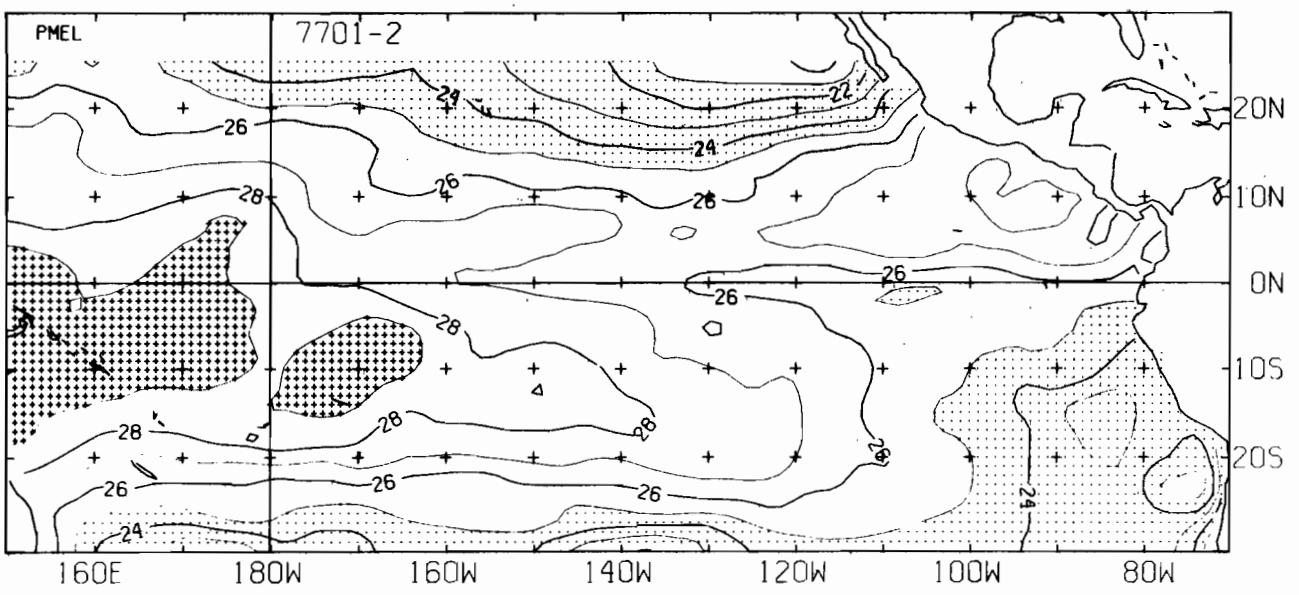

7701-2 SST. 0 E-BUØY. 0 BT. 22 XBT. 1921 SPØT DATA

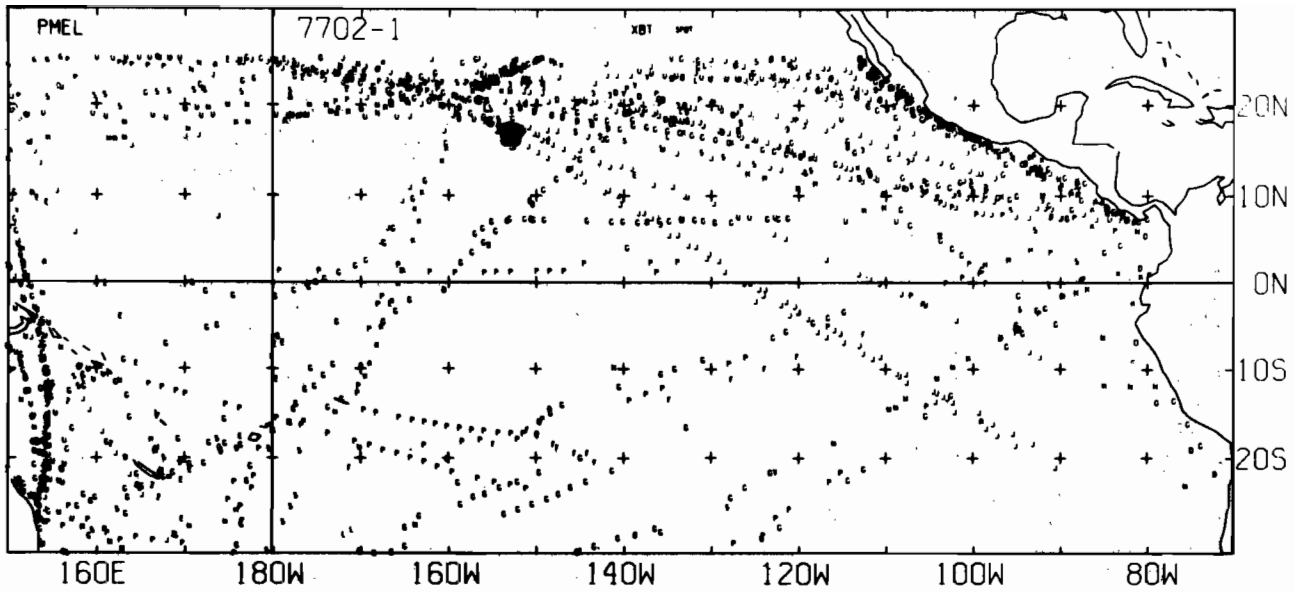

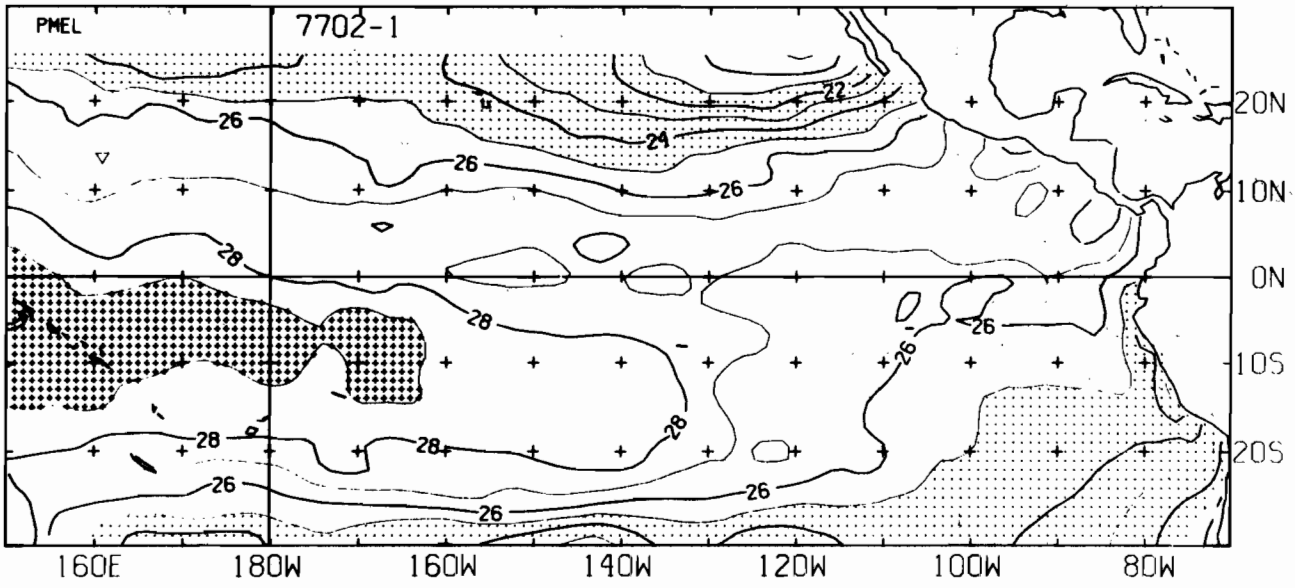

7702-1 SST. 0 E-BUØY. 0 BT. 60 XBT. 1645 SPØT DATA

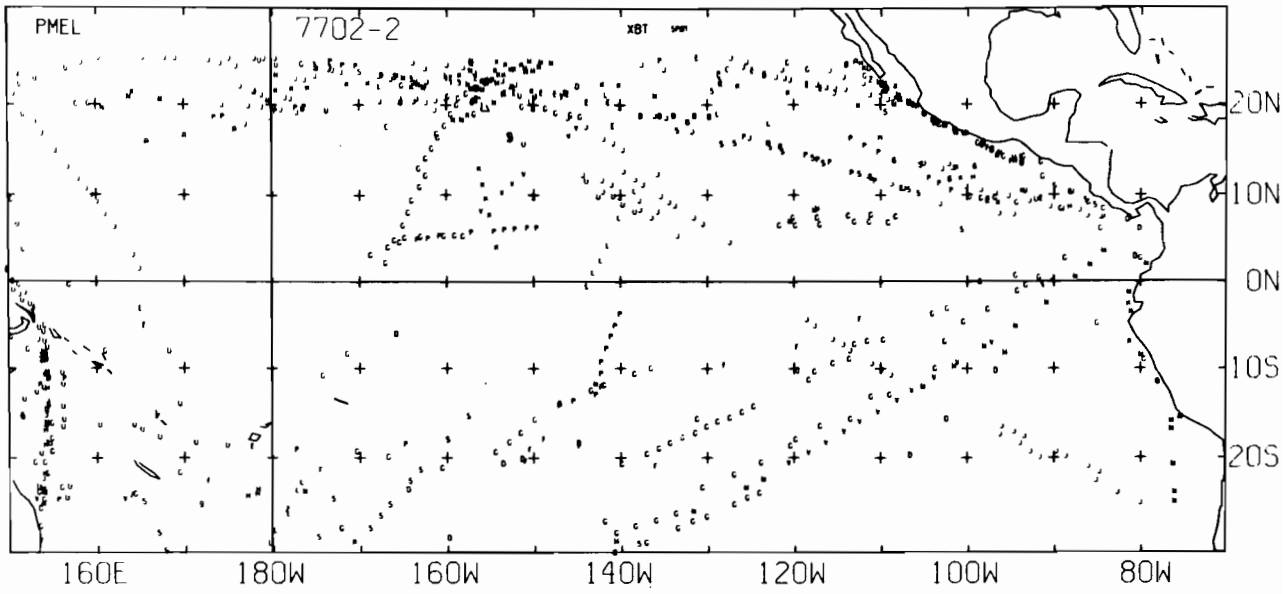

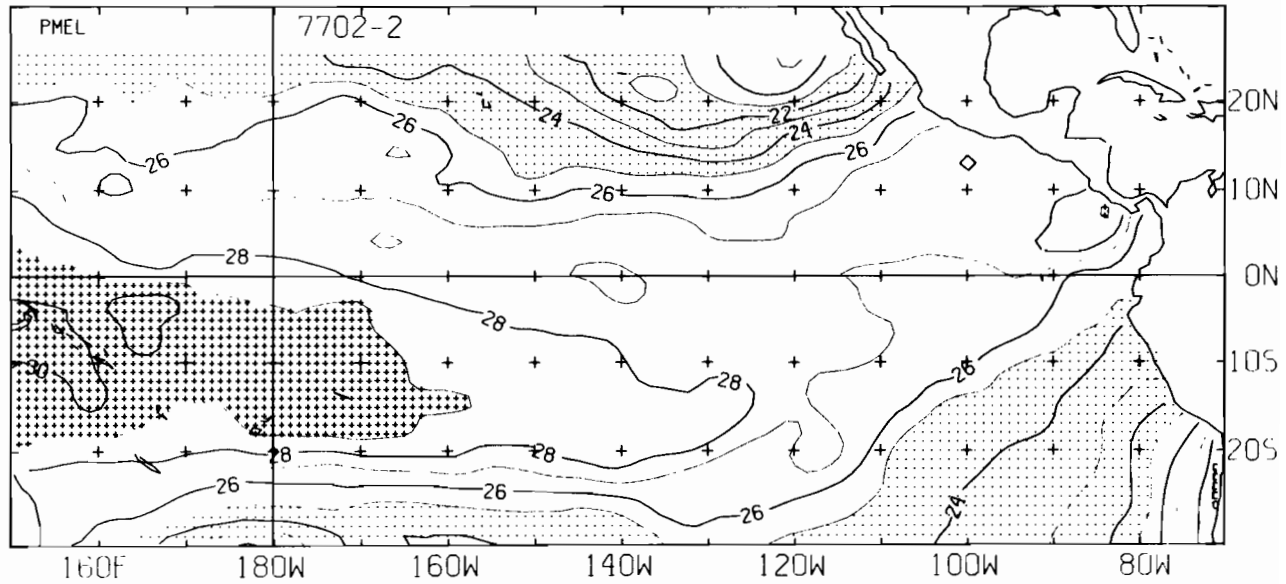

7702-2 SST. 0 E-BUØY. 0 BT. 1 XBT. 779 SPØT DATA

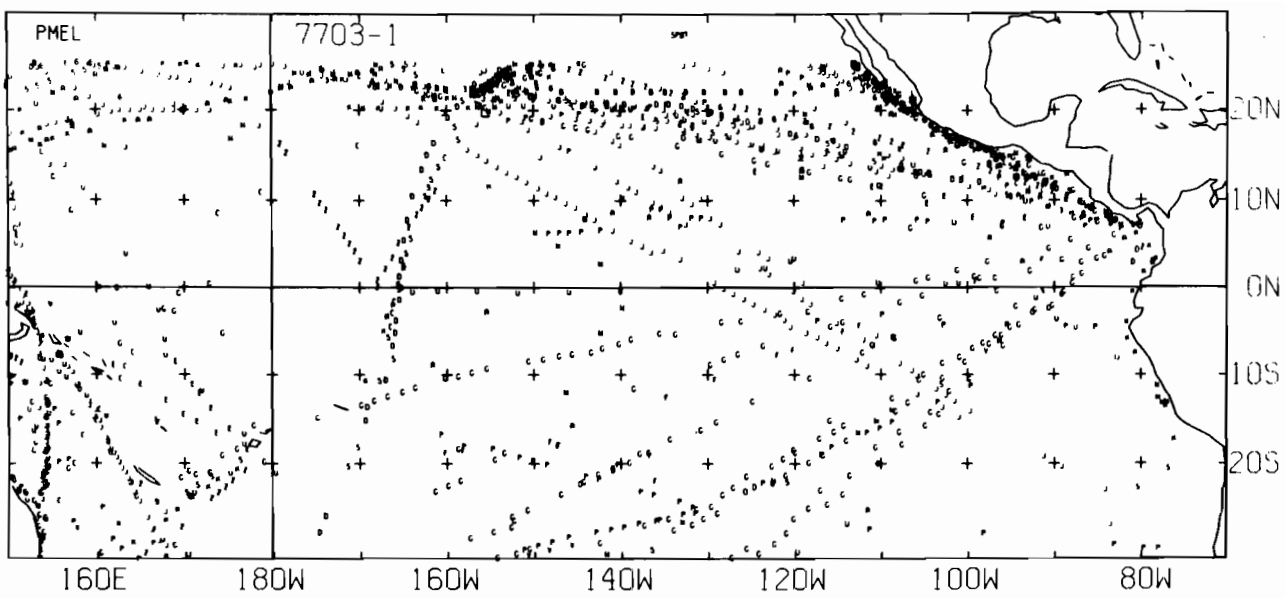

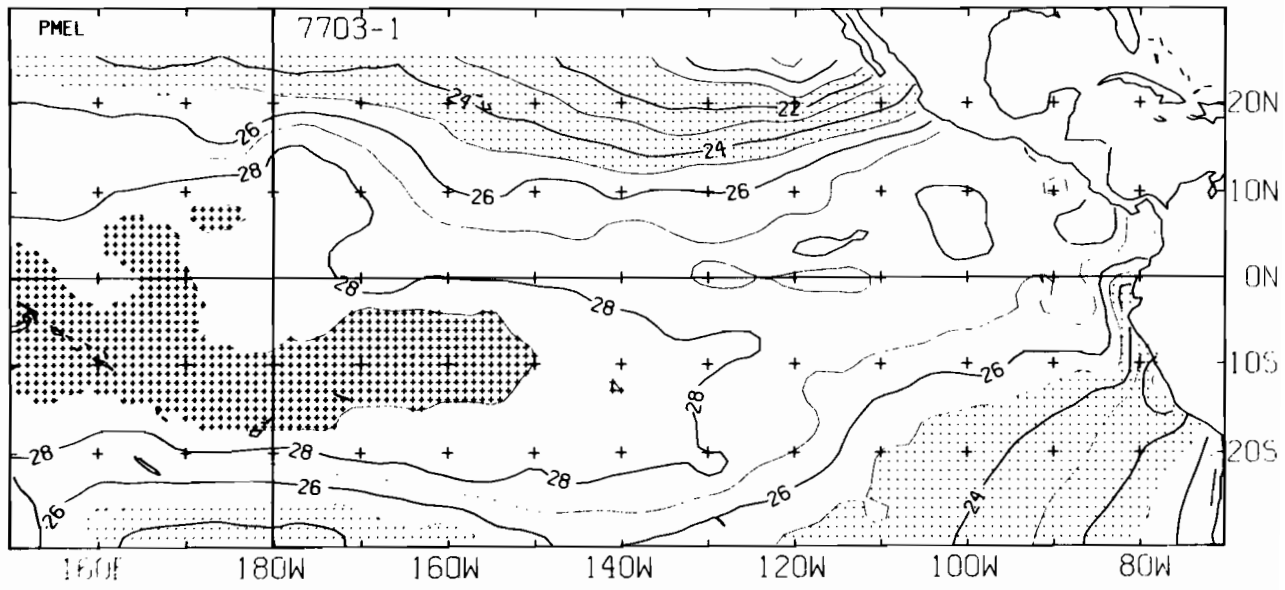

7703-1 SST. 0 E-BUØY. 0 BT. 0 XBT. 1538 SPØT DATA

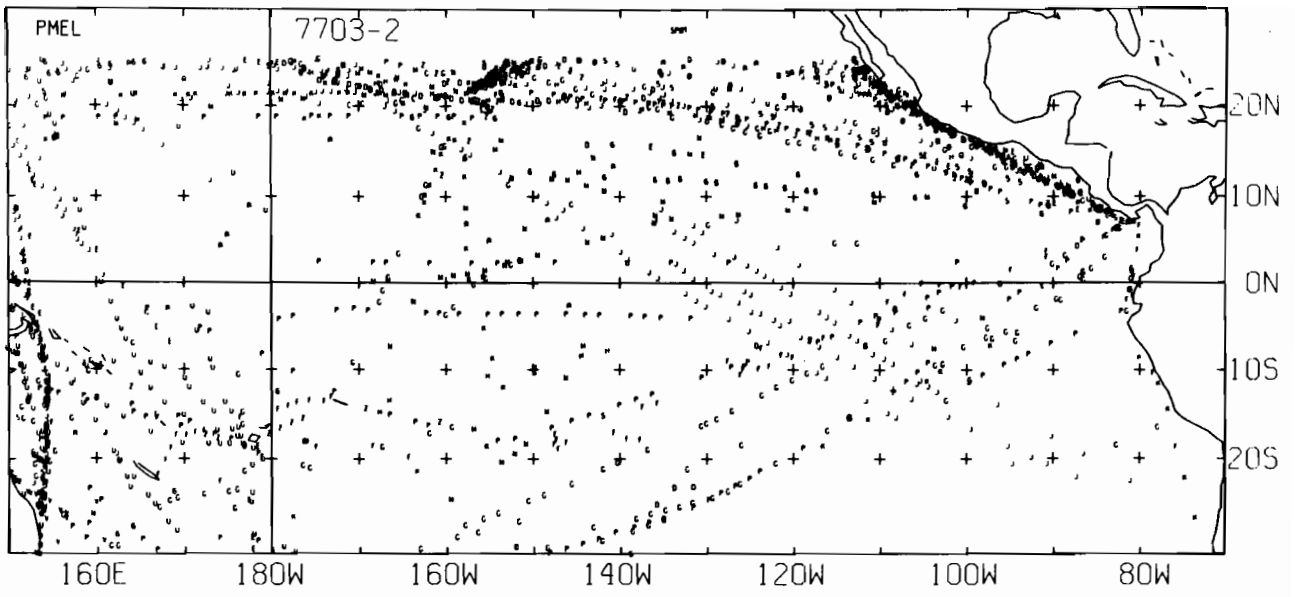

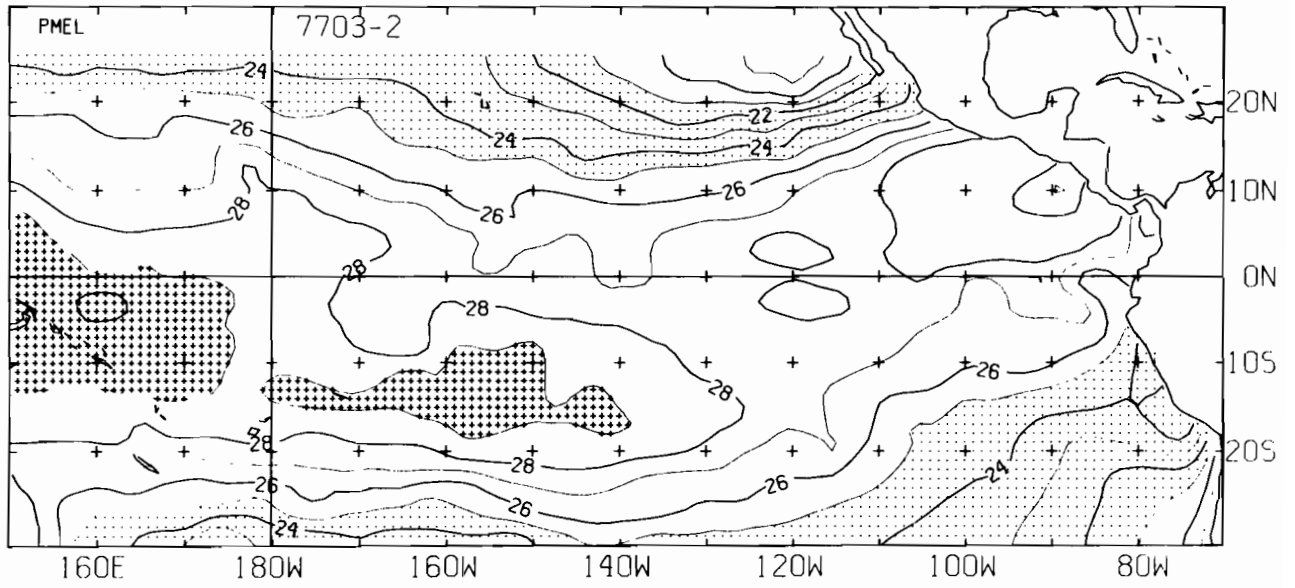

7703-2 SST. 0 E-BUØY. 0 BT. 0 XBT. 1647 SPØT DATA

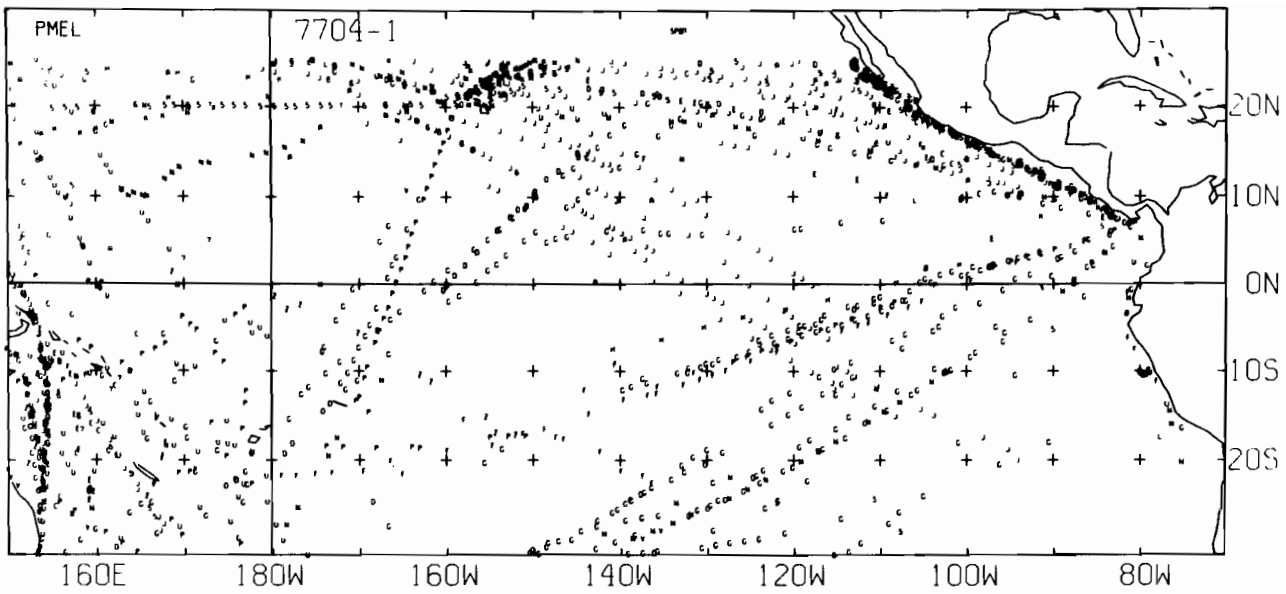

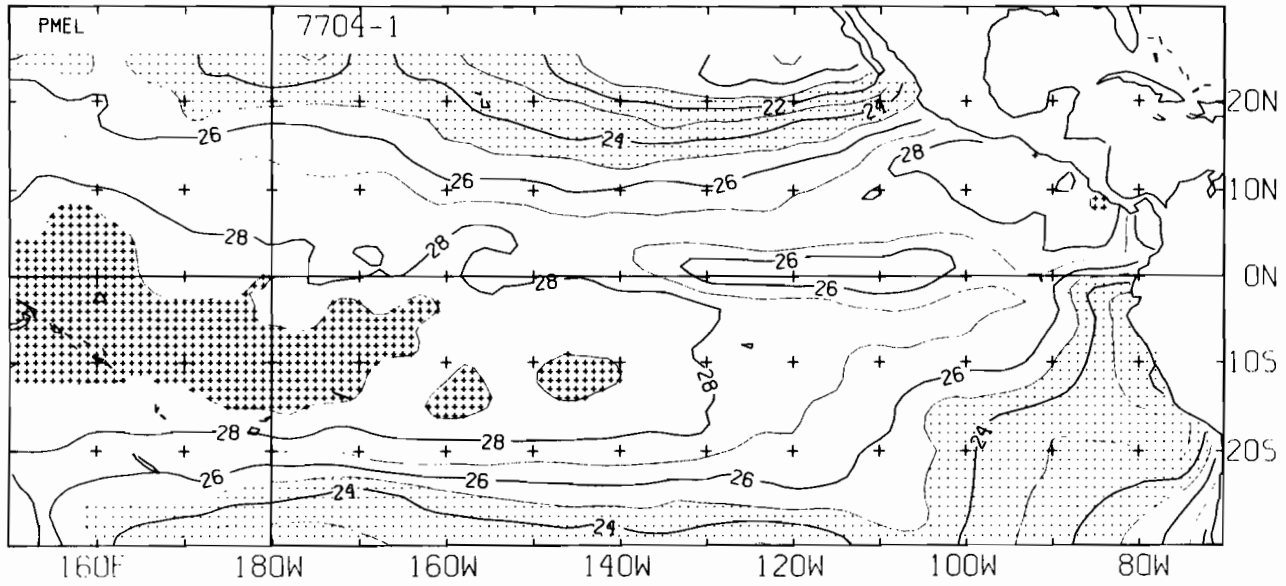

7704-1 SST. 0 E-BUØY. 0 BT. 0 XBT. 1590 SPØT DATA

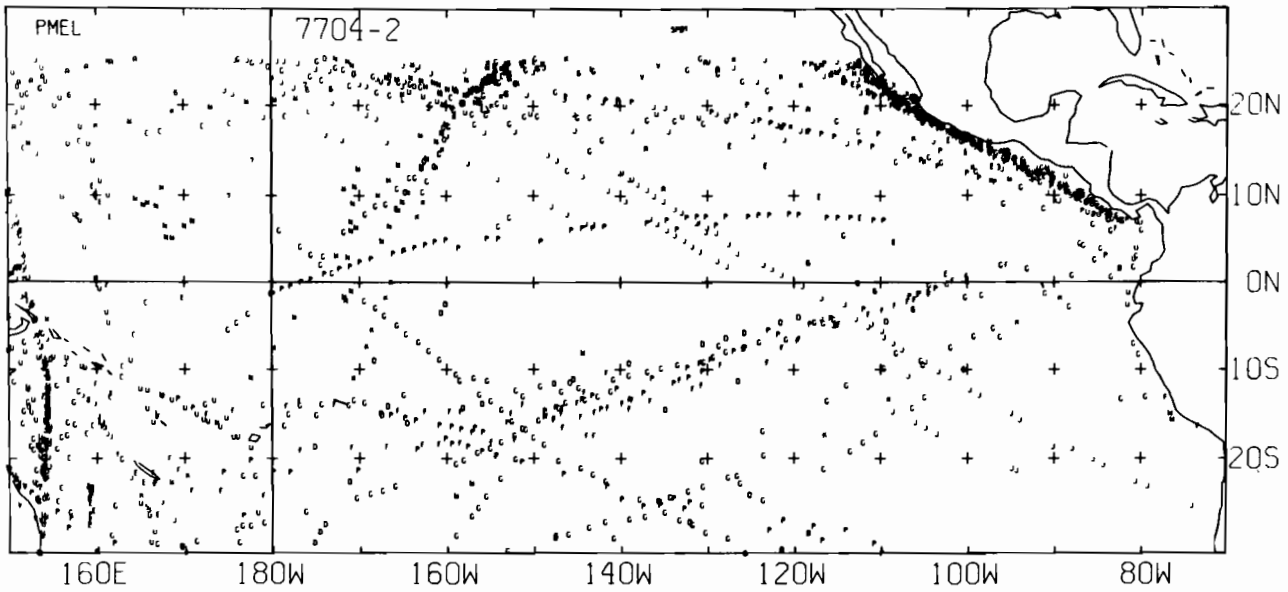

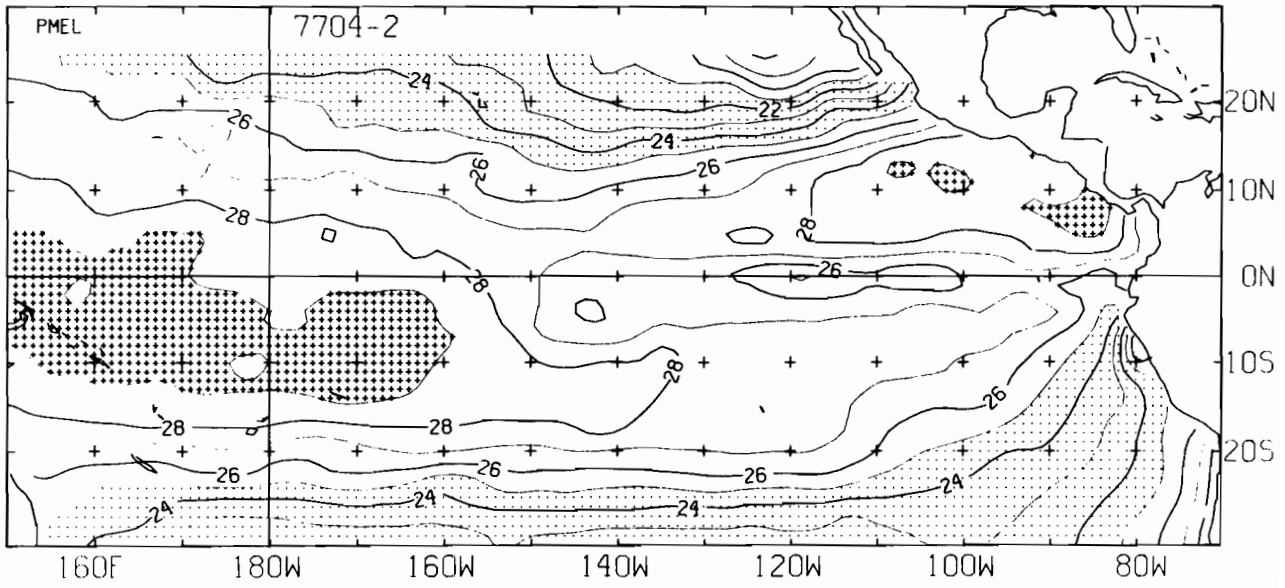

7704-2 SST. 0 E-BUØY. 0 BT. 0 XBT. 1463 SPØT DATA

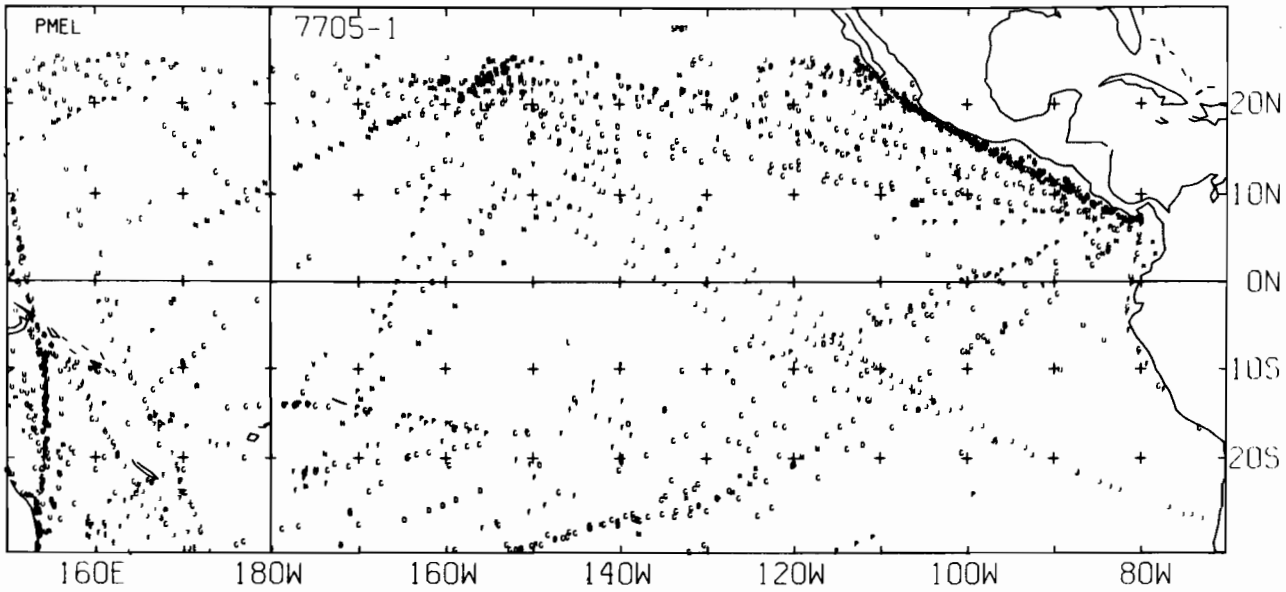

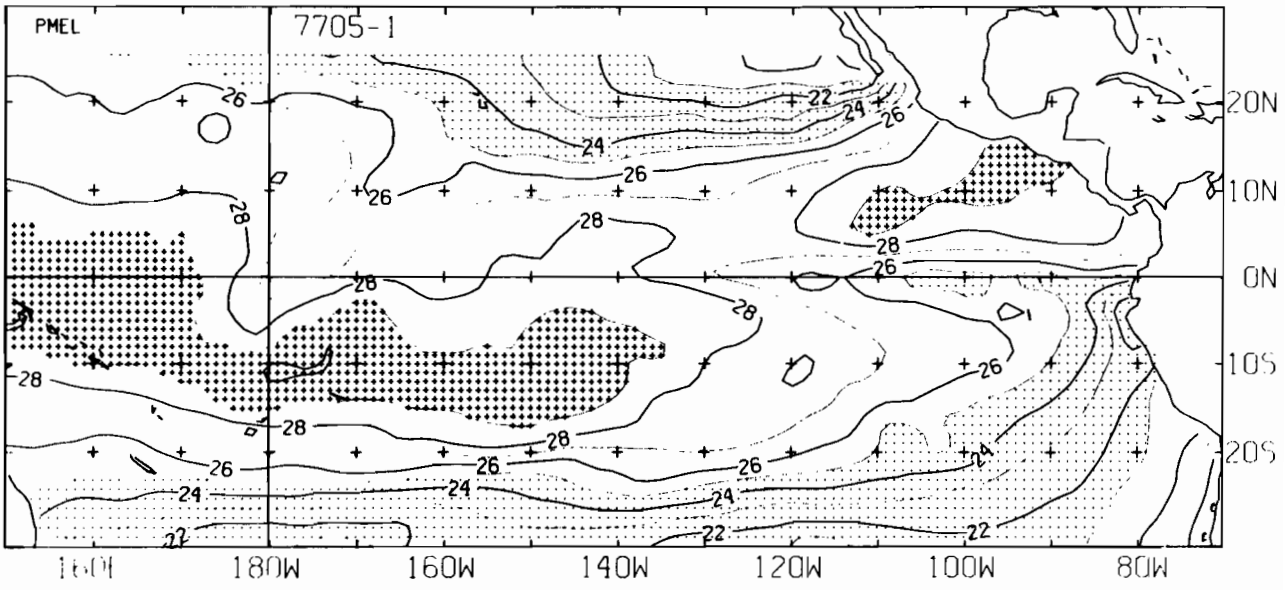

7705 1 SST. 0 E-BUØY. 0 BT. 0 XBT. 1540 SPØT DATA

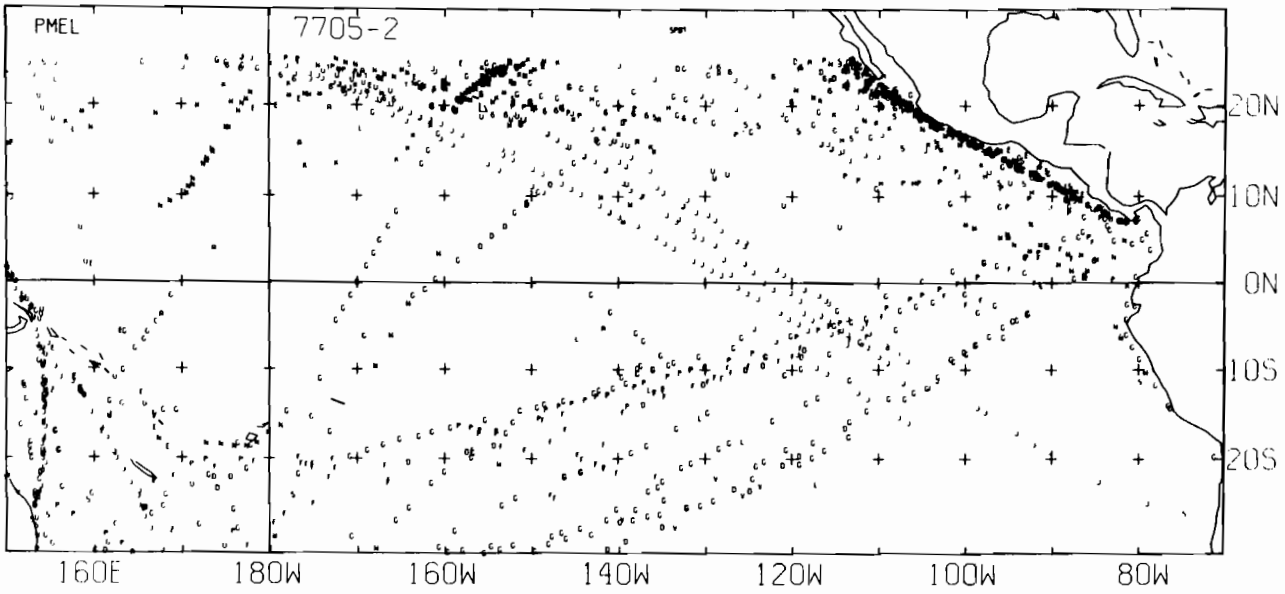

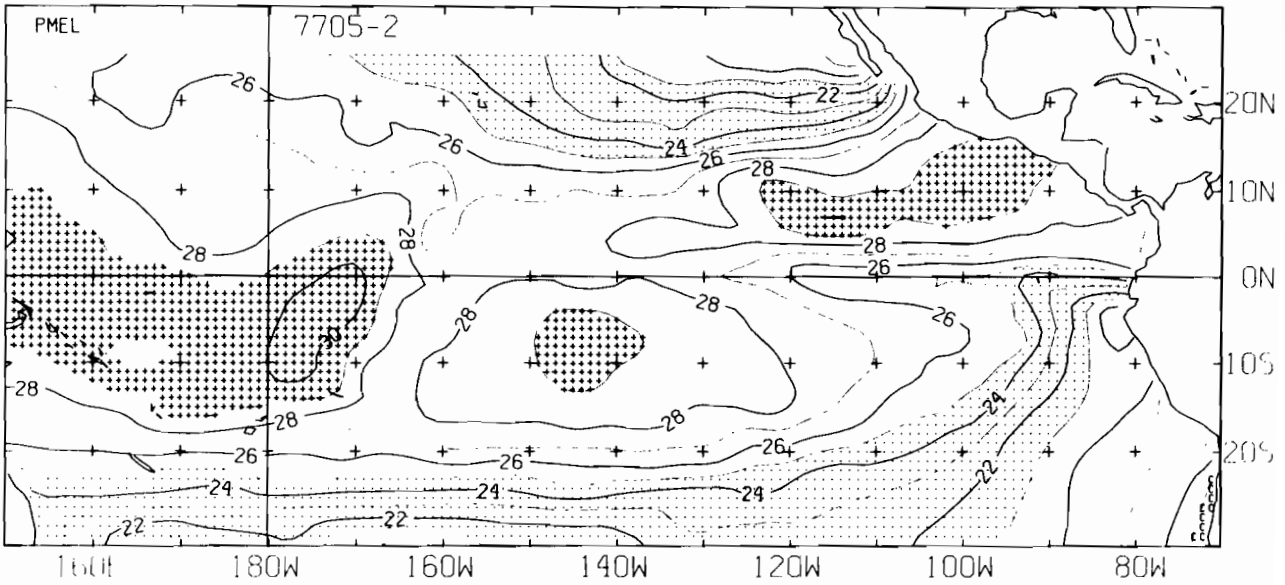

7705-2 SST. 0 E-BUØY. 0 BT. 0 XBT. 1410 SPØT DATA

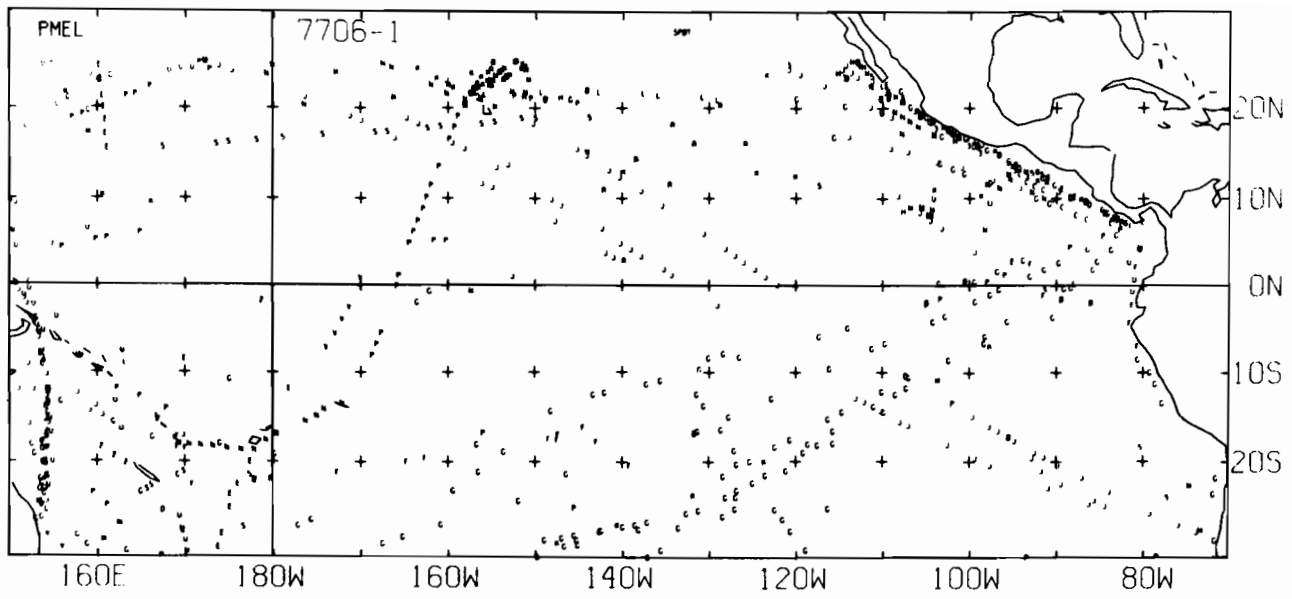

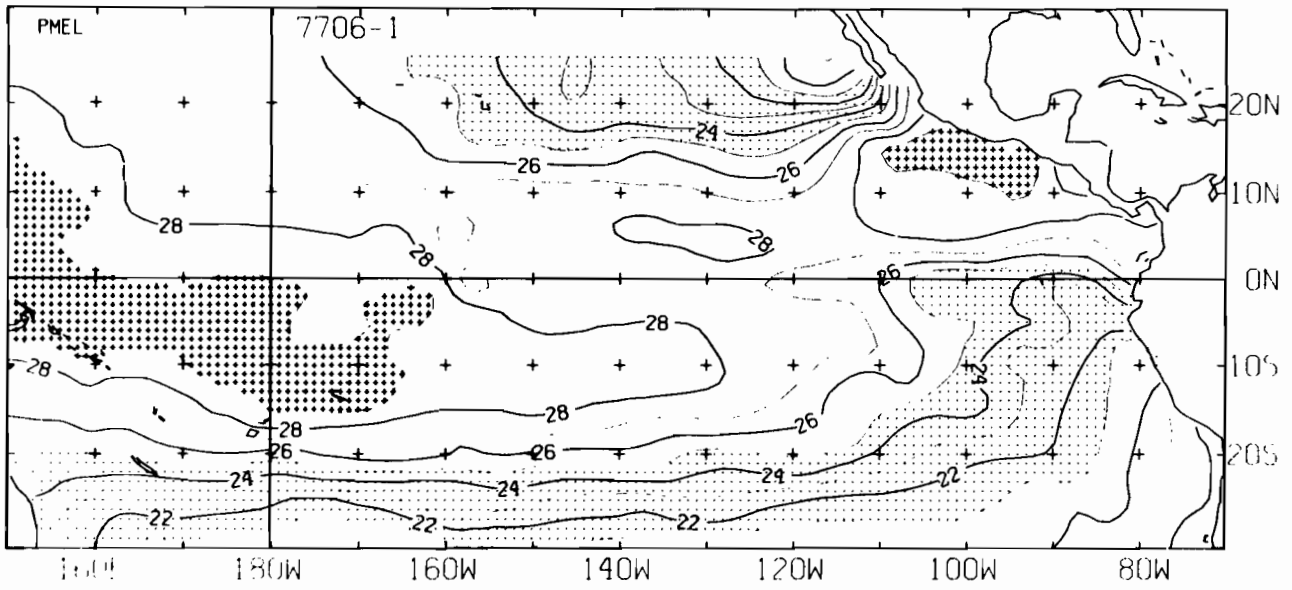

7706 1 SST. 0 E-BUØY. 0 BT. 0 XBT. 729 SPØT DATA

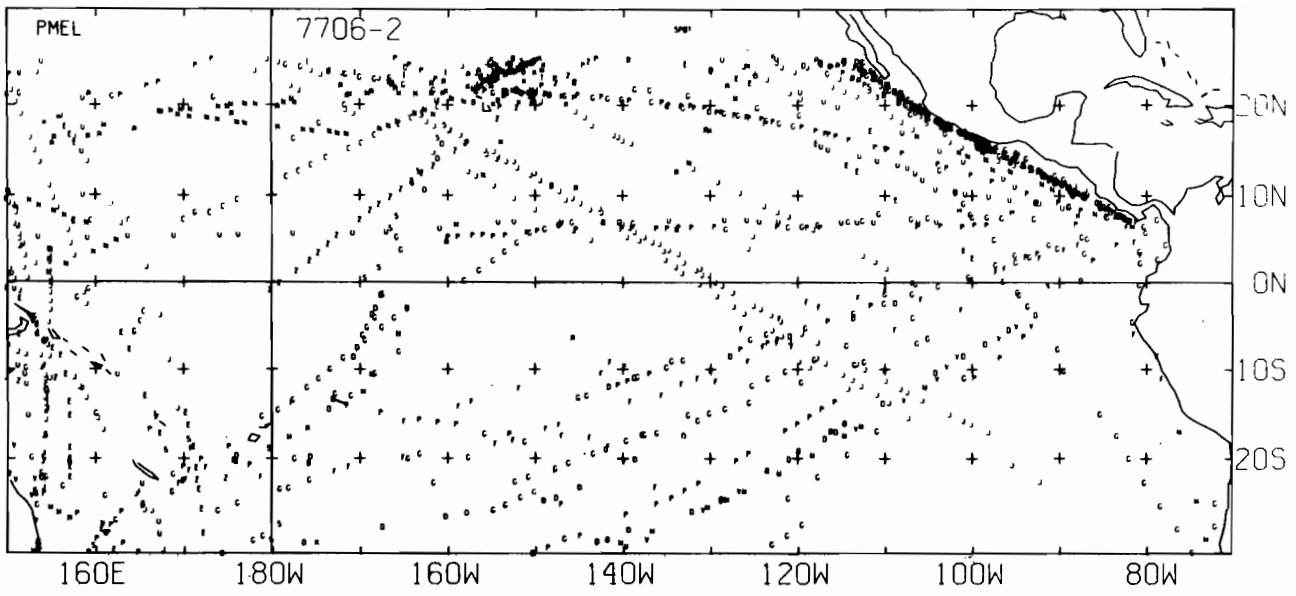

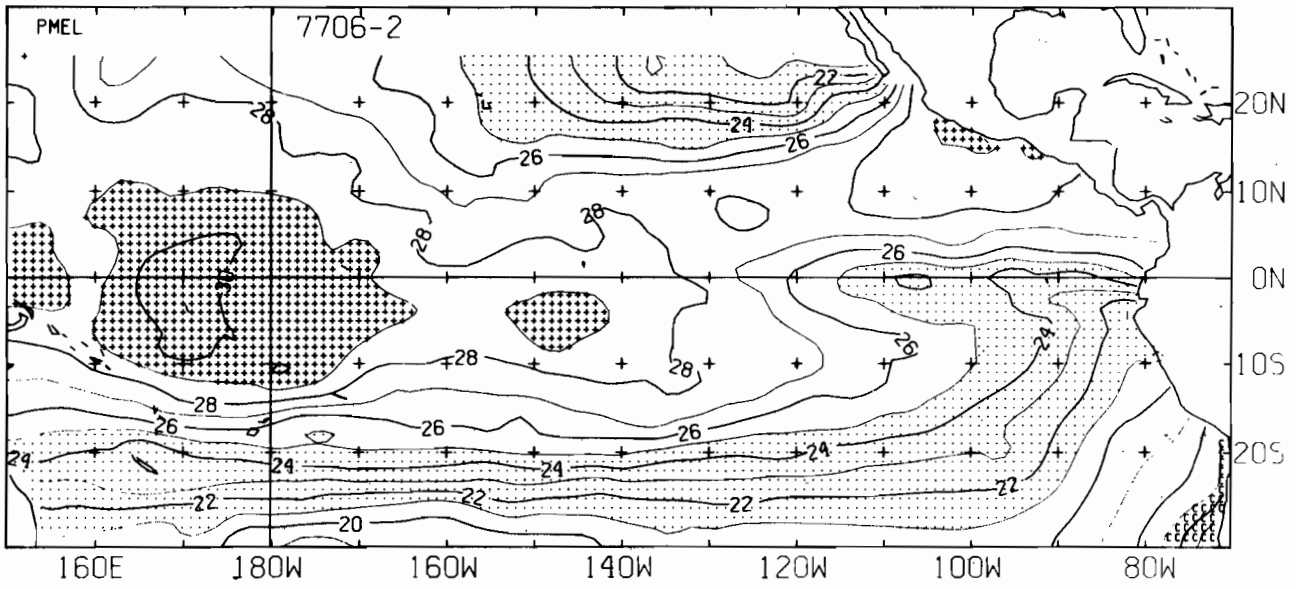

7706-2 SST. 0 E-BUØY. 0 BT. 0 XBT. 1362 SPØT DATA

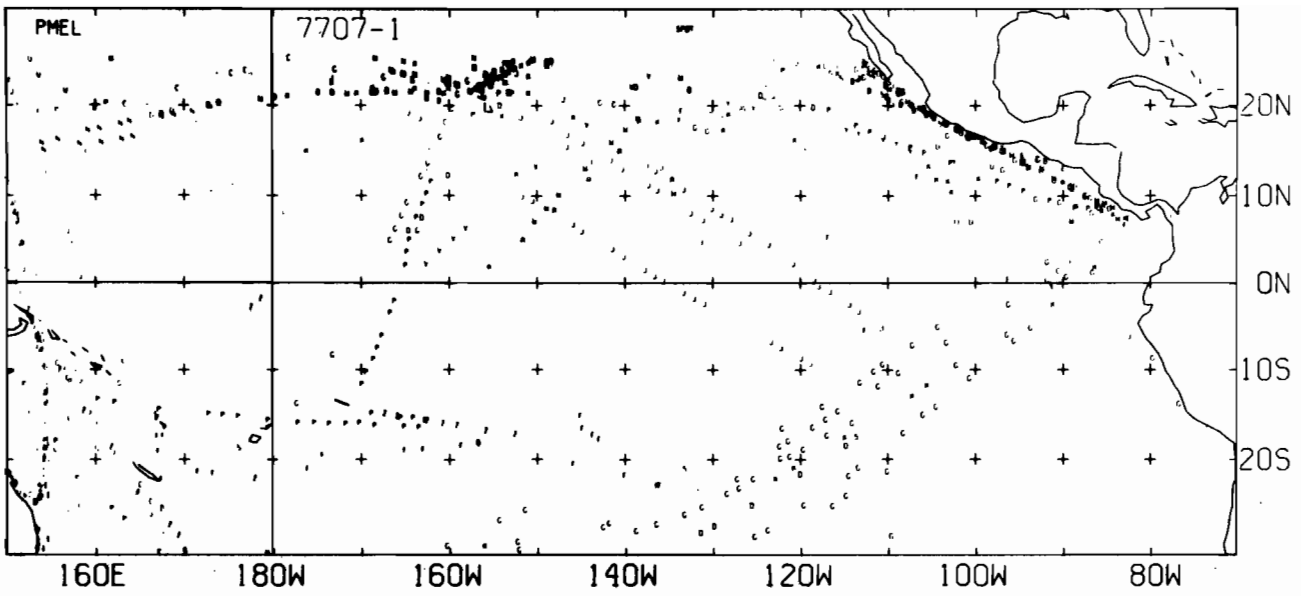

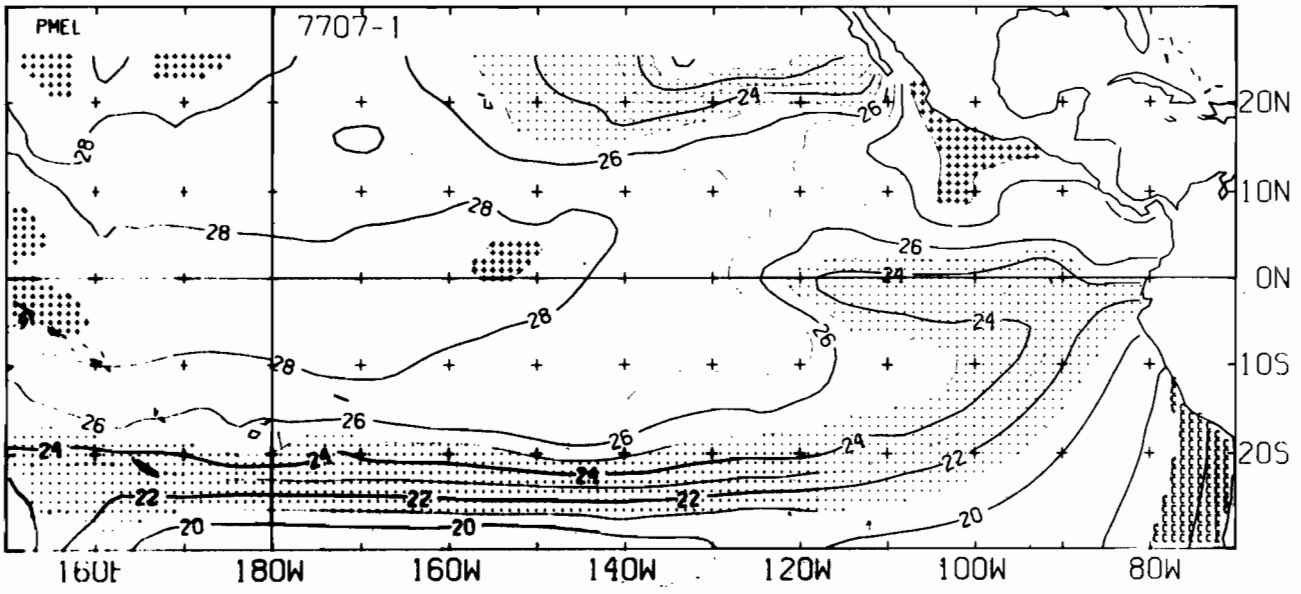

7707-1 SST. 0 E-BUØY. 0 BT. 0 XBT. 701 SPØT DATA

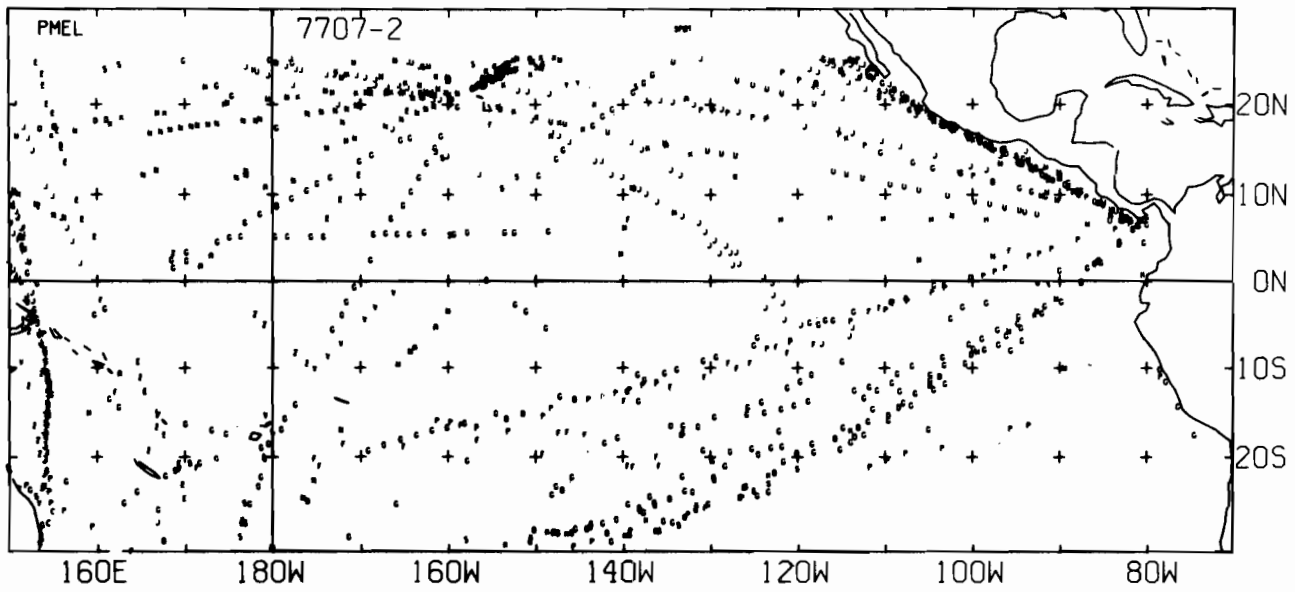

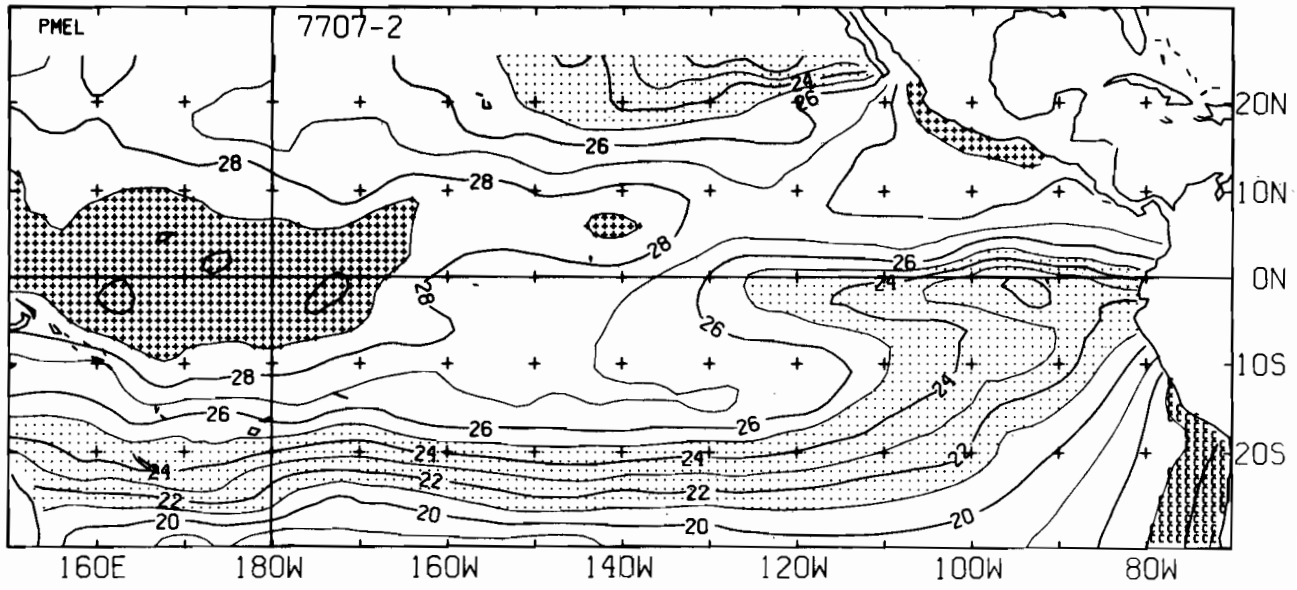

7707-2 SST. 0 E-BUØY. 0 BT. 0 XBT. 1076 SPØT DATA

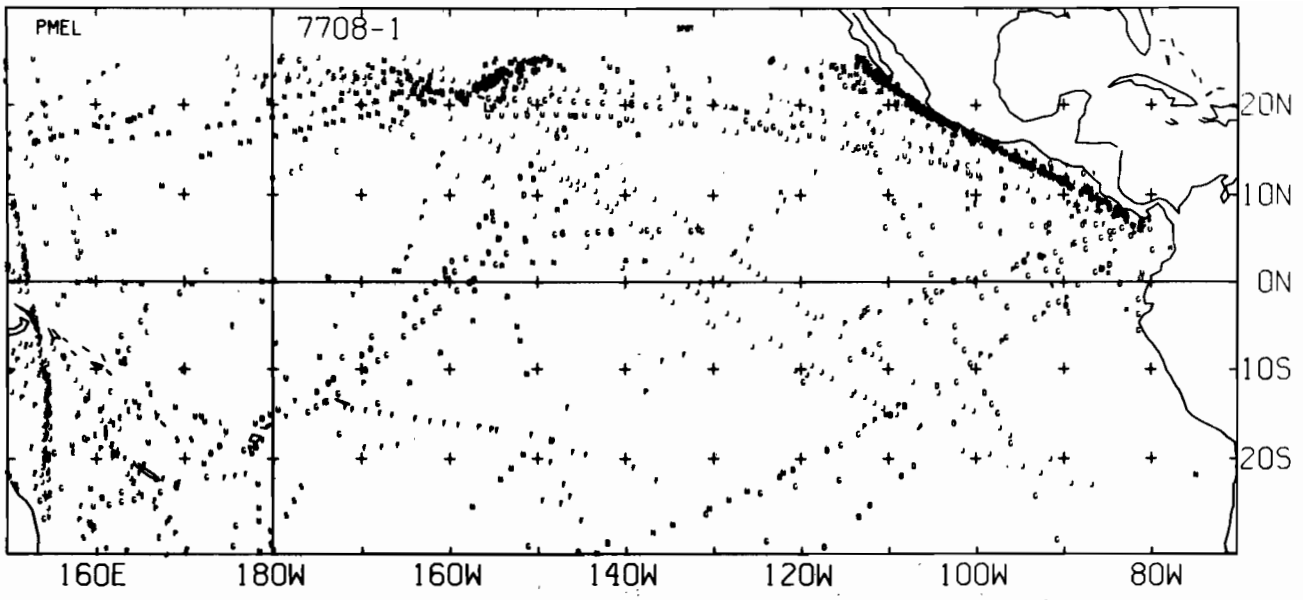

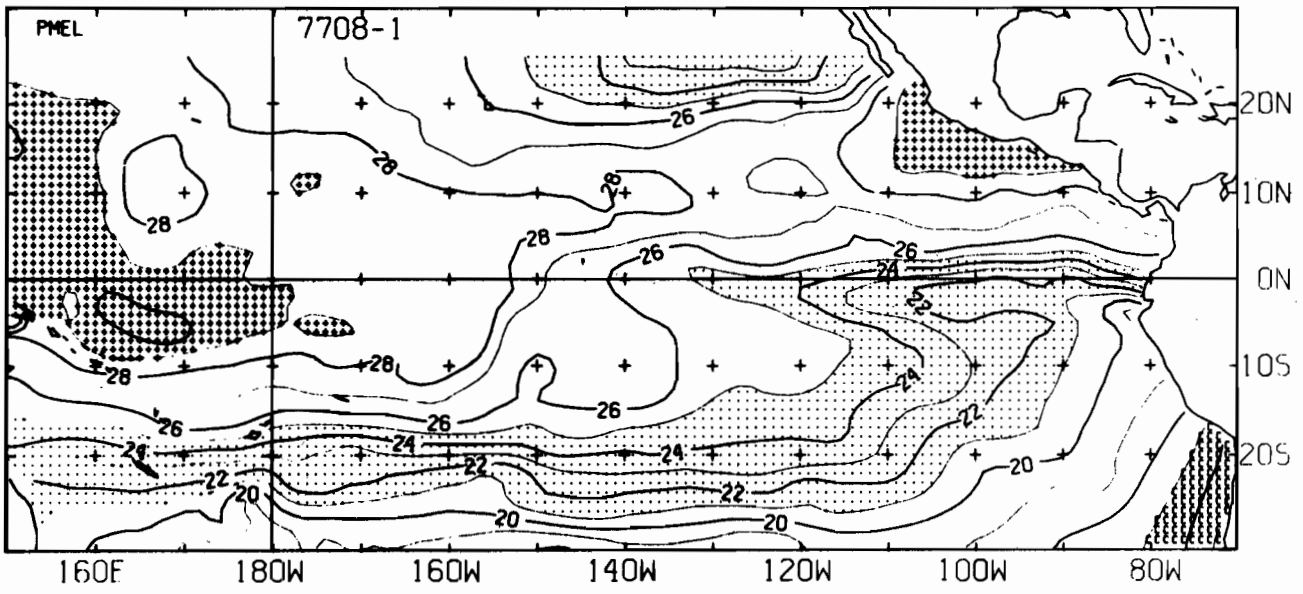

7708-1 SST. 0 E-BUØY. 0 BT. 0 XBT. 1389 SPØT DATA

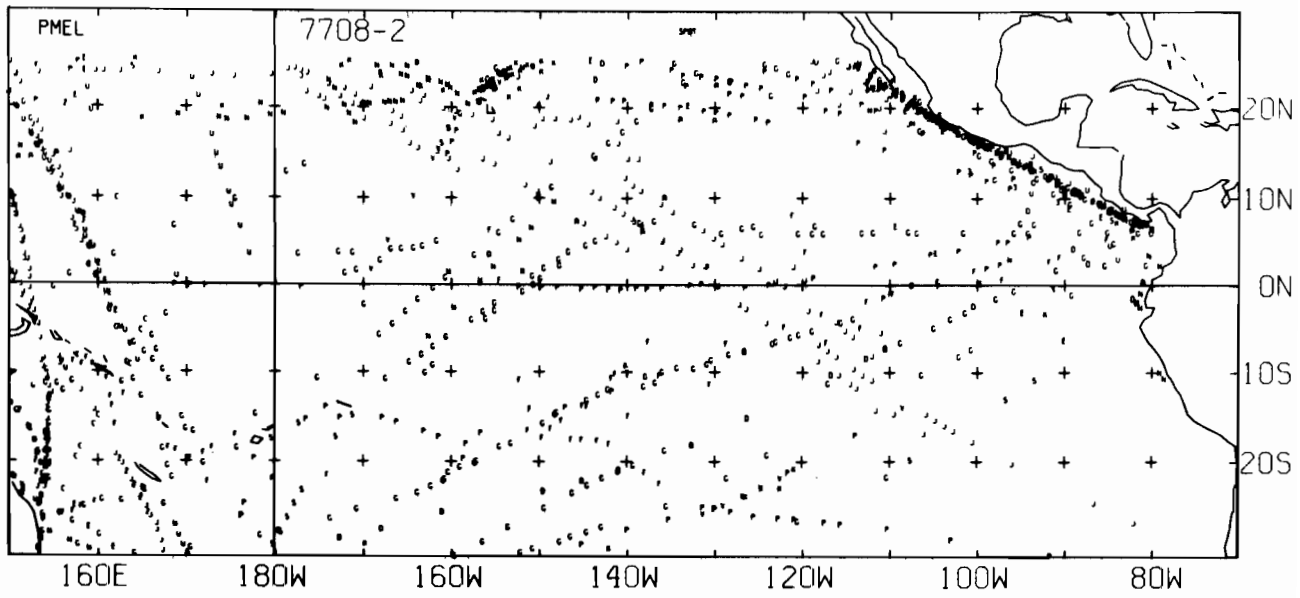

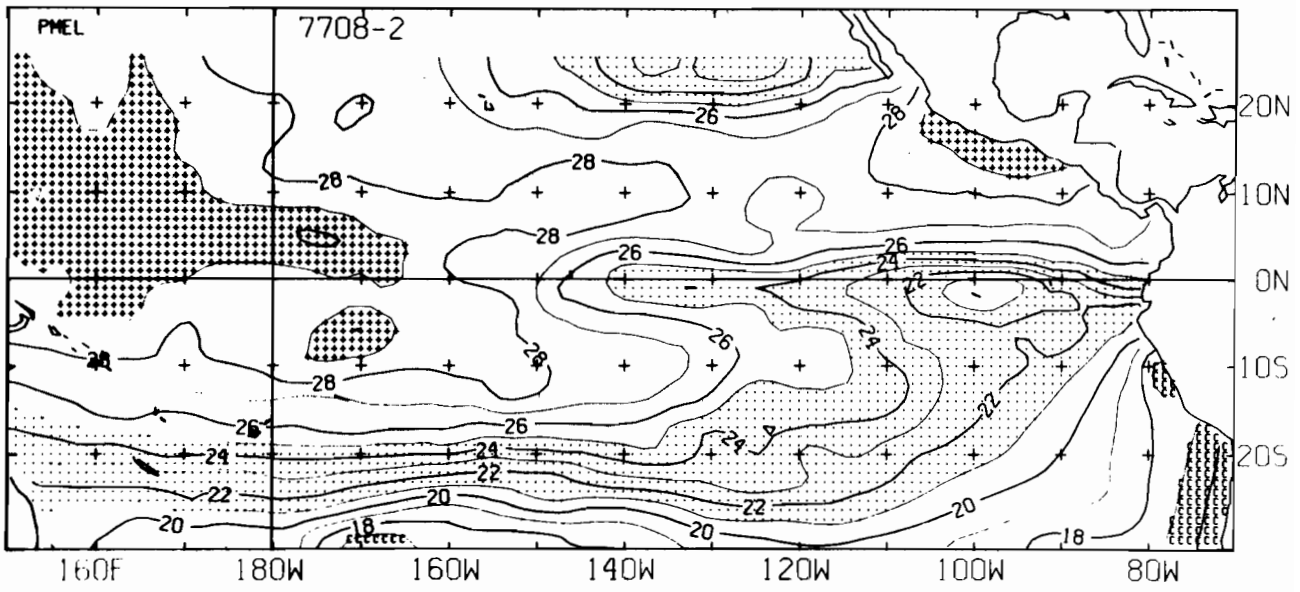

7708-2 SST. 0 E-BUØY. 0 BT. 0 XBT. 1172 SPØT DATA

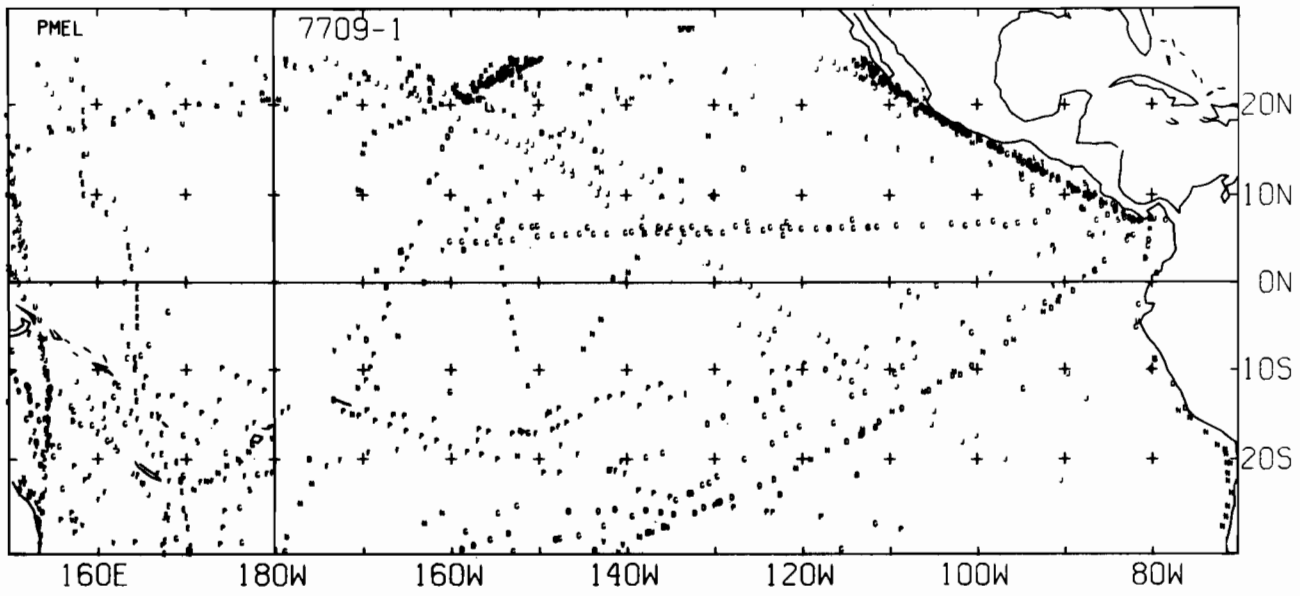

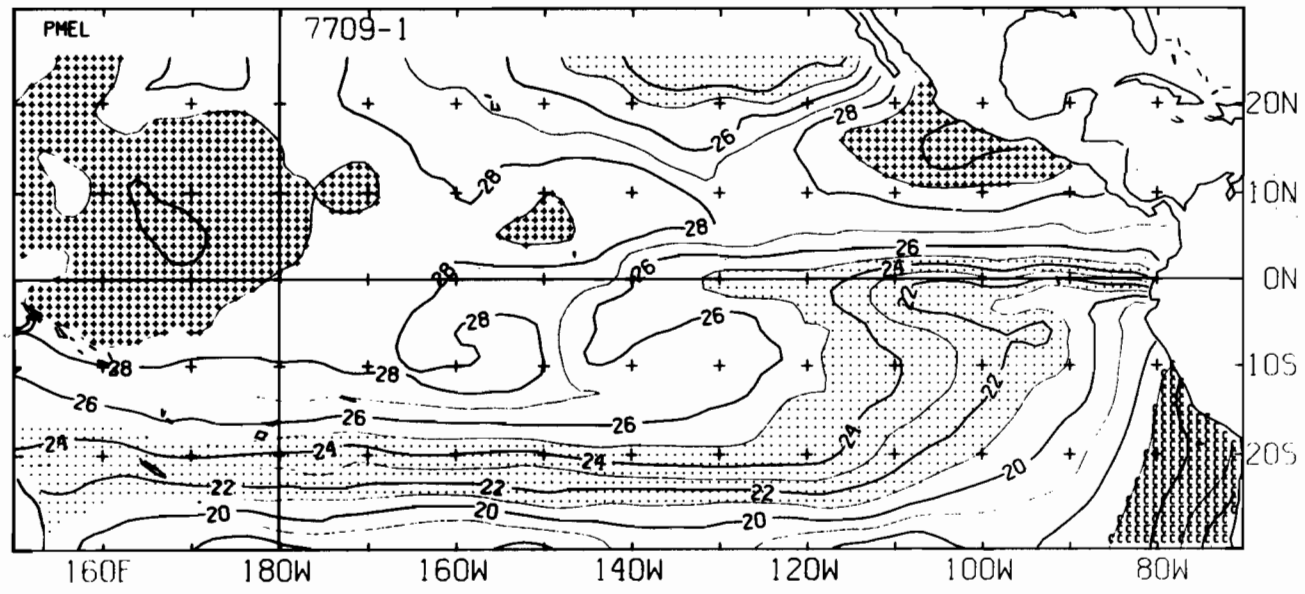

7709-1 SST. 0 E-BUØY. 0 BT. 0 XBT. 1095 SPØT DATA

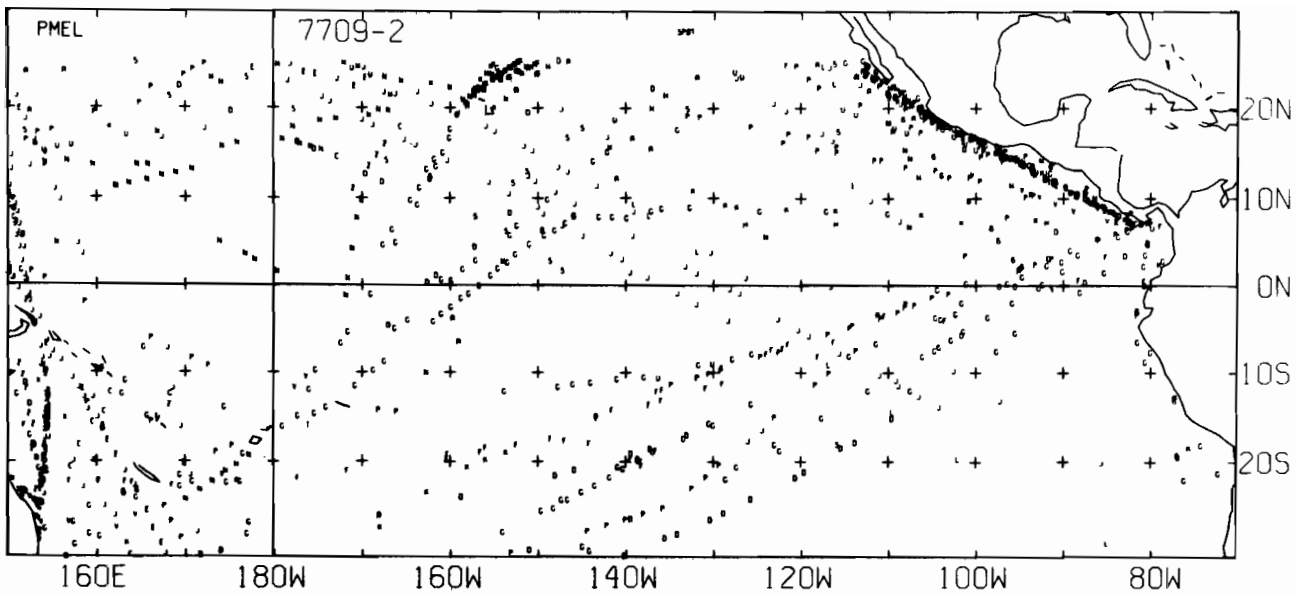

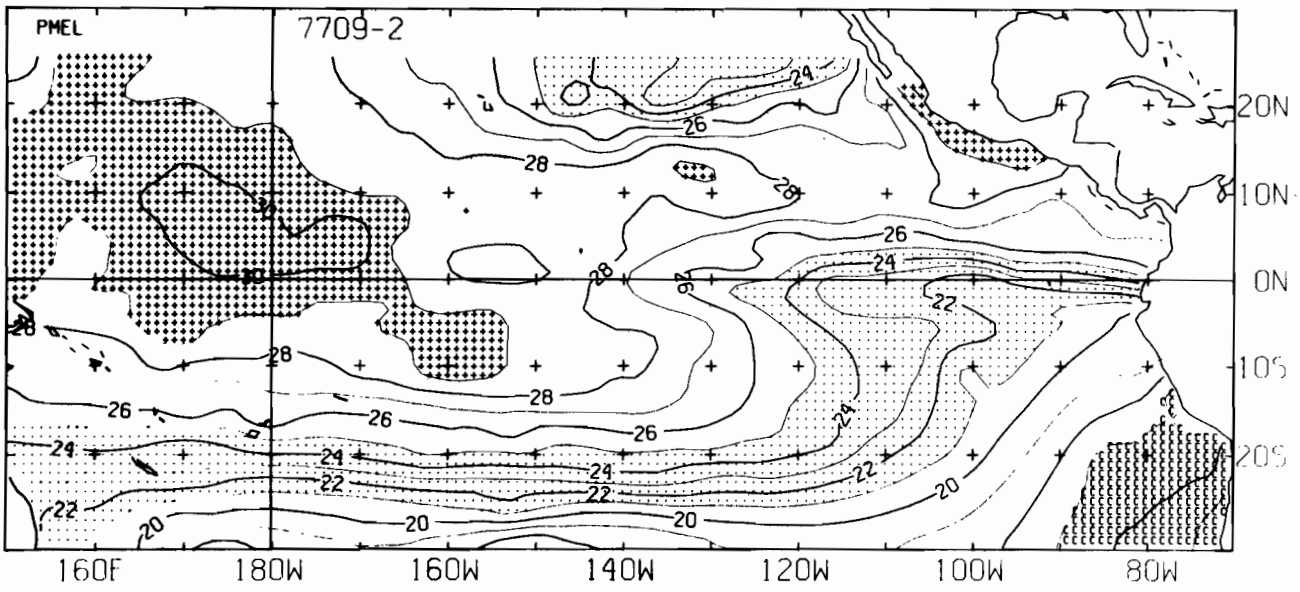

7709-2 SST. 0 E-BUØY. 0 BT. 0 XBT. 1058 SPØT DATA

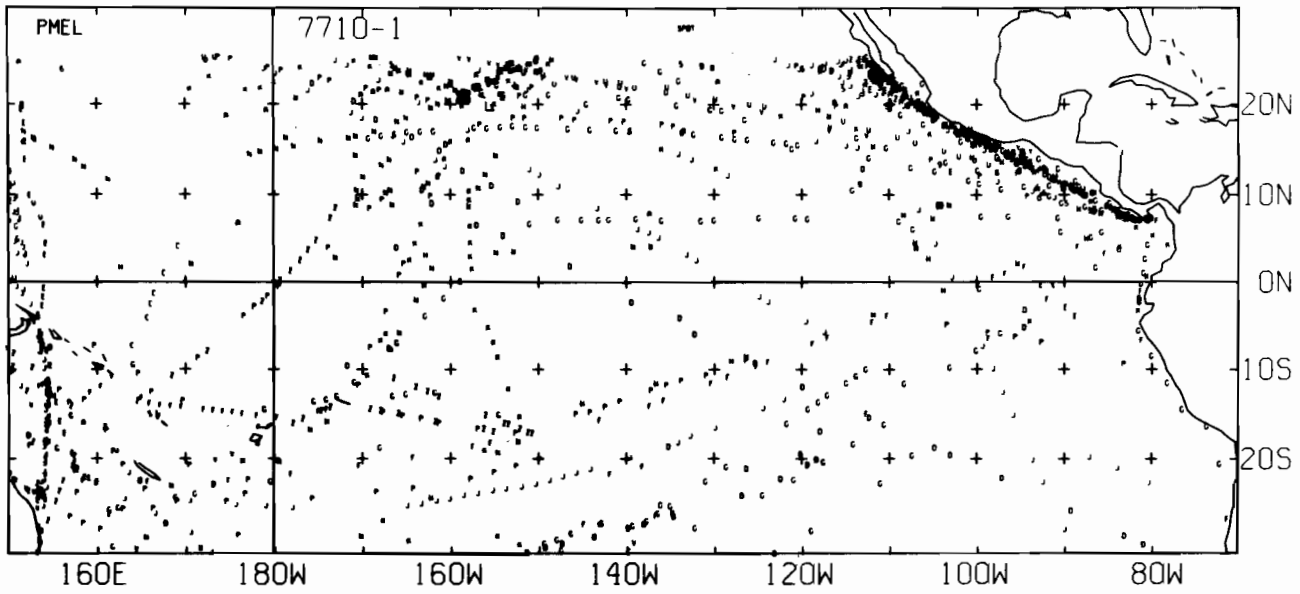

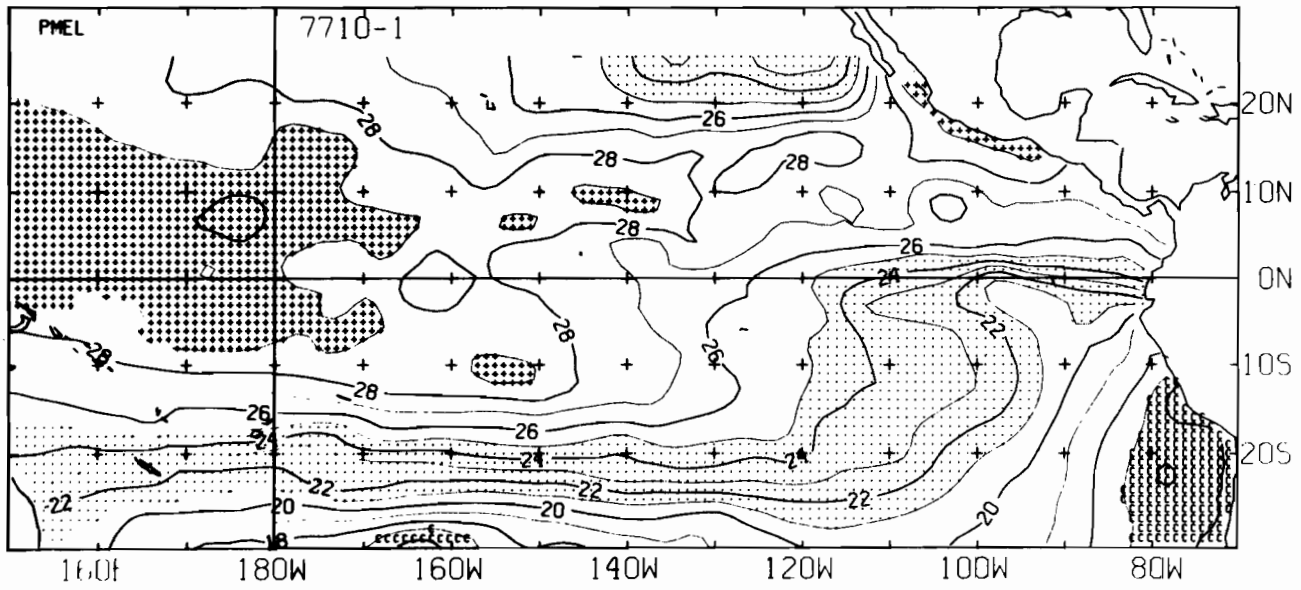

7710-1 SST. 0 E-BUØY. 0 BT. 0 XBT. 1234 SPØT DATA

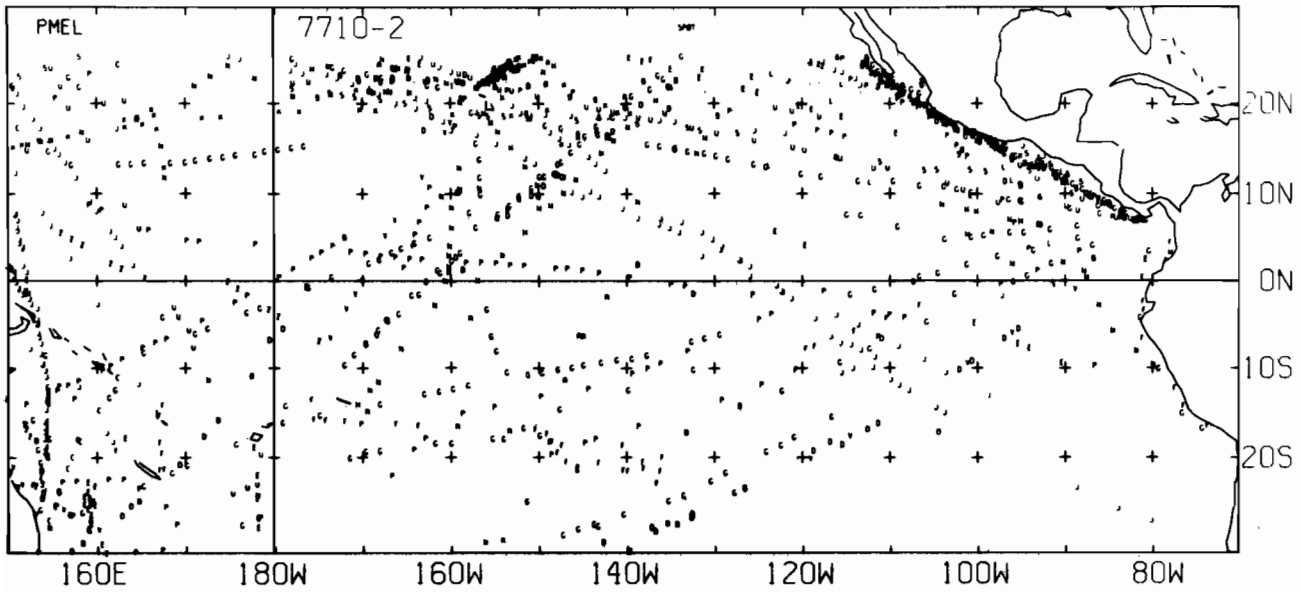

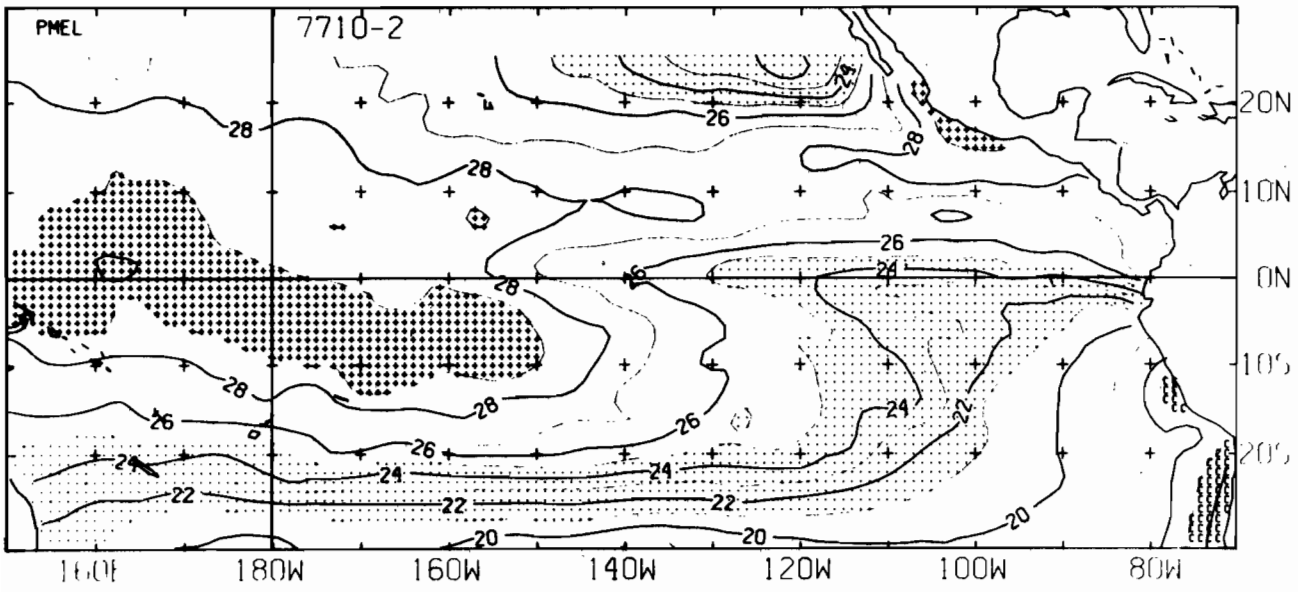

7710-2 SST. 0 E-BUØY. 0 BT. 0 XBT. 1256 SPØT DATA

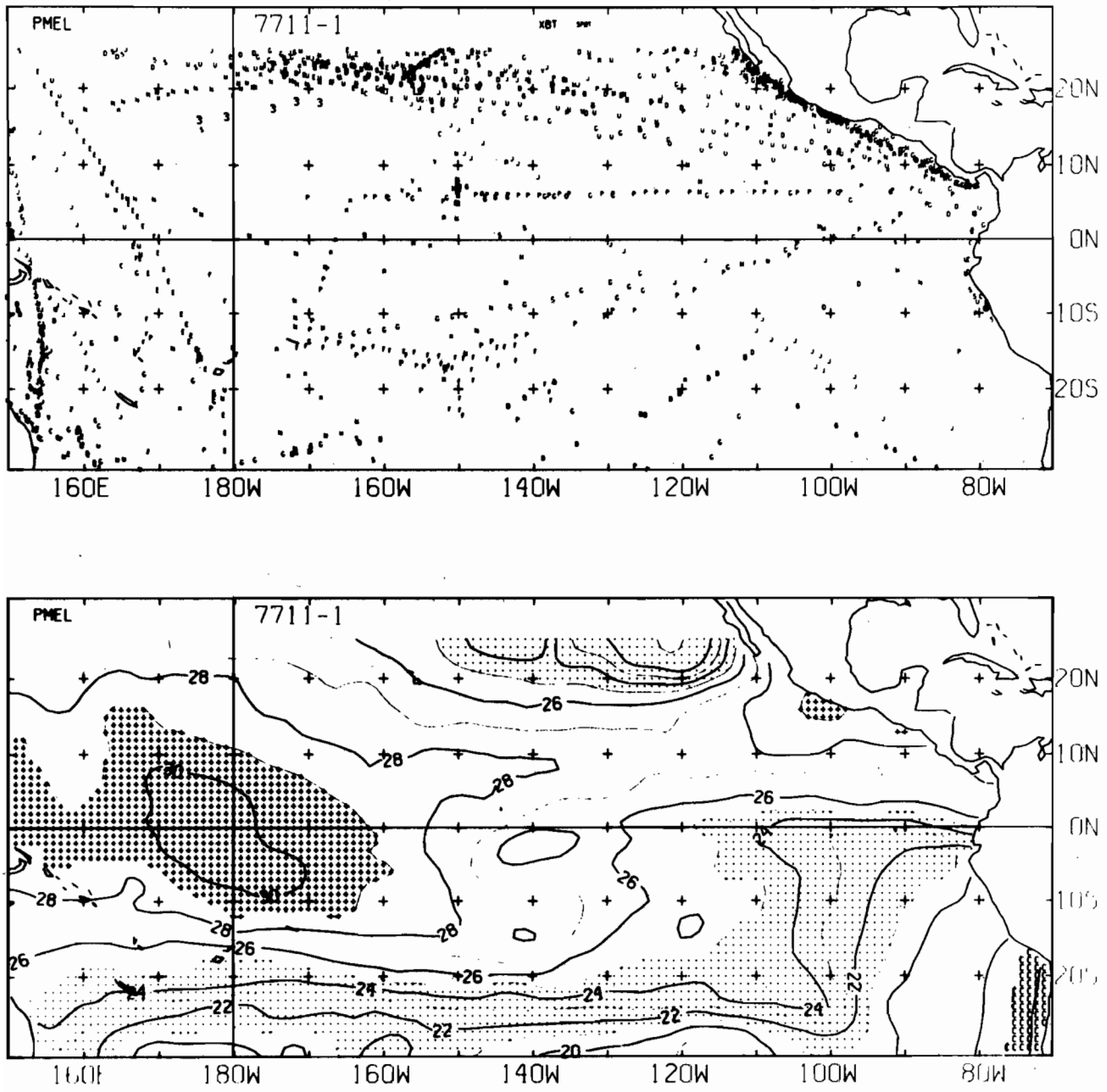

7711-1 SST. 0 E-BUØY. 0 BT. 5 XBT. 1186 SPØT DATA

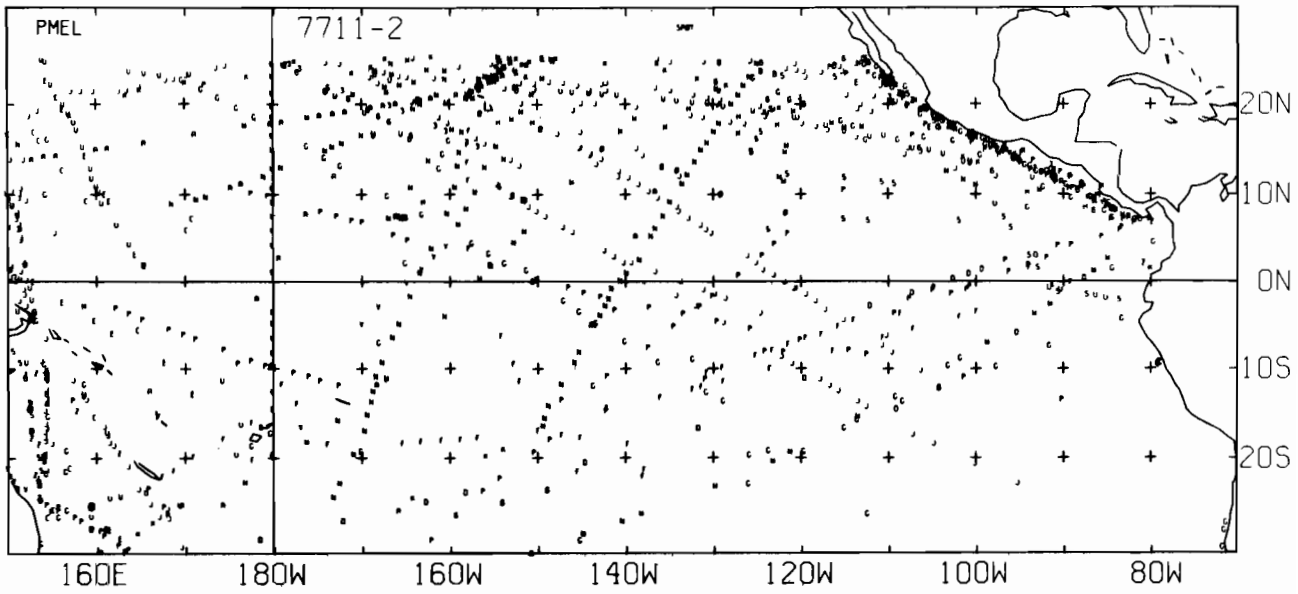

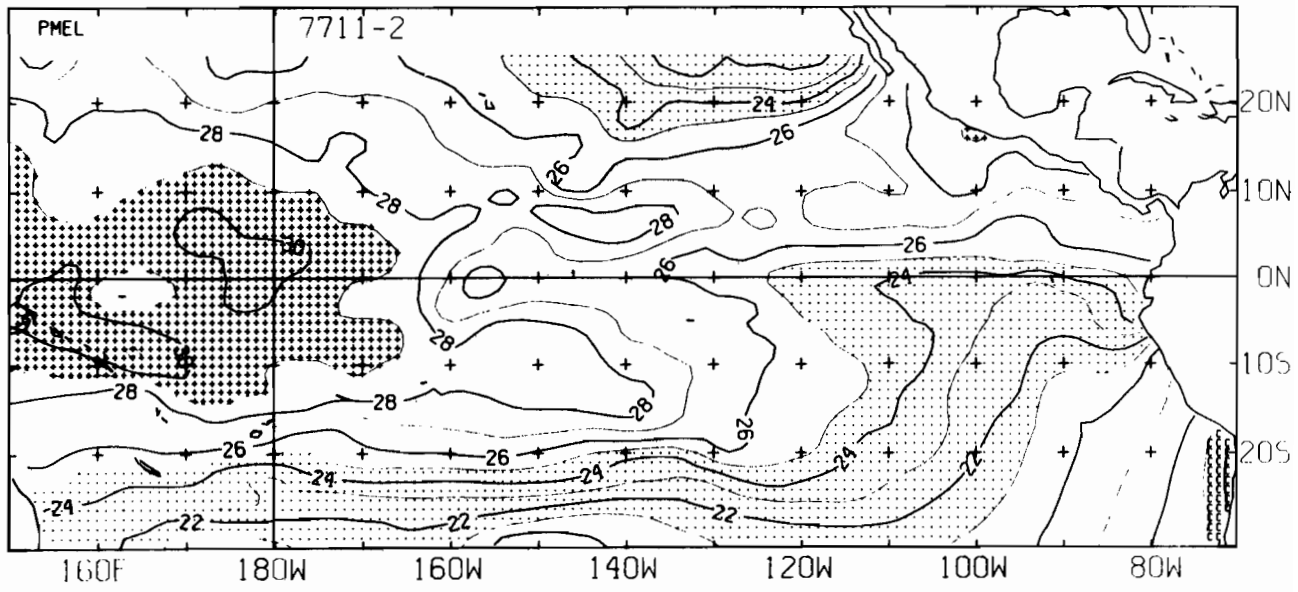

7711-2 SST. 0 E-BUØY. 0 BT. 0 XBT. 1163 SPØT DATA

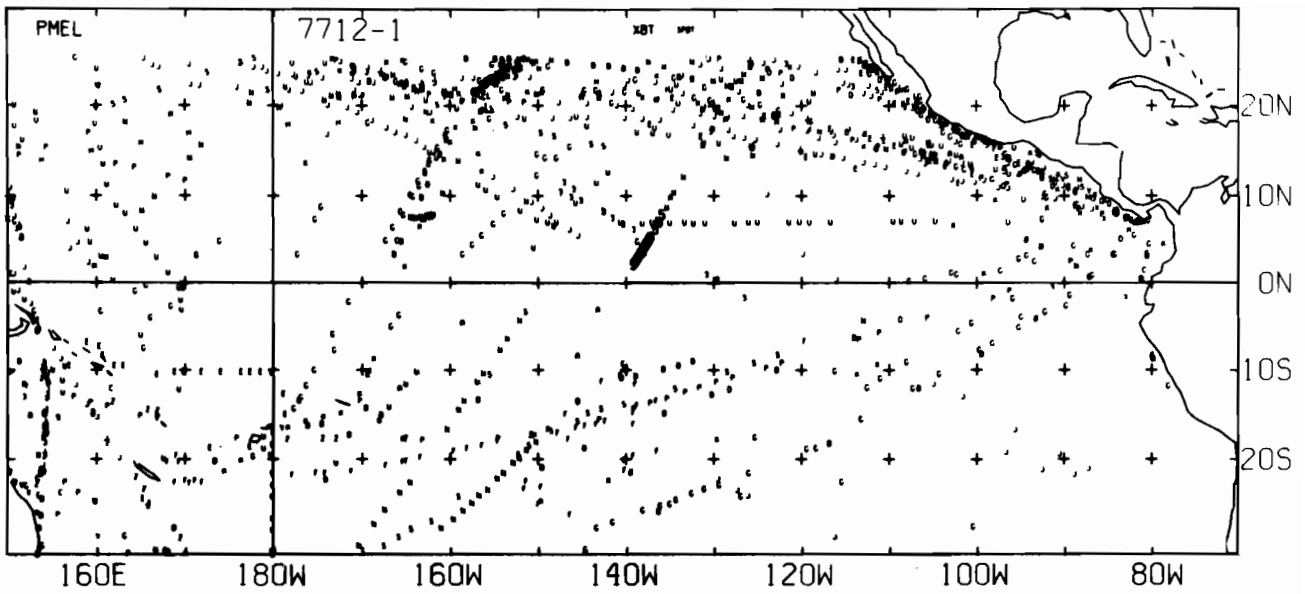

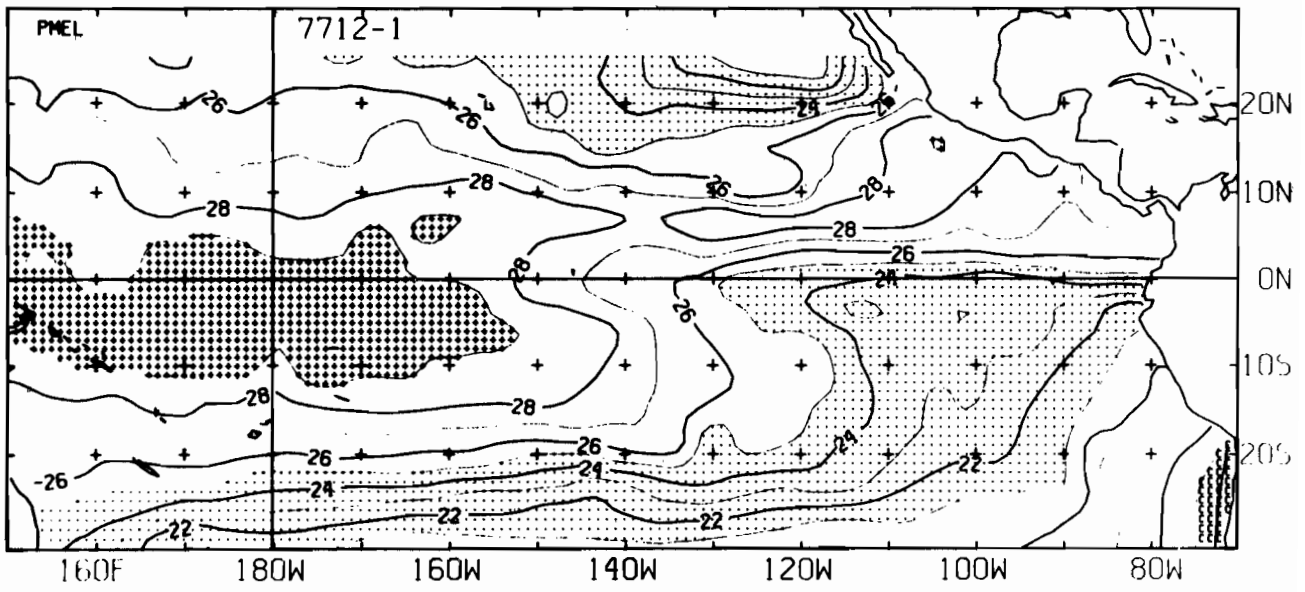

7712-1 SST. 0 E-BUØY. 0 BT. 15 XBT. 1277 SPØT DATA

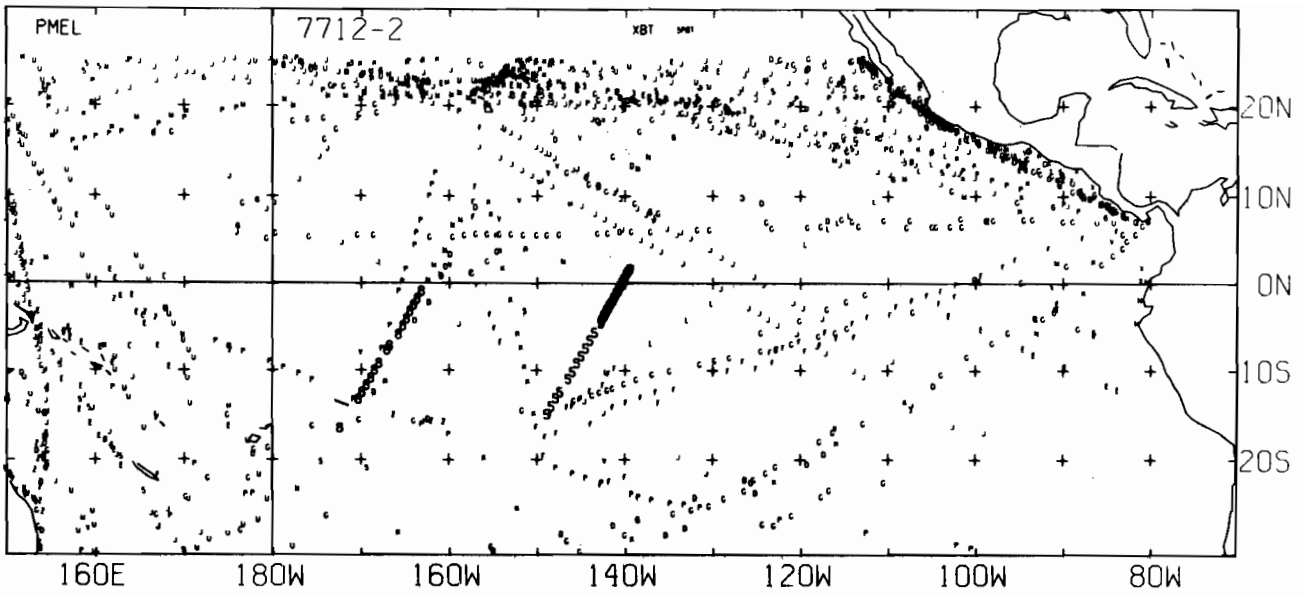

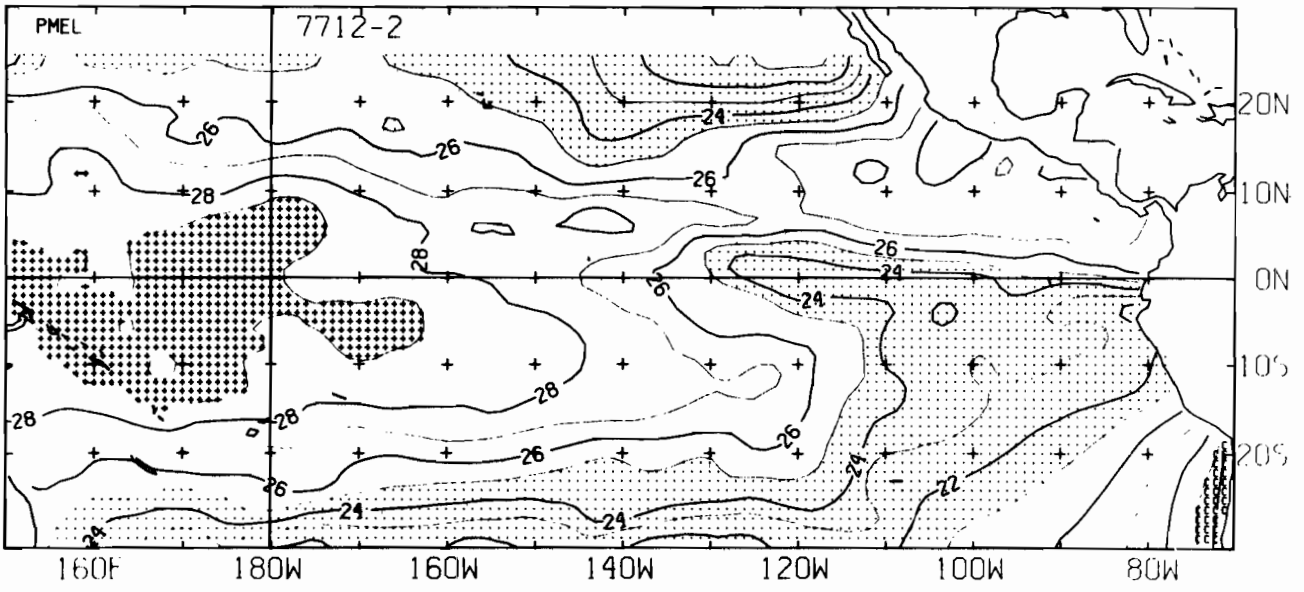

7712-2 SST. 0 E-BUØY. 0 BT. 50 XBT. 1417 SPØT DATA

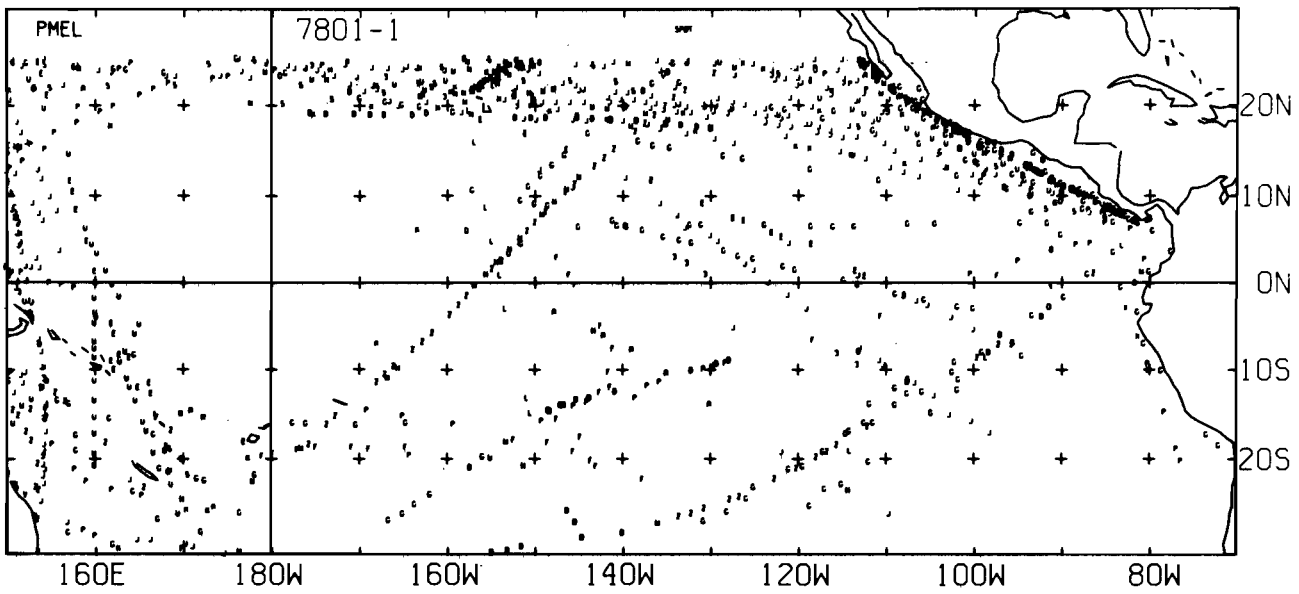

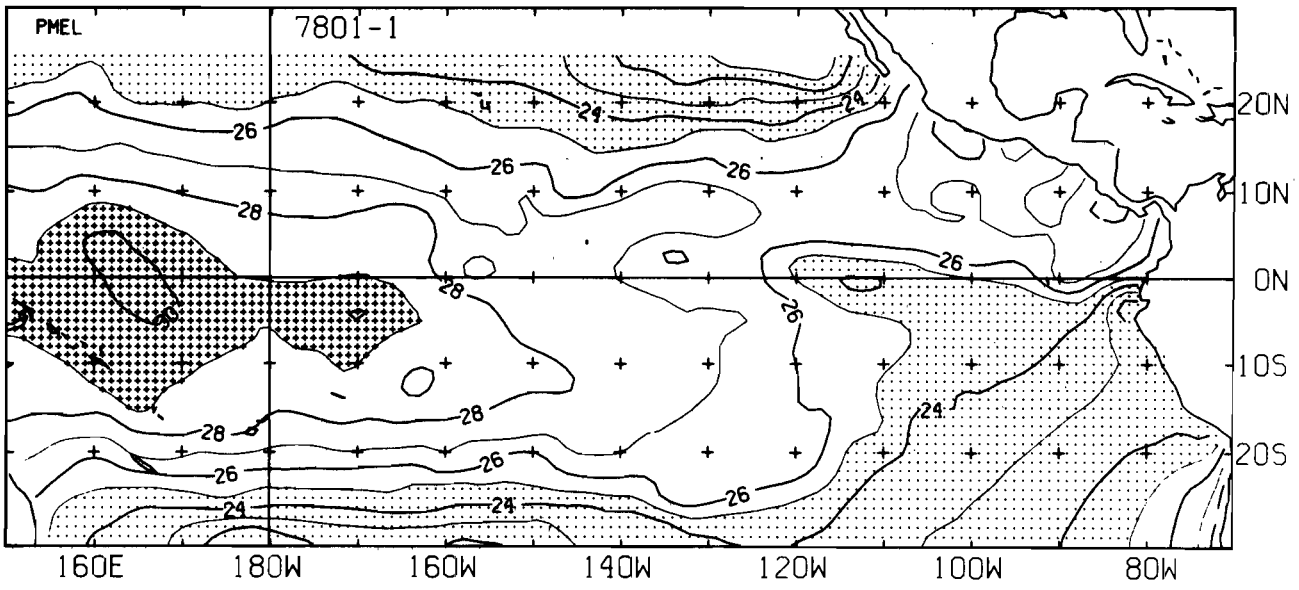

7801-1 SST. 0 E-BUØY. 0 BT. 0 XBT. 1113 SPØT DATA

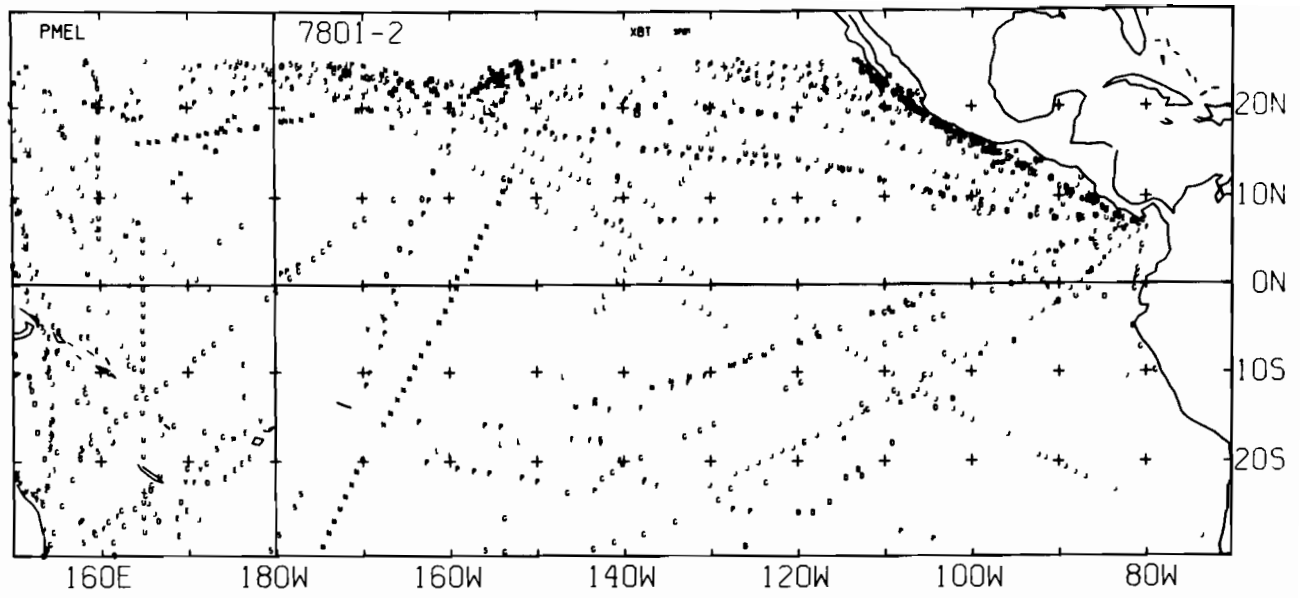

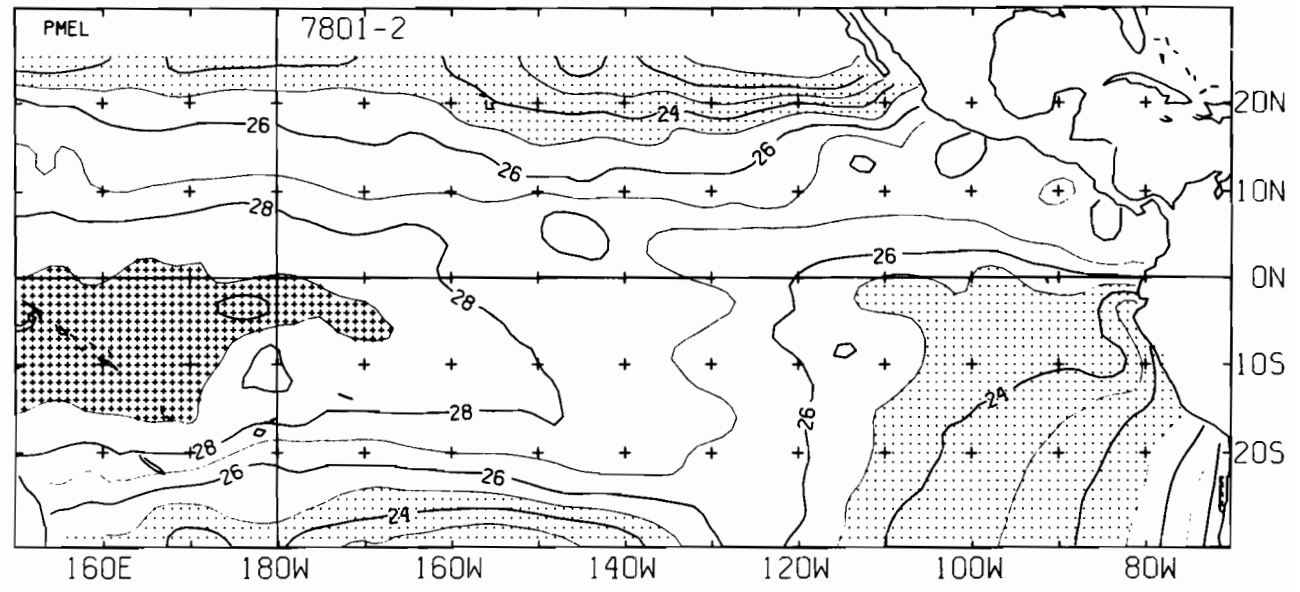

7801-2 SST. 0 E-BUØY. 0 BT. 1 XBT. 1218 SPØT DATA

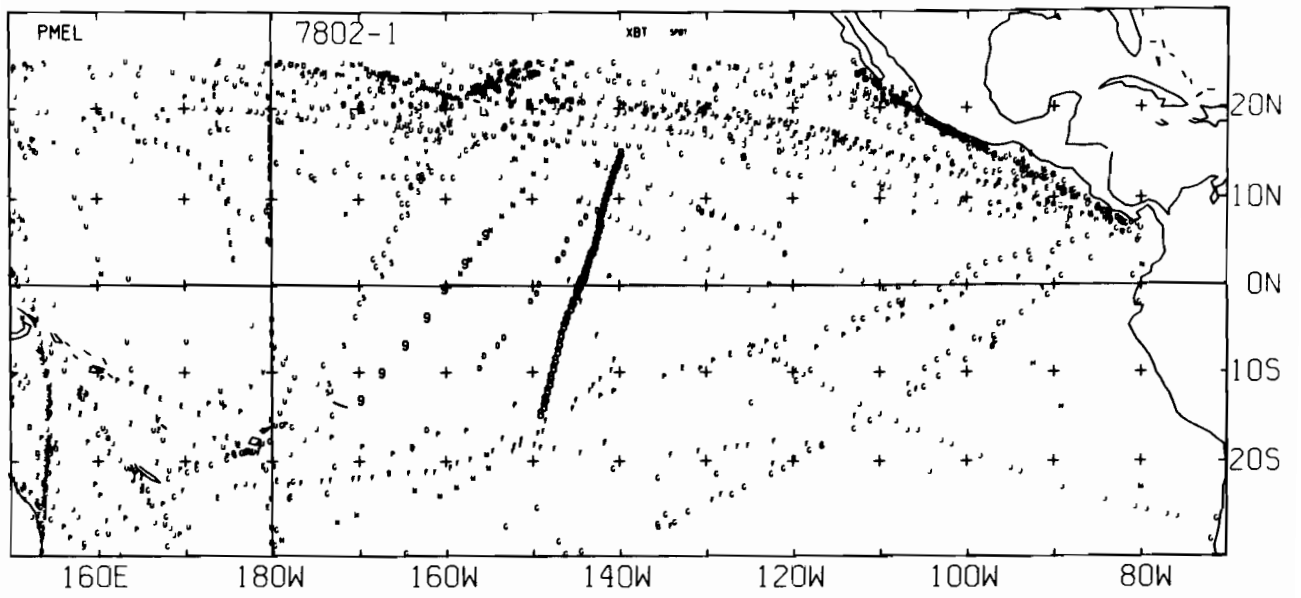

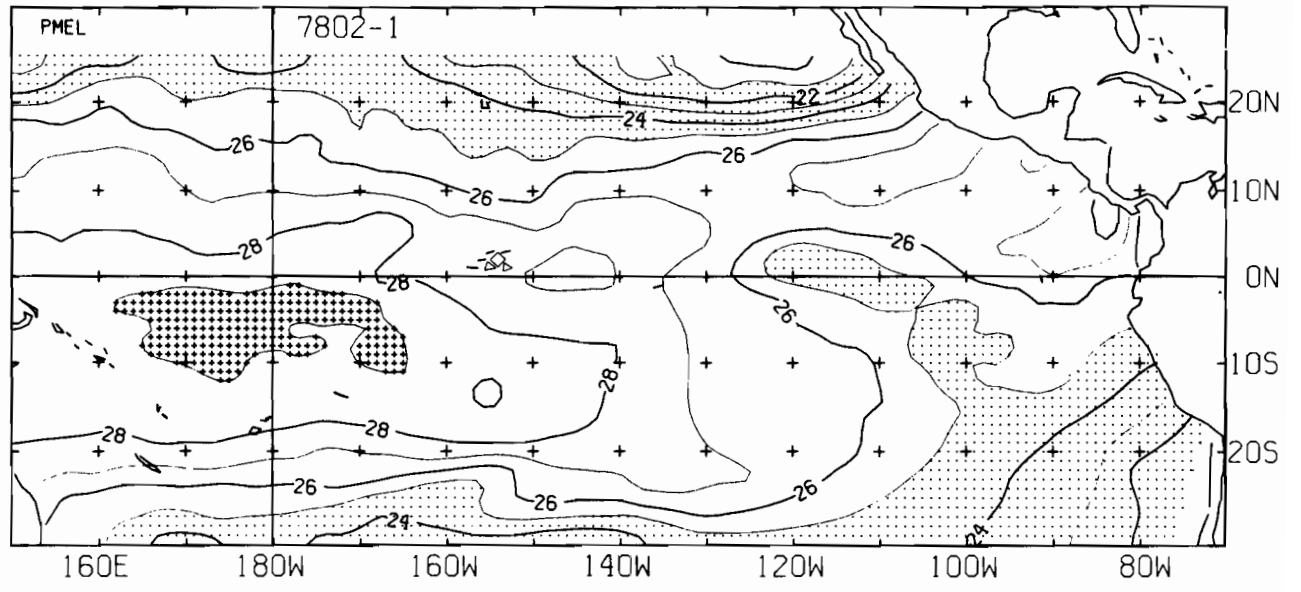

7802-1 SST. 0 E-BUØY. 0 BT. 61 XBT. 1536 SPØT DATA

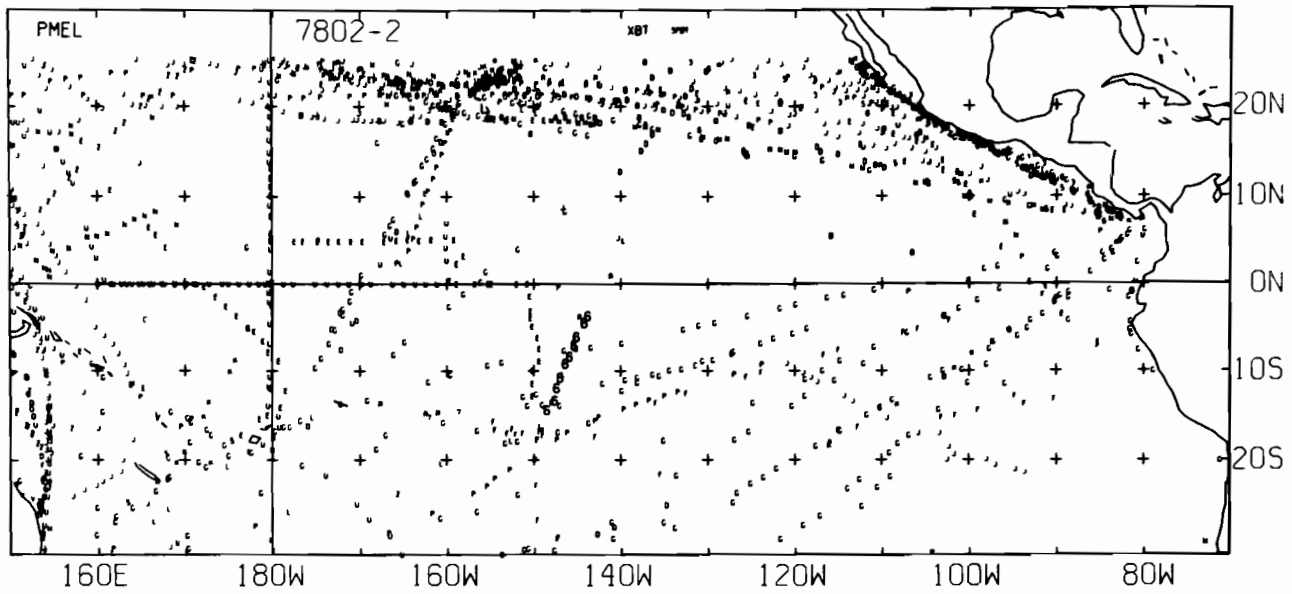

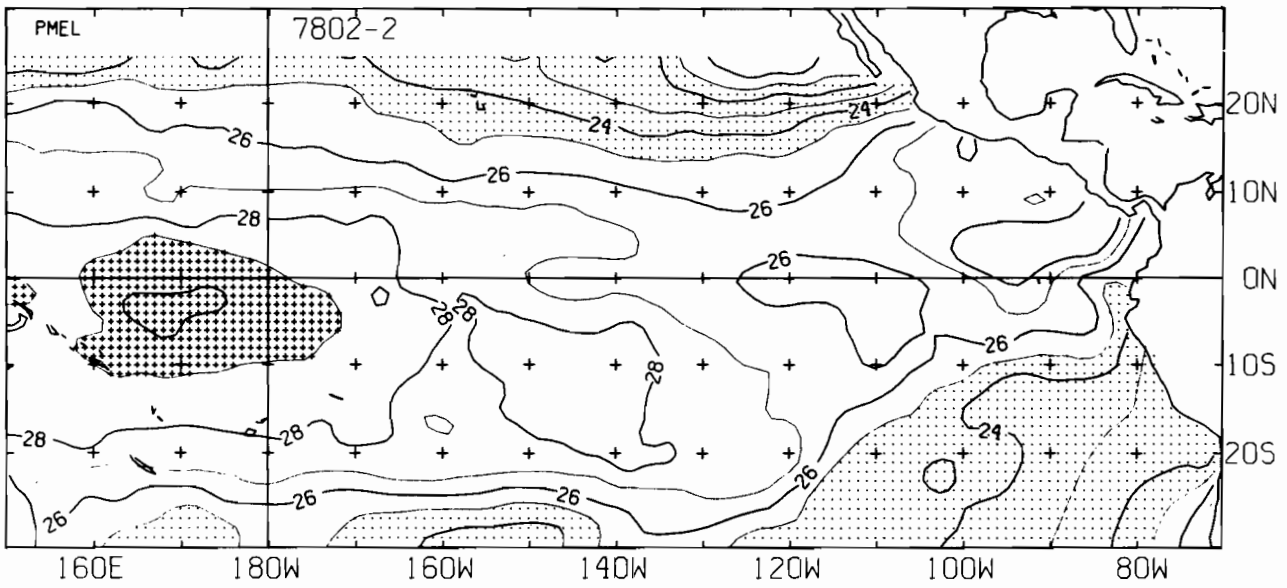

7802-2 SST. 0 E-BUØY. 0 BT. 10 XBT. 1532 SPØT DATA

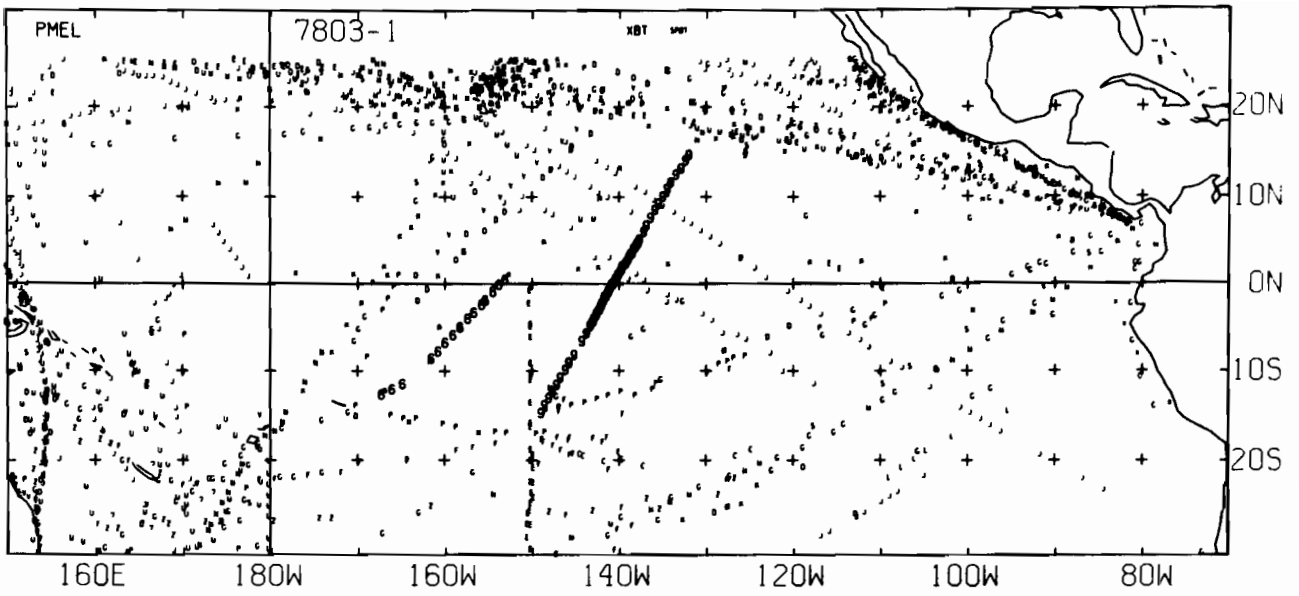

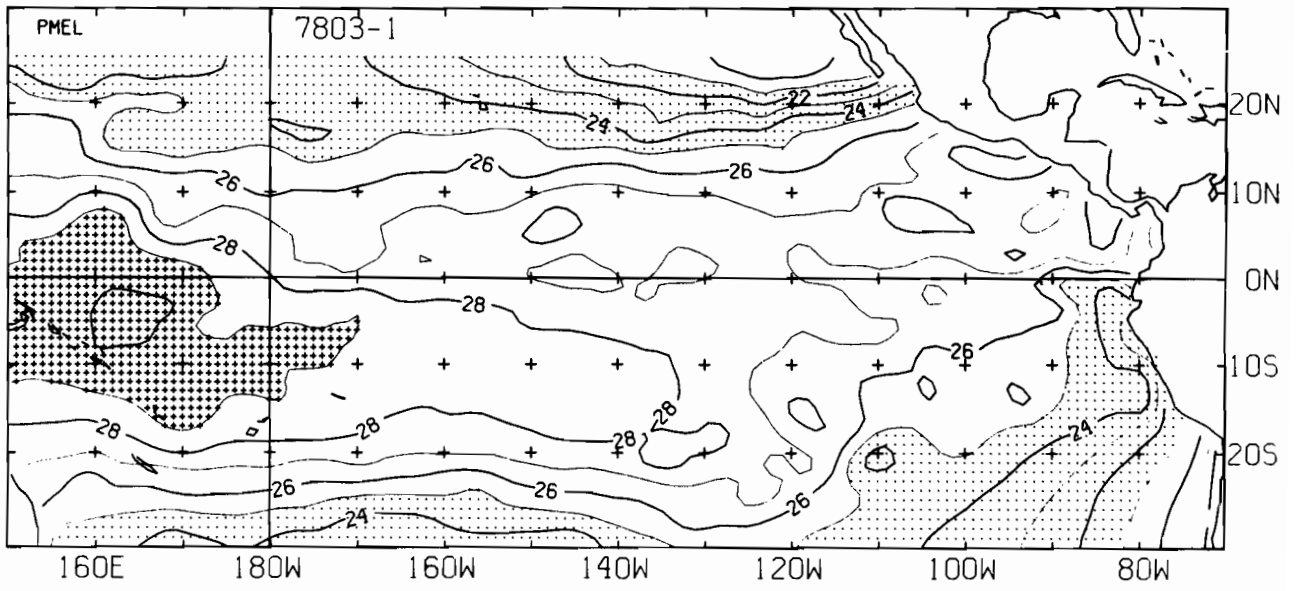

7803-1 SST. 0 E-BUØY. 0 BT. 75 XBT. 1443 SPØT DATA

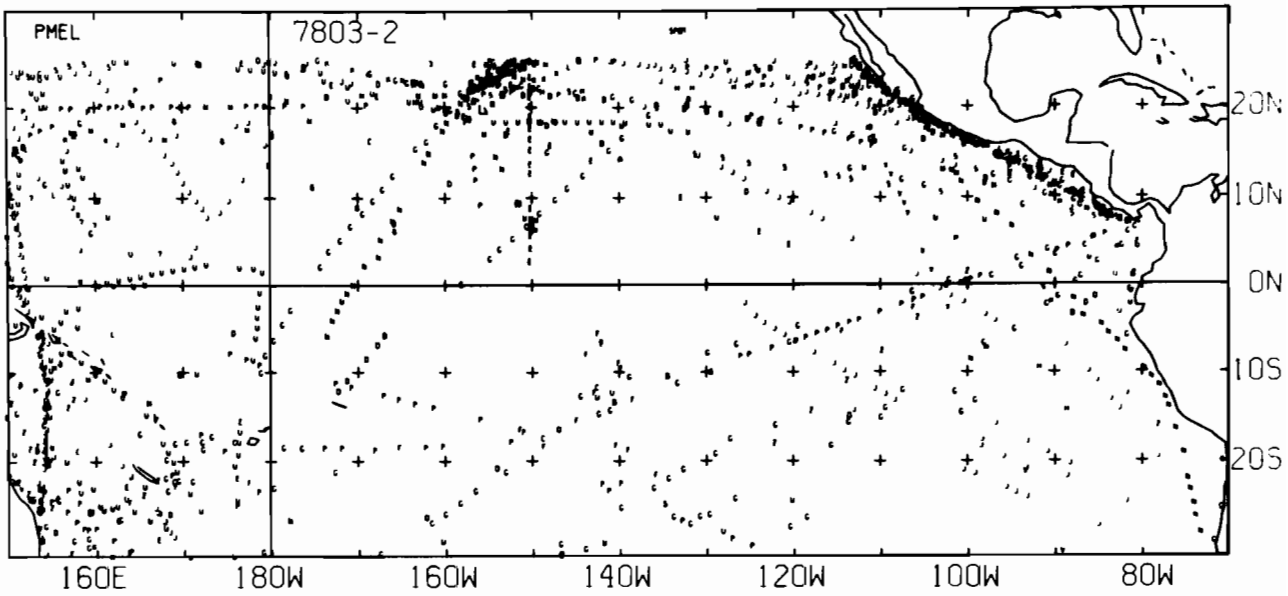

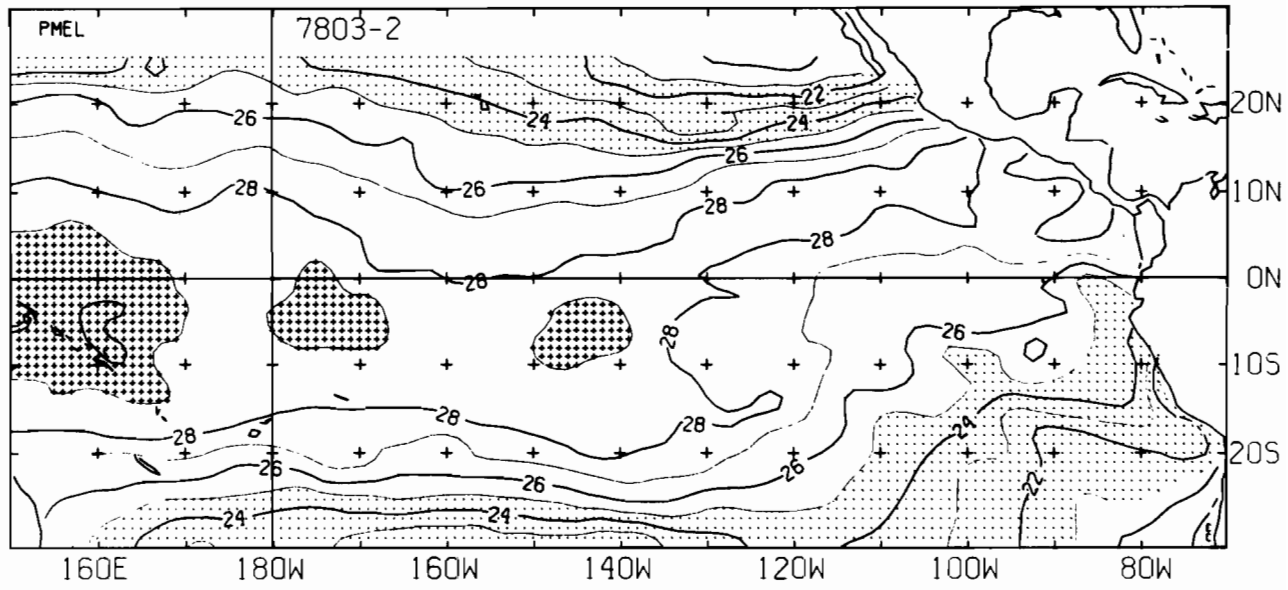

7803-2 SST. 0 E-BUØY. 0 BT. 0 XBT. 1348 SPØT DATA

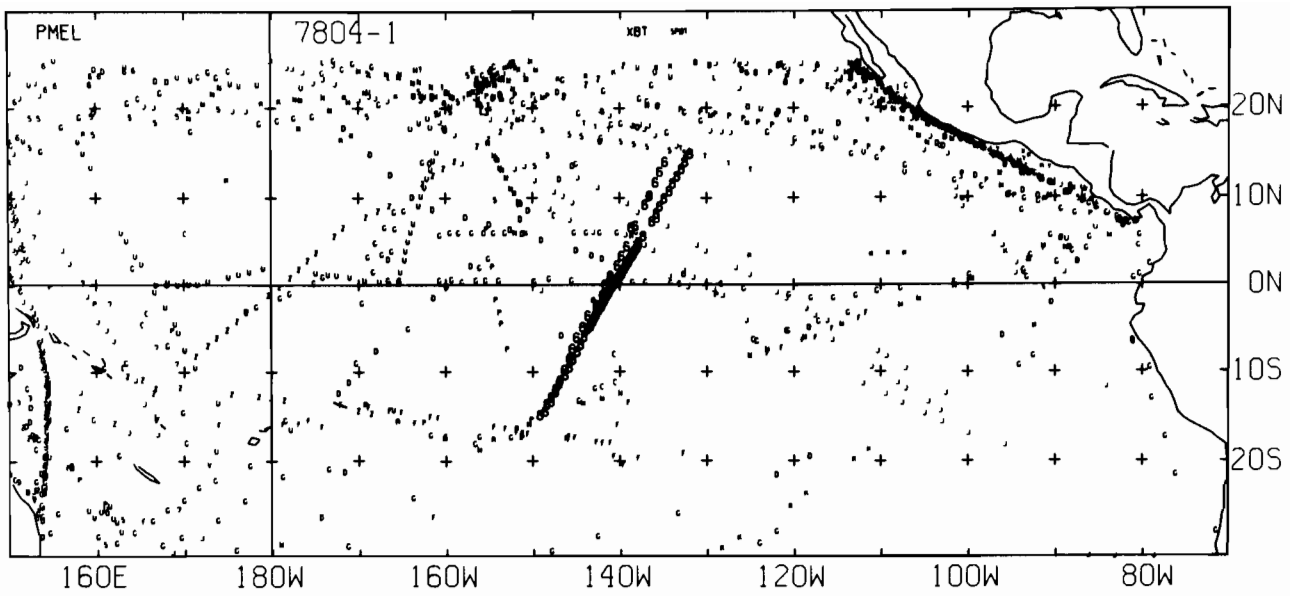

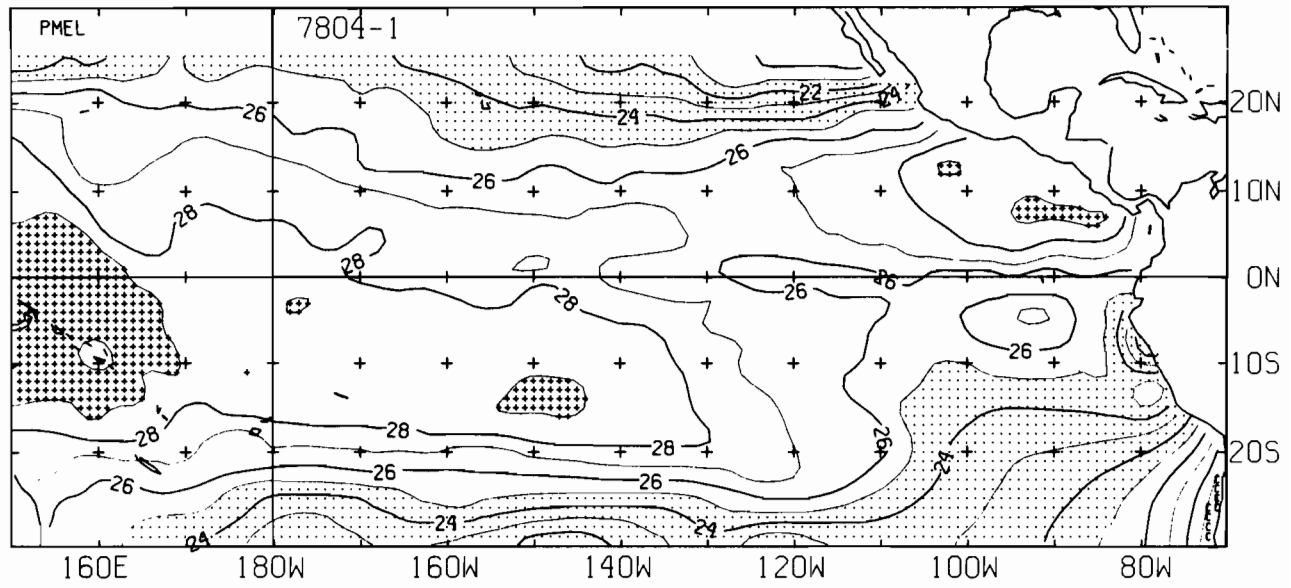

7804-1 SST. 0 E-BUØY. 0 BT. 83 XBT. 1227 SPØT DATA

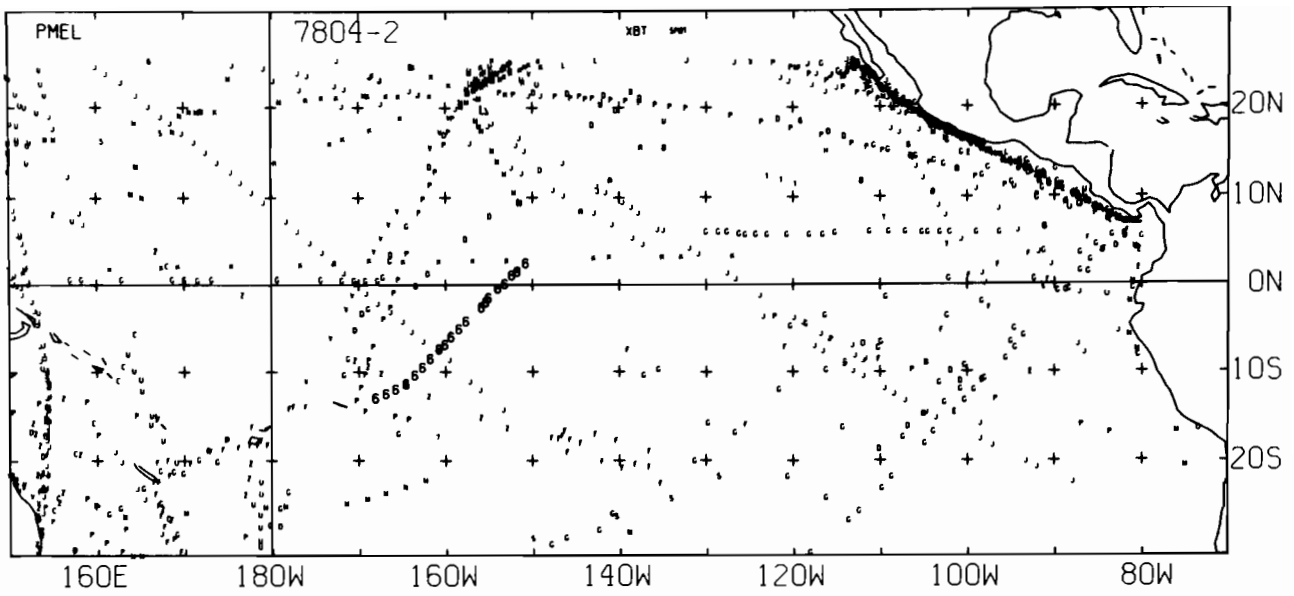

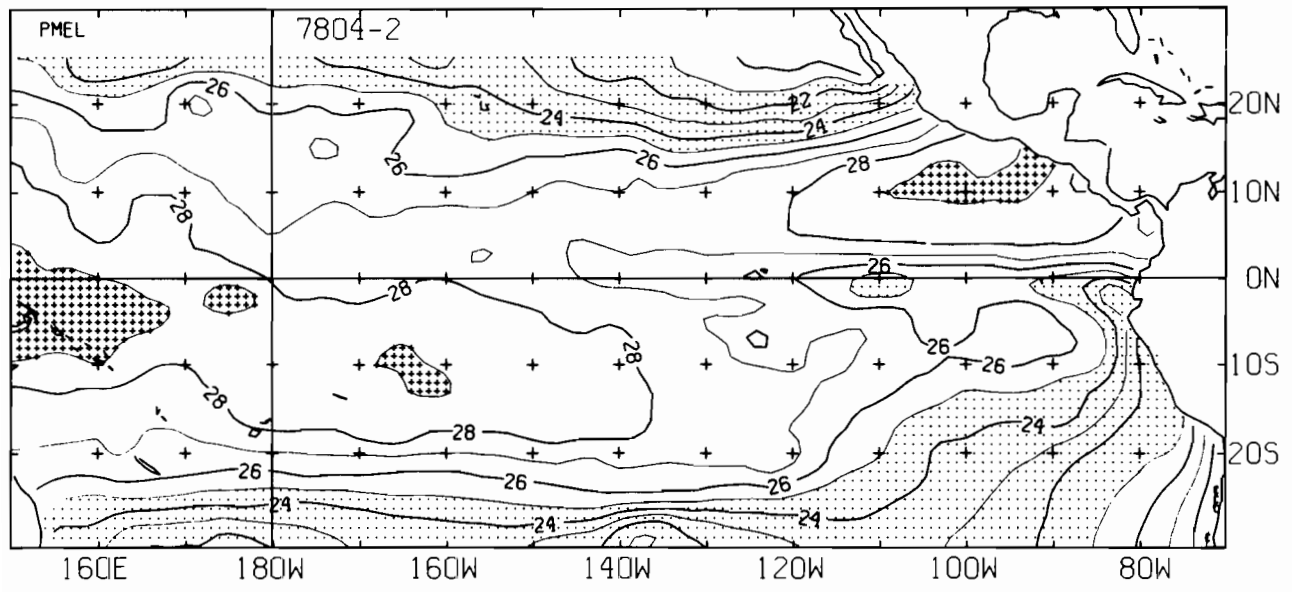

7804-2 SST. 0 E-BUØY. 0 BT. 20 XBT. 1042 SPØT DATA

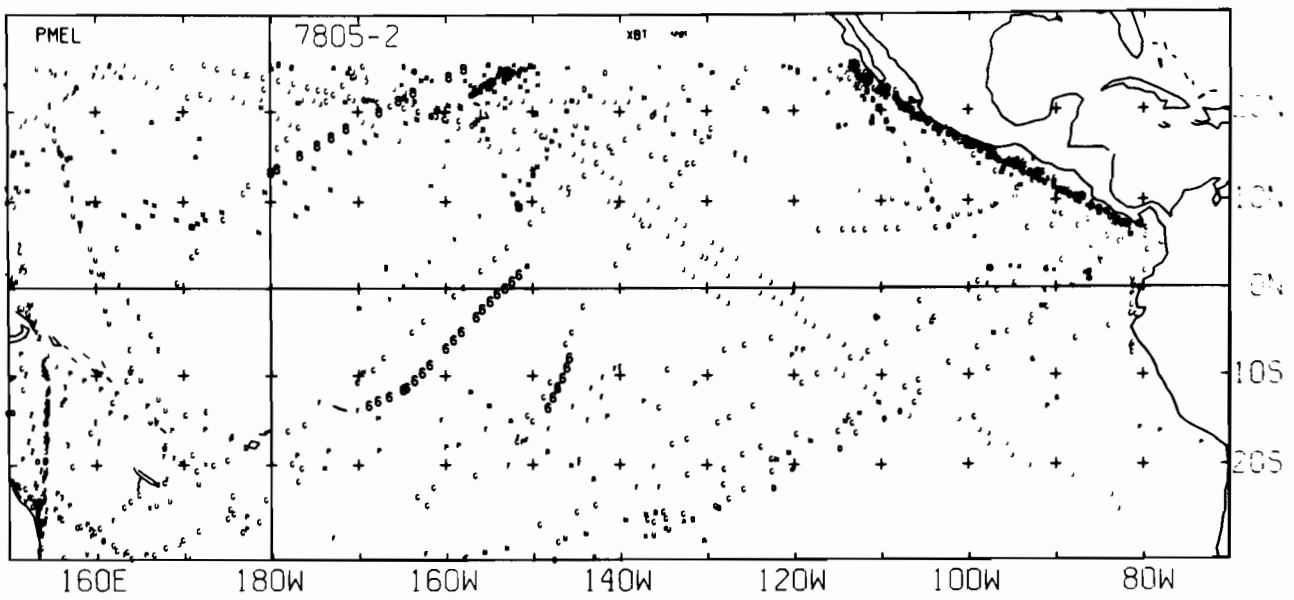

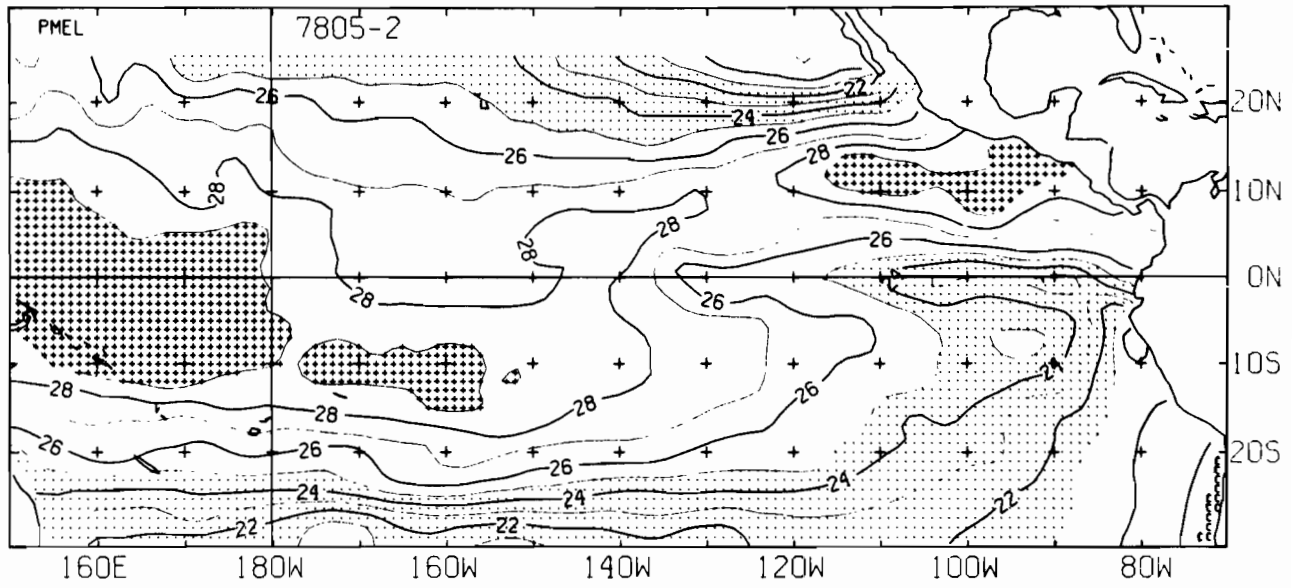

7805-2 SST. 0 E-BUØY. 0 BT. 35 XBT. 1191 SPØT DATA

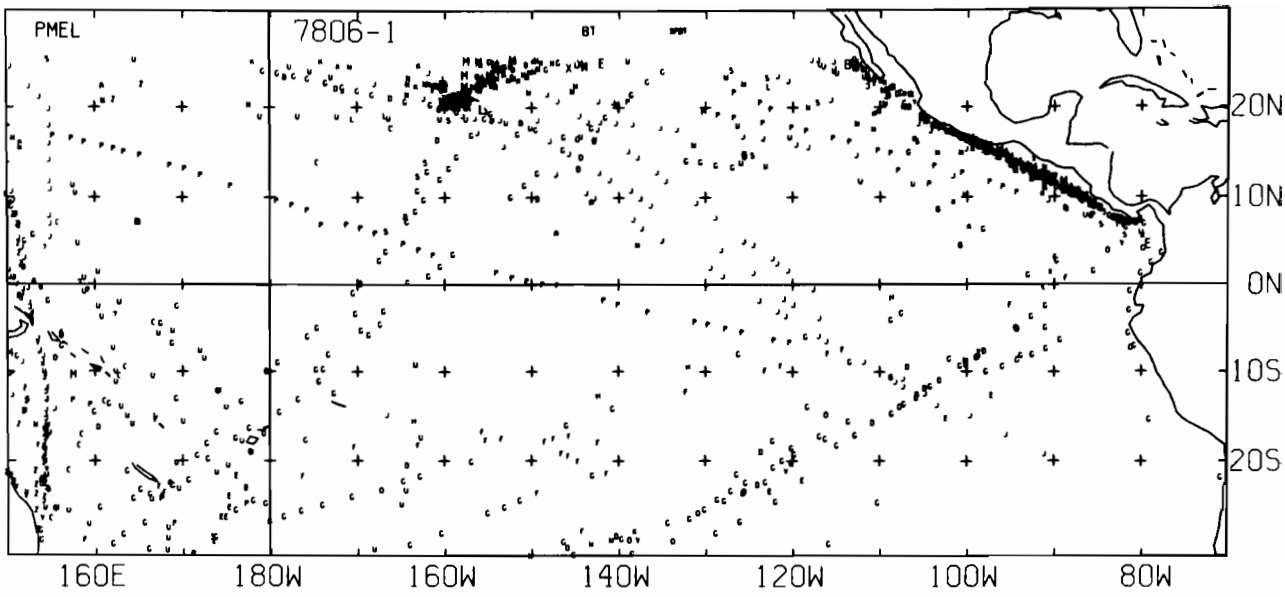

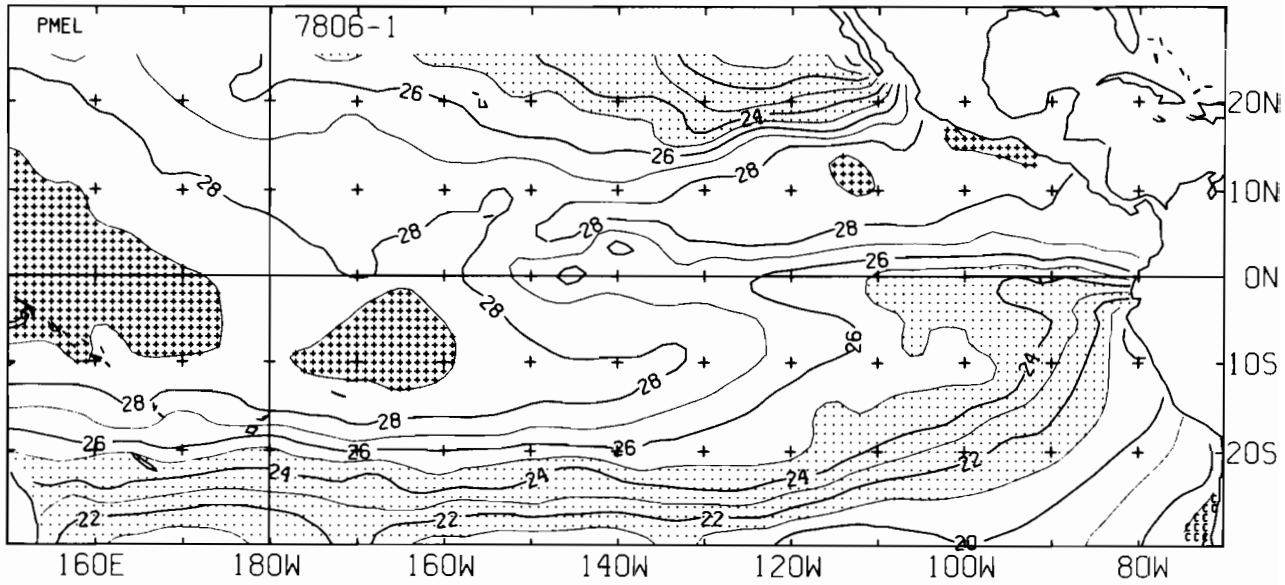

7806-1 SST. 0 E-BUØY. 128 BT. 0 XBT. 1018 SPØT DATA

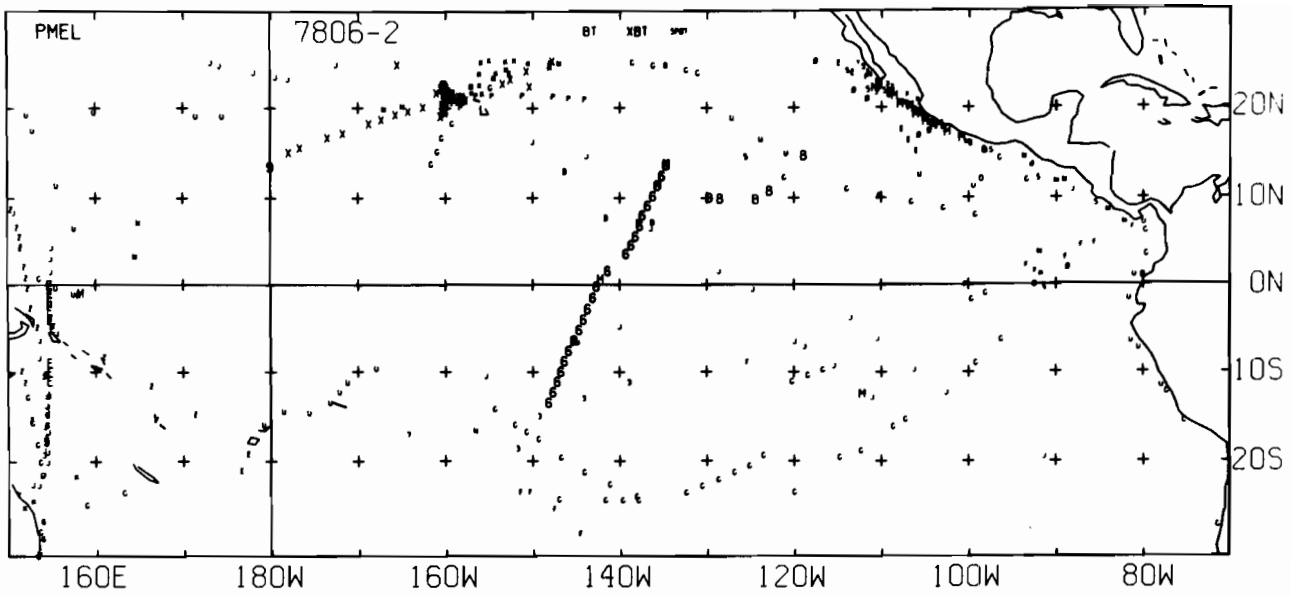

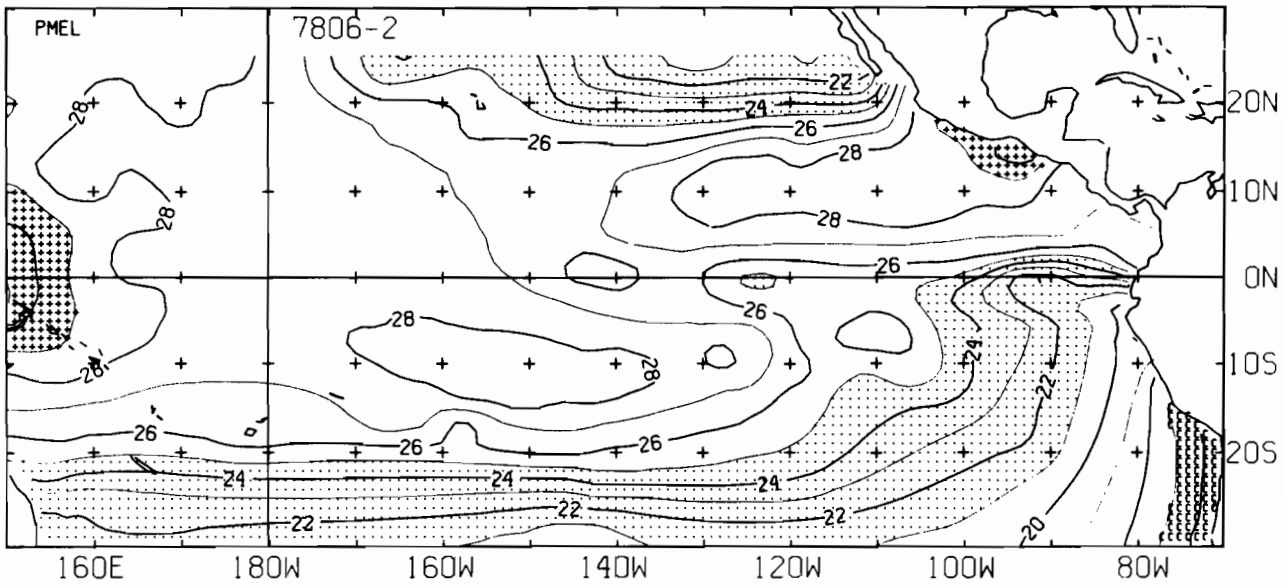

7806-2 SST. 0 E-BUØY. 111 BT. 24 XBT. 292 SPØT DATA

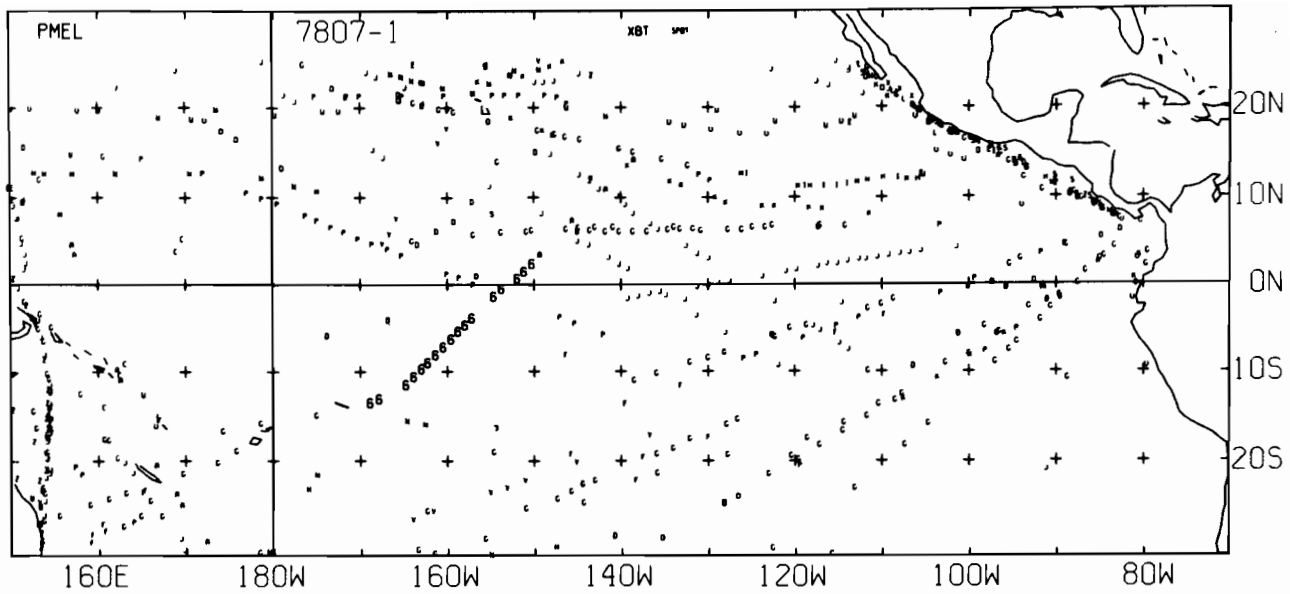

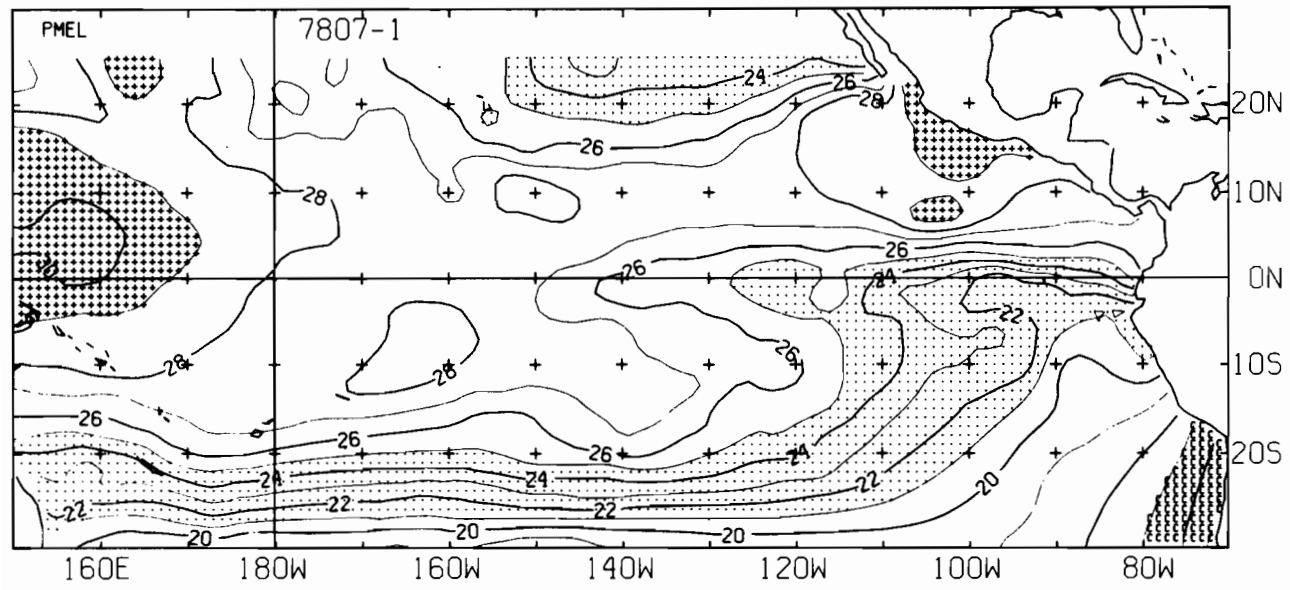

7807-1 SST. 0 E-BUØY. 0 BT. 17 XBT. 641 SPØT DATA

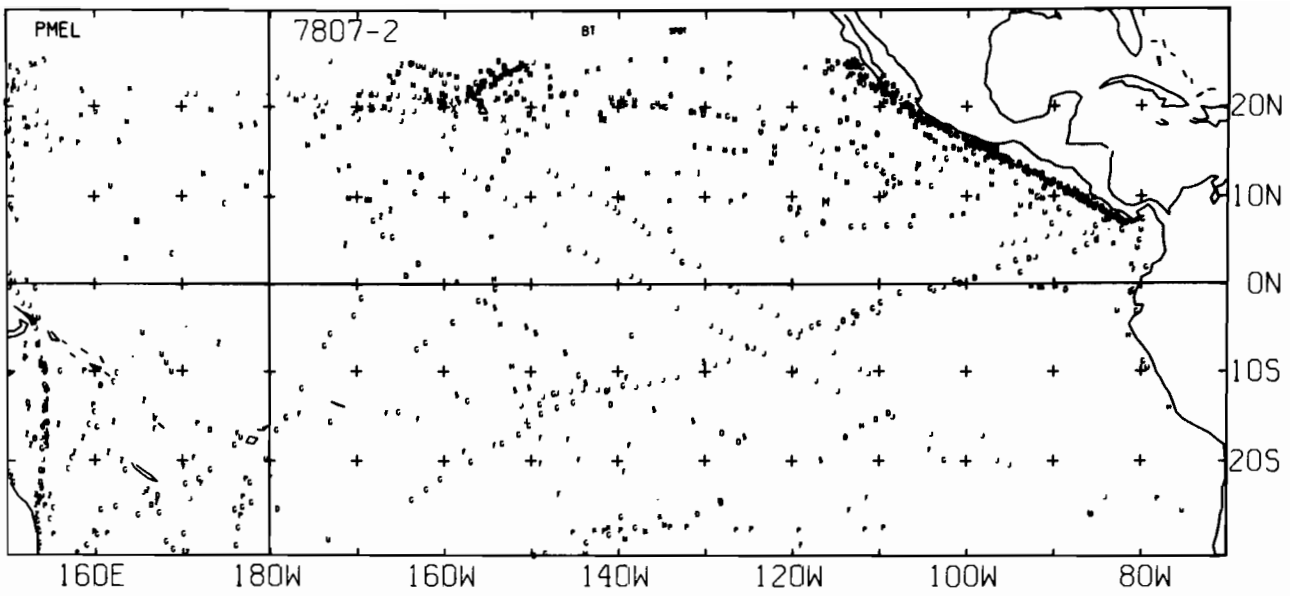

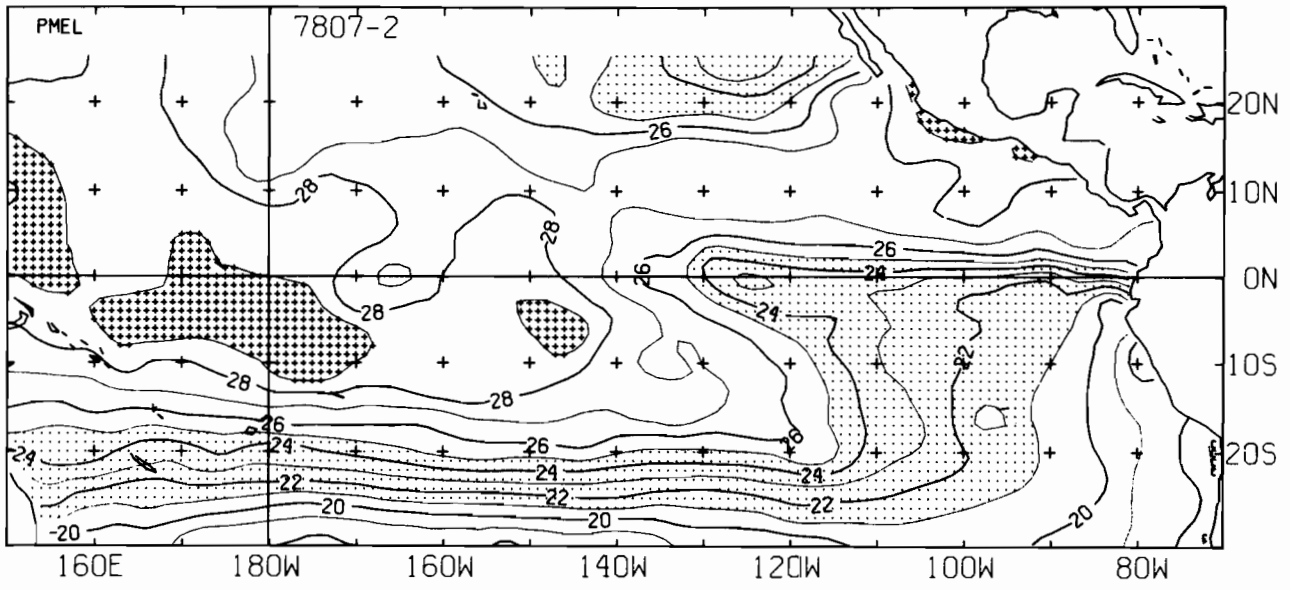

7807-2 SST. 0 E-BUØY. 9 BT. 0 XBT. 979 SPØT DATA

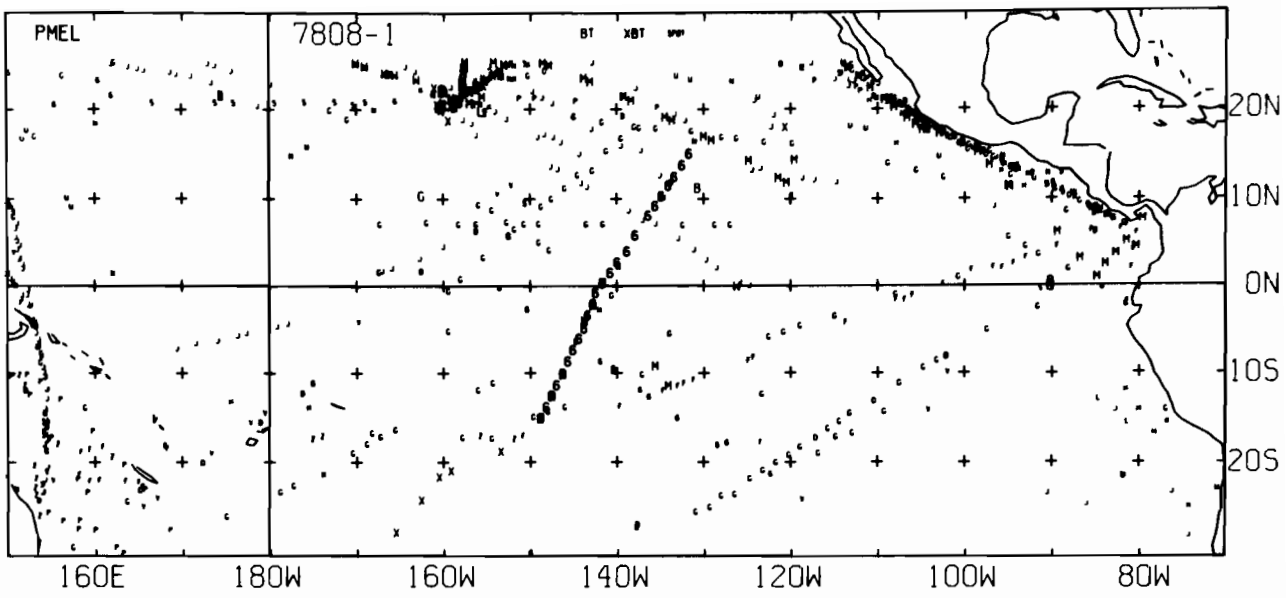

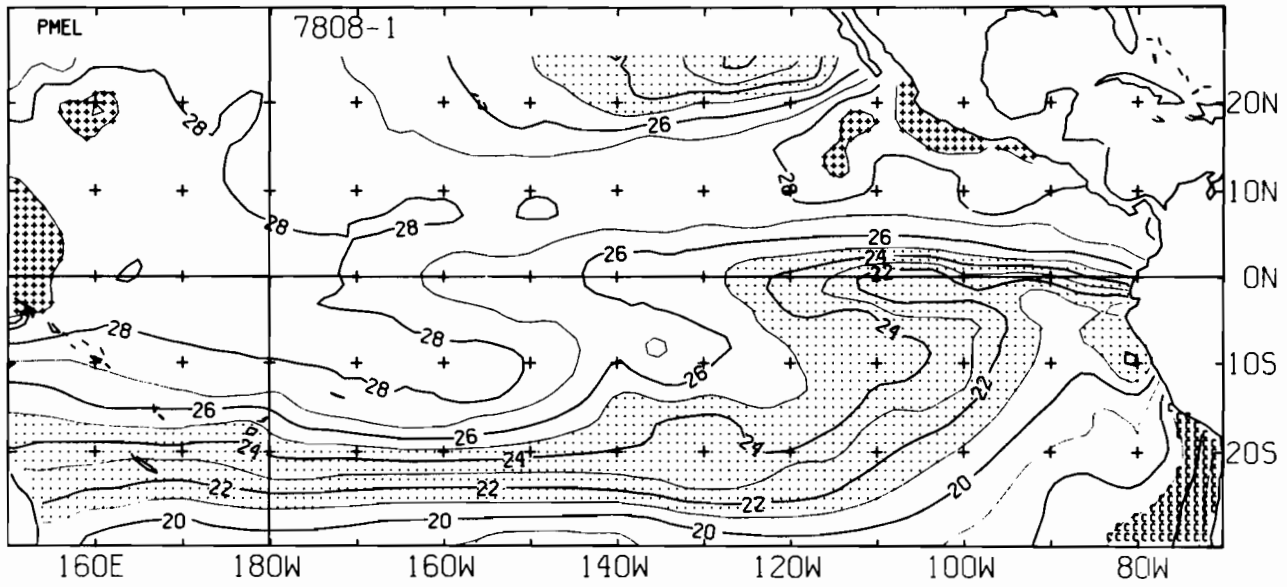

7808-1 SST. 0 E-BUØY. 111 BT. 24 XBT. 619 SPØT DATA

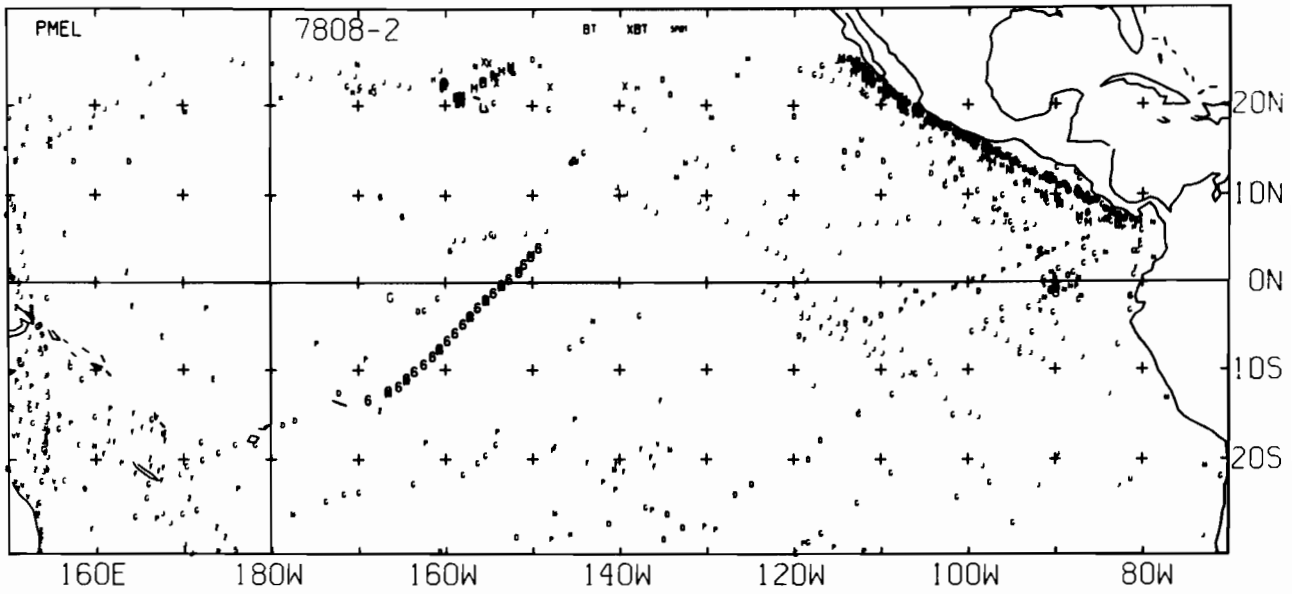

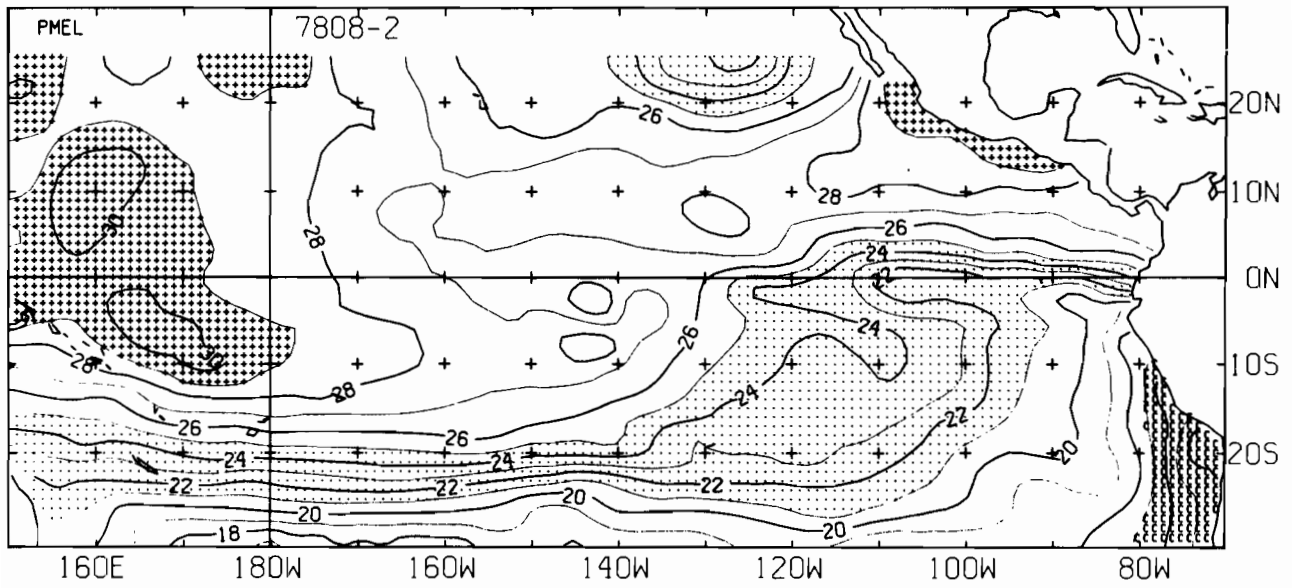

7808-2 SST. 0 E-BUØY. 73 BT. 21 XBT. 771 SPØT DATA

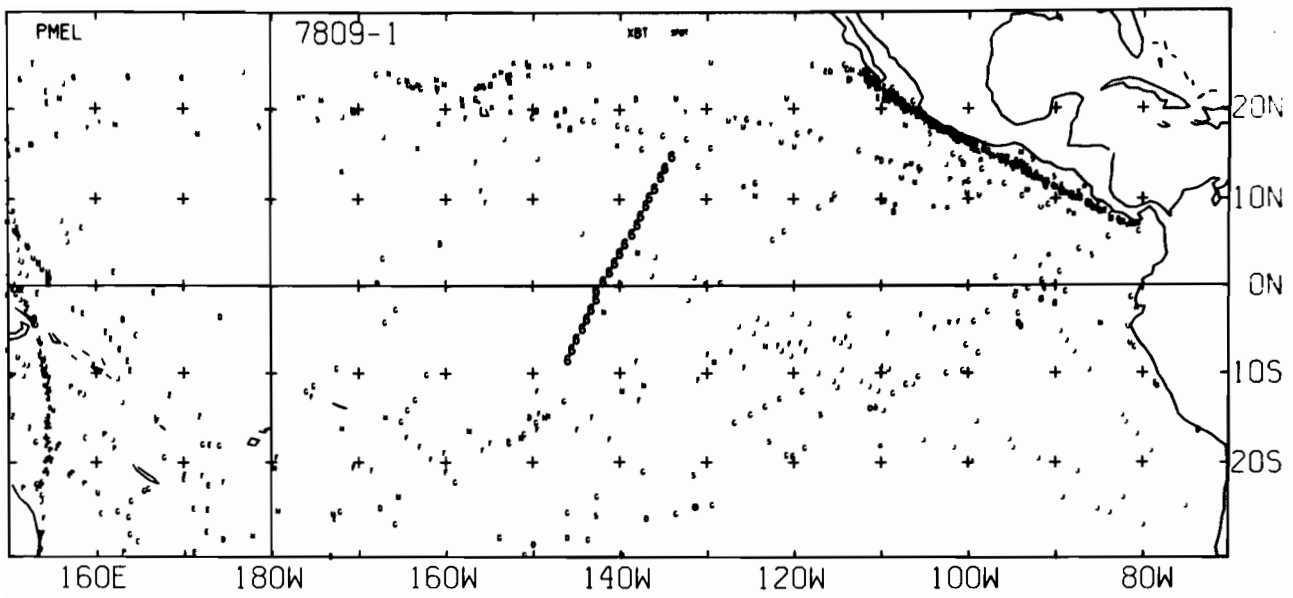

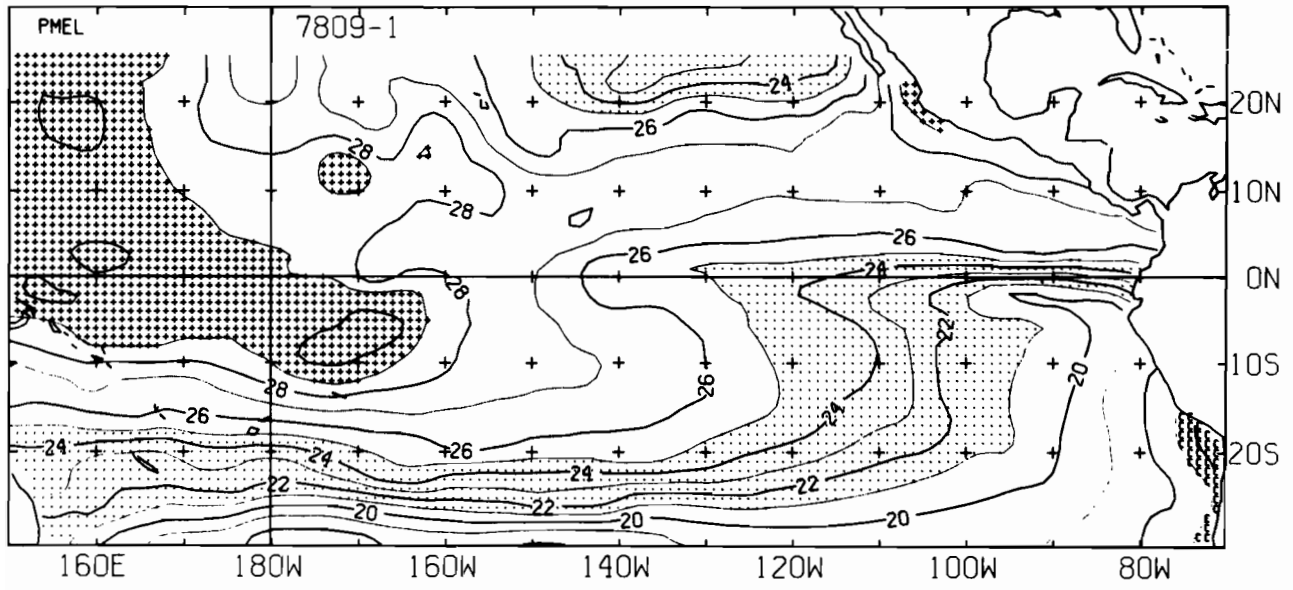

7809-1 SST. 0 E-BUØY. 0 BT. 22 XBT. 736 SPØT DATA

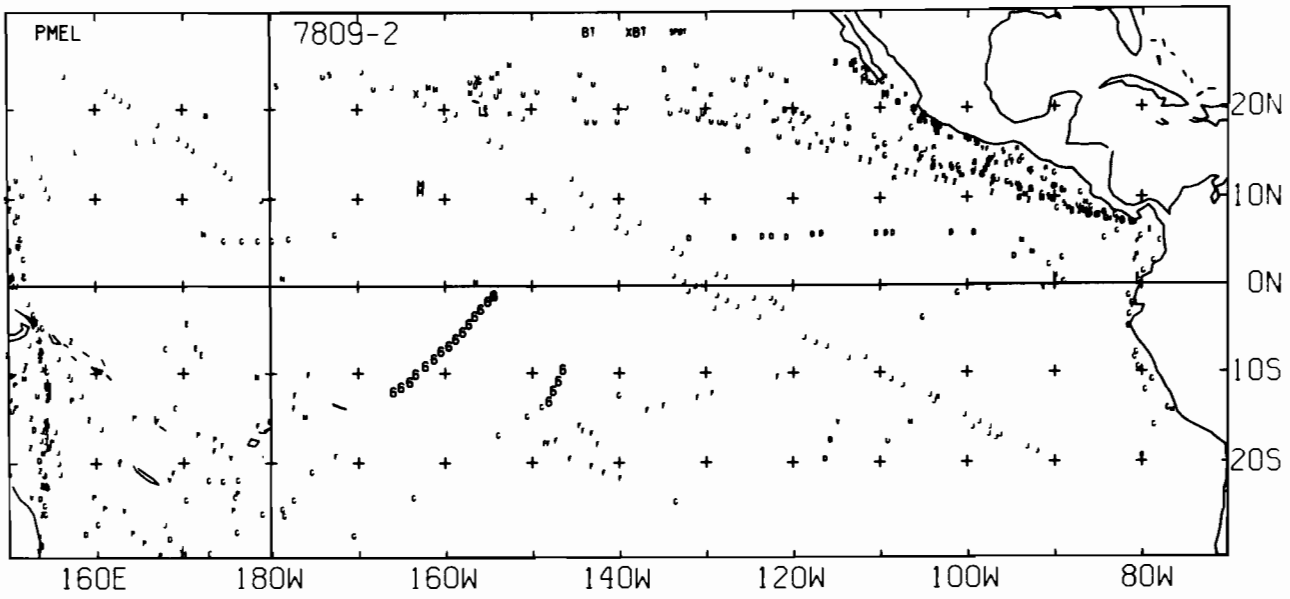

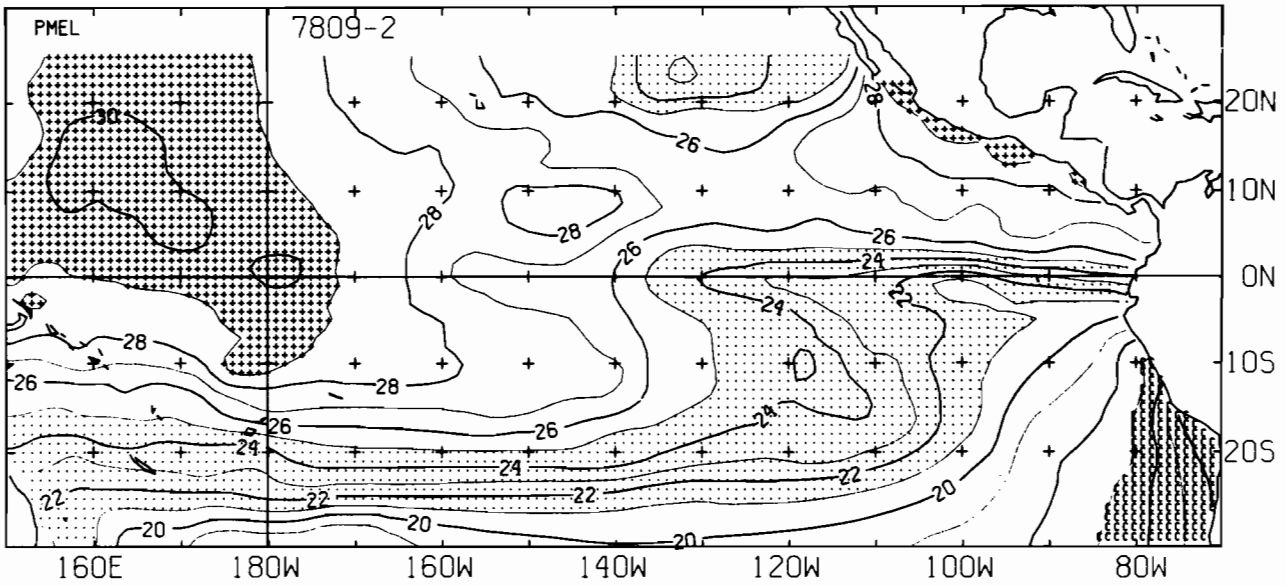

7809-2 SST. 0 E-BUØY. 7 BT. 19 XBT. 551 SPØT DATA

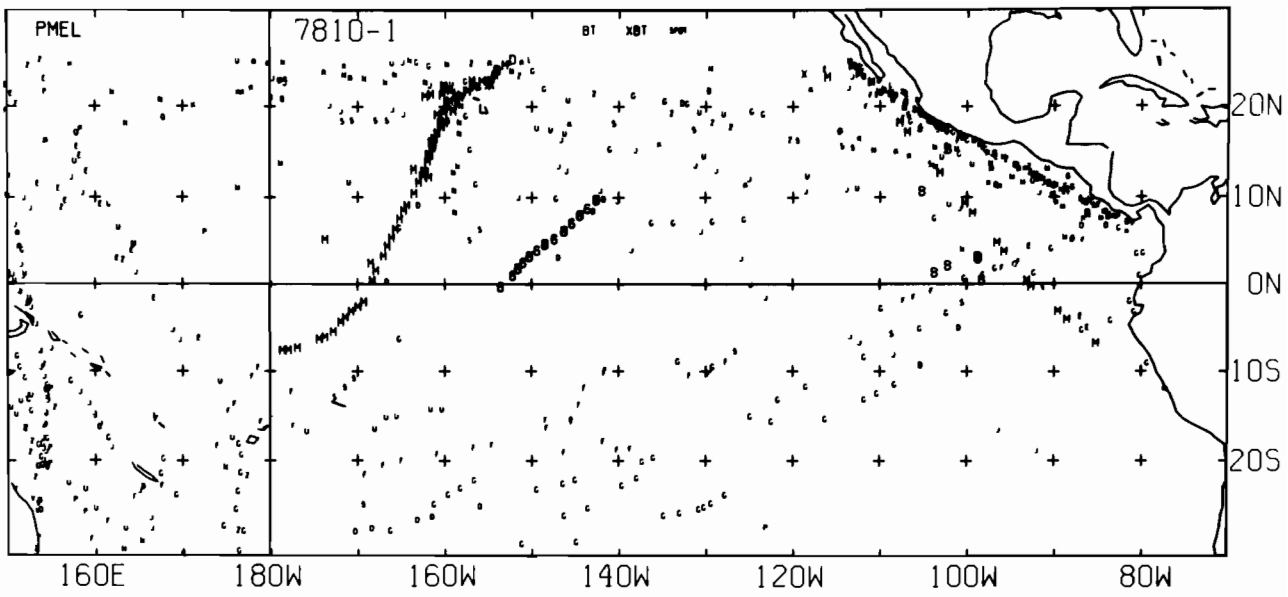

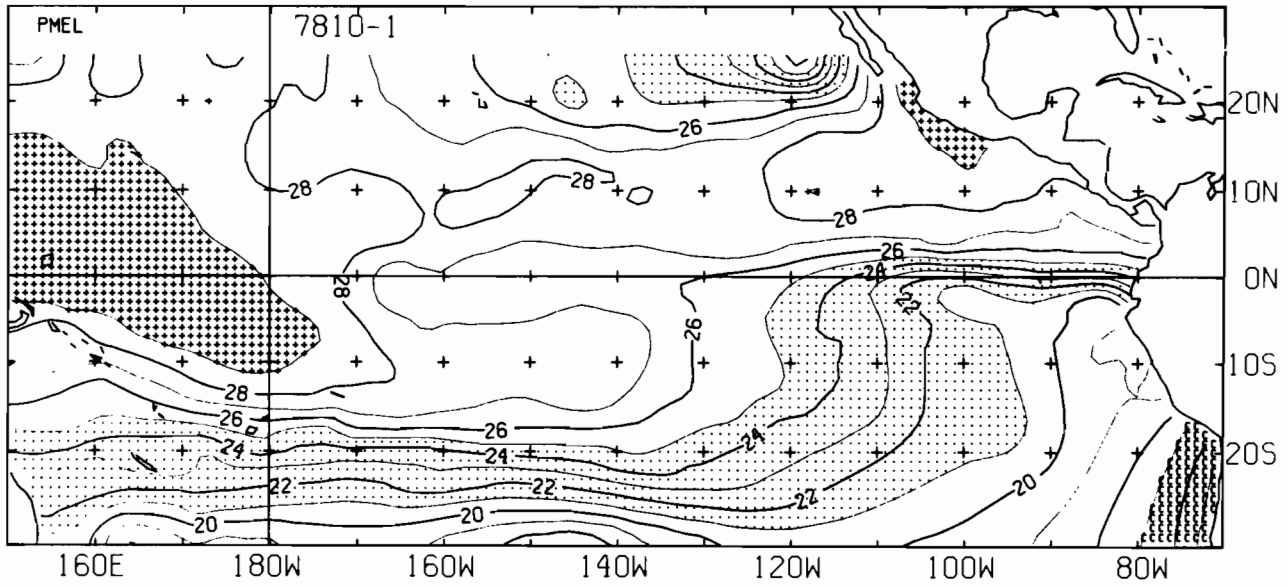

7810-1 SST. 0 E-BUØY. 107 BT. 13 XBT. 598 SPØT DATA

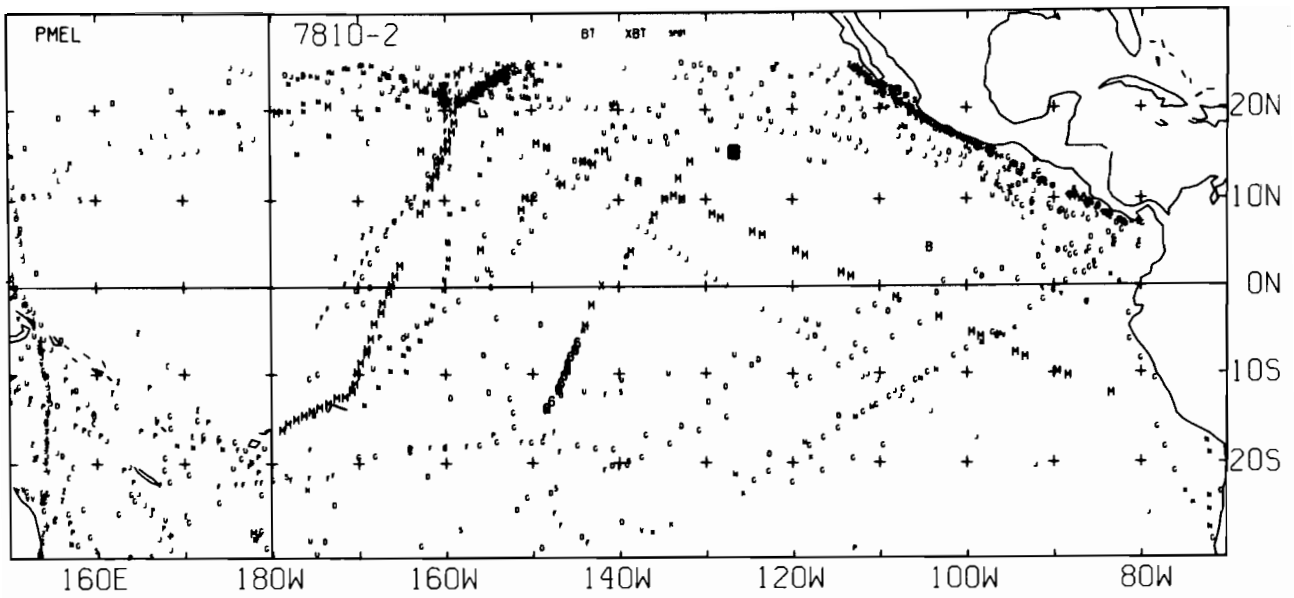

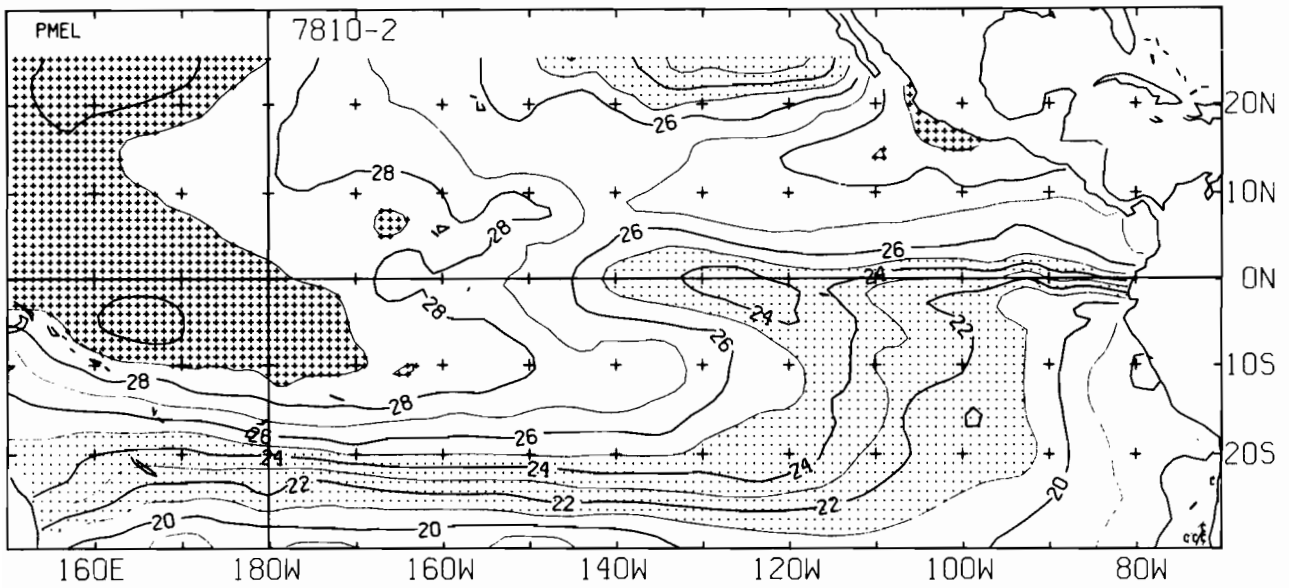

7810-2 SST. 0 E-BUØY. 140 BT. 10 XBT. 1030 SPØT DATA

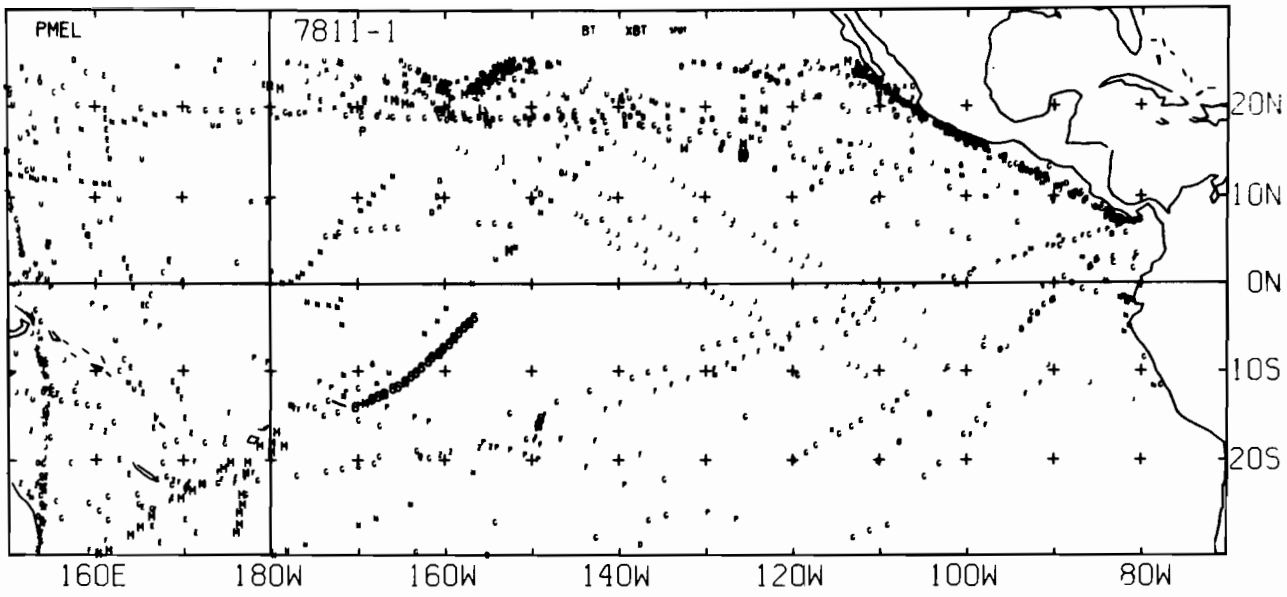

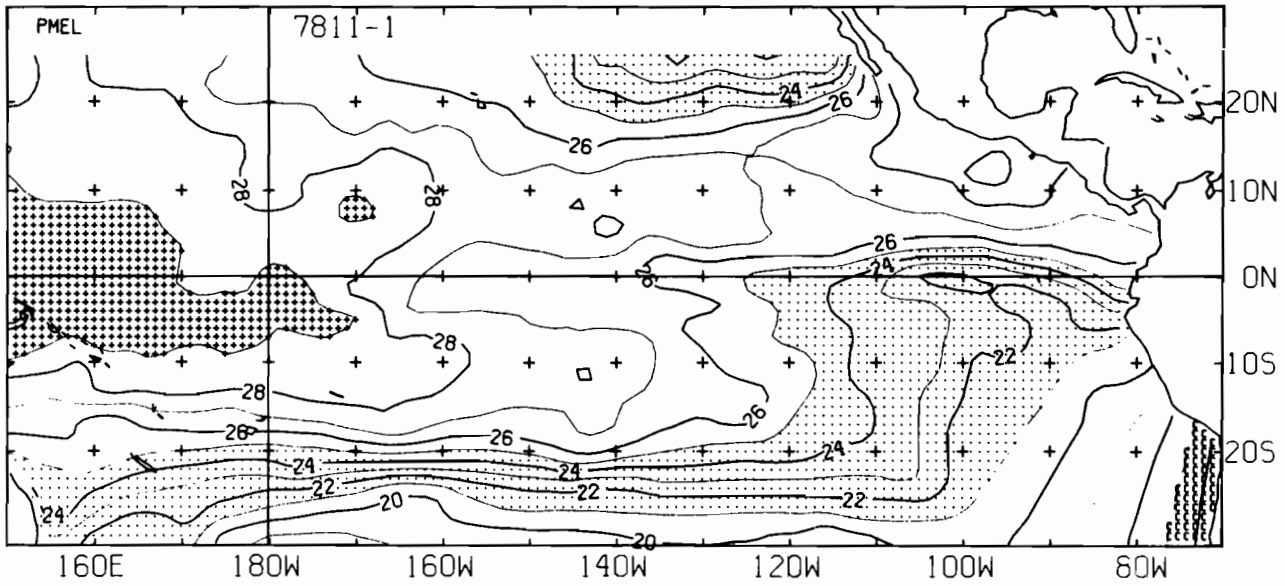

7811-1 SST. 0 E-BUØY. 106 BT. 22 XBT. 1128 SPØT DATA

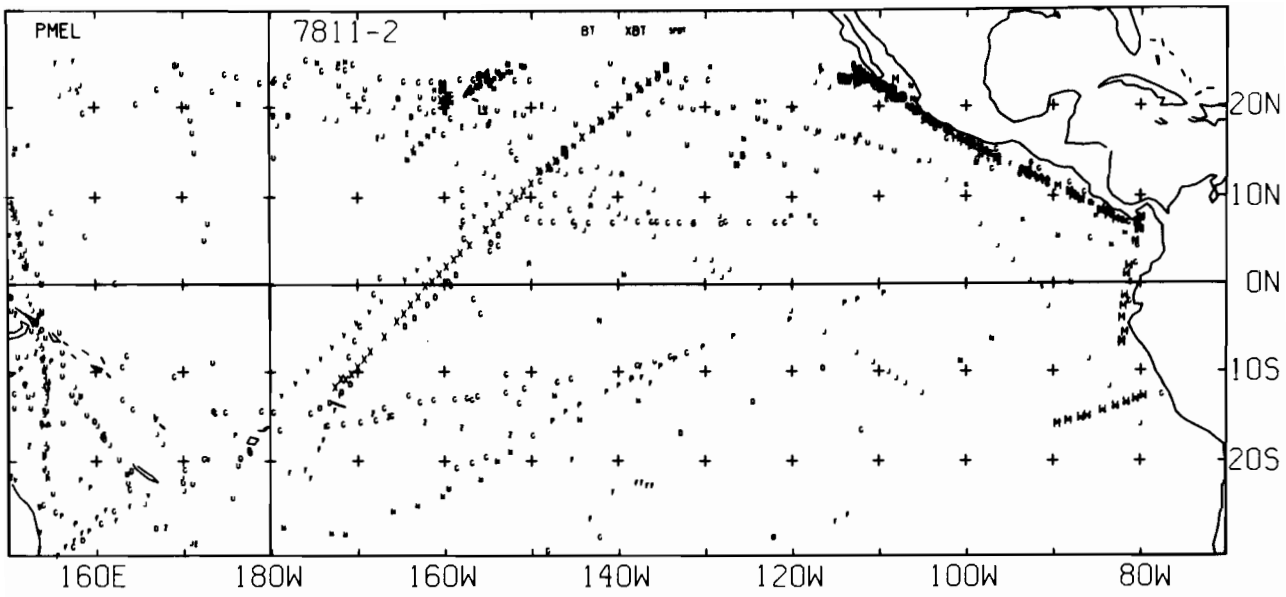

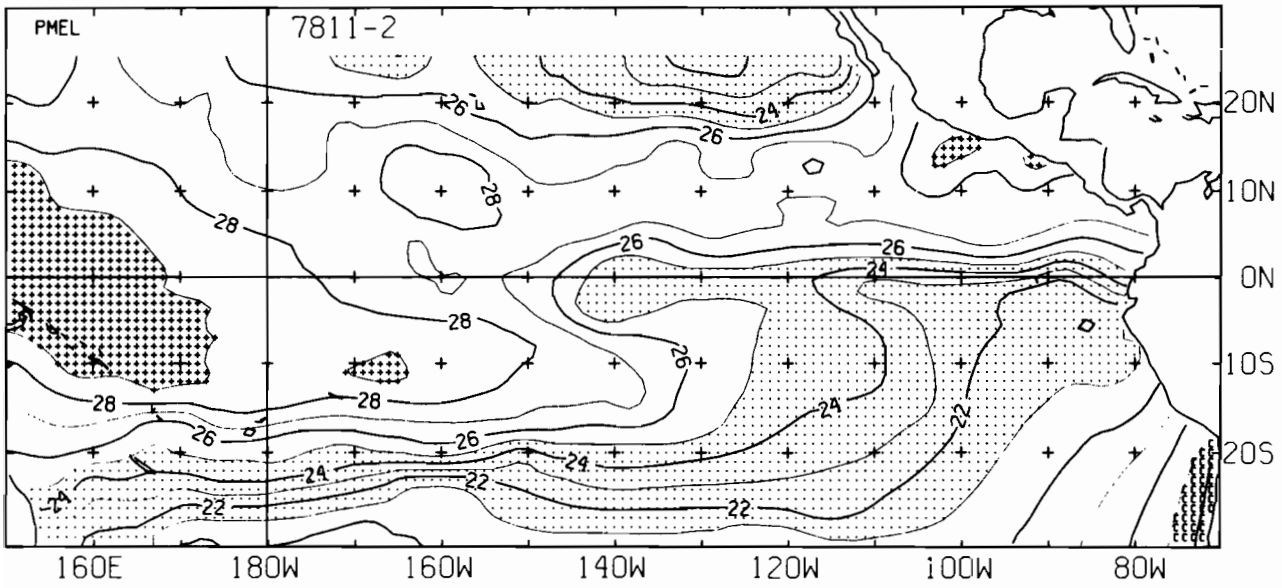

7811-2 SST. 0 E-BUØY. 142 BT. 3 XBT. 750 SPØT DATA

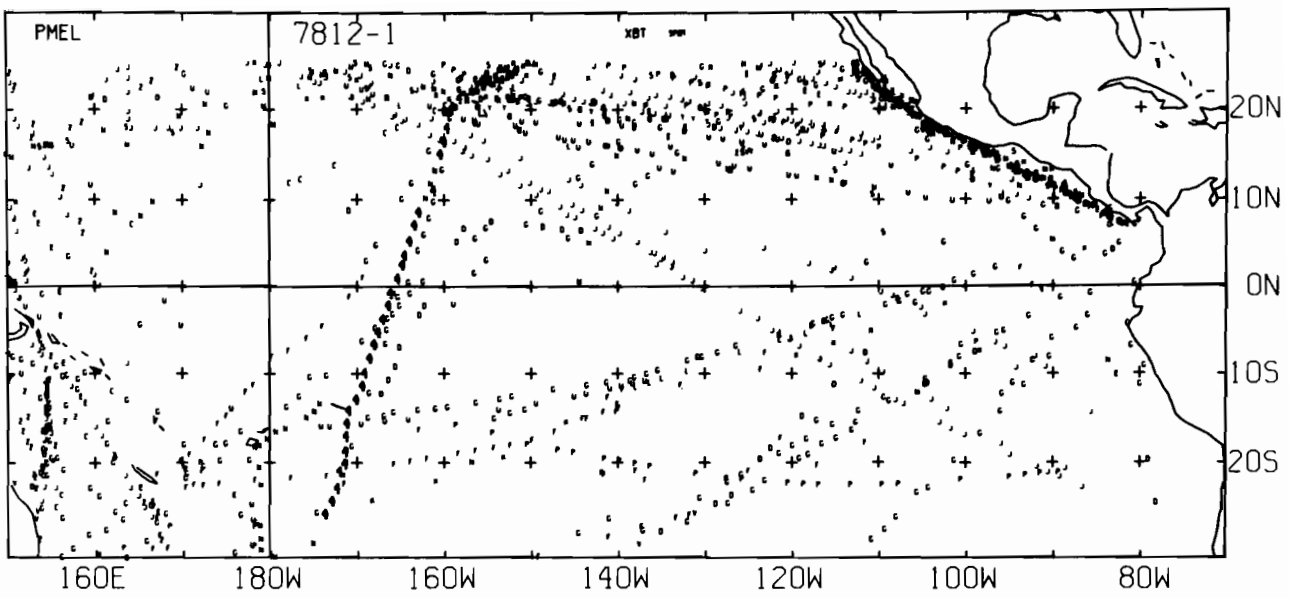

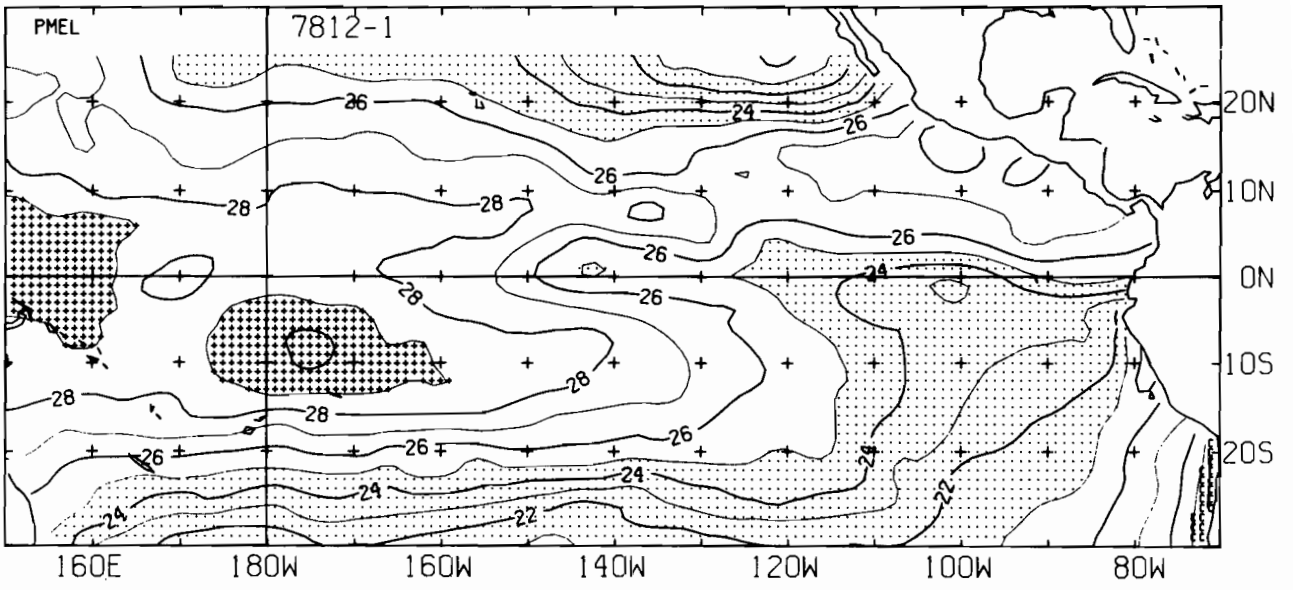

7812-1 SST. 0 E-BUØY. 0 BT. 30 XBT. 1360 SPØT DATA

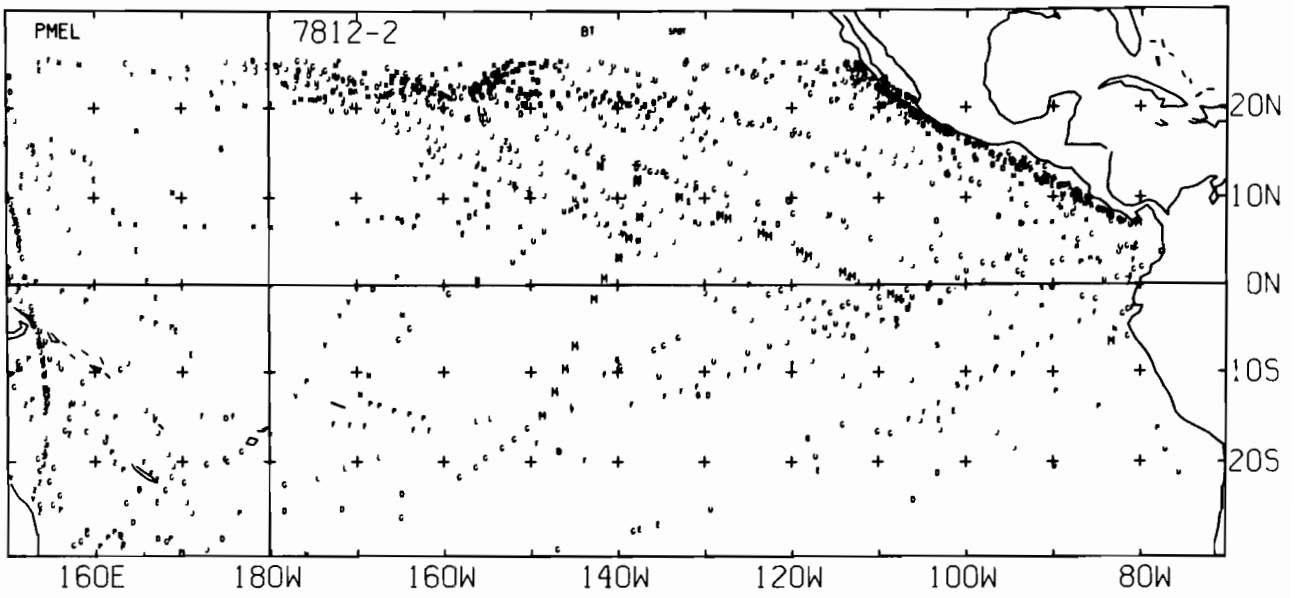

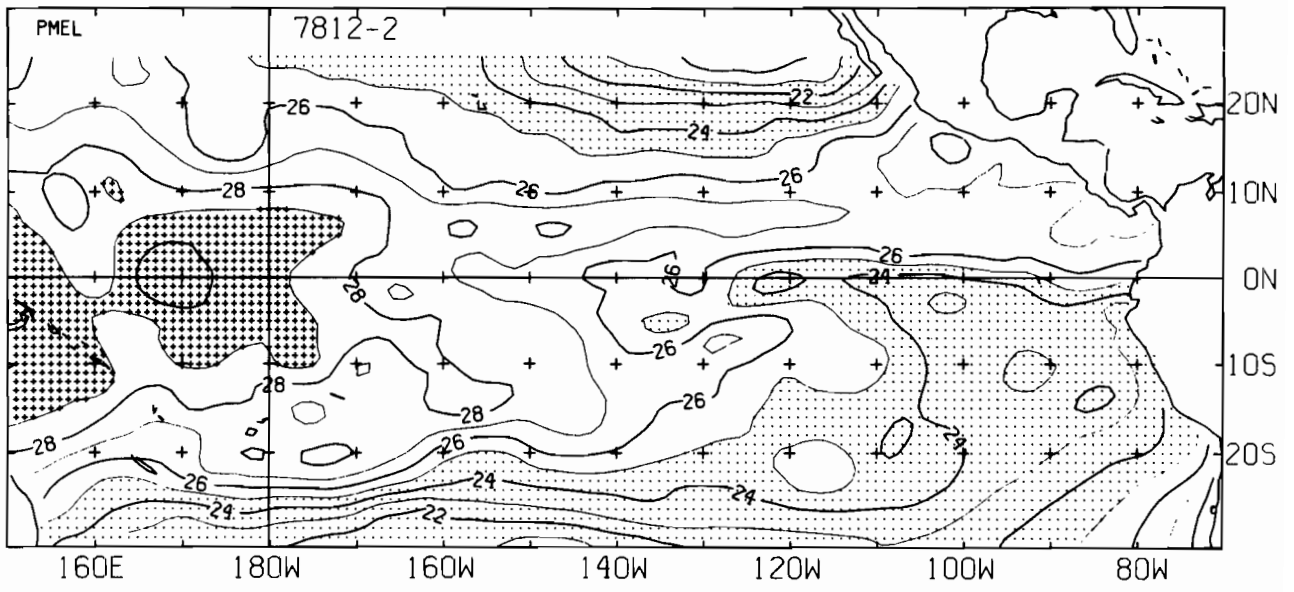

7812-2 SST. 0 E-BUØY. 26 BT. 0 XBT. 1173 SPØT DATA

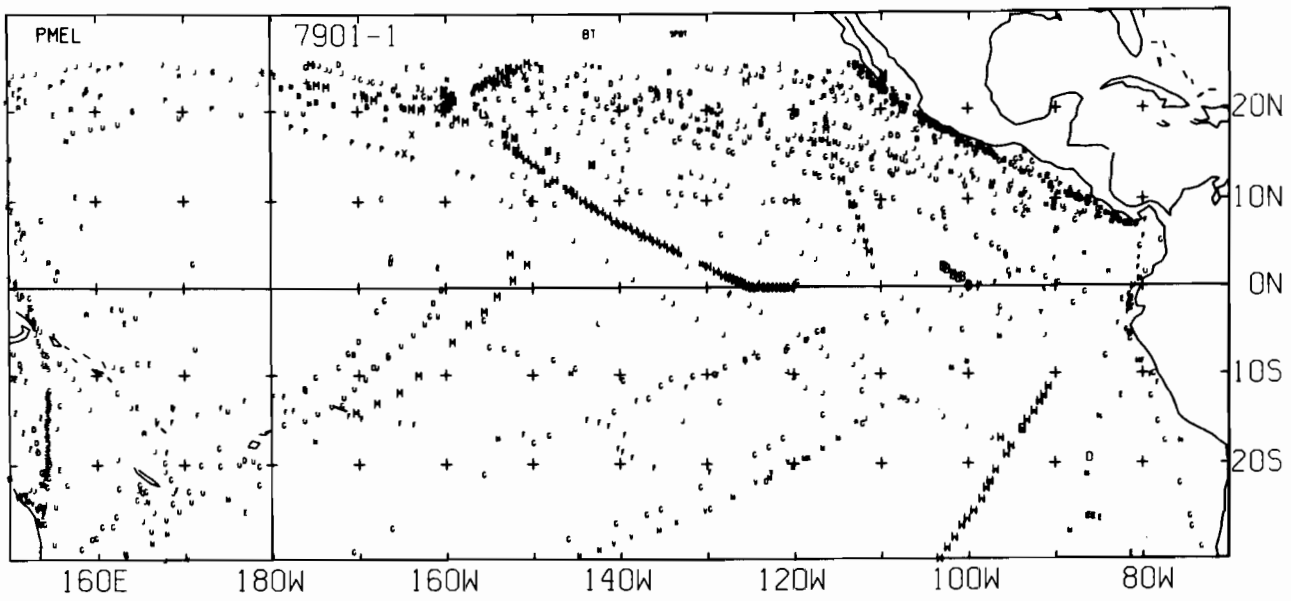

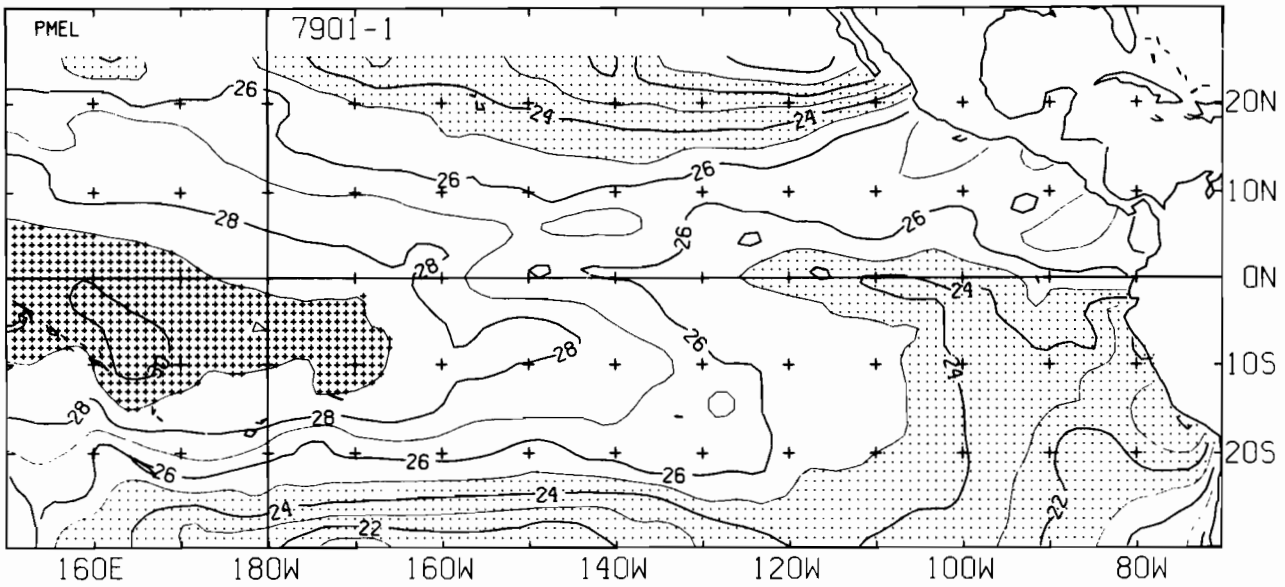

7901-1 SST. 0 E-BUØY. 159 BT. 0 XBT. 1101 SPØT DATA

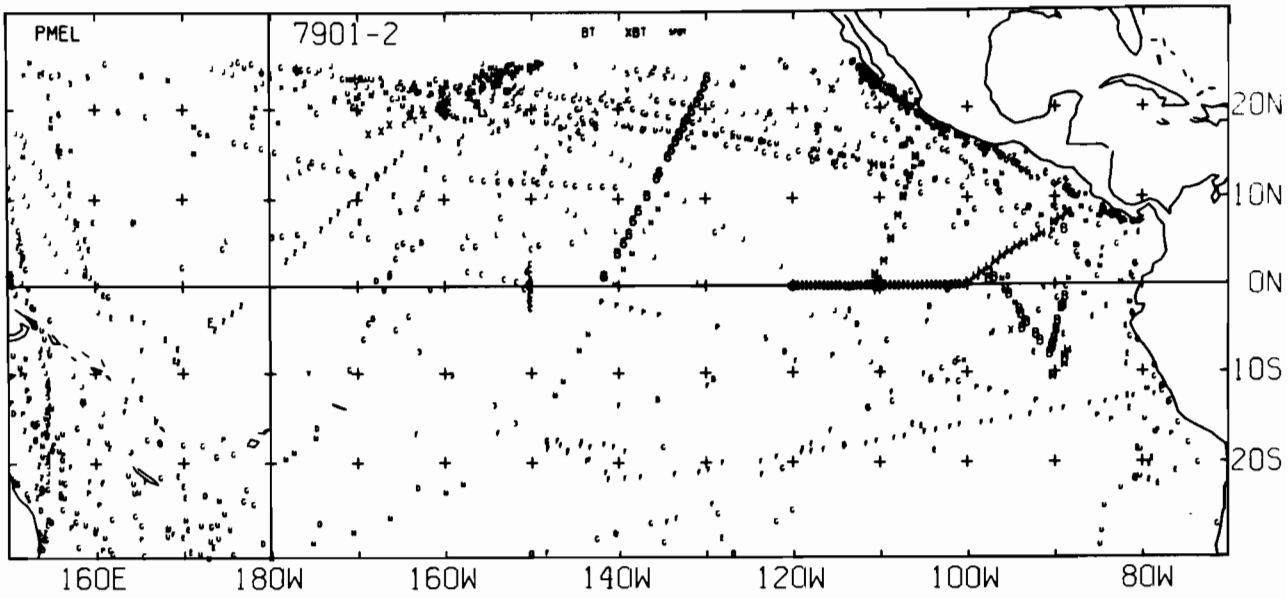

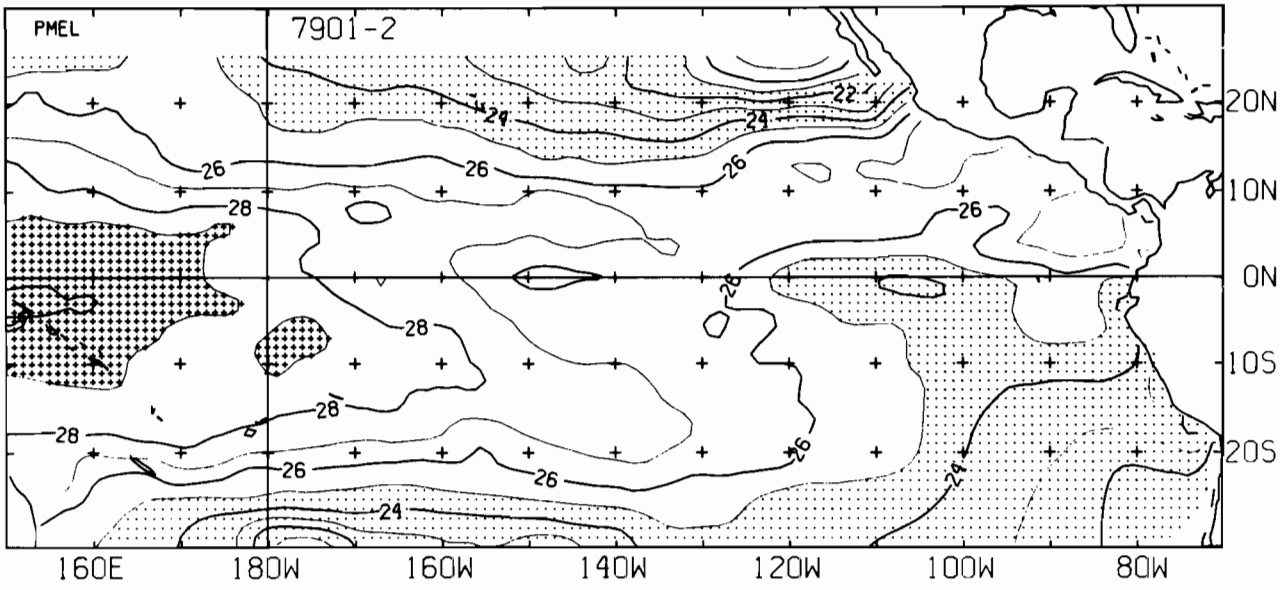

7901-2 SST. 0 E-BUØY, 121 BT, 20 XBT, 1261 SPØT DATA

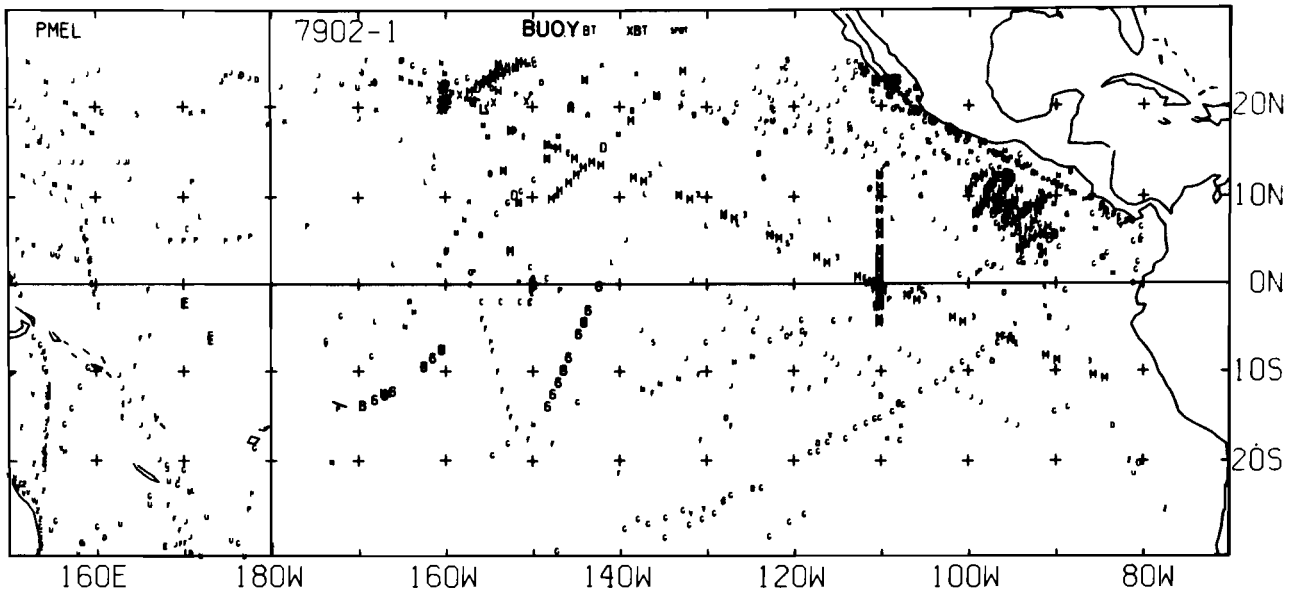

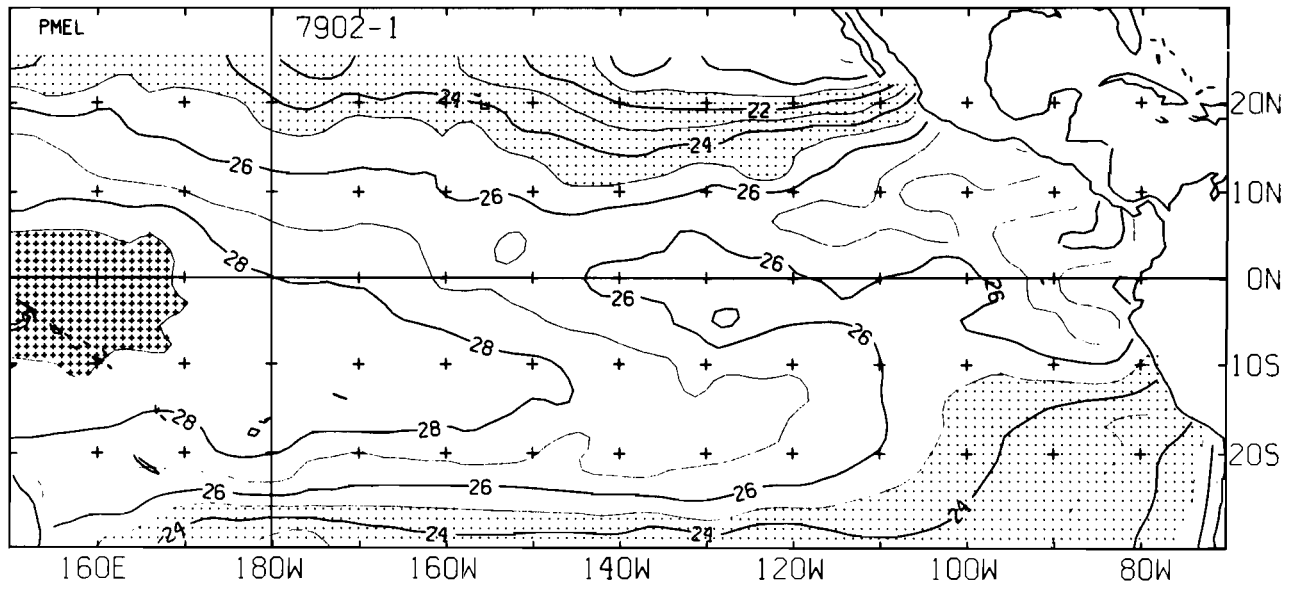

7902-1 SST. 2 E-BUØY. 210 BT. 16 XBT. 790 SPØT DATA

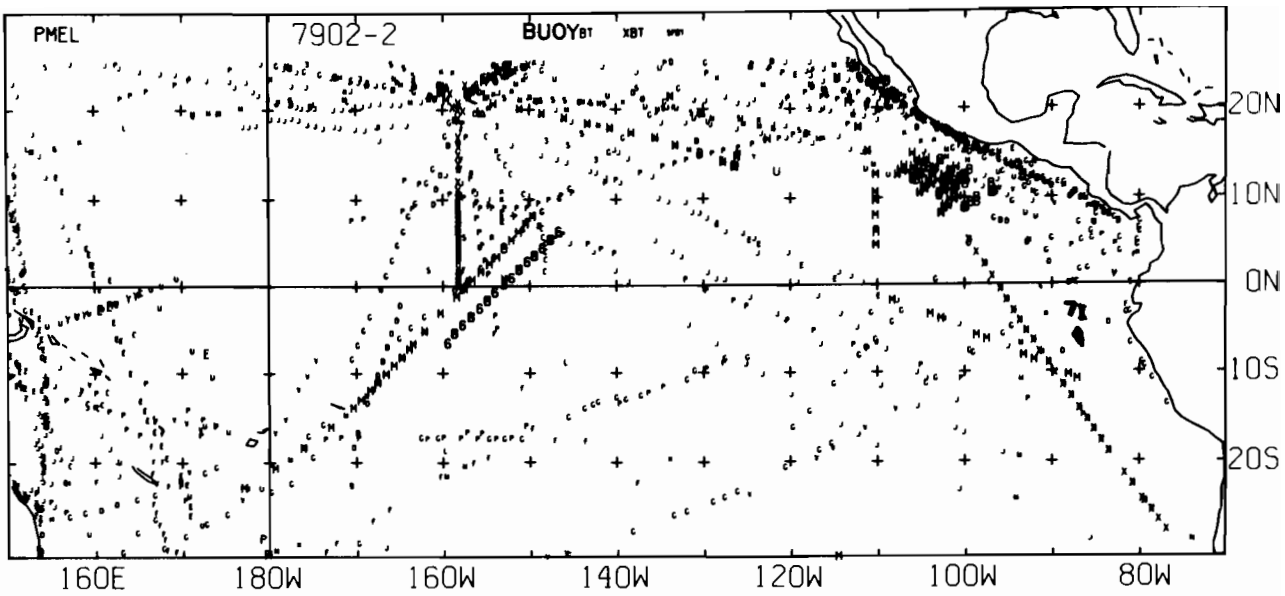

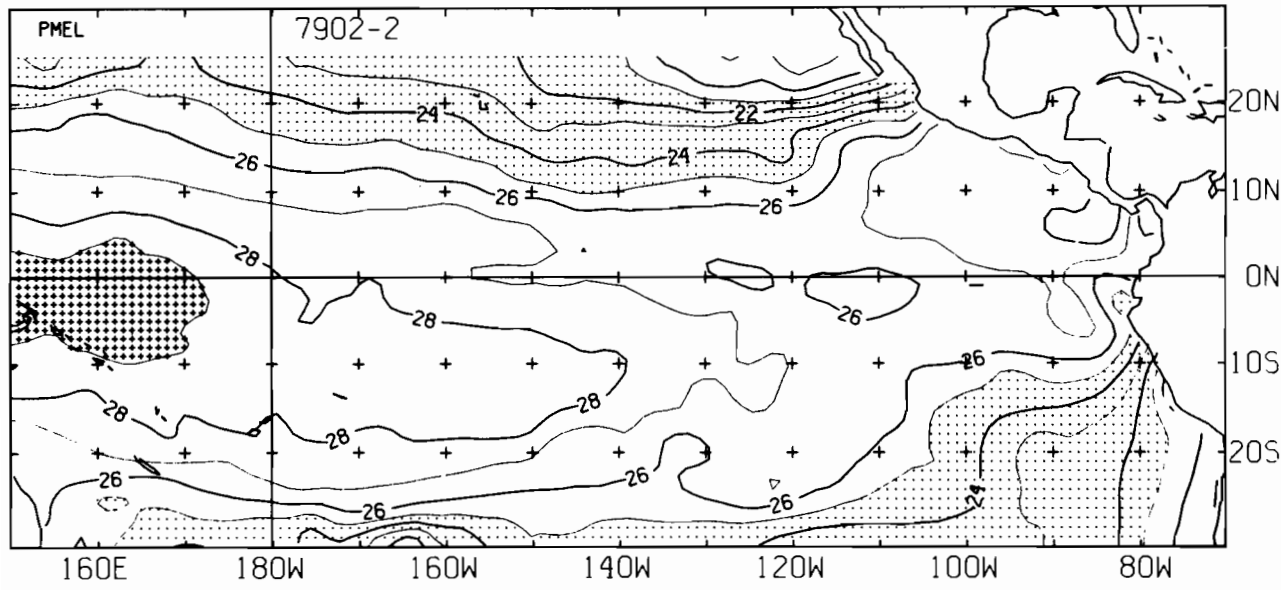

7902-2 SST. 39 E-BUØY. 245 BT. 15 XBT. 1270 SPØT DATA

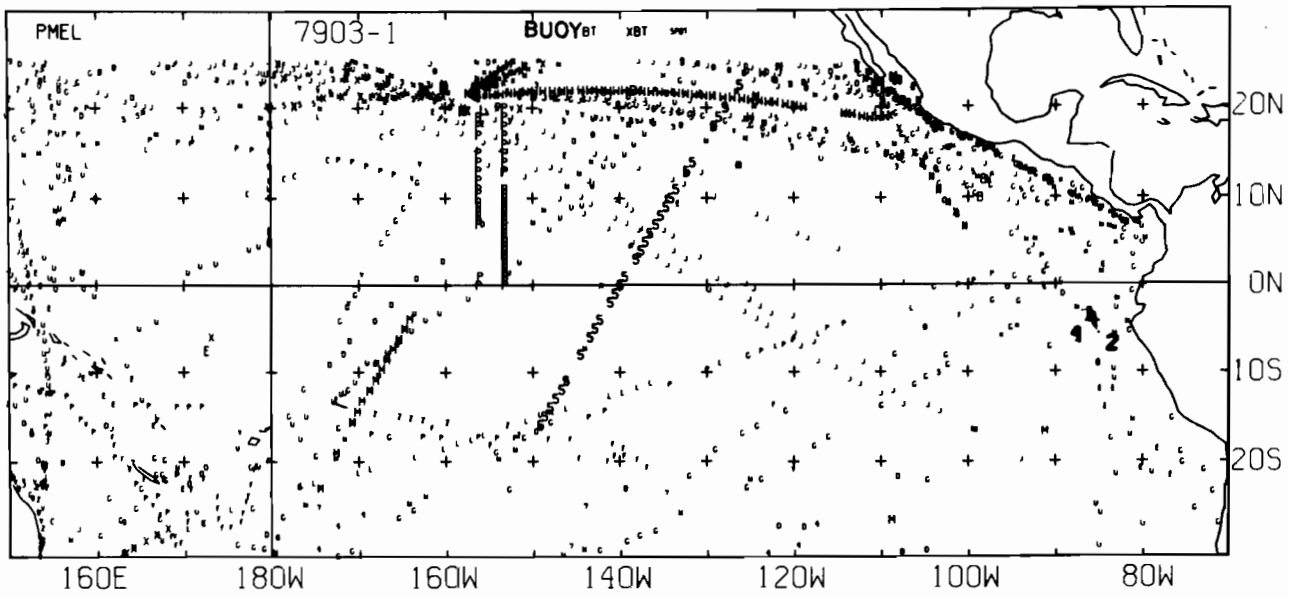

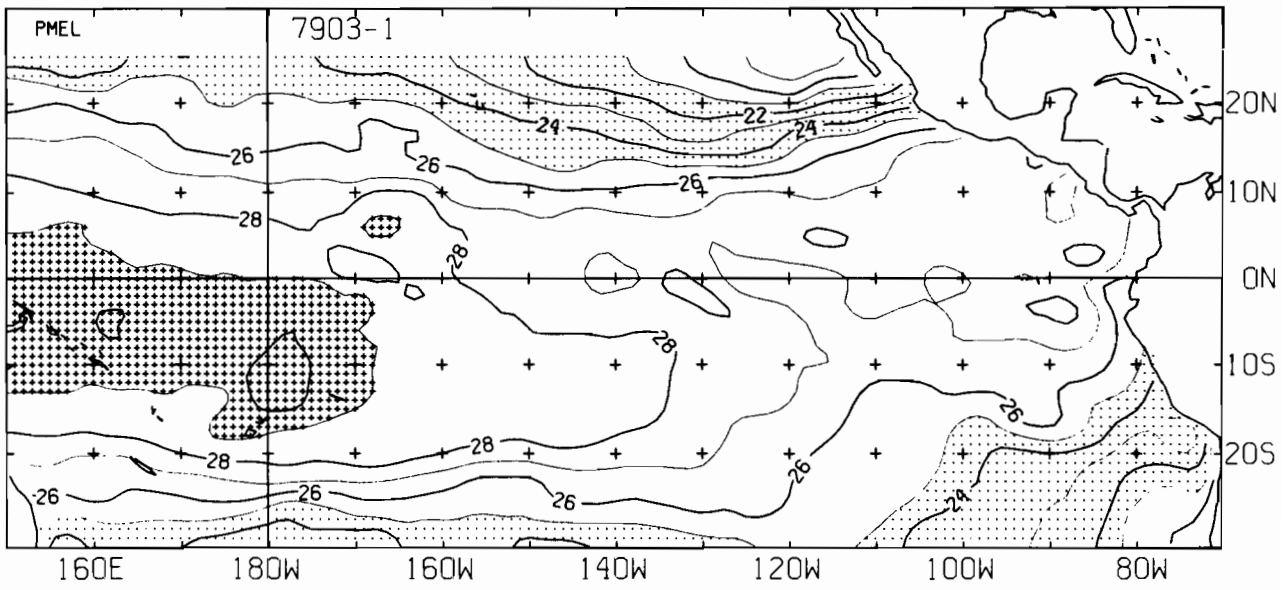

7903-1 SST. 40 E-BUØY. 202 BT. 29 XBT. 1344 SPØT DATA

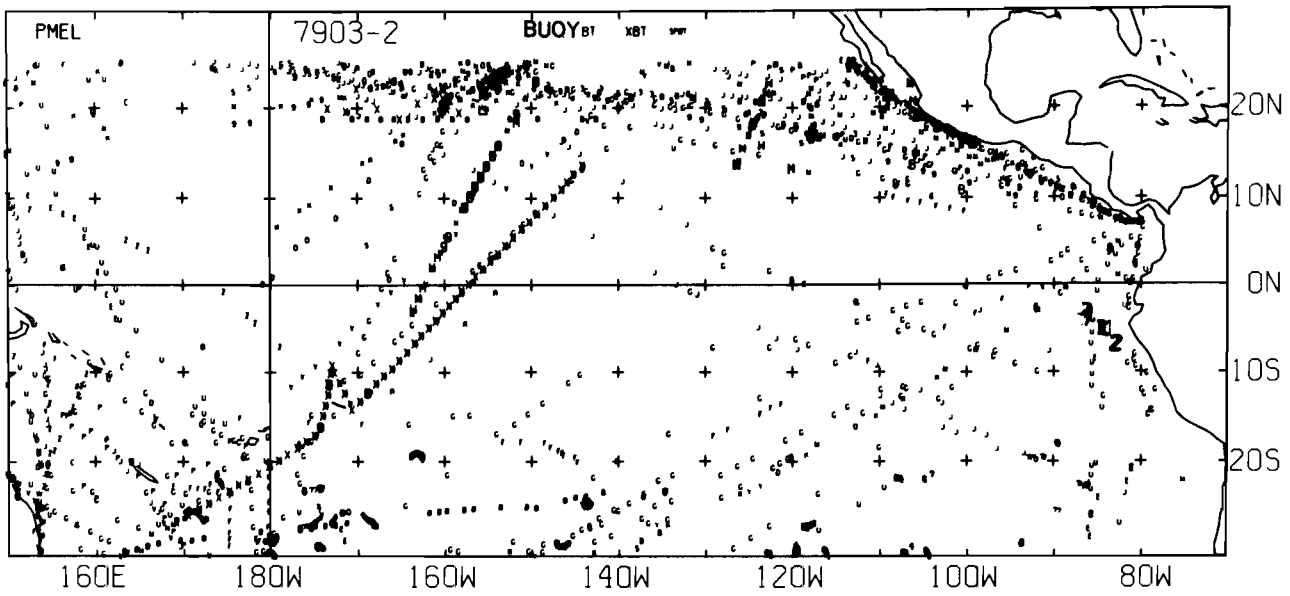

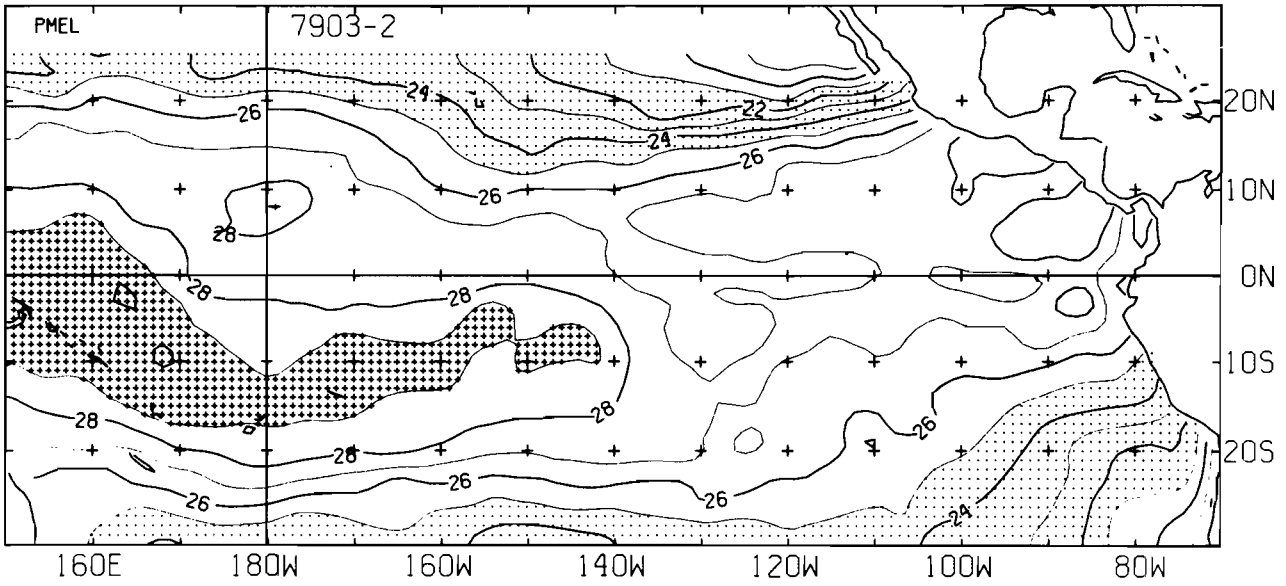

7903-2 SST. 48 E-BUØY. 136 BT. 11 XBT. 1800 SPØT DATA

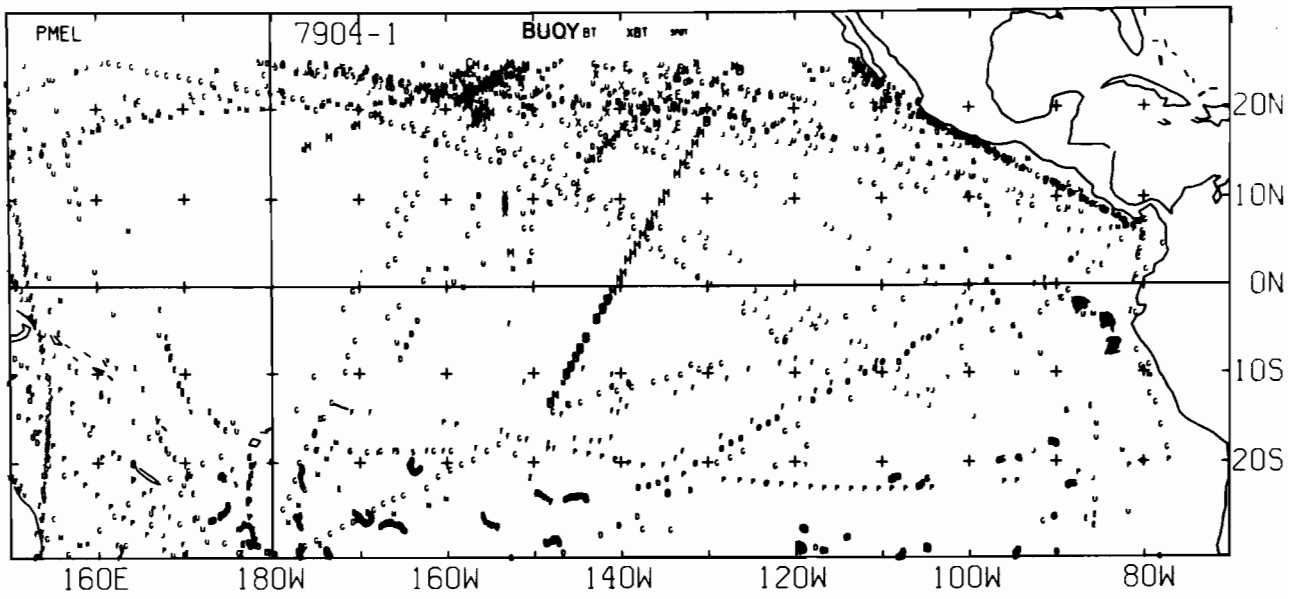

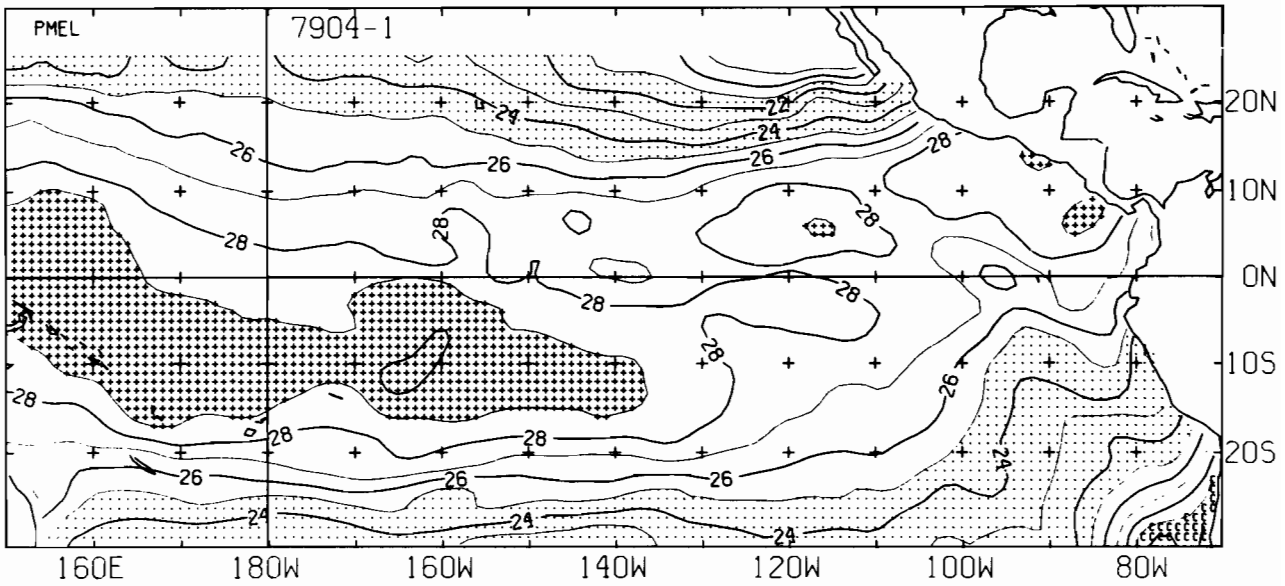

7904-1 SST. 45 E-BUØY. 132 BT. 9 XBT. 1812 SPØT DATA

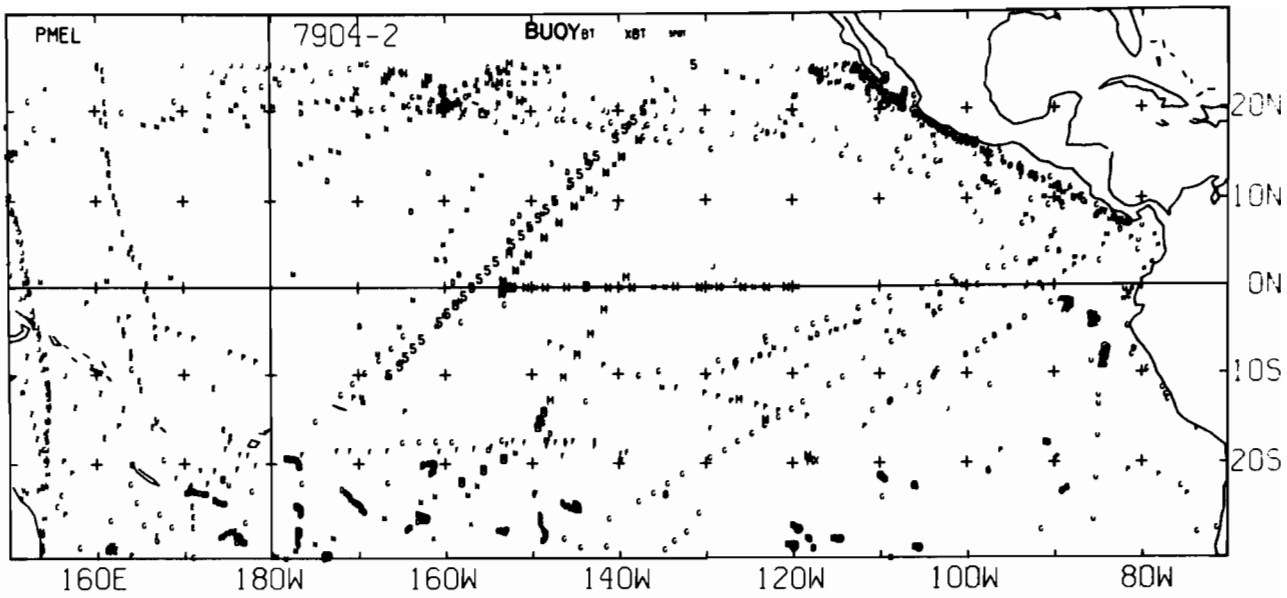

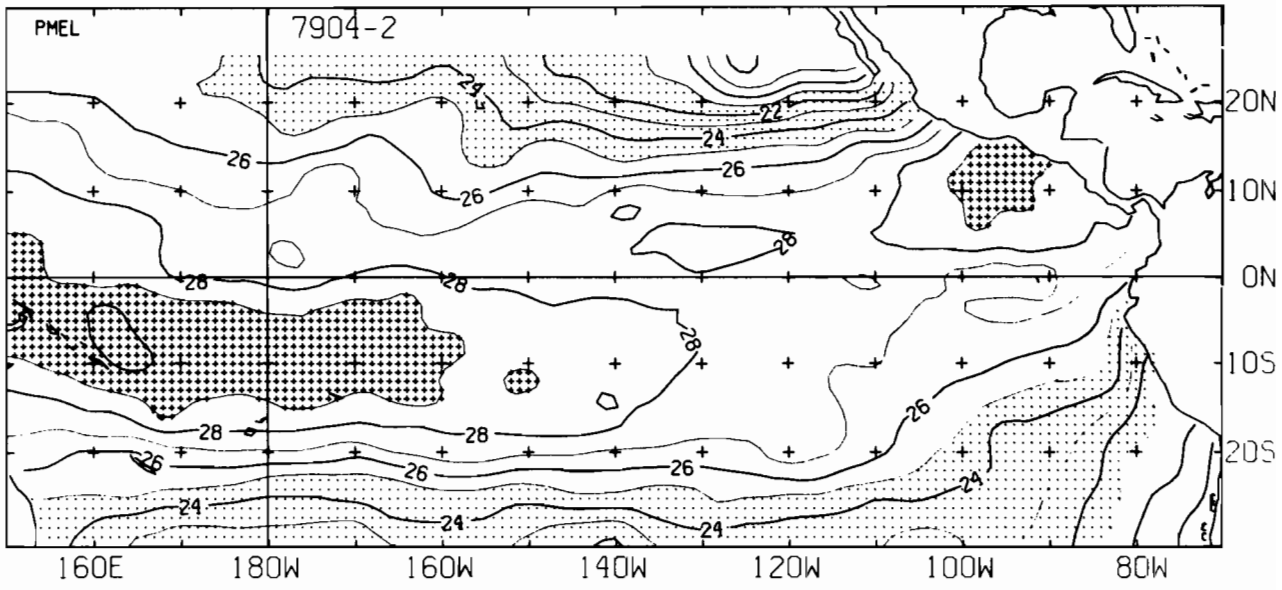

7904-2 SST. 45 E-BUØY. 93 BT. 34 XBT. 1253 SPØT DATA

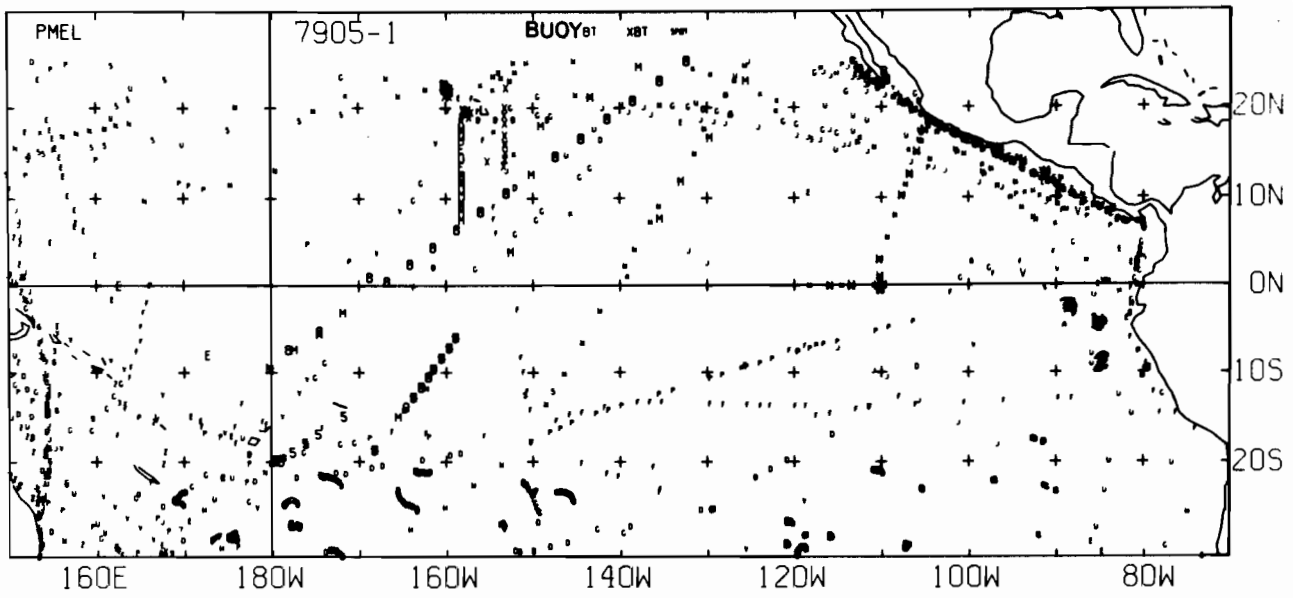

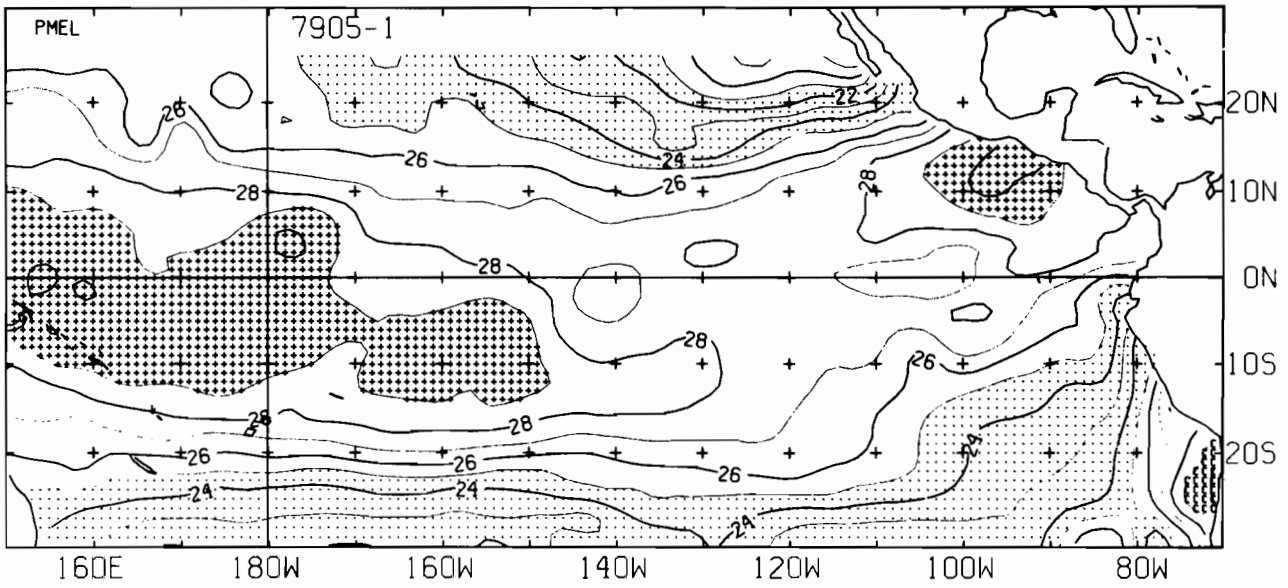

7905-1 SST. 44 E-BUØY. 146 BT. 29 XBT. 1191 SPØT DATA

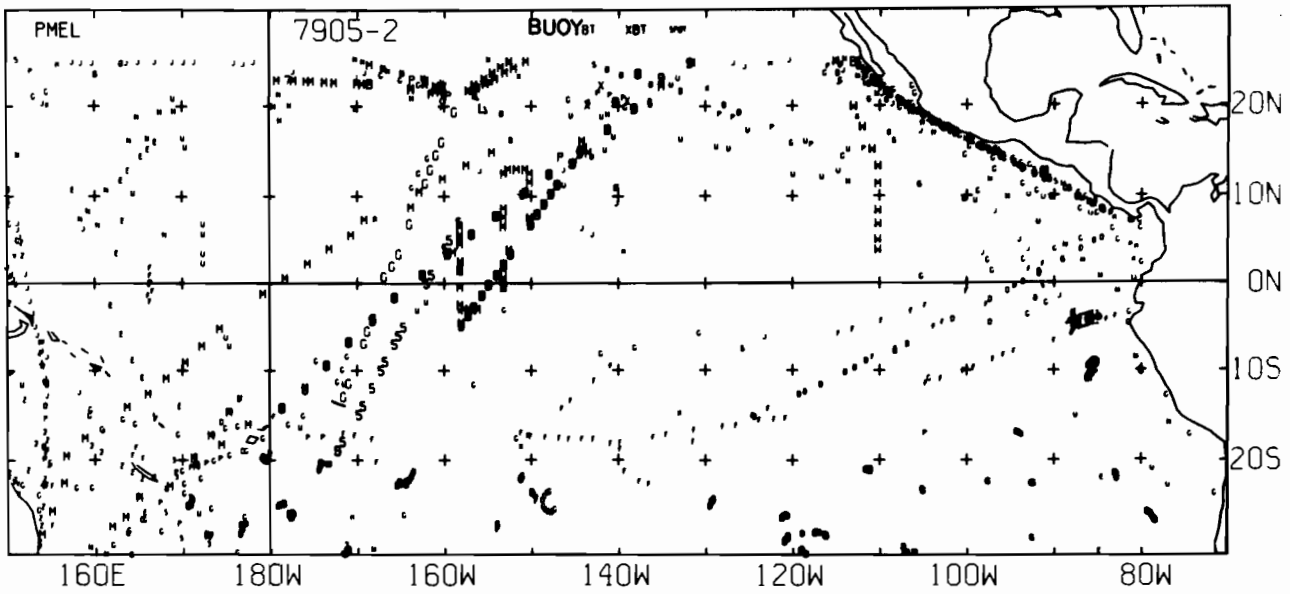

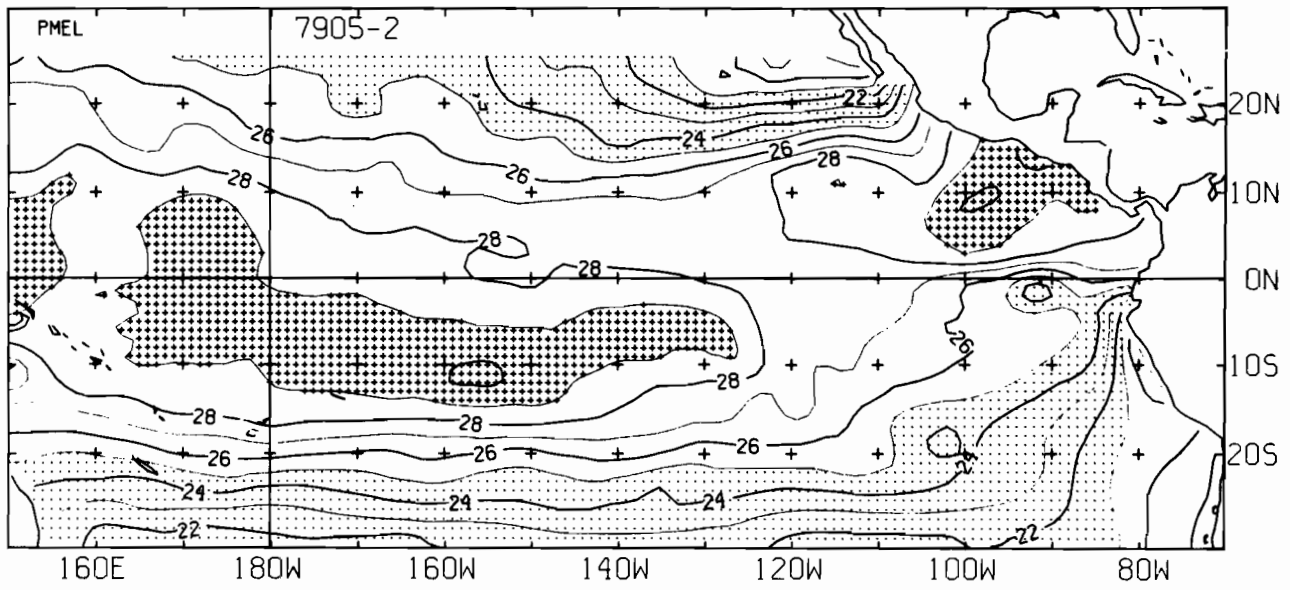

7905-2 SST, 48 E-BUØY, 165 BT, 49 XBT, 941 SPØT DATA

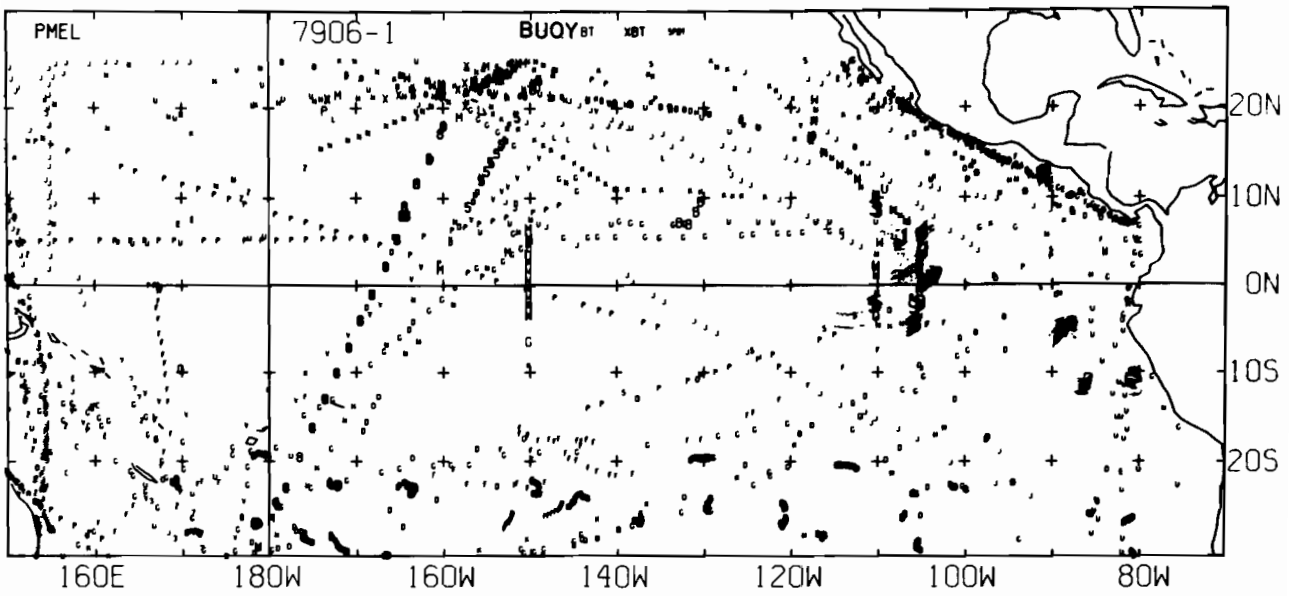

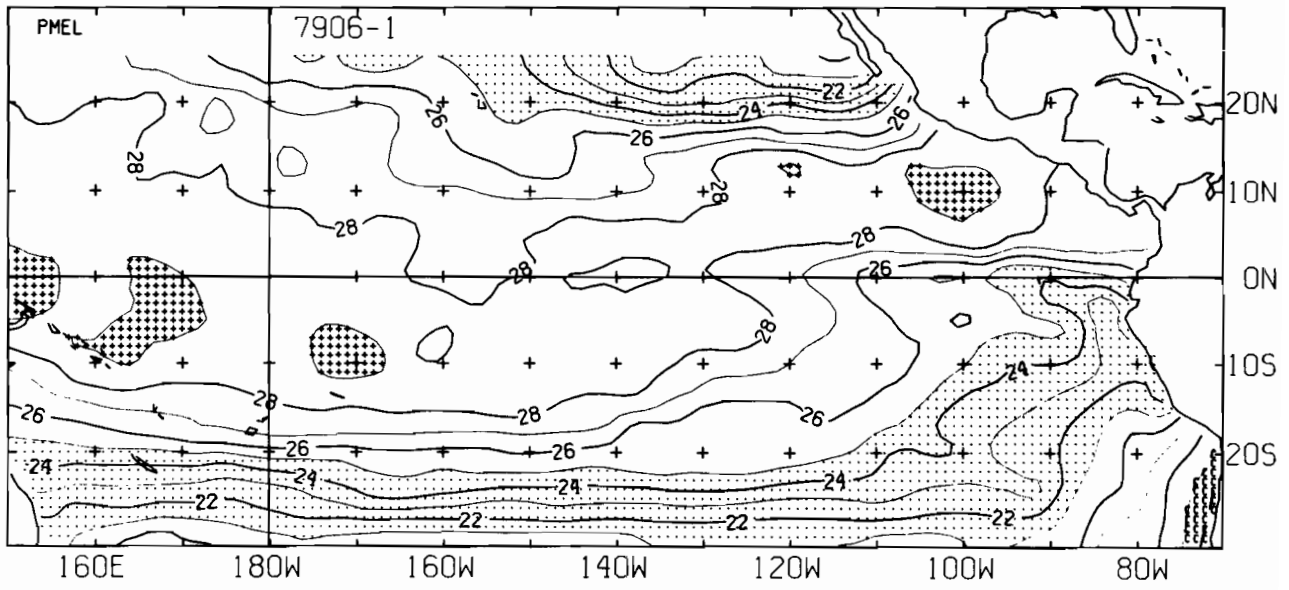

7906-1 SST, 183 E-BUØY, 118 BT, 27 XBT, 1769 SPØT DATA

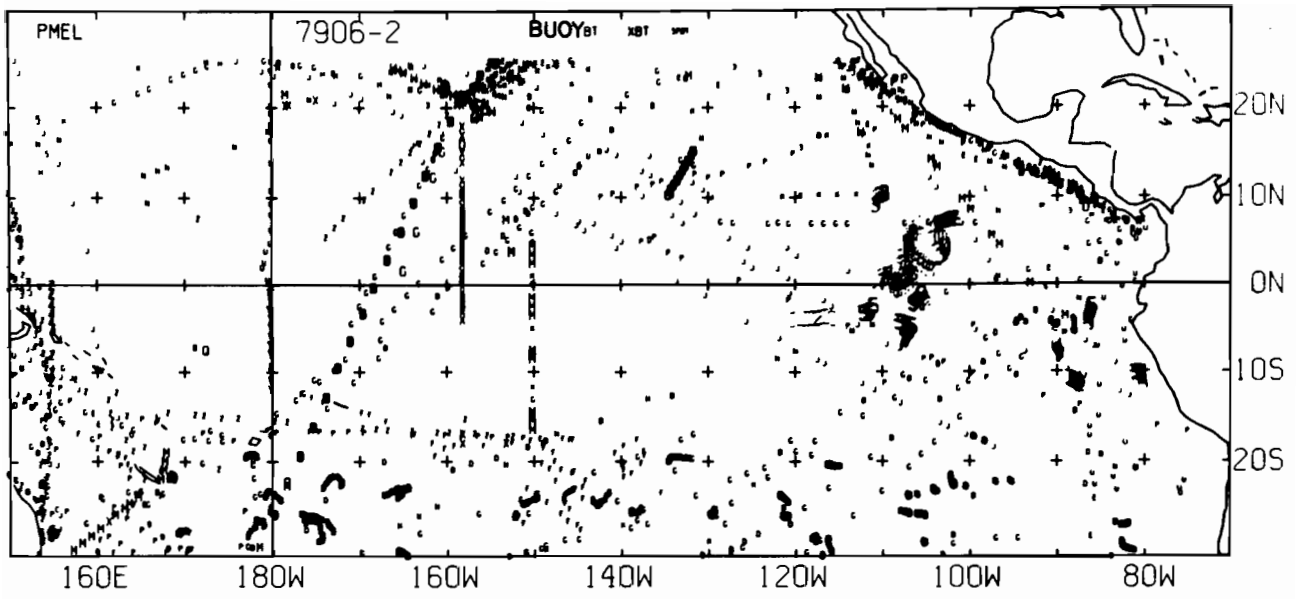

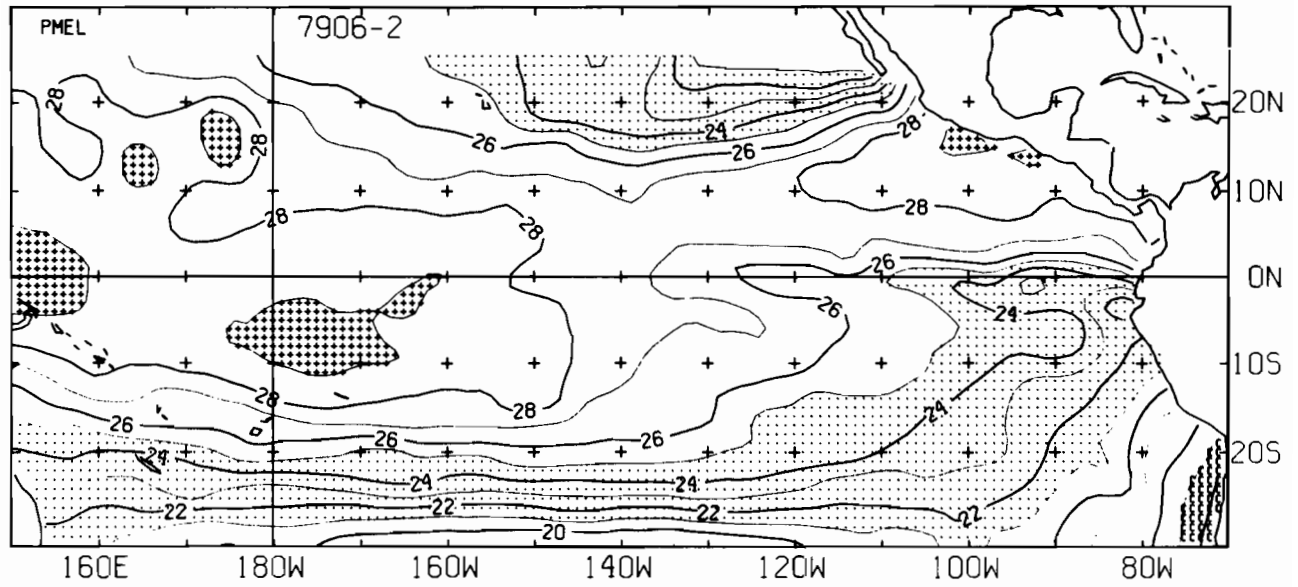

7906-2 SST. 296 E-BUØY. 224 BT. 28 XBT. 1599 SPØT DATA

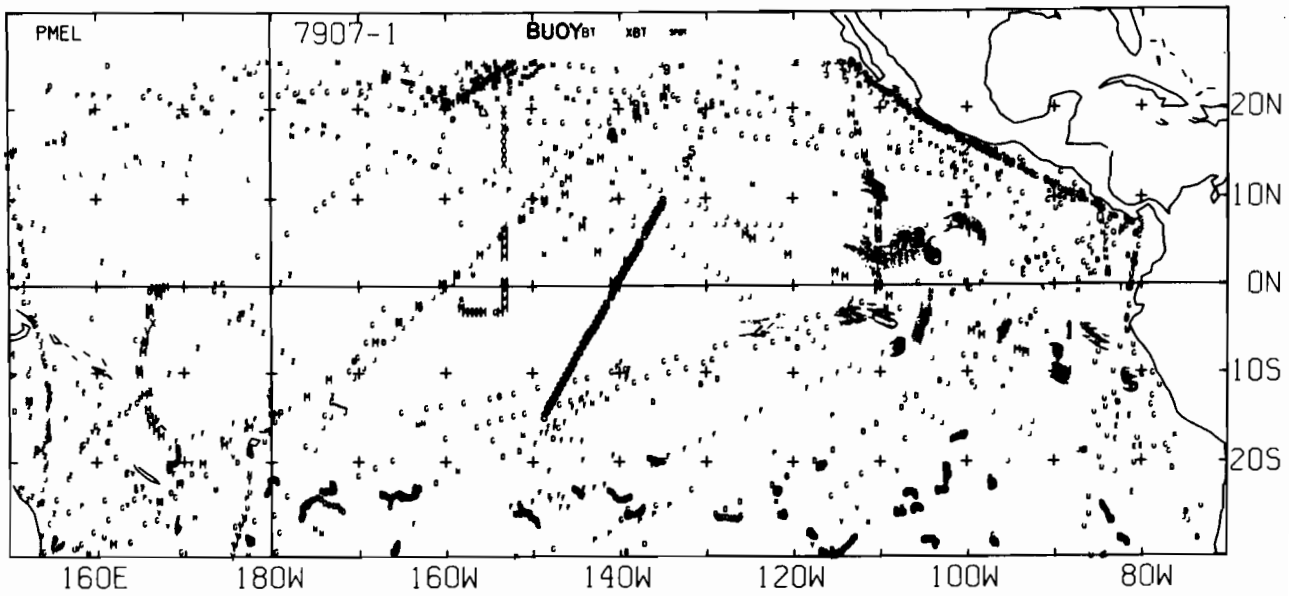

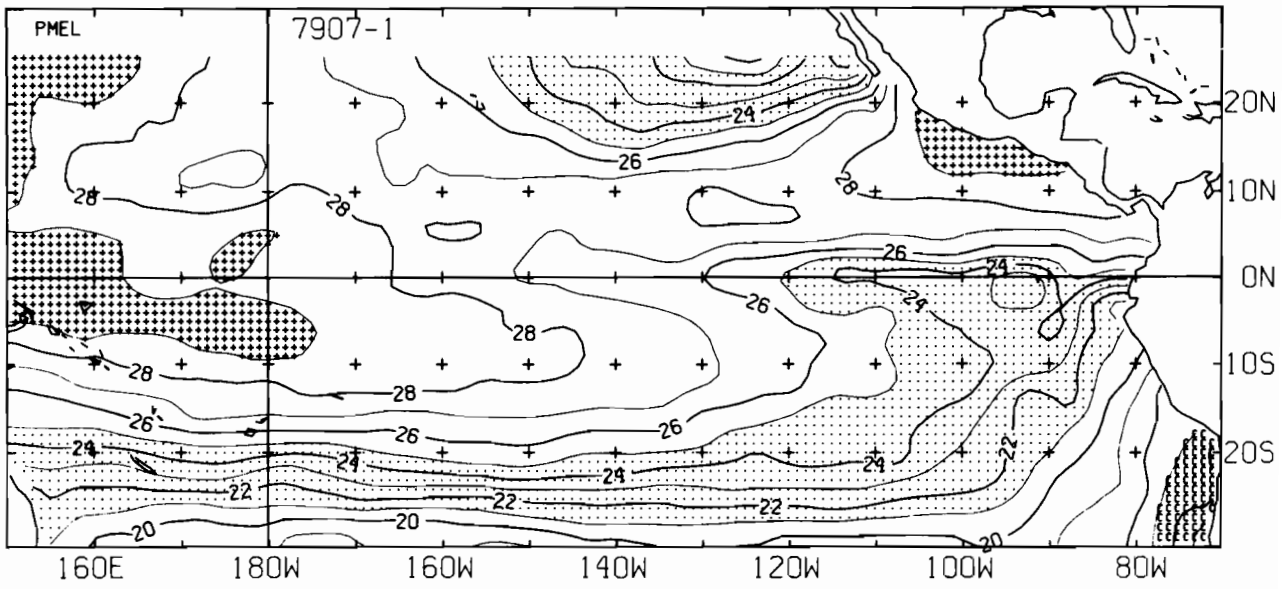

7907-1 SST. 295 E-BUØY. 158 BT. 49 XBT. 1846 SPØT DATA

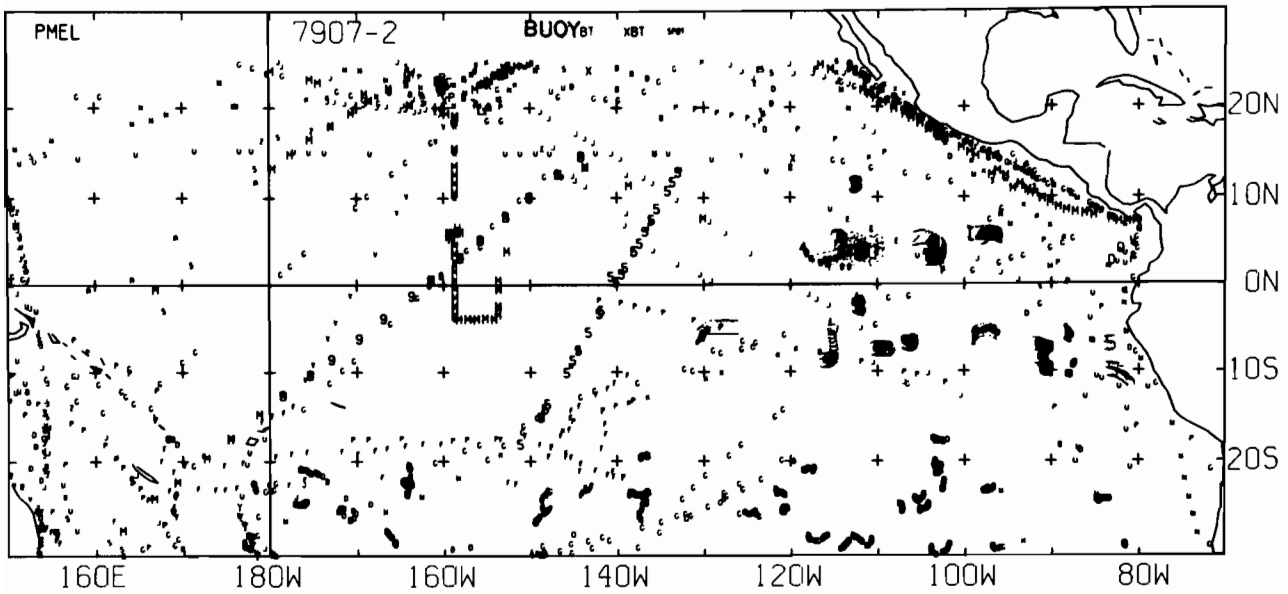

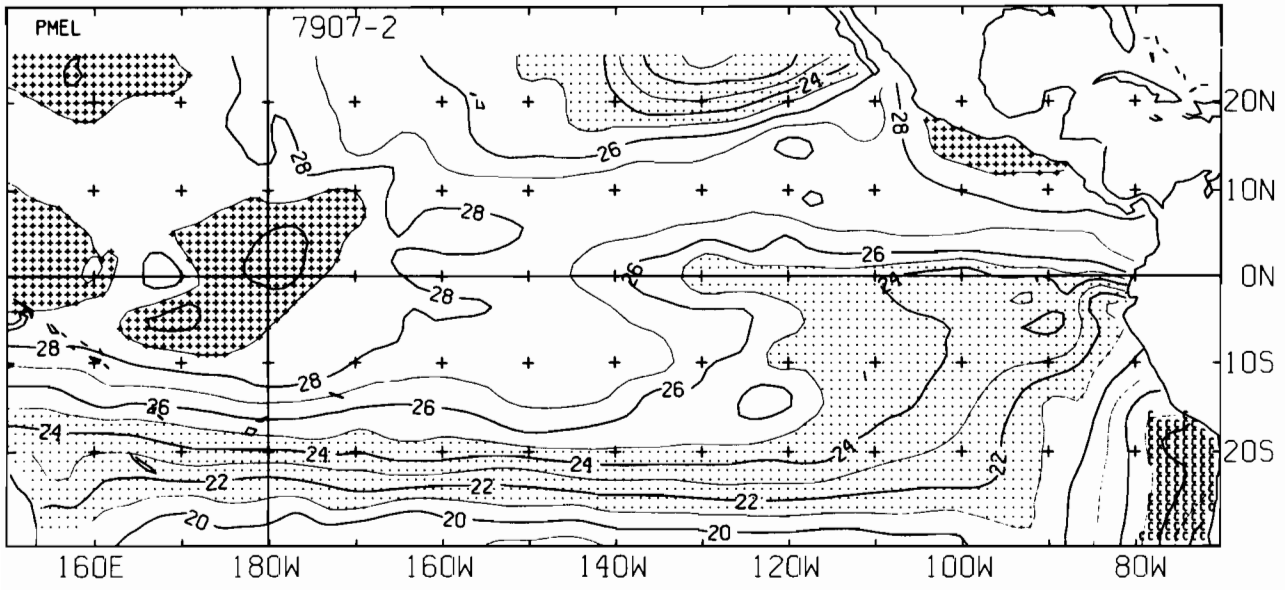

7907-2 SST, 305 E-BUØY, 167 BT, 35 XBT, 1517 SPØT DATA

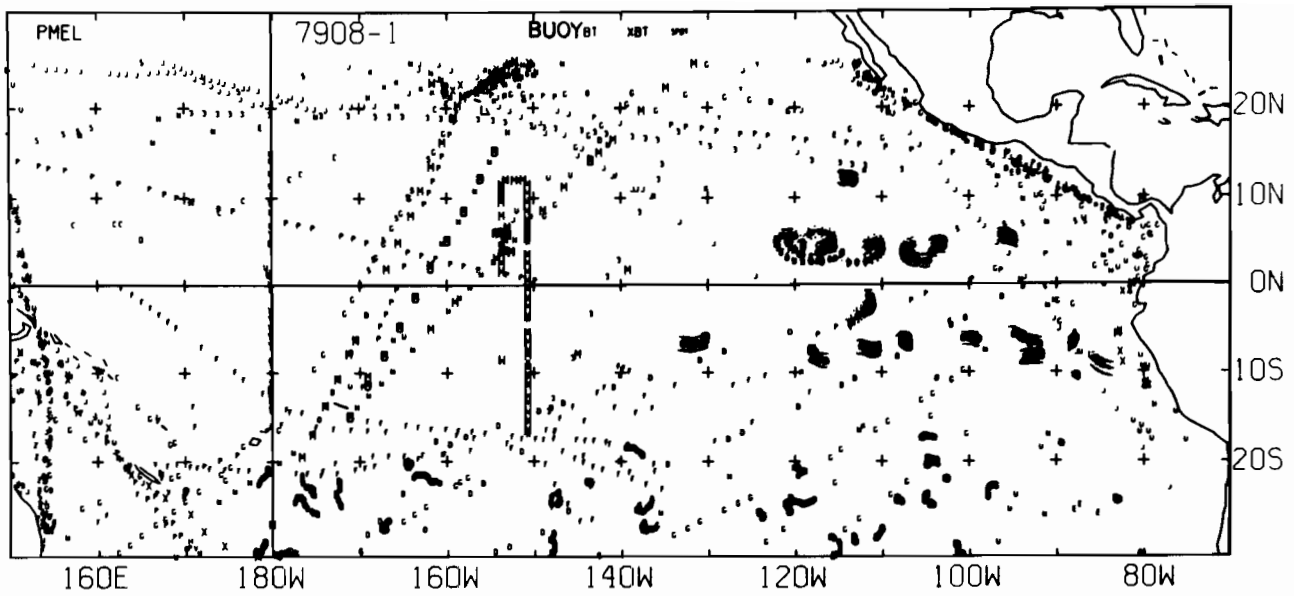

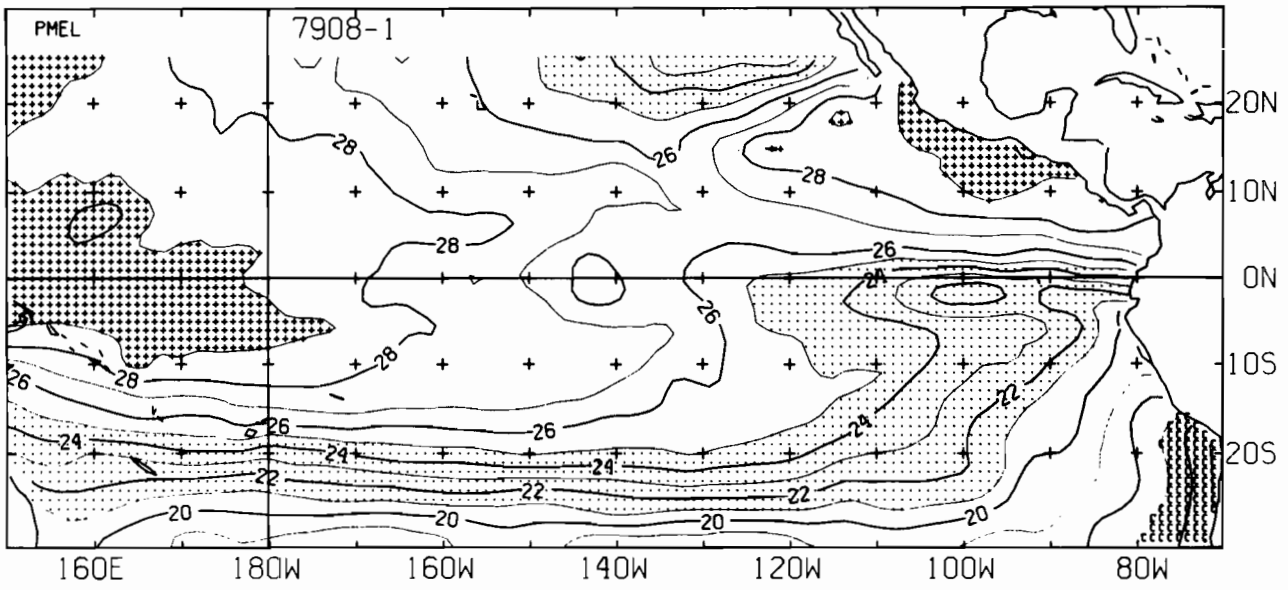

7908-1 SST. 285 E-BUØY. 156 BT. 10 XBT. 1899 SPØT DATA

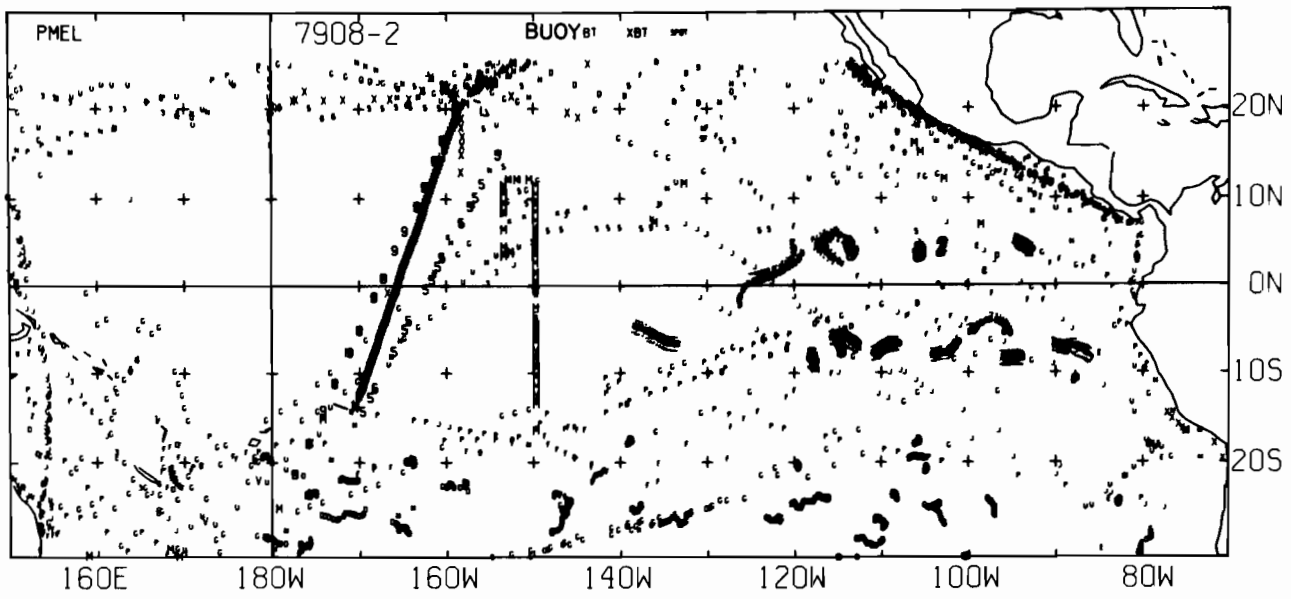

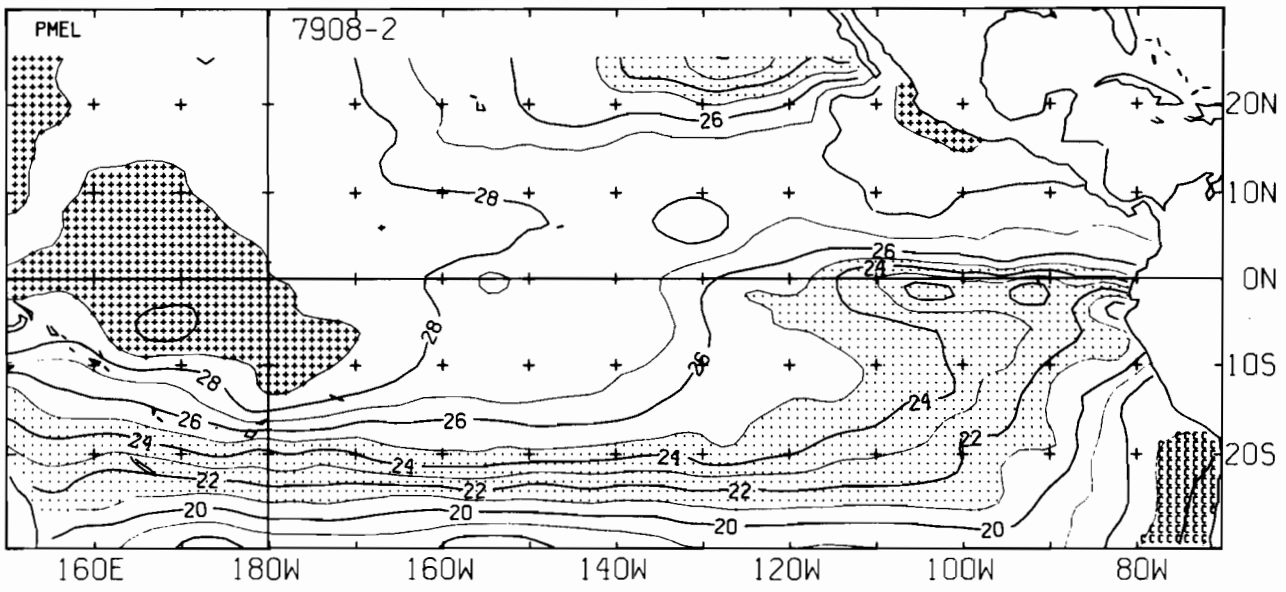

7908-2 SST. 284 E-BUØY. 250 BT. 31 XBT. 2021 SPØT DATA

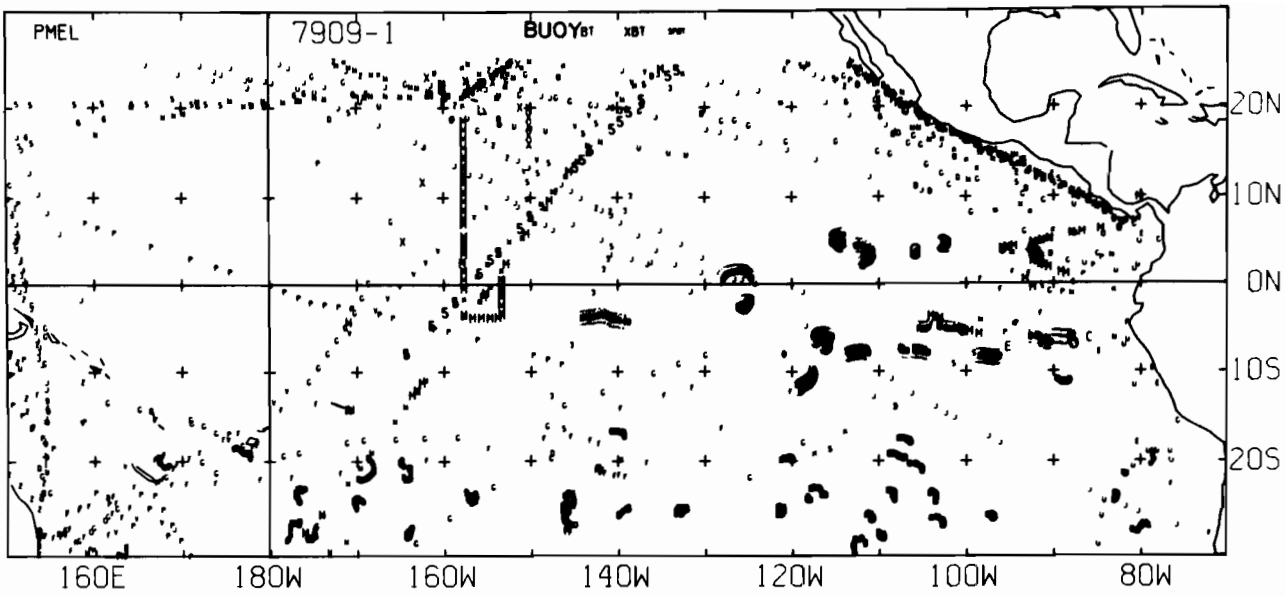

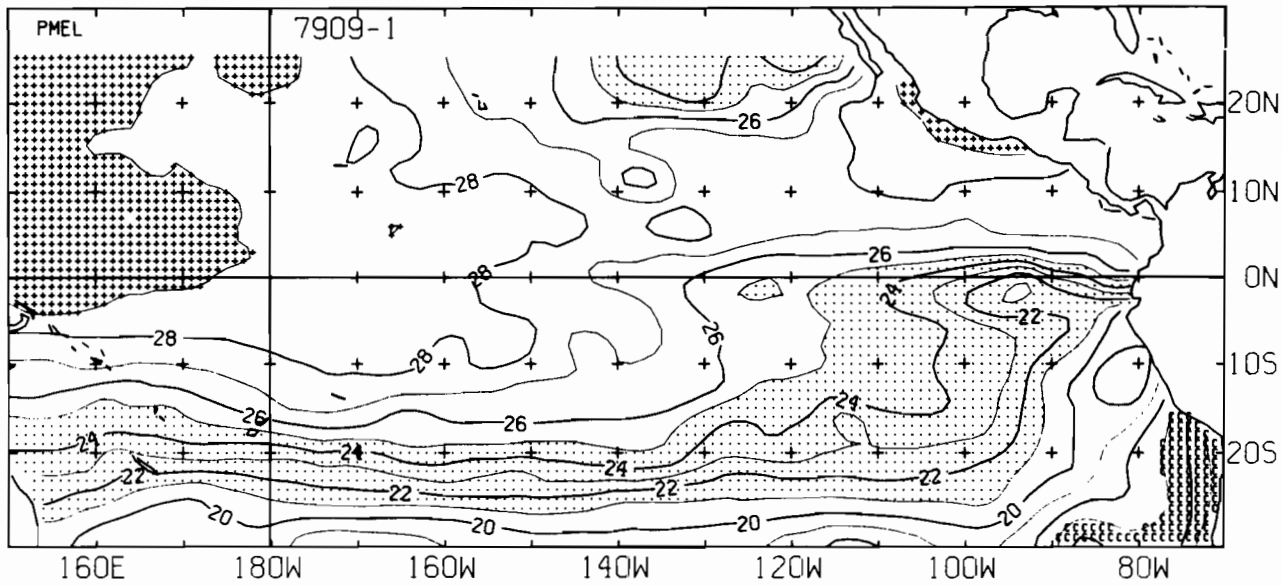

7909-1 SST. 259 E-BUØY. 103 BT. 18 XBT. 1685 SPØT DATA

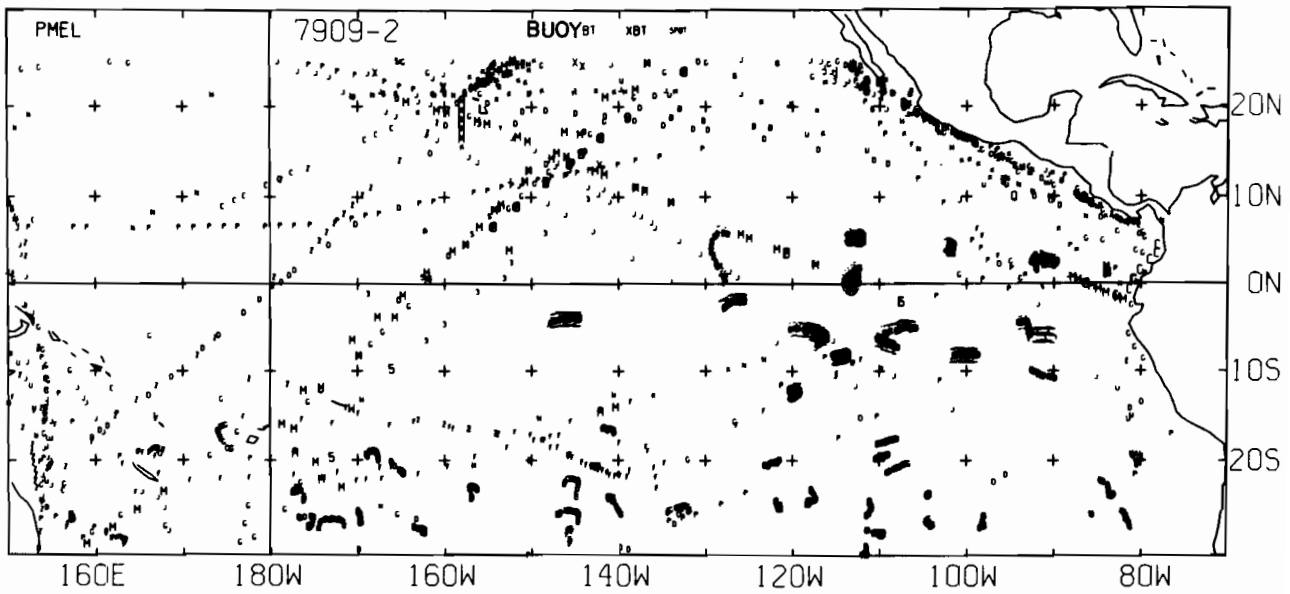

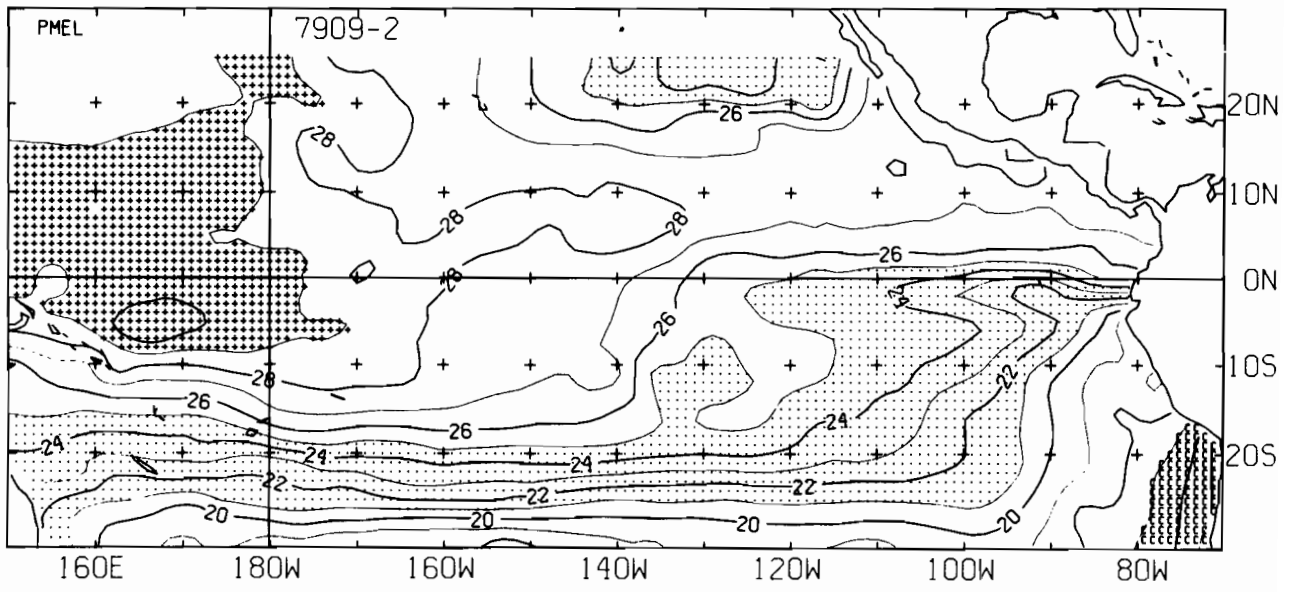

7909-2 SST, 255 E-BUØY, 110 BT, 10 XBT, 1523 SPØT DATA

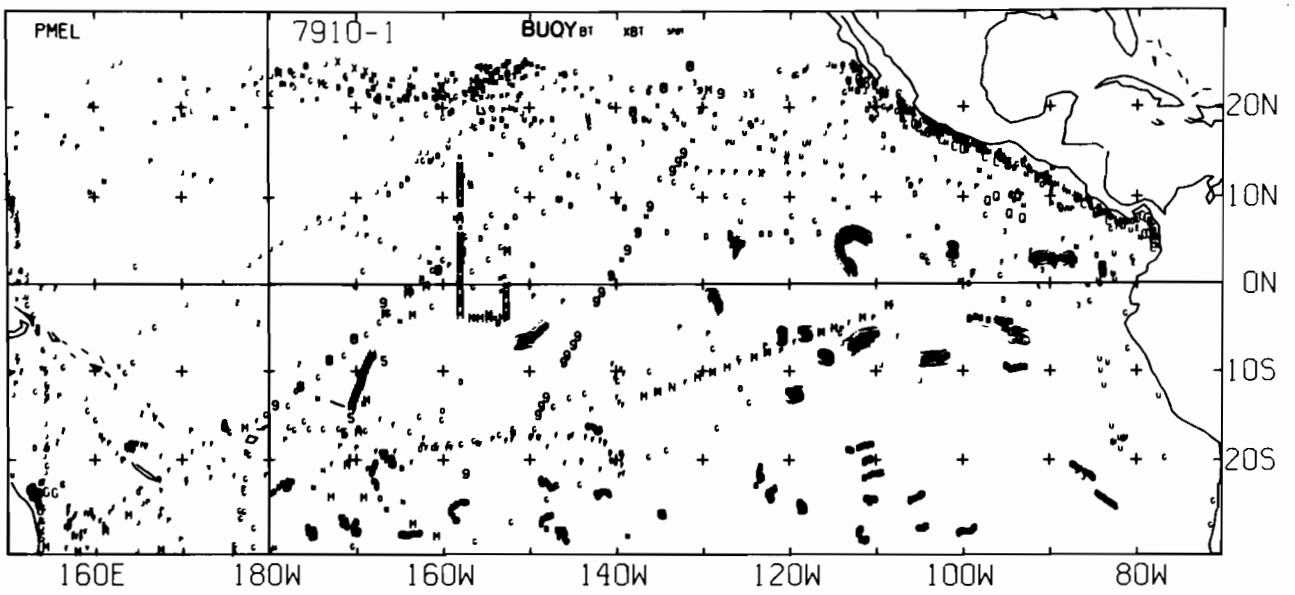

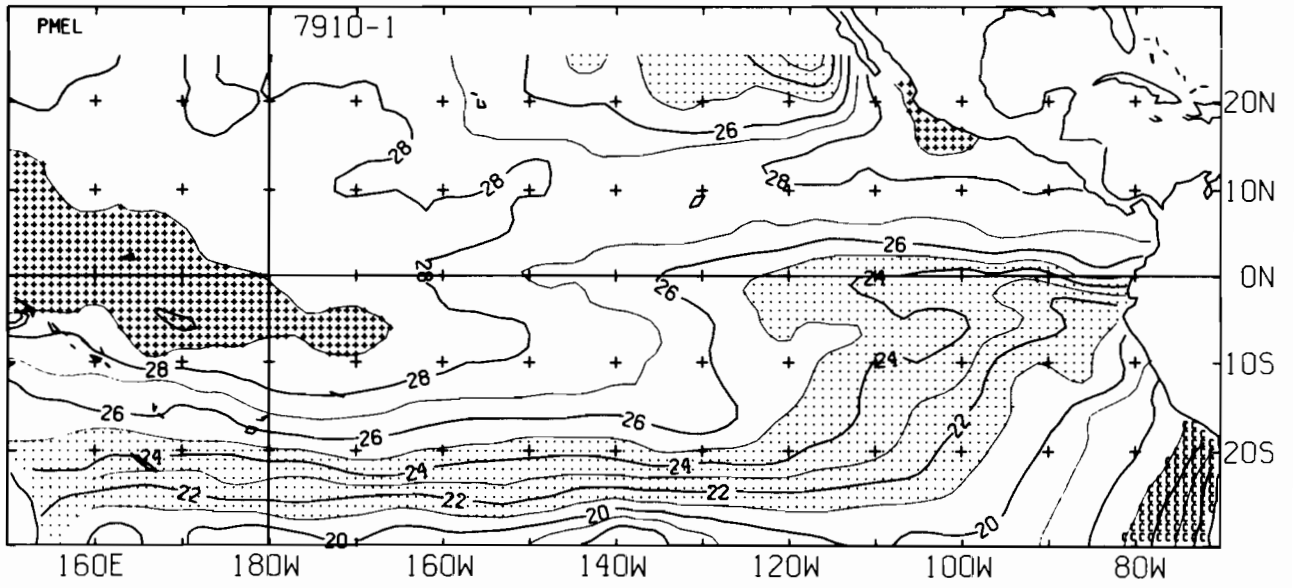

7910-1 SST, 255 E-BUØY, 164 BT, 32 XBT, 1690 SPØT DATA

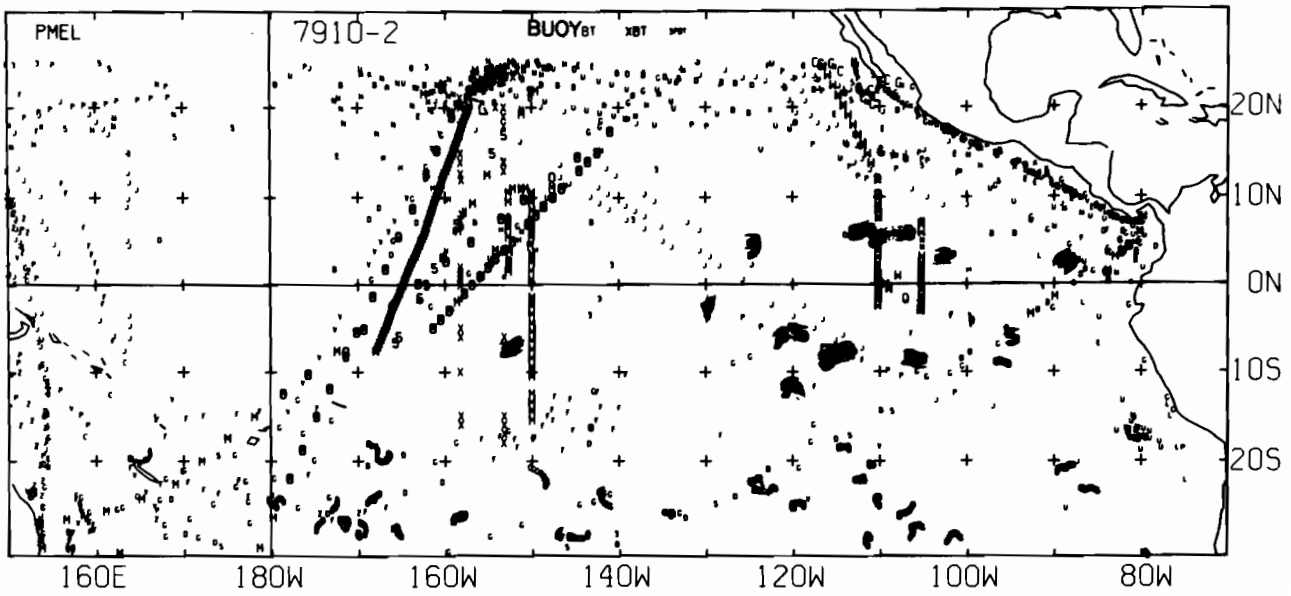

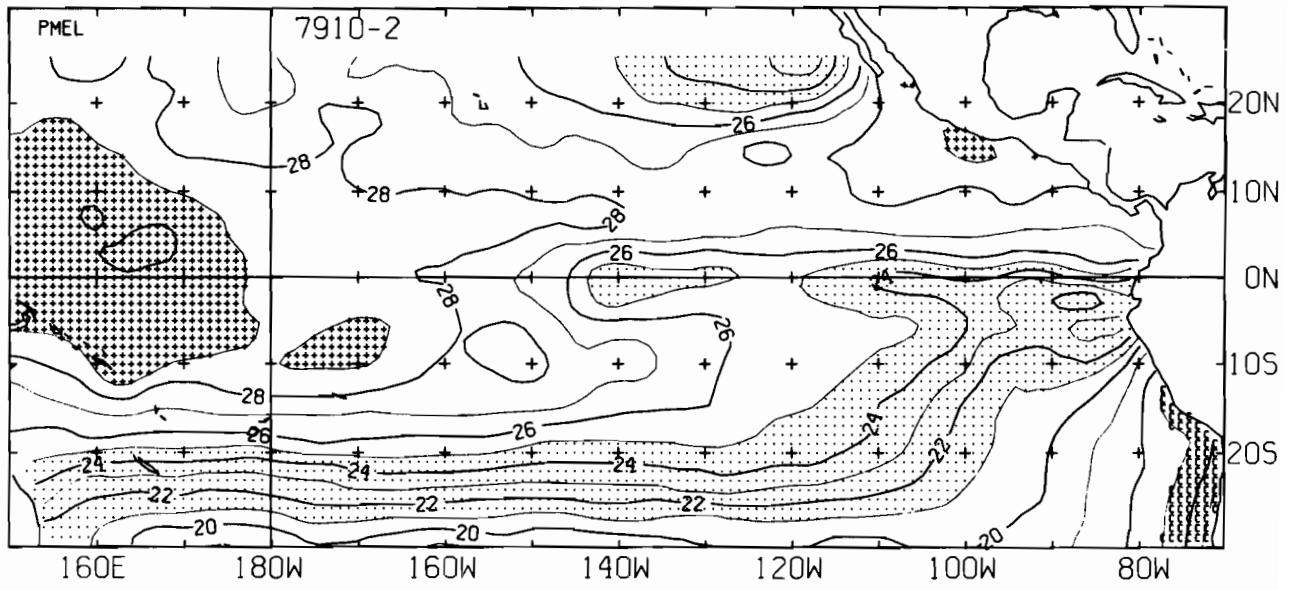

7910-2 SST, 272 E-BUØY, 319 BT, 55 XBT, 1750 SPØT DATA

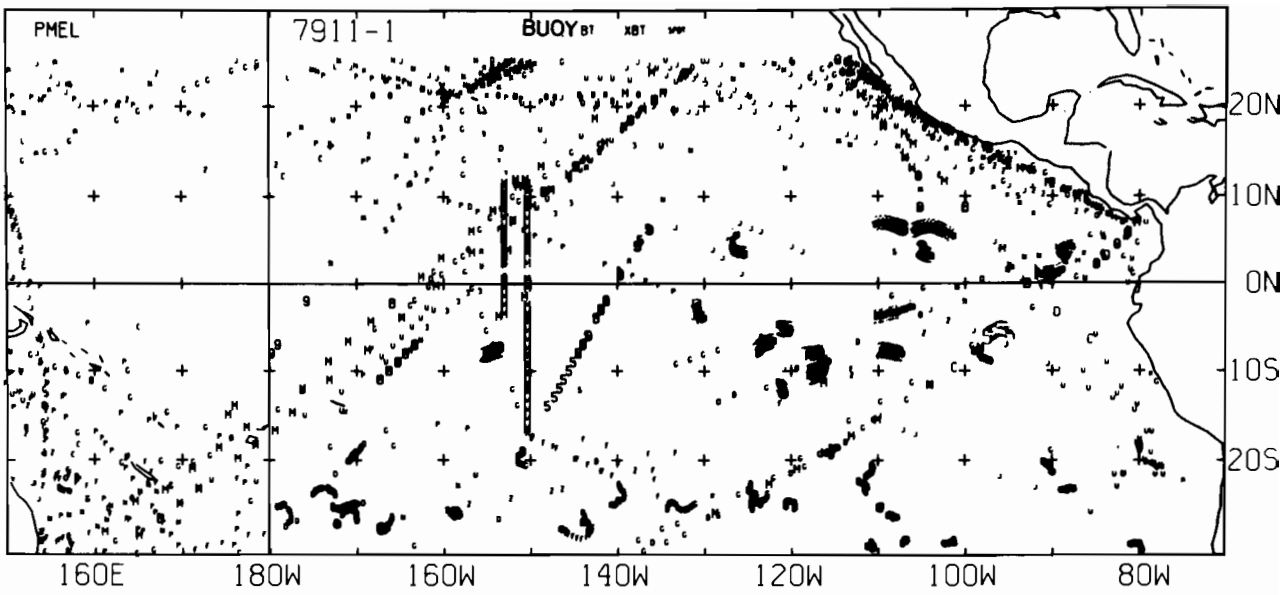

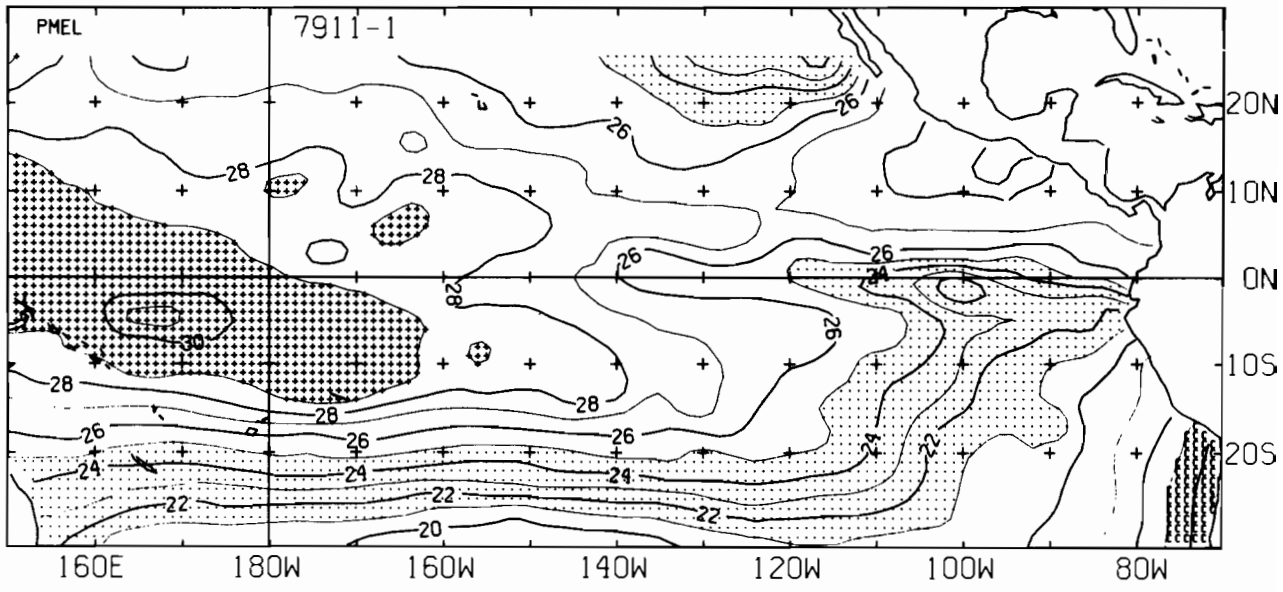

7911-1 SST. 255 E-BUØY. 186 BT. 30 XBT. 1723 SPØT DATA

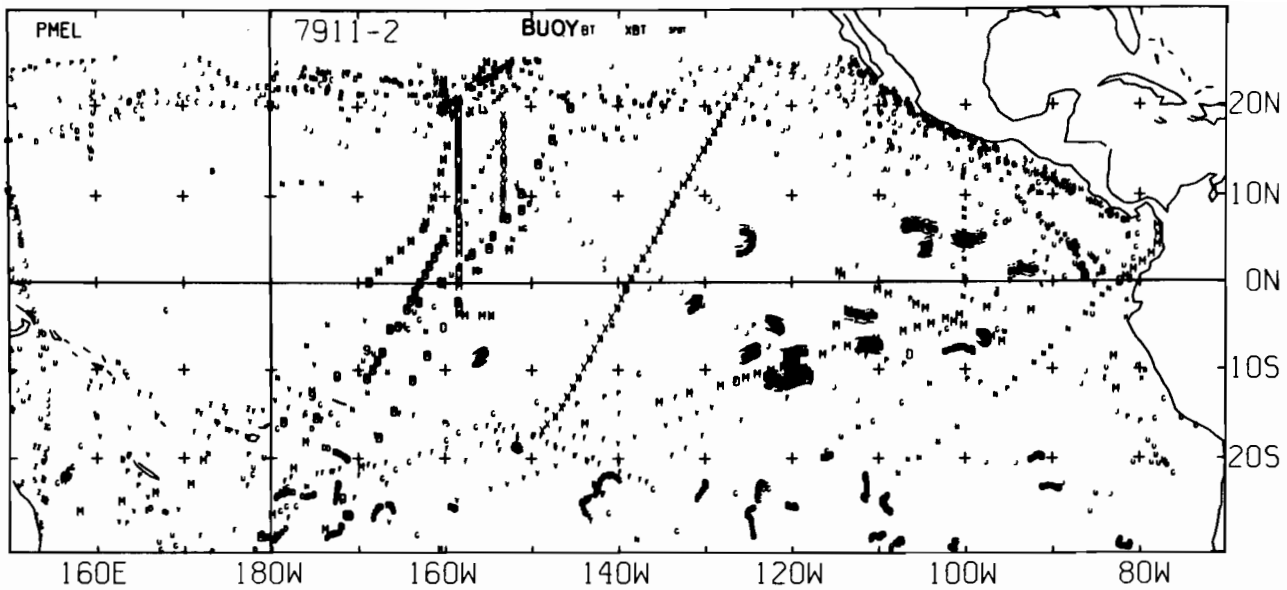

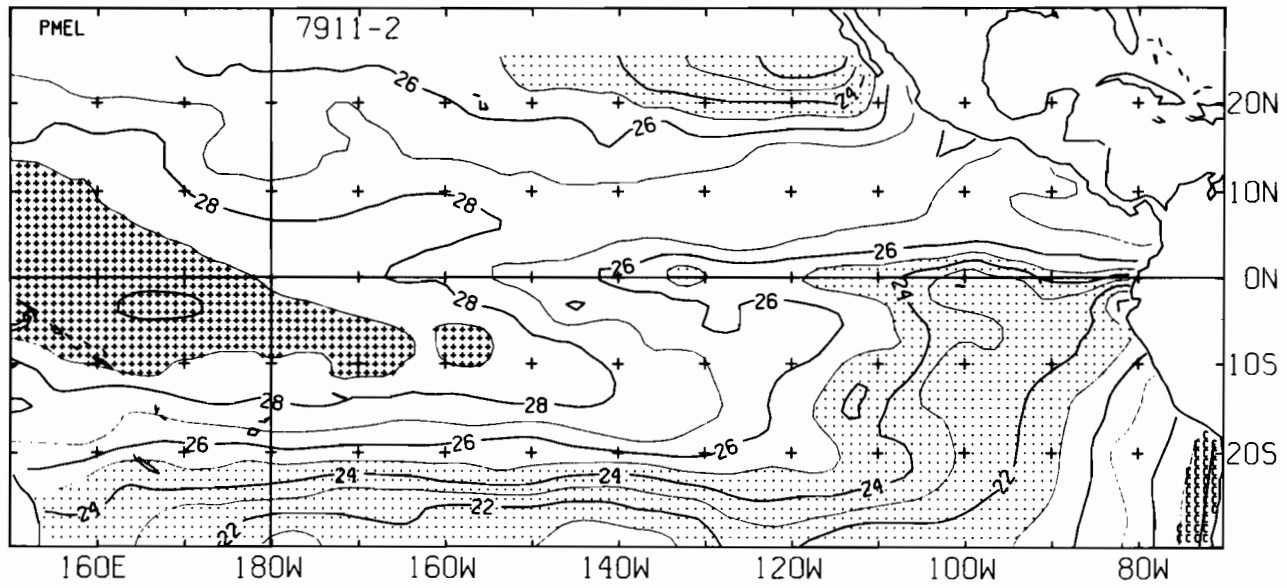

7911-2 SST. 252 E-BUØY. 248 BT. 37 XBT. 1731 SPØT DATA

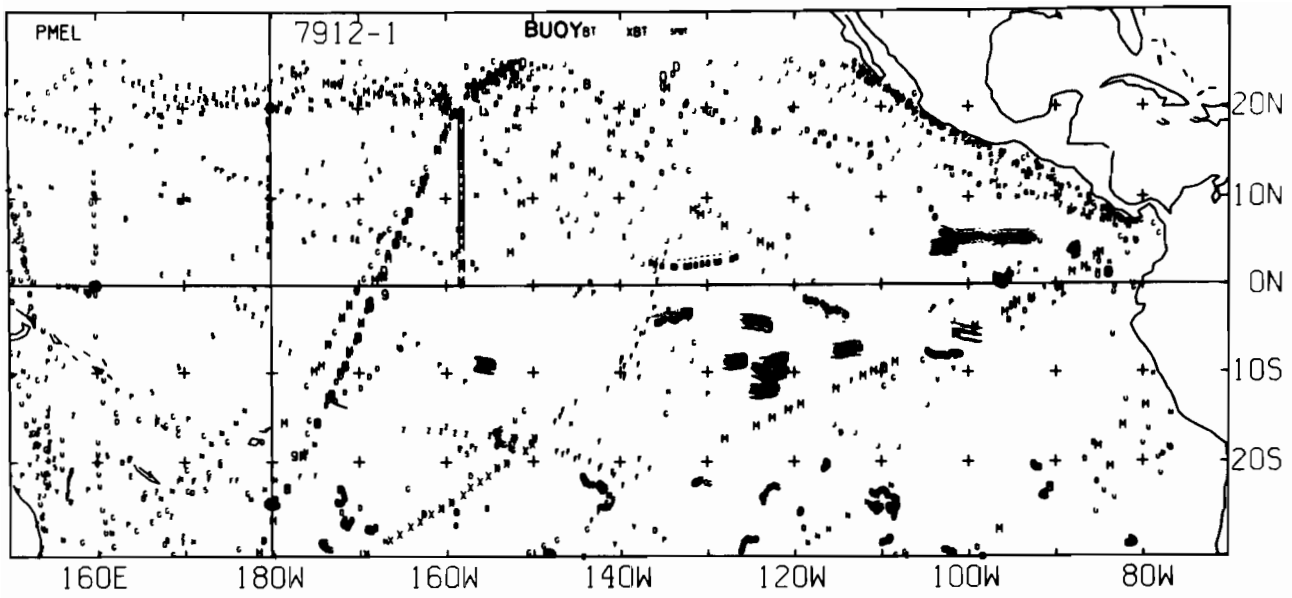

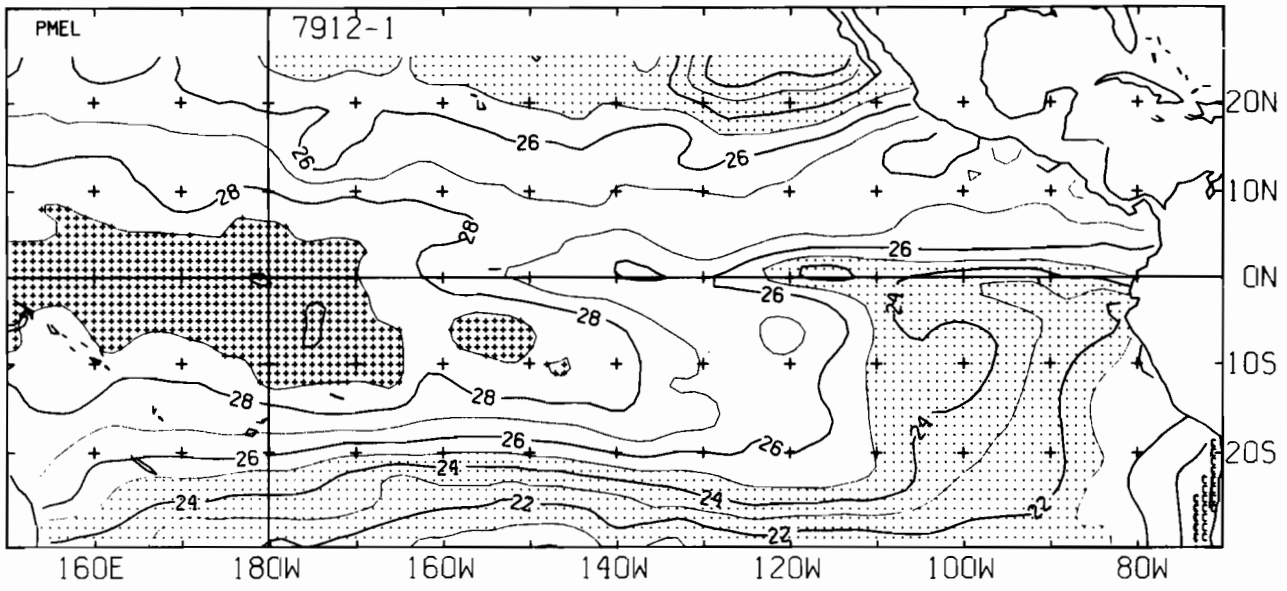

7912-1 SST. 255 E-BUØY. 171 BT. 12 XBT. 1688 SPØT DATA

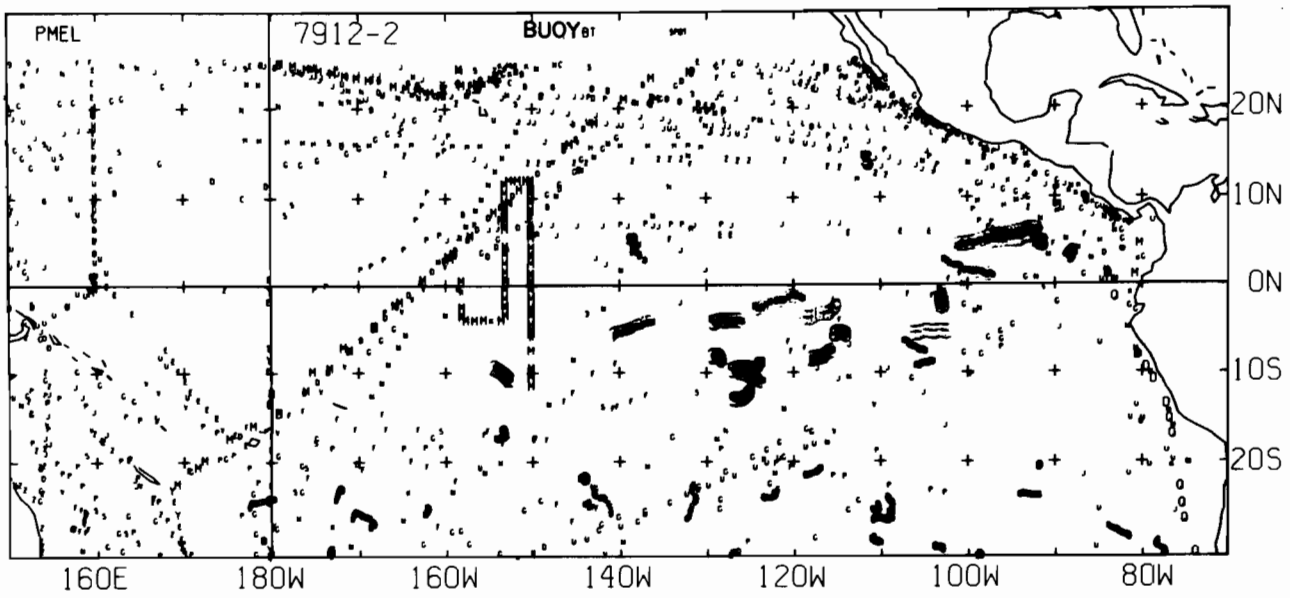

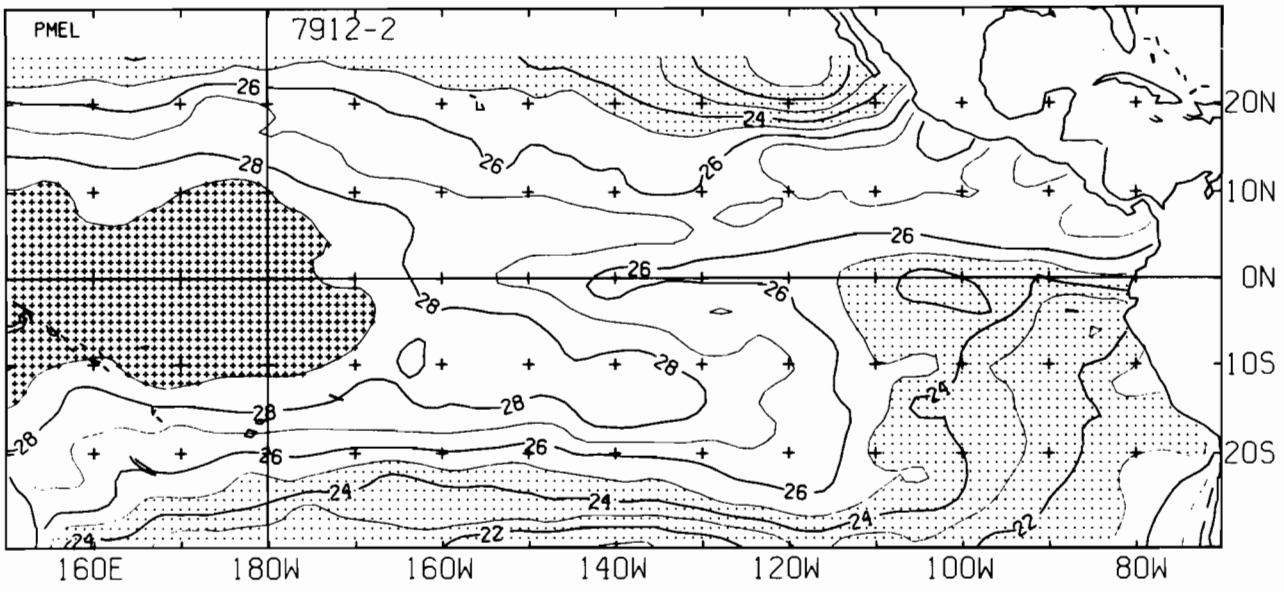

7912-2 SST. 347 E-BUØY. 135 BT. 0 XBT. 1883 SPØT DATA

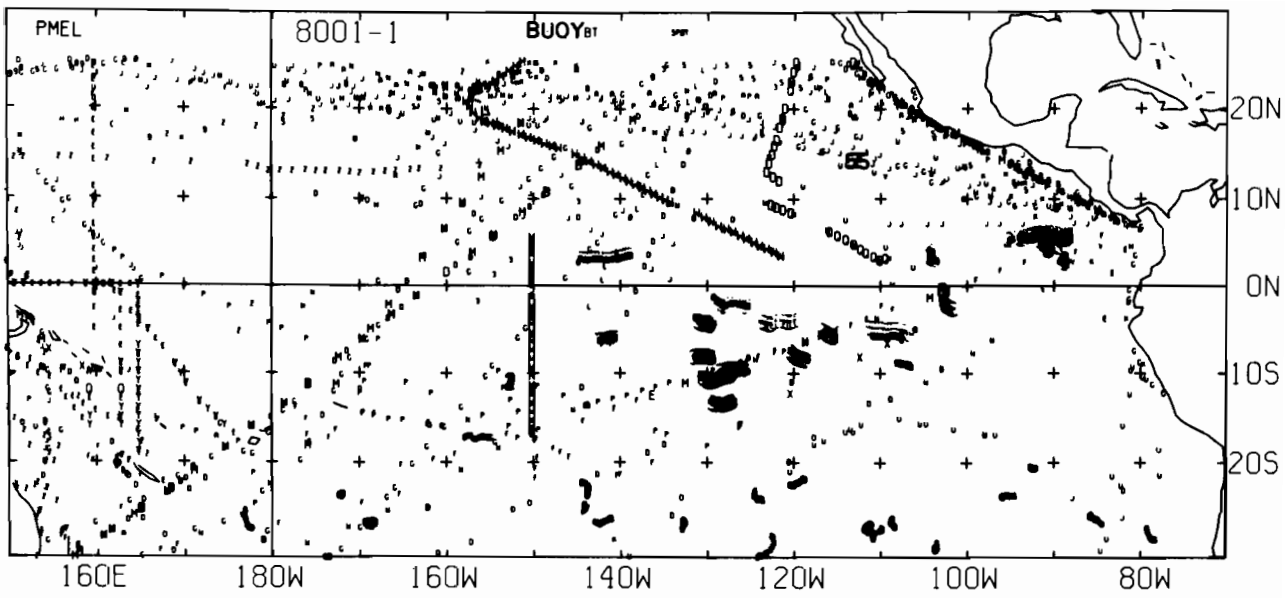

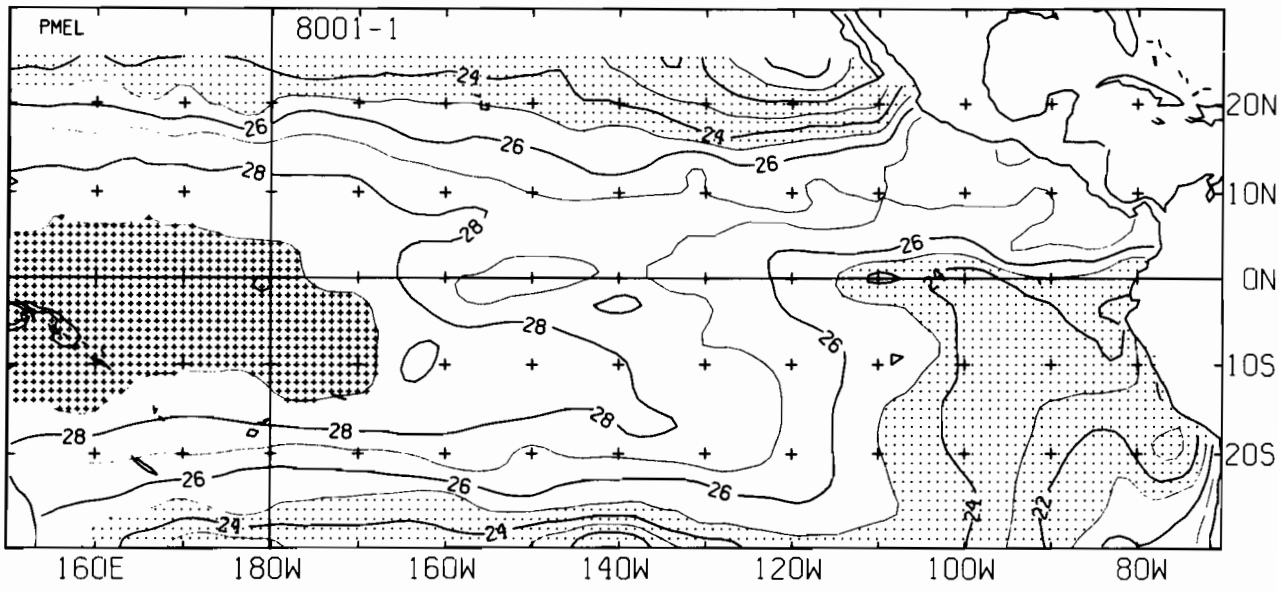

8001-1 SST. 330 E-BUØY. 222 BT. 0 XBT. 1790 SPØT DATA

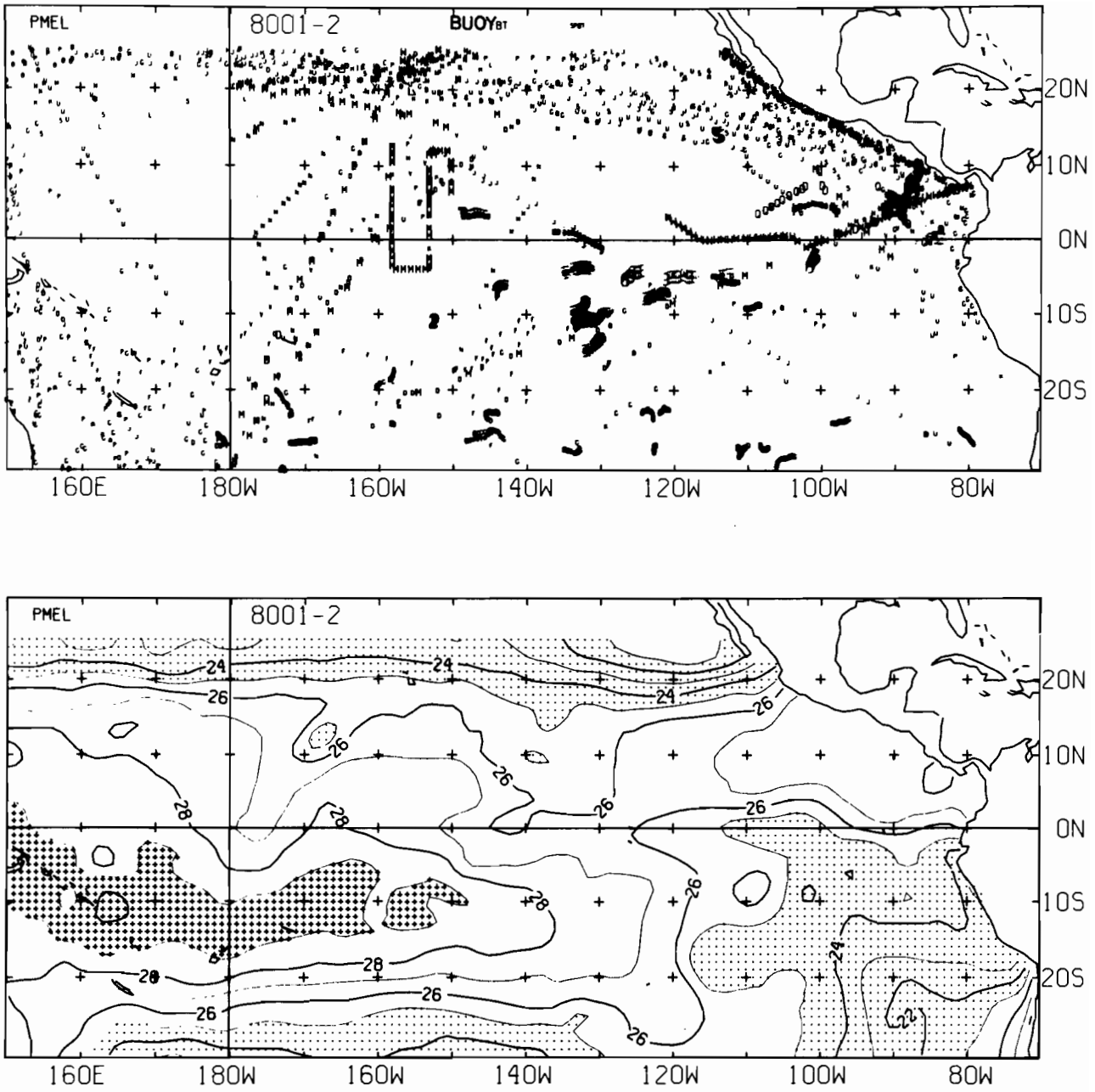

8001-2 SST. 347 E-BUØY. 243 BT. 0 XBT. 1955 SPØT DATA

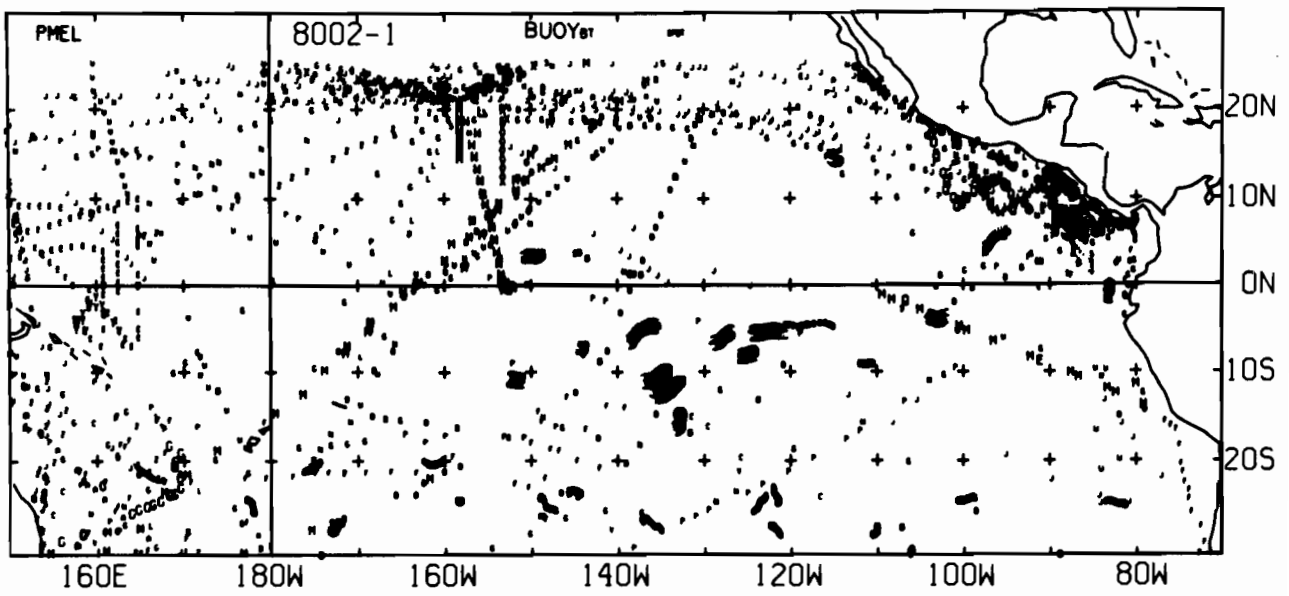

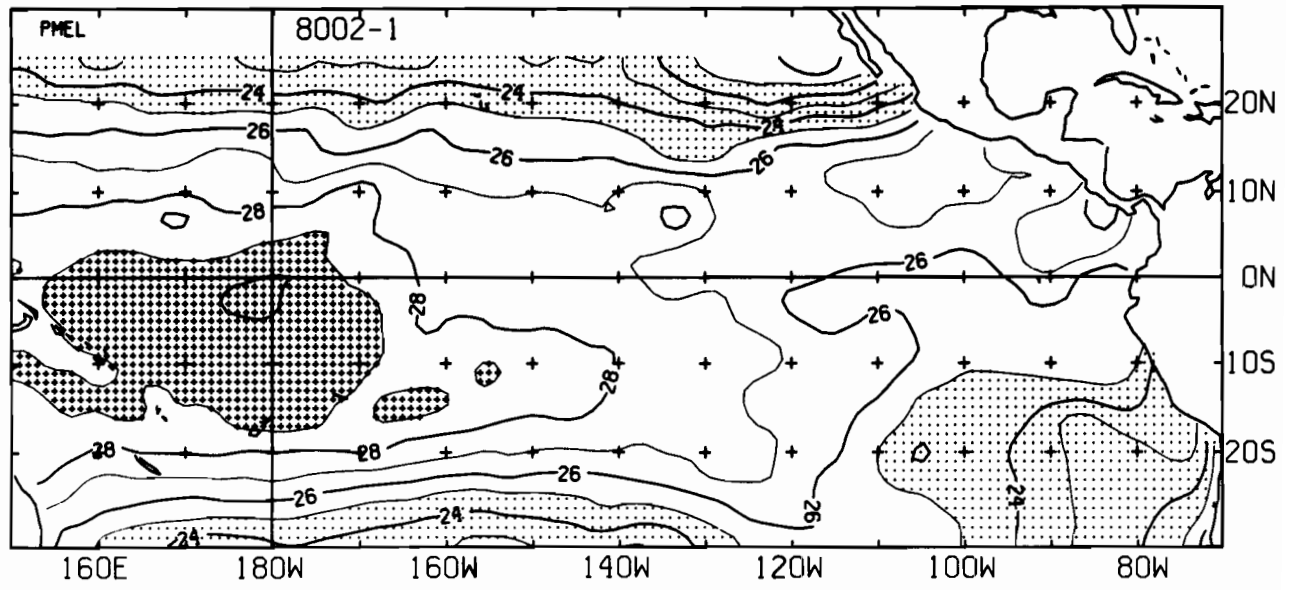

8002-1 SST. 293 E-BUØY. 250 BT. 0 XBT. 1760 SPØT DATA

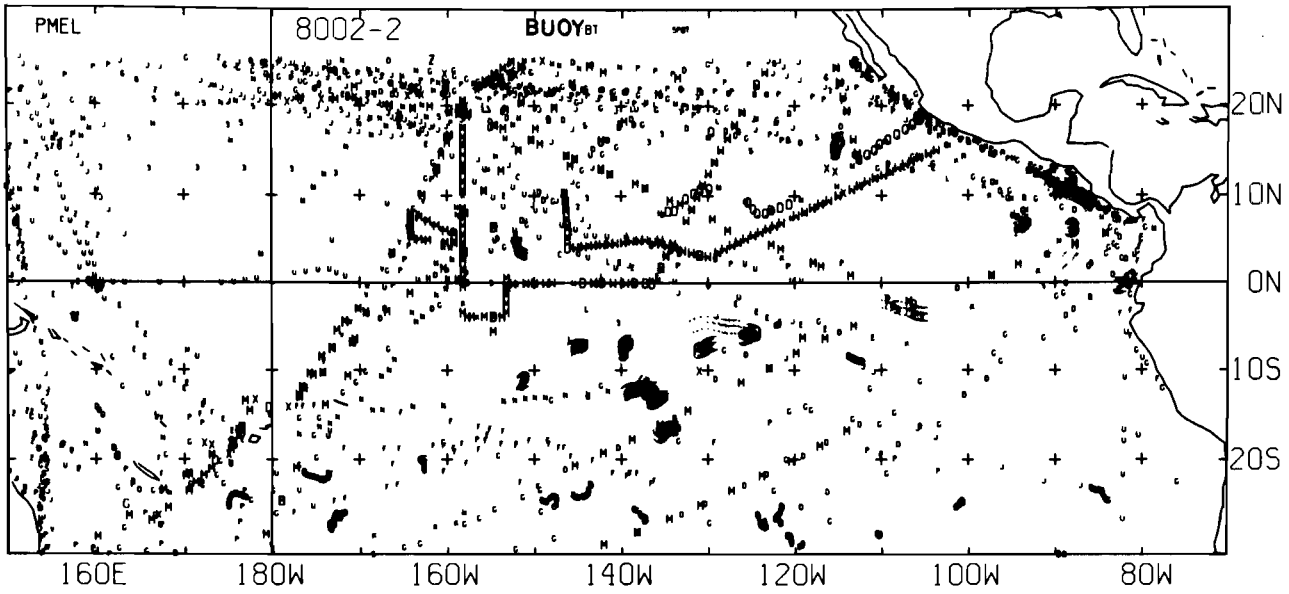

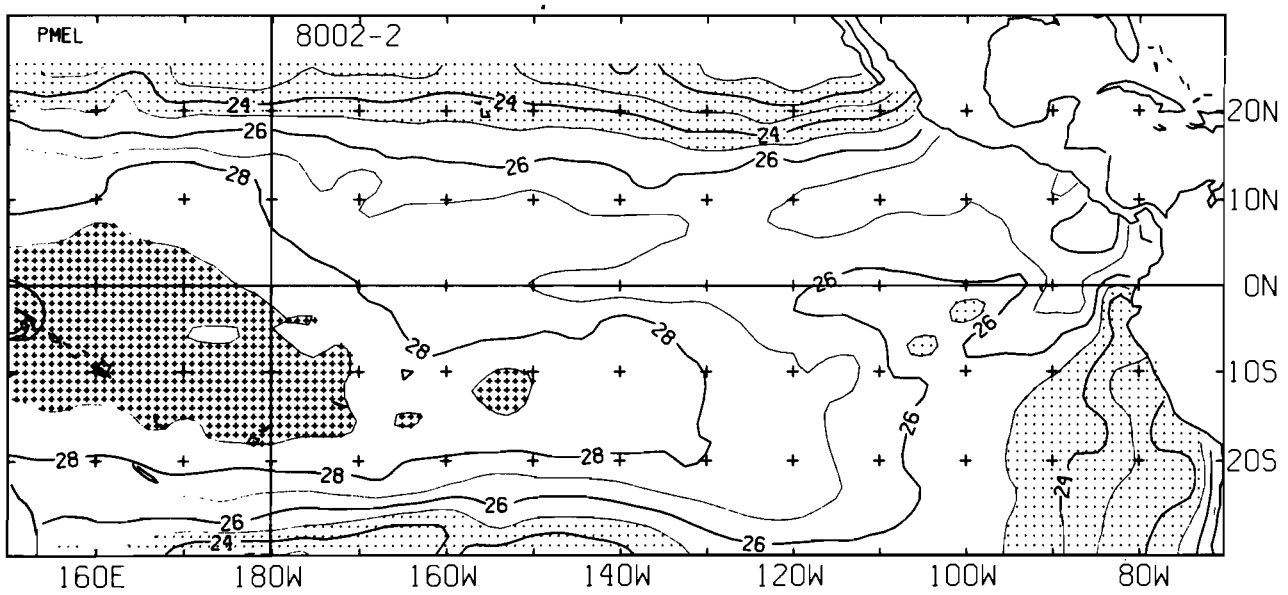

8002-2 SST. 297 E-BUØY. 377 BT. 0 XBT. 1831 SPØT DATA

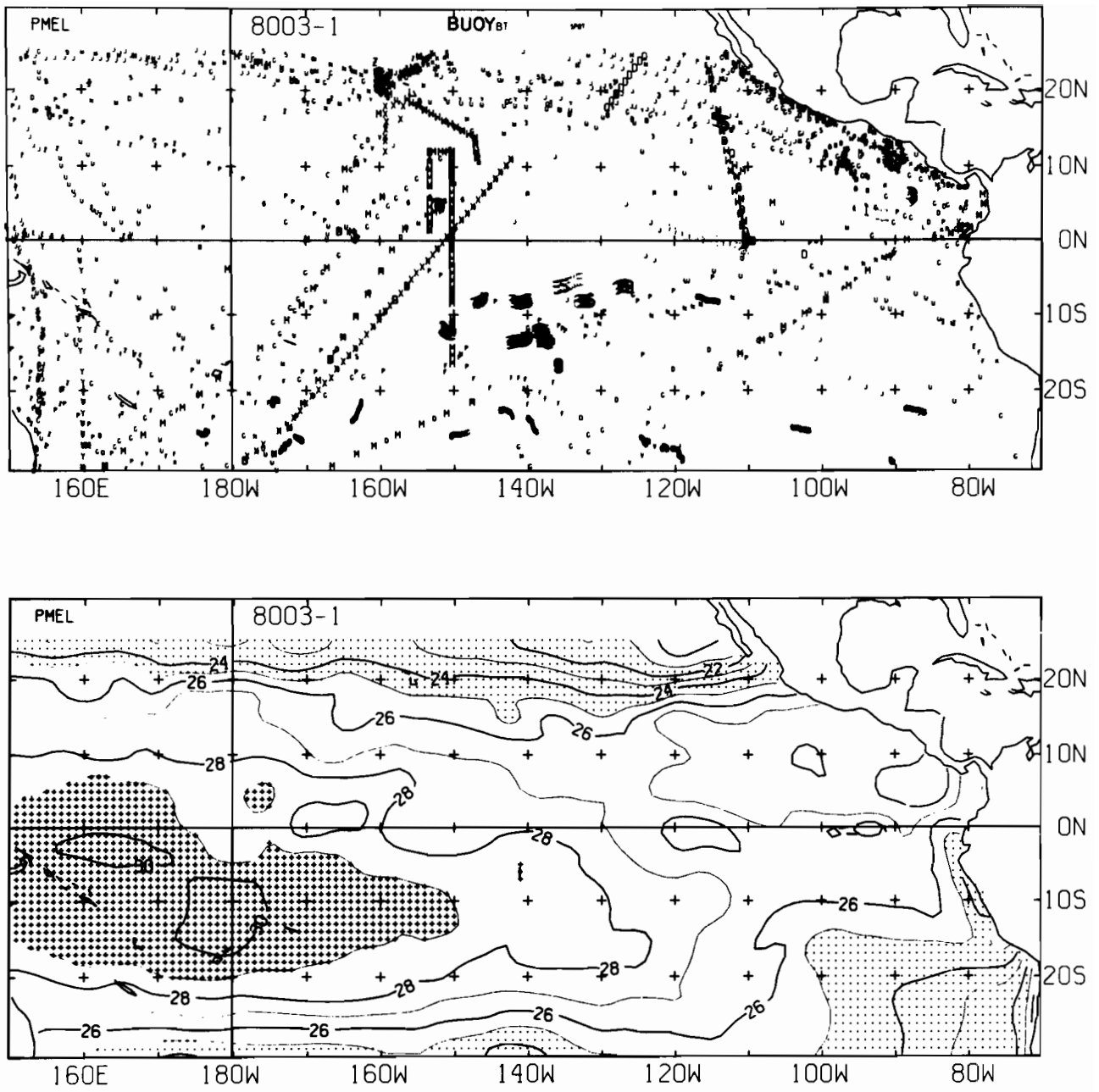

8003-1 SST. 282 E-BUØY. 298 BT. 0 XBT. 1644 SPØT DATA

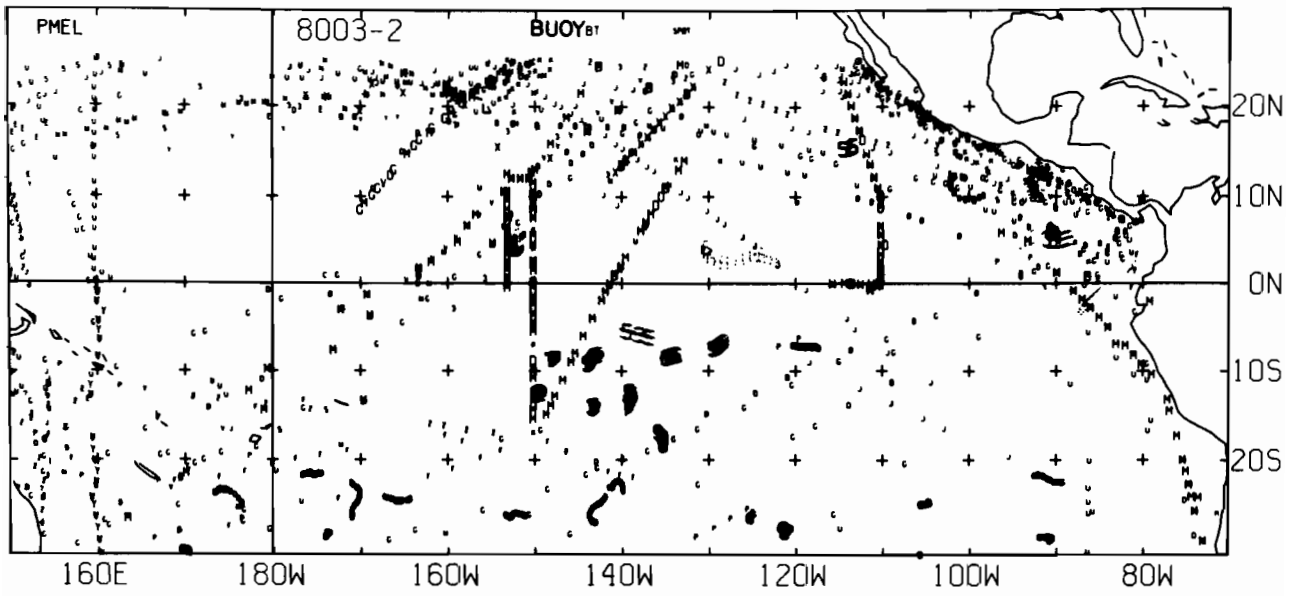

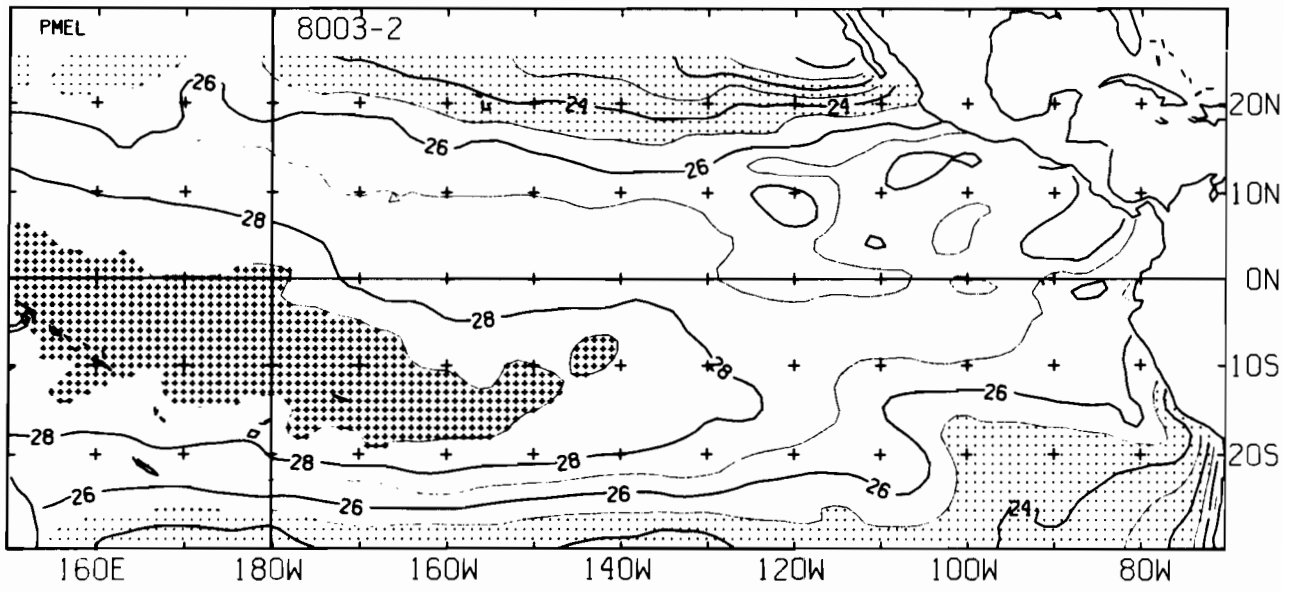

8003-2 SST. 304 E-BUØY. 236 BT. 0 XBT. 1406 SPØT DATA

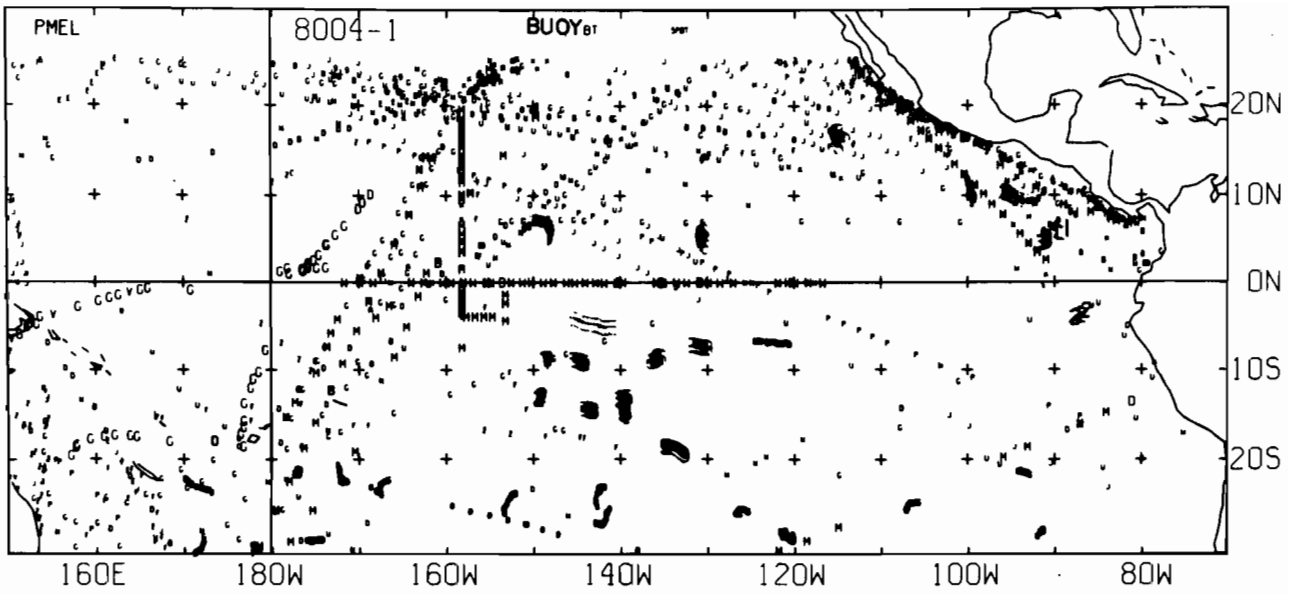

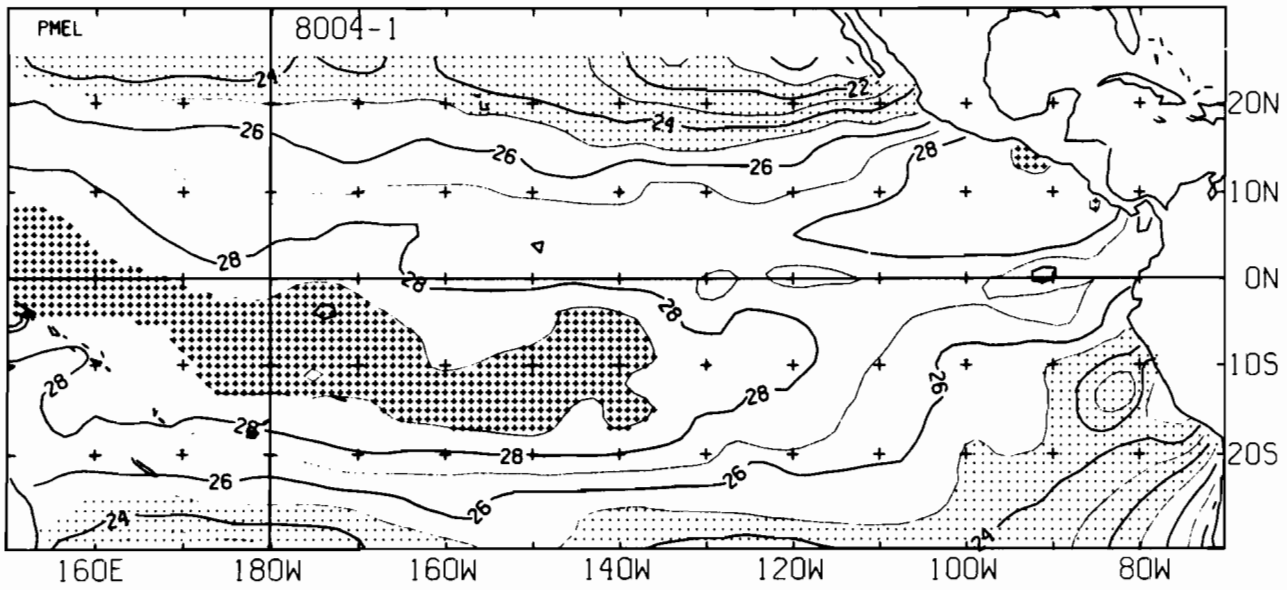

8004-1 SST. 285 E-BUØY. 232 BT. 0 XBT. 1443 SPØT DATA

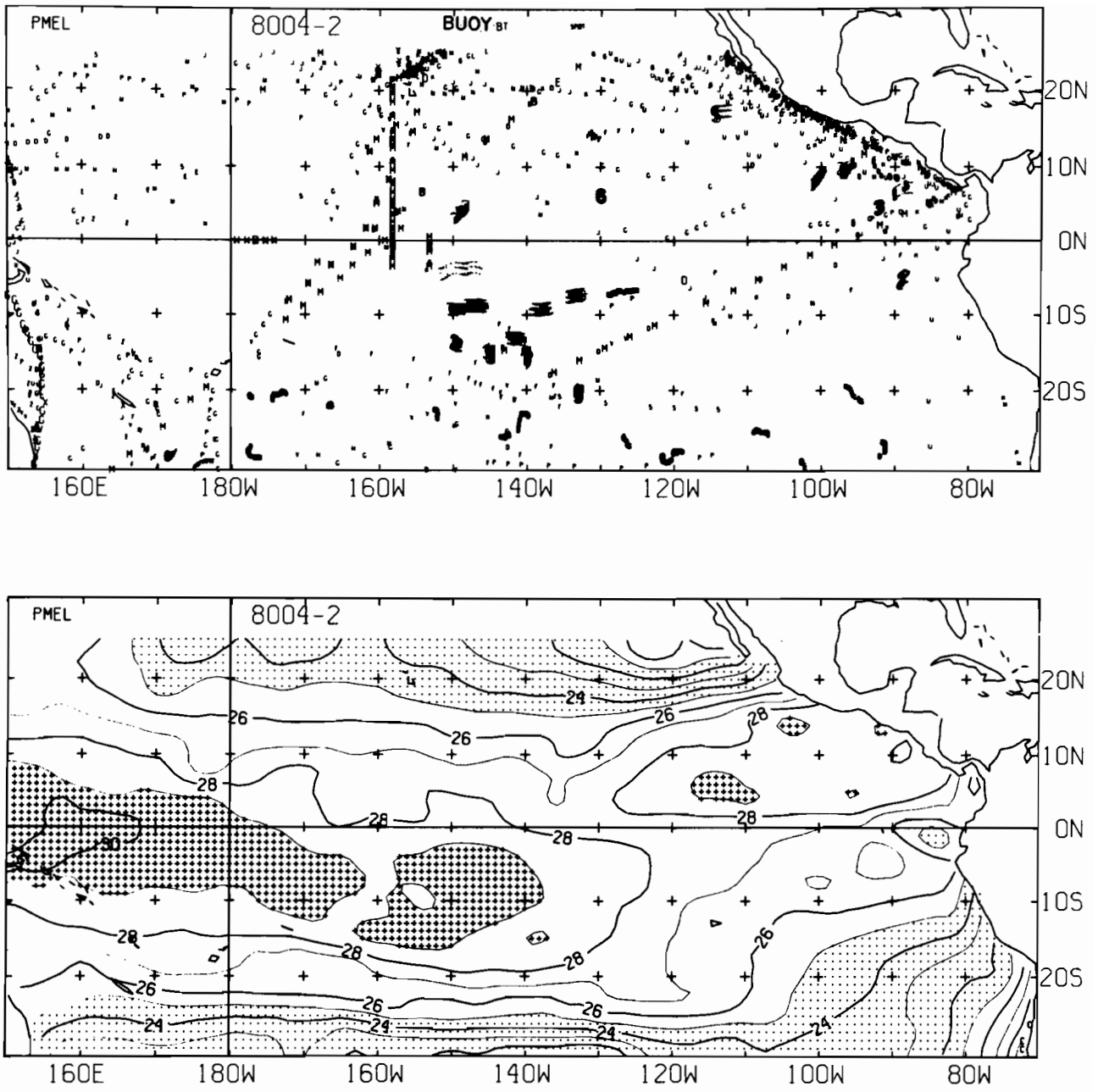

8004-2 SST. 278 E-BUØY. 155 BT. 0 XBT. 1241 SPØT DATA

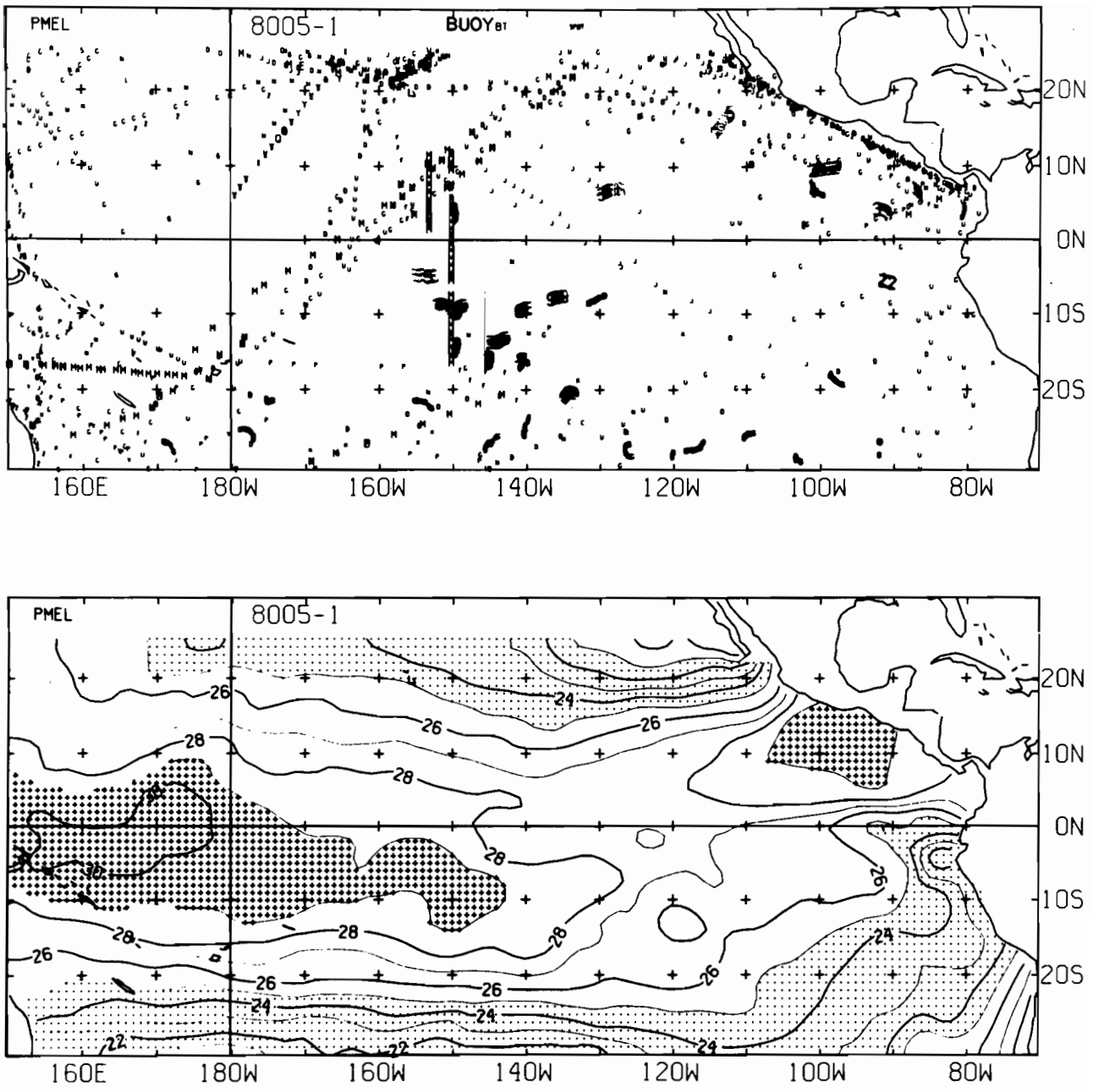

8005-1 SST. 270 E-BUØY. 178 BT. 0 XBT. 1244 SPØT DATA

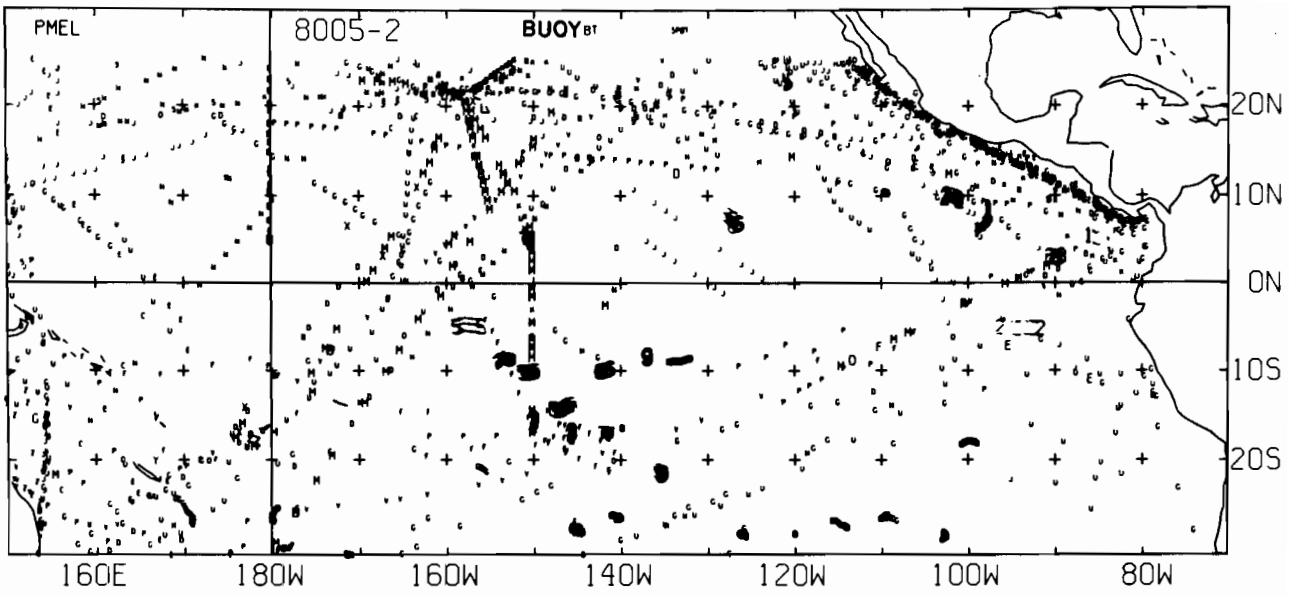

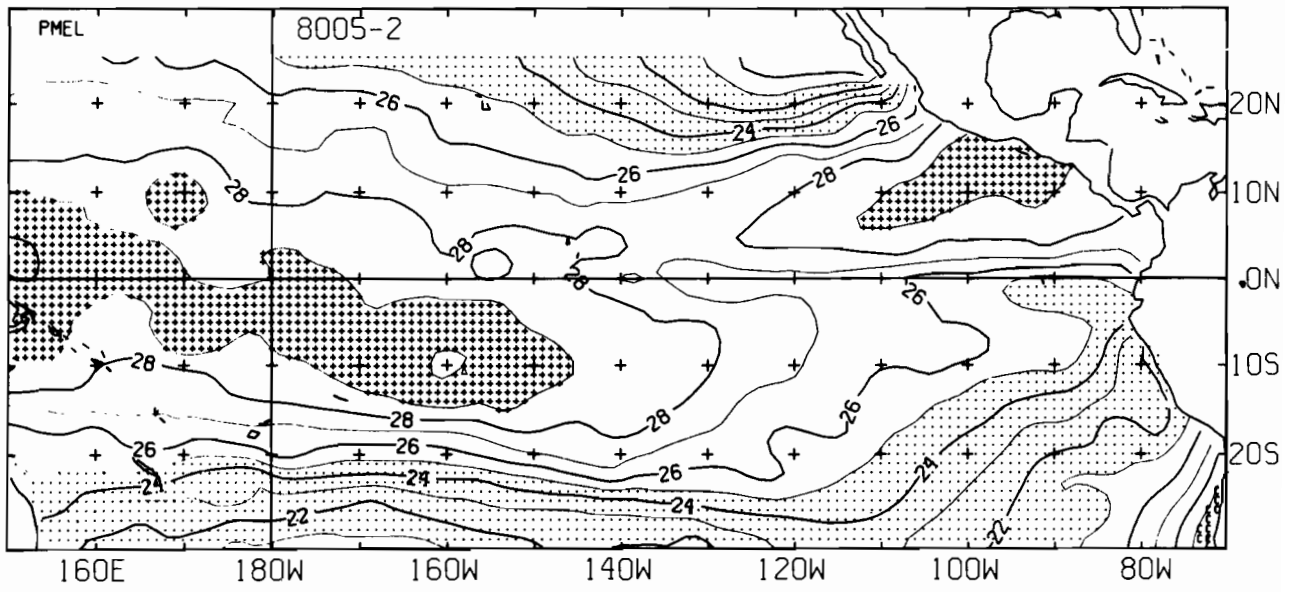

8005-2 SST. 263 E-BUØY. 127 BT. 0 XBT. 1645 SPØT DATA

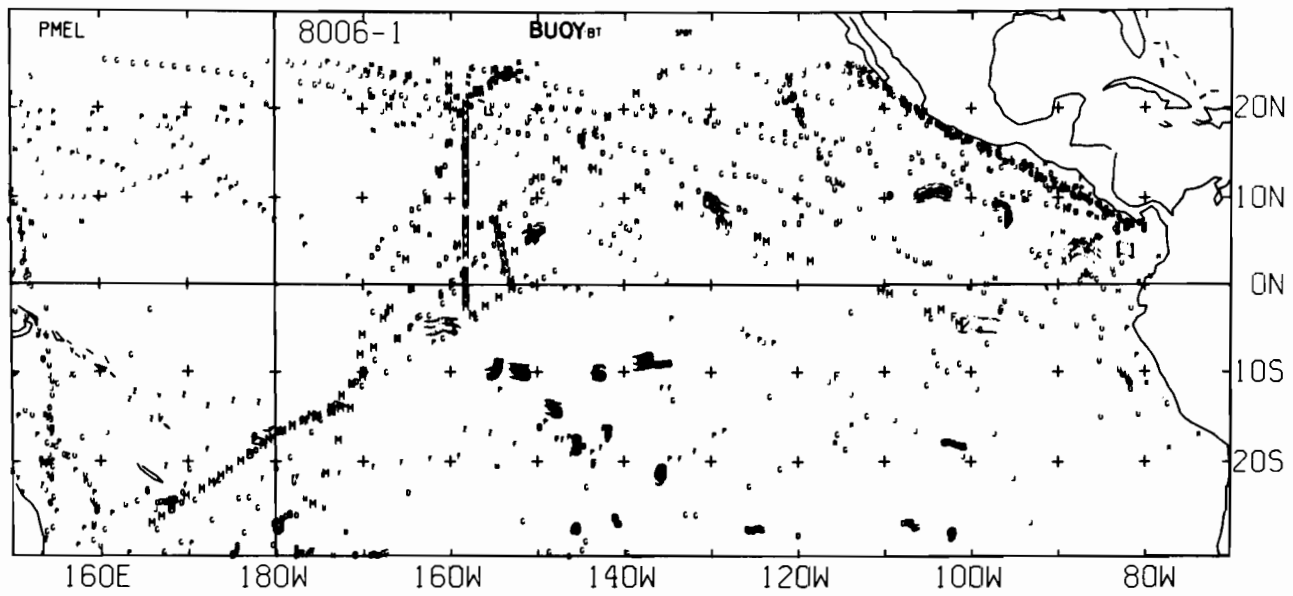

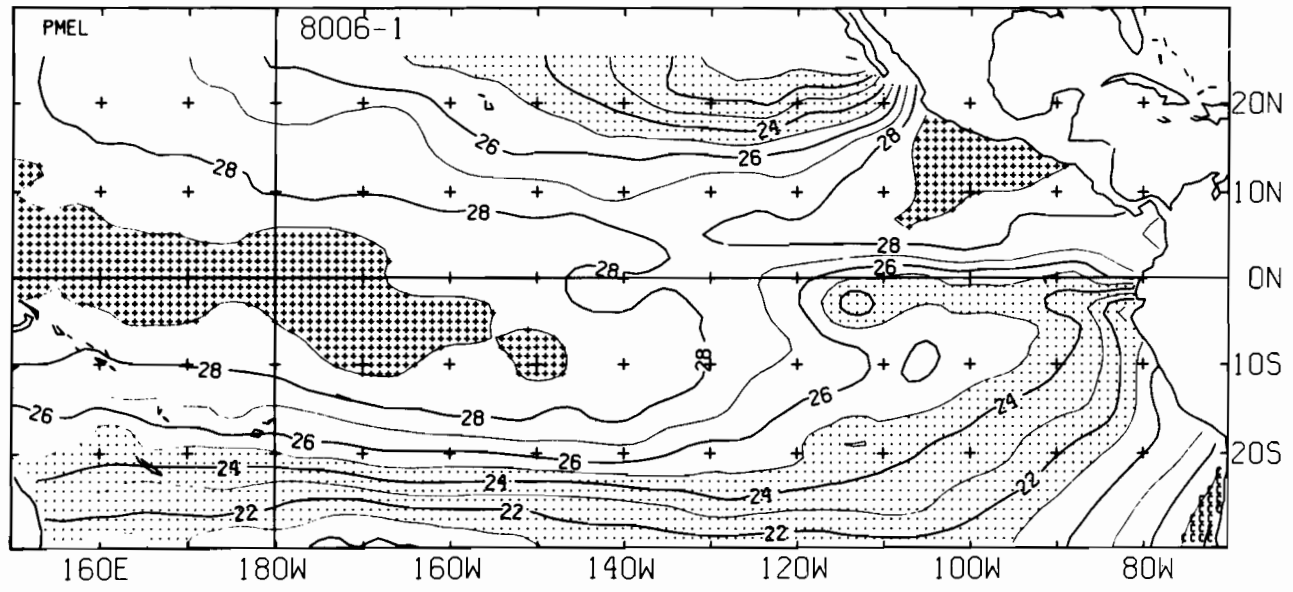

8006-1 SST. 235 E-BUØY. 141 BT. 0 XBT. 1359 SPØT DATA

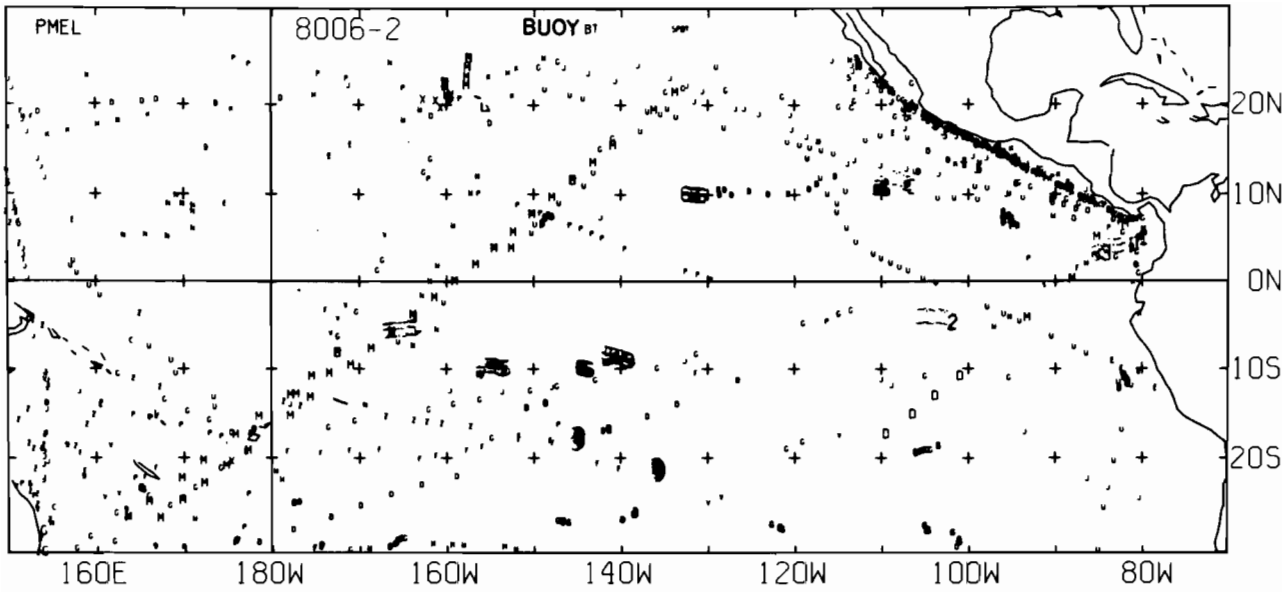

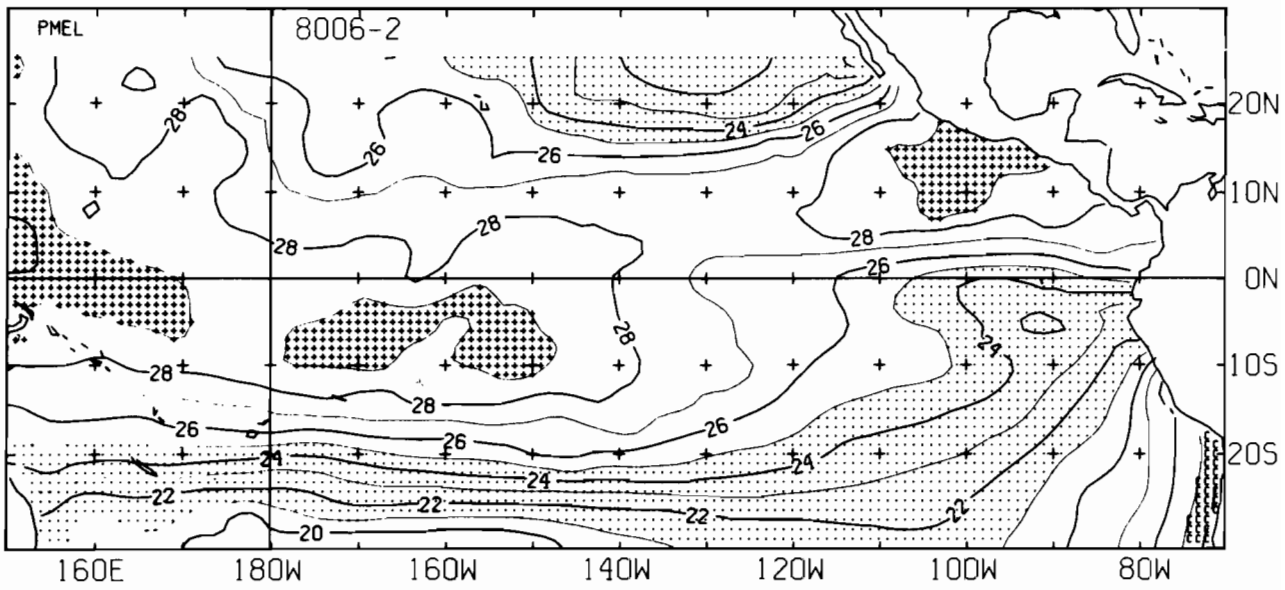

8006-2 SST. 176 E-BUØY. 76 BT. 0 XBT. 825 SPØT DATA

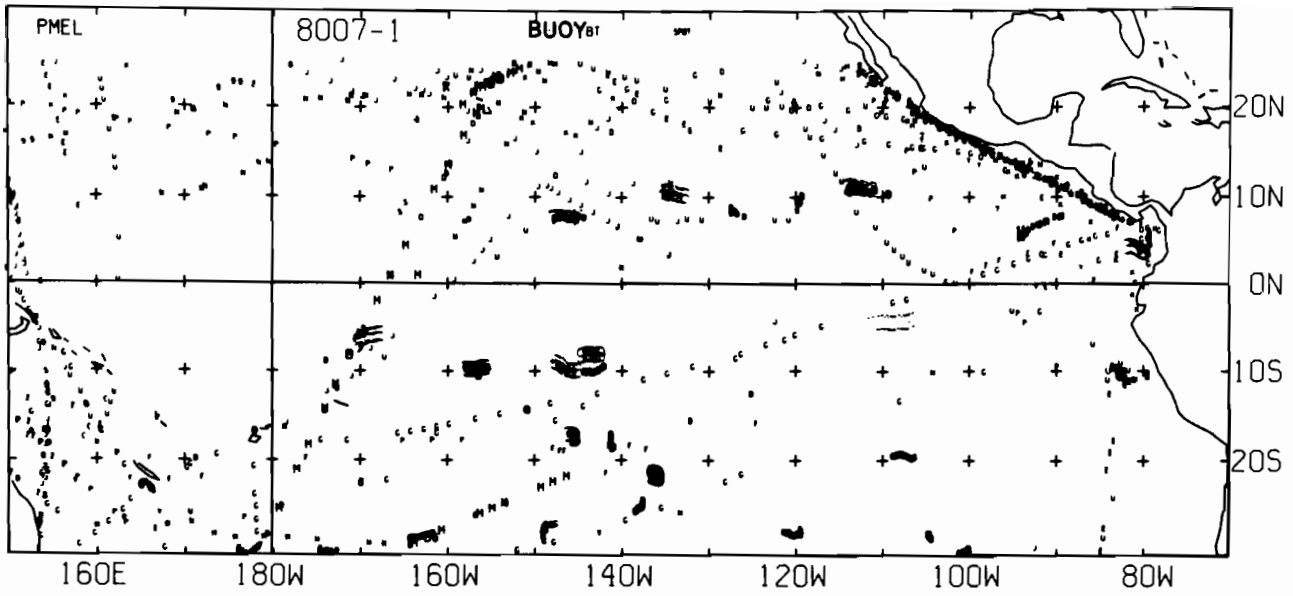

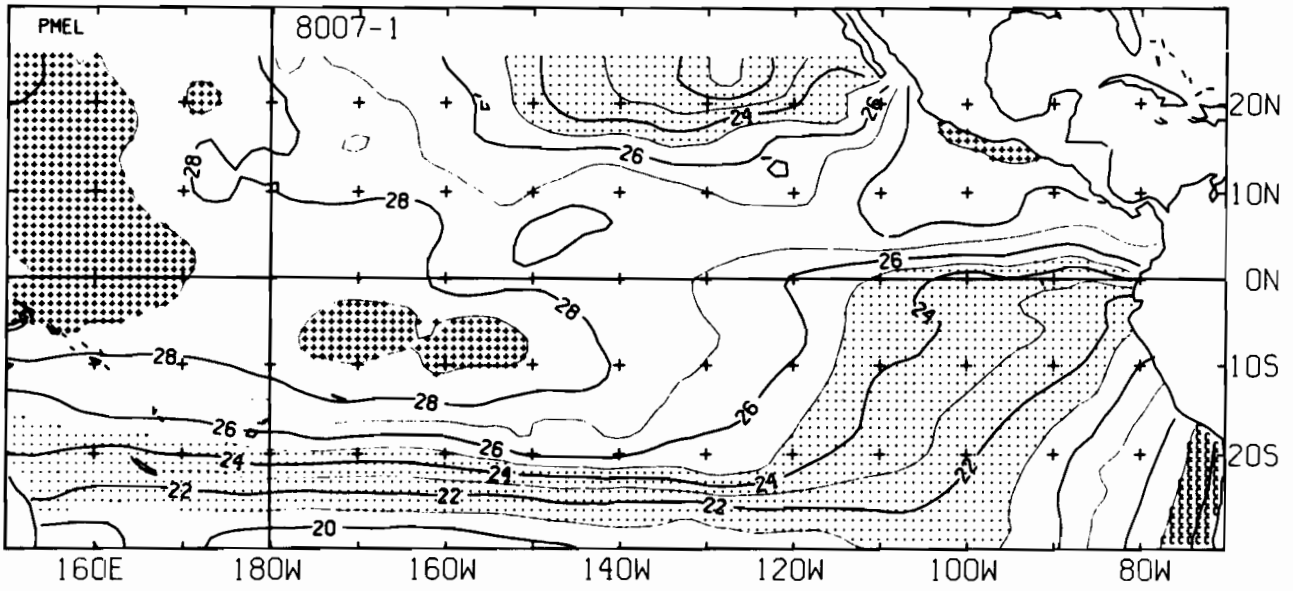

8007-1 SST. 195 E-BUØY. 37 BT. 0 XBT. 1131 SPØT DATA

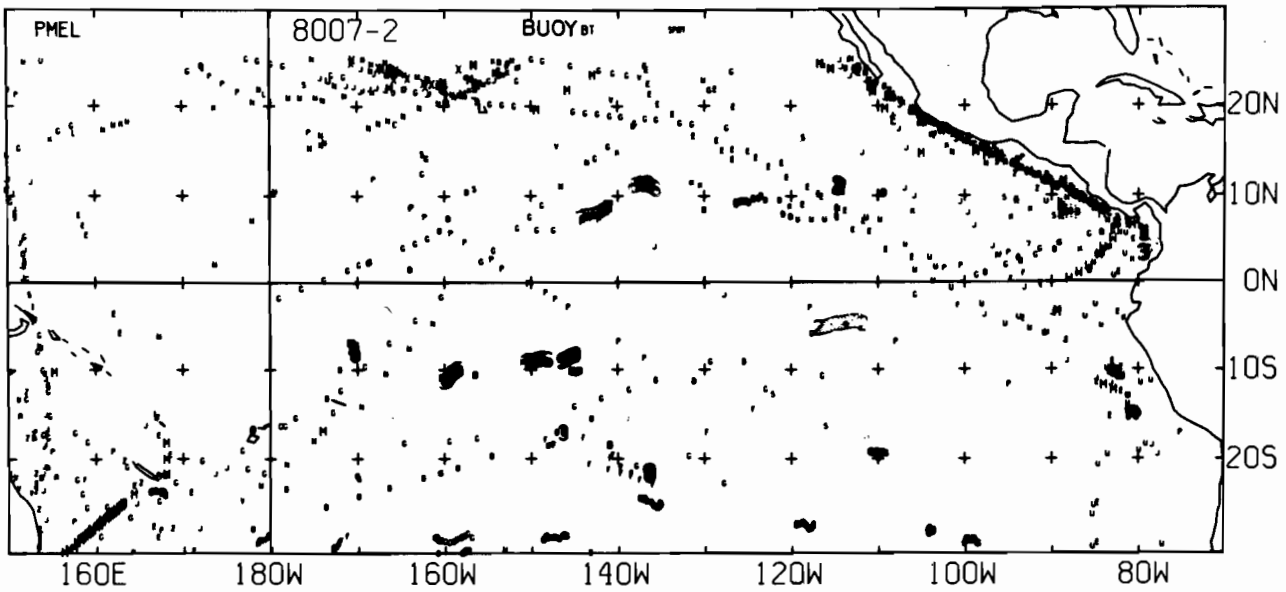

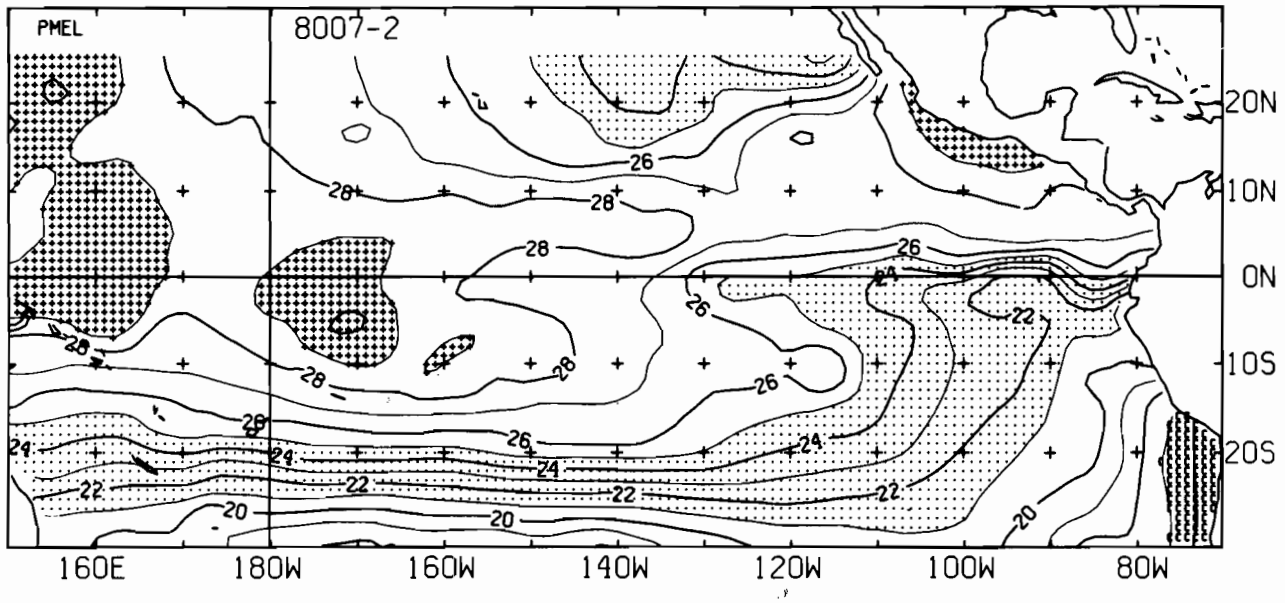

8007-2 SST, 177 E-BUØY, 103 BT, 0 XBT, 1114 SPØT DATA

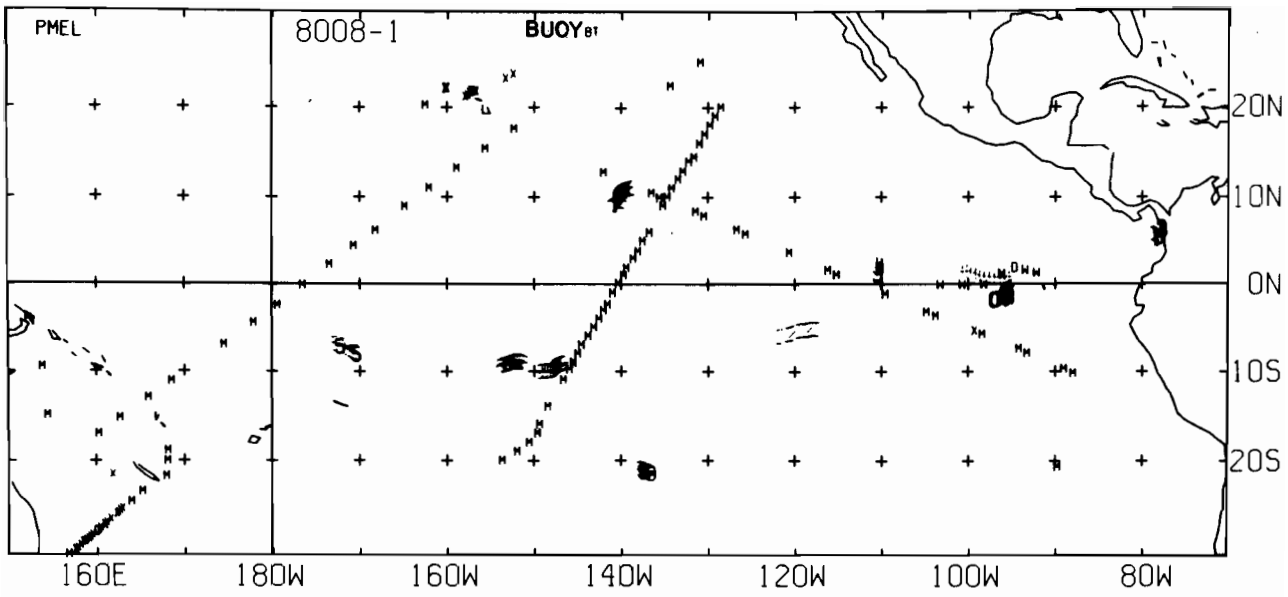

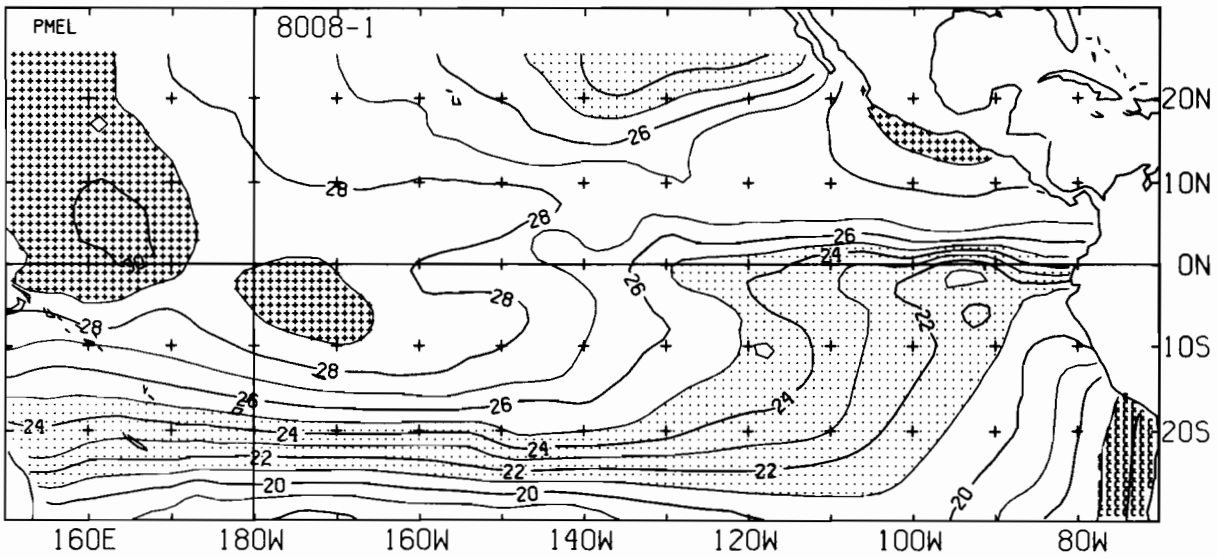

8008-1 SST, 172 E-BUØY, 132 BT, 0 XBT, 0 SPØT DATA

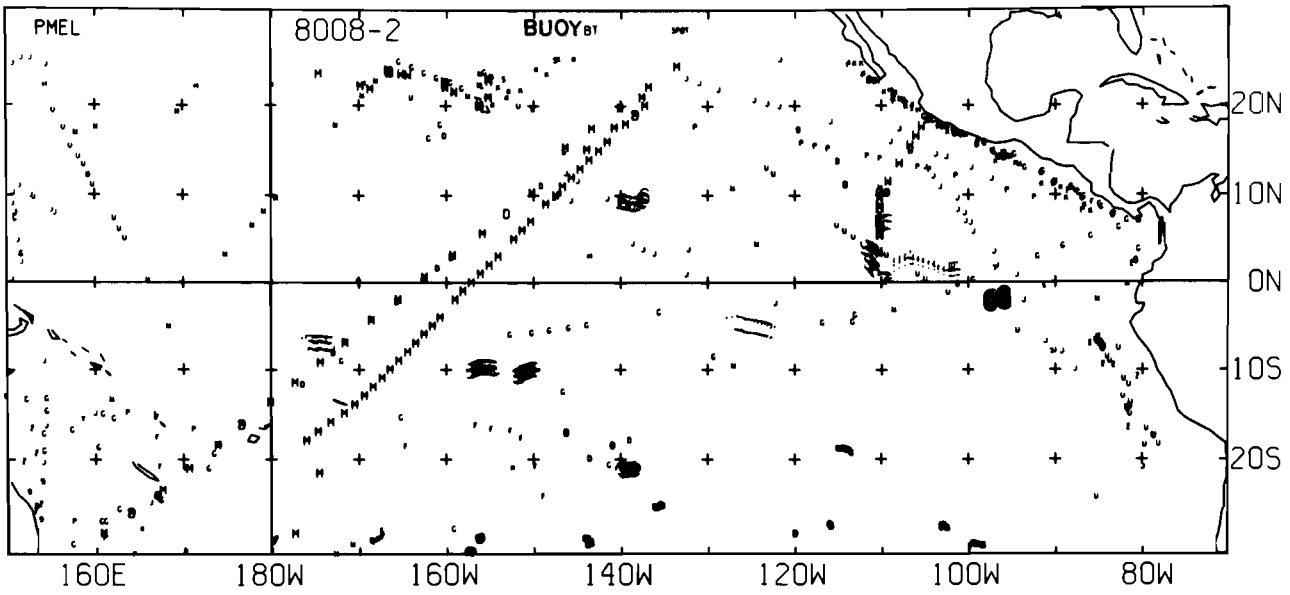

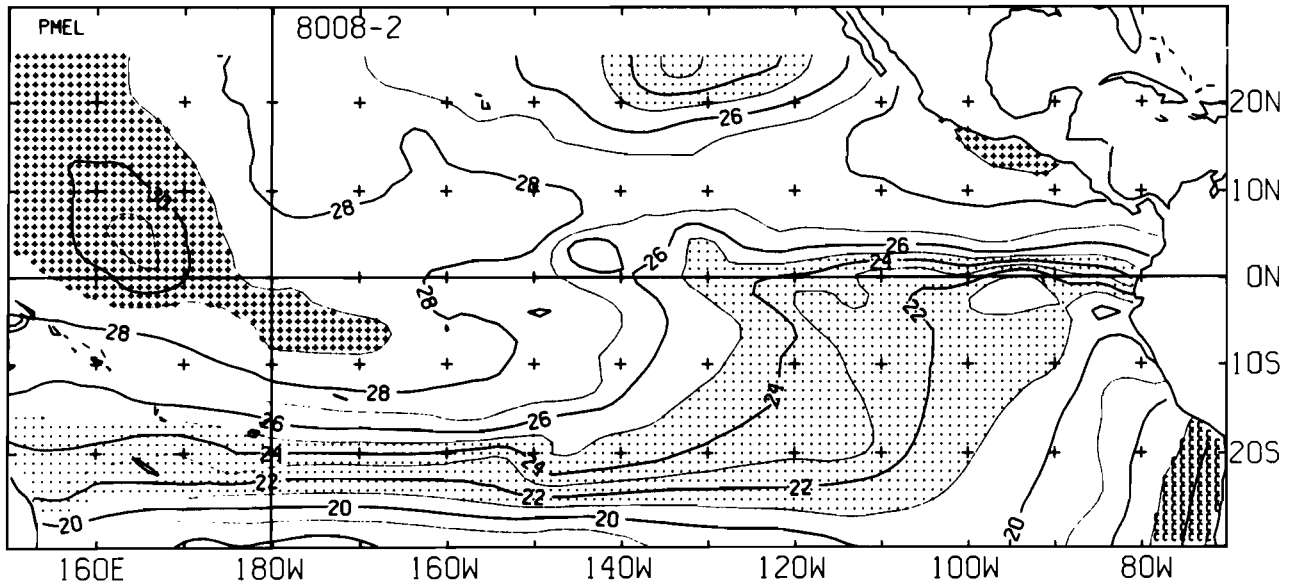

8008-2 SST. 180 E-BUØY. 118 BT. 0 XBT. 509 SPØT DATA

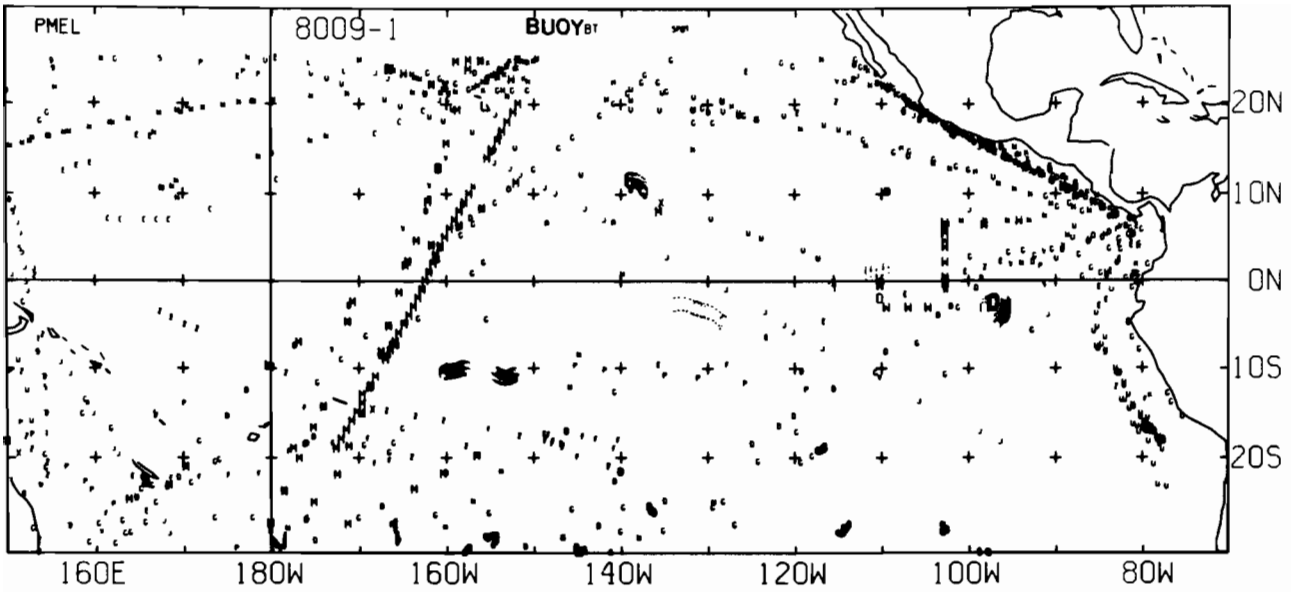

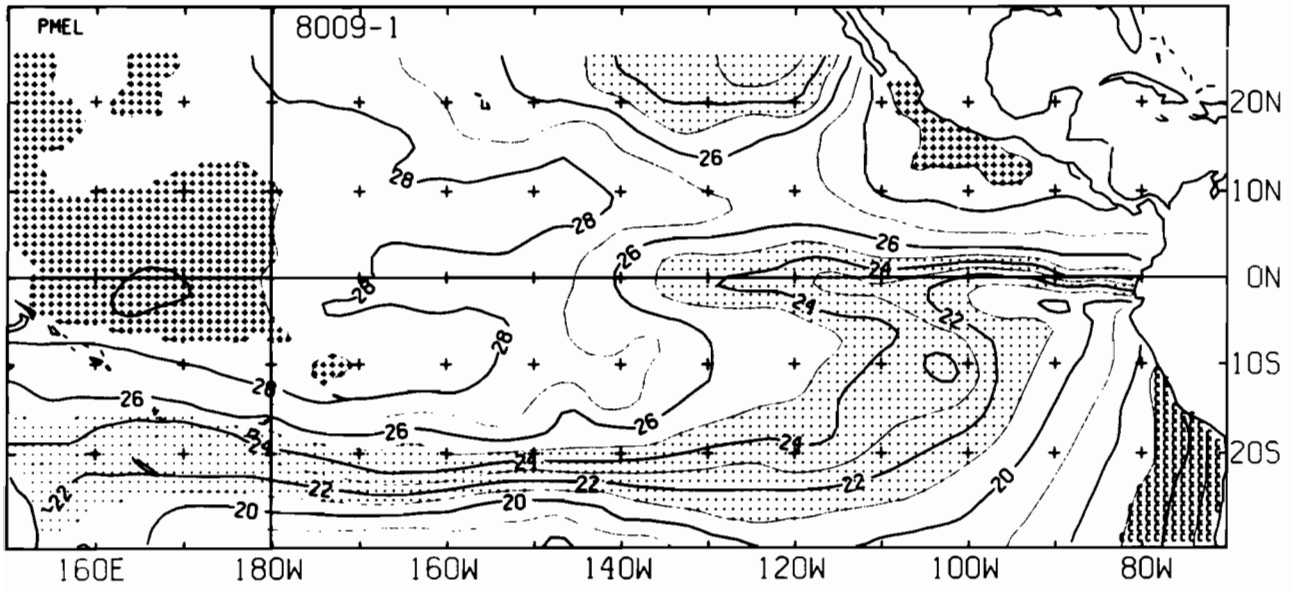

8009-1 SST. 113 E-BUØY. 116 BT. 0 XBT. 991 SPØT DATA

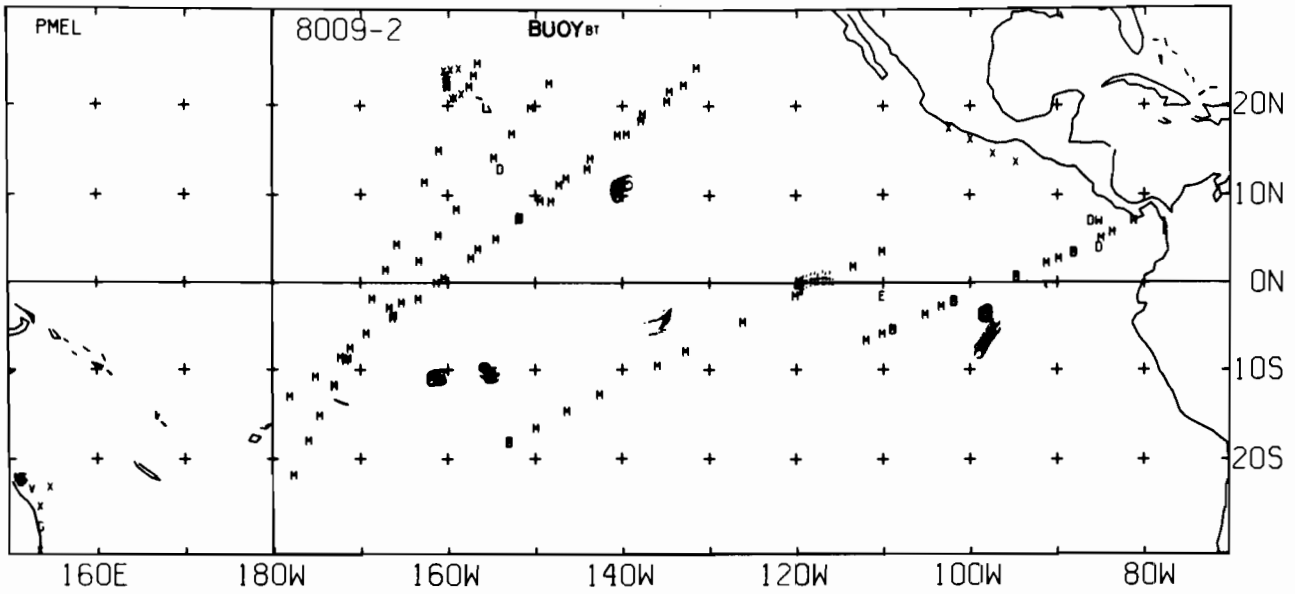

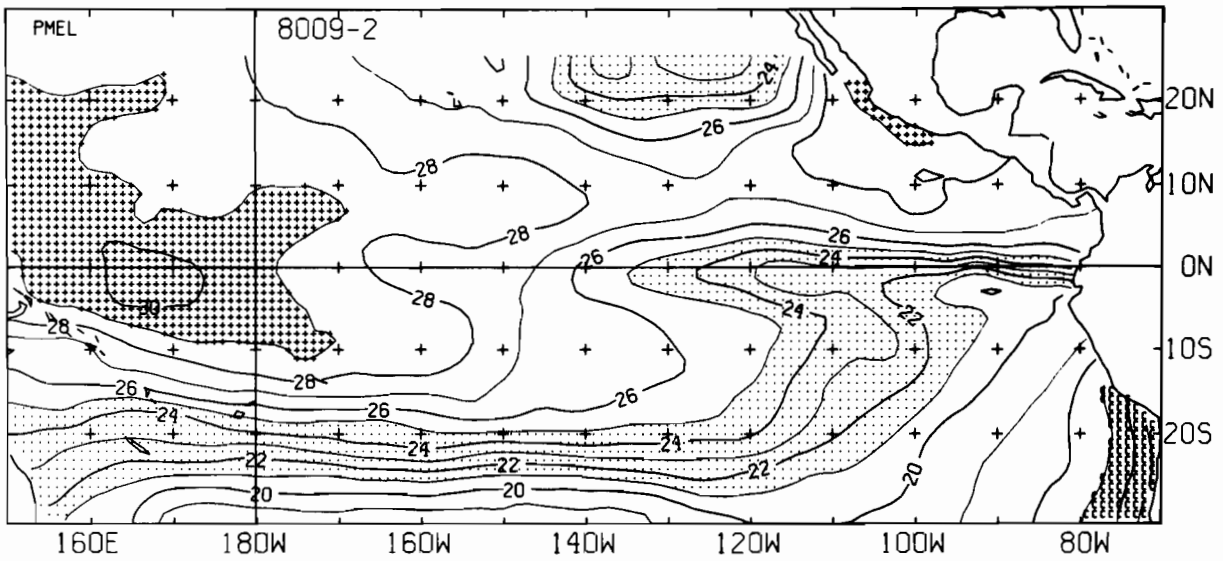

8009-2 SST, 112 E-BUØY, 125 BT, 0 XBT, 0 SPØT DATA

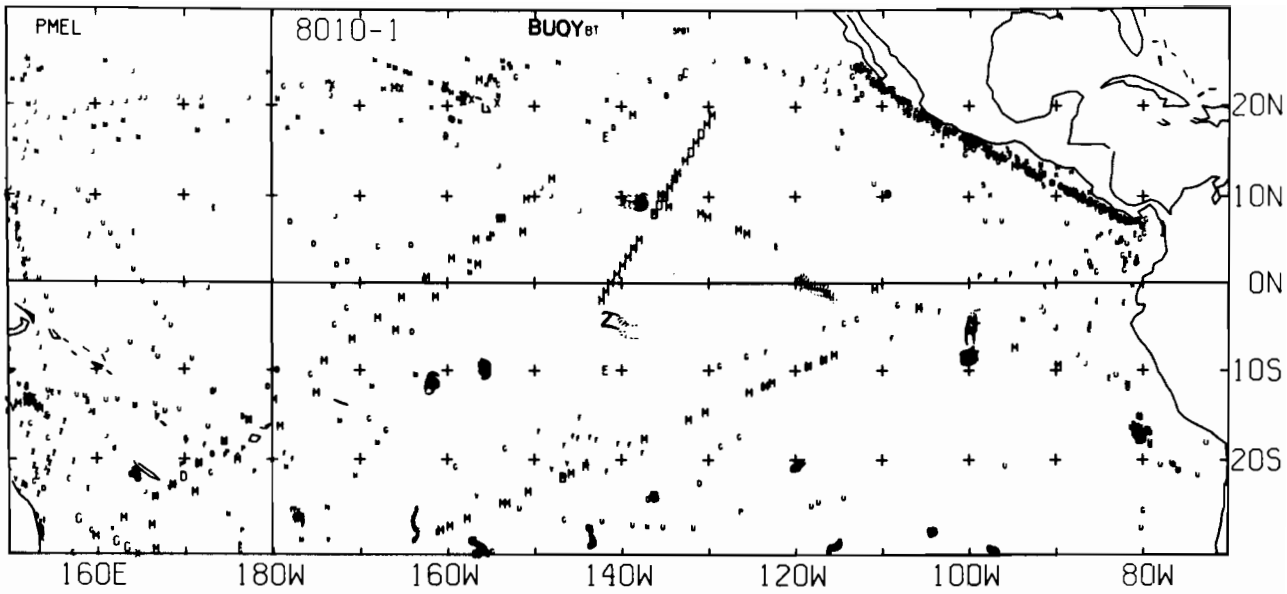

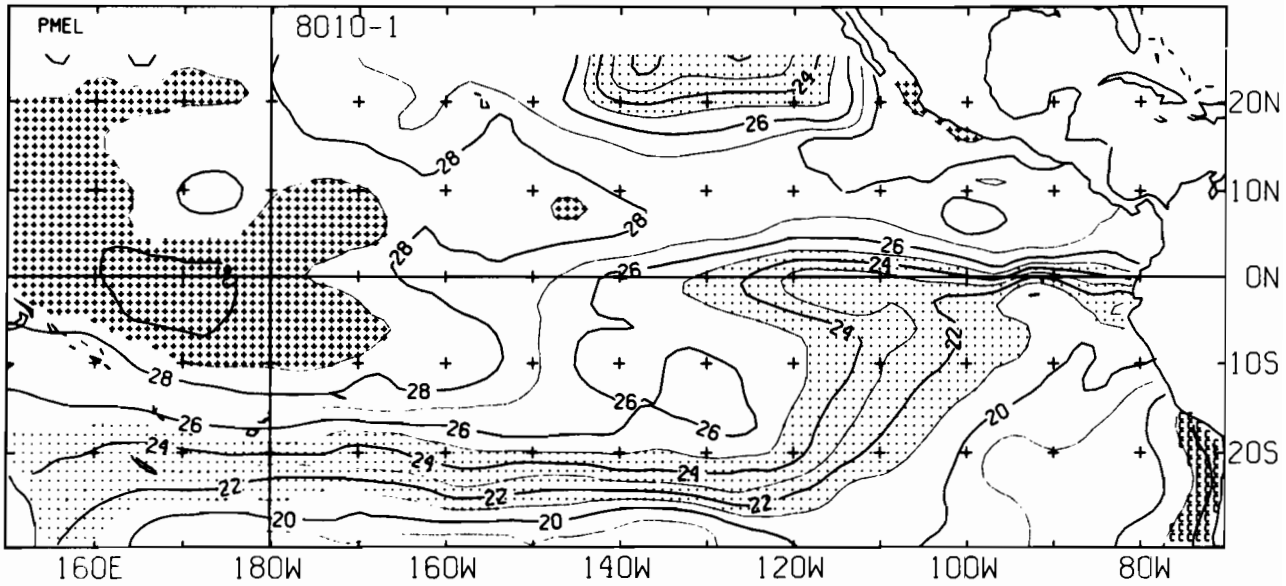

8010-1 SST. 114 E-BUØY. 136 BT. 0 XBT. 839 SPØT DATA

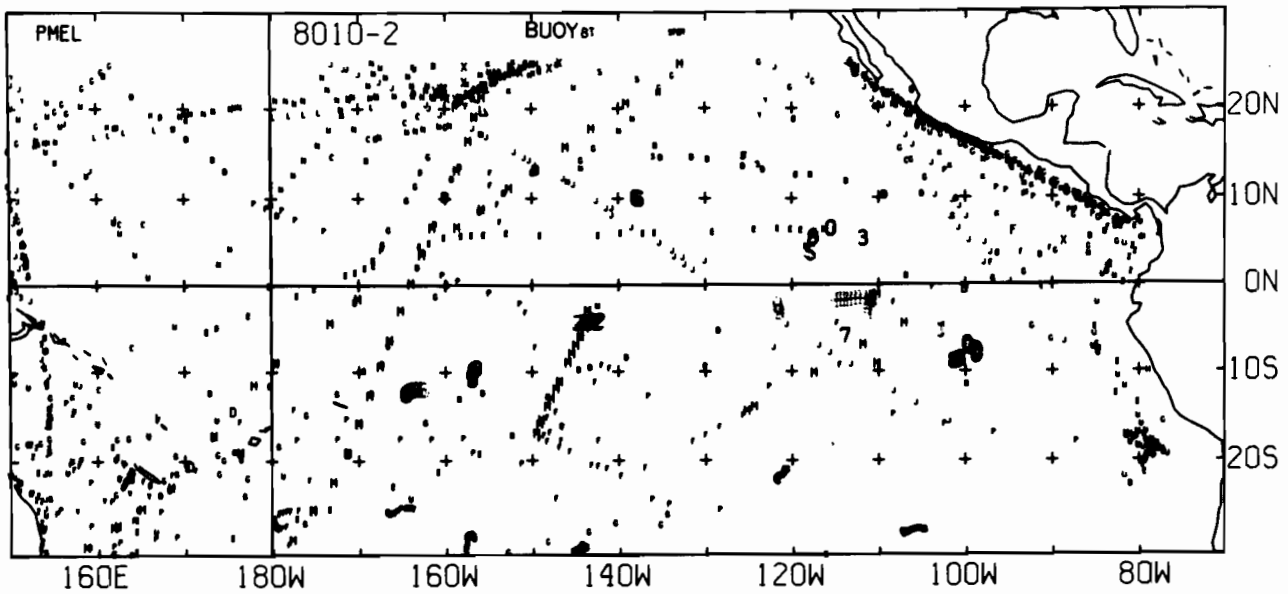

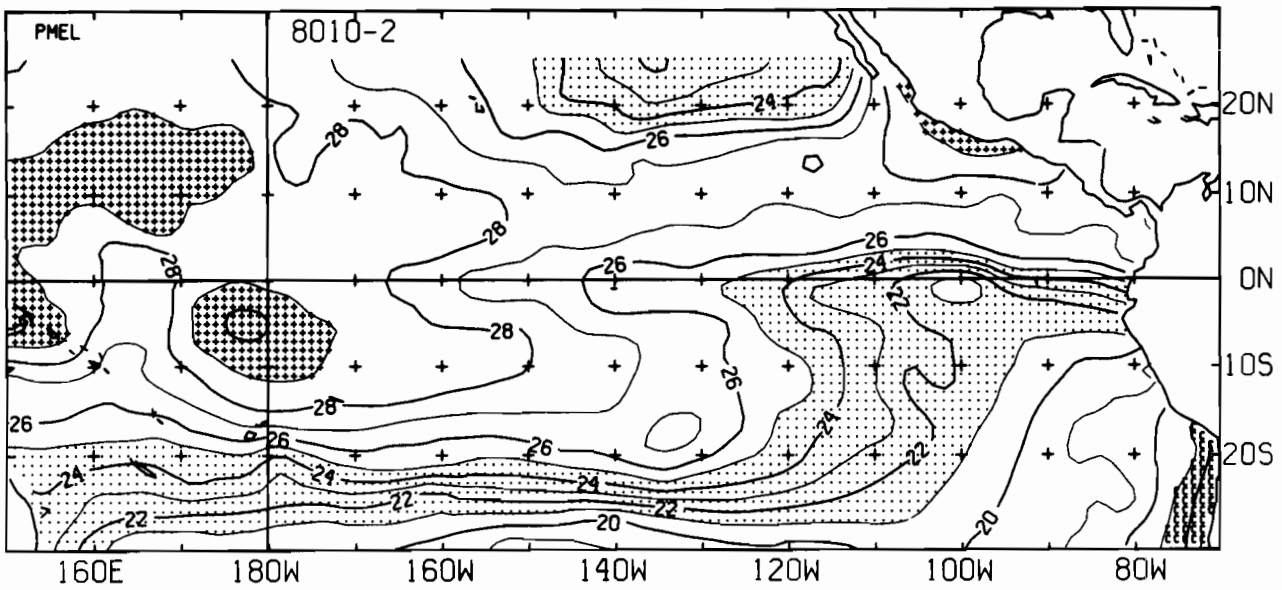

8010-2 SST. 145 E-BUØY. 98 BT. 0 XBT. 1048 SPØT DATA

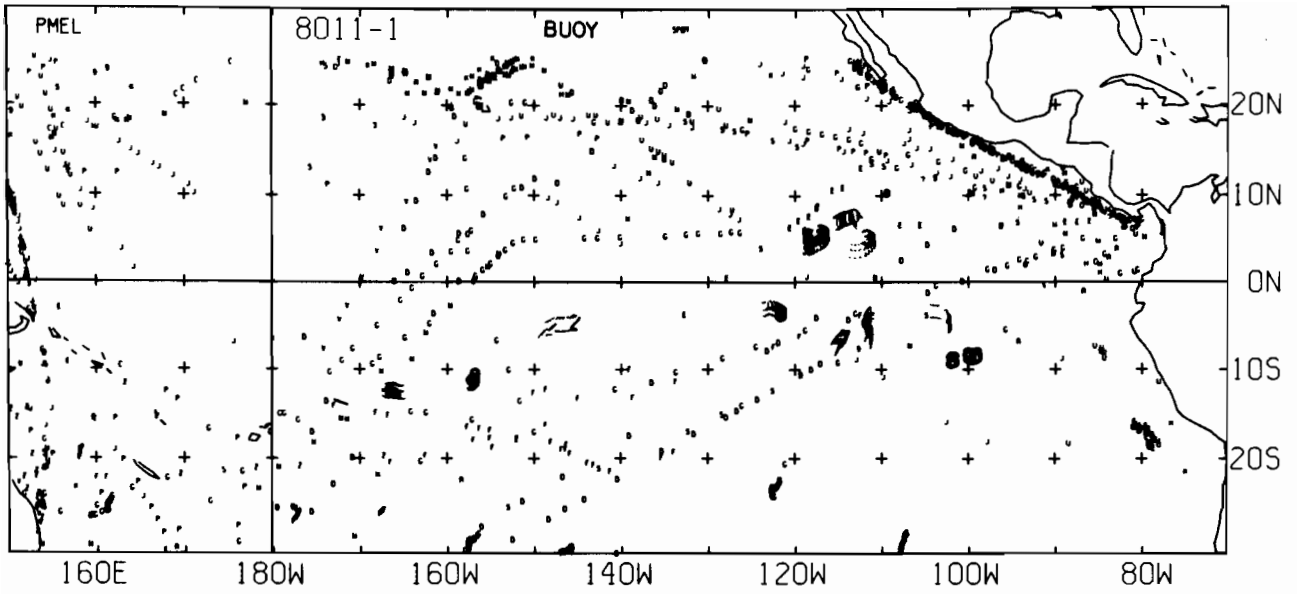

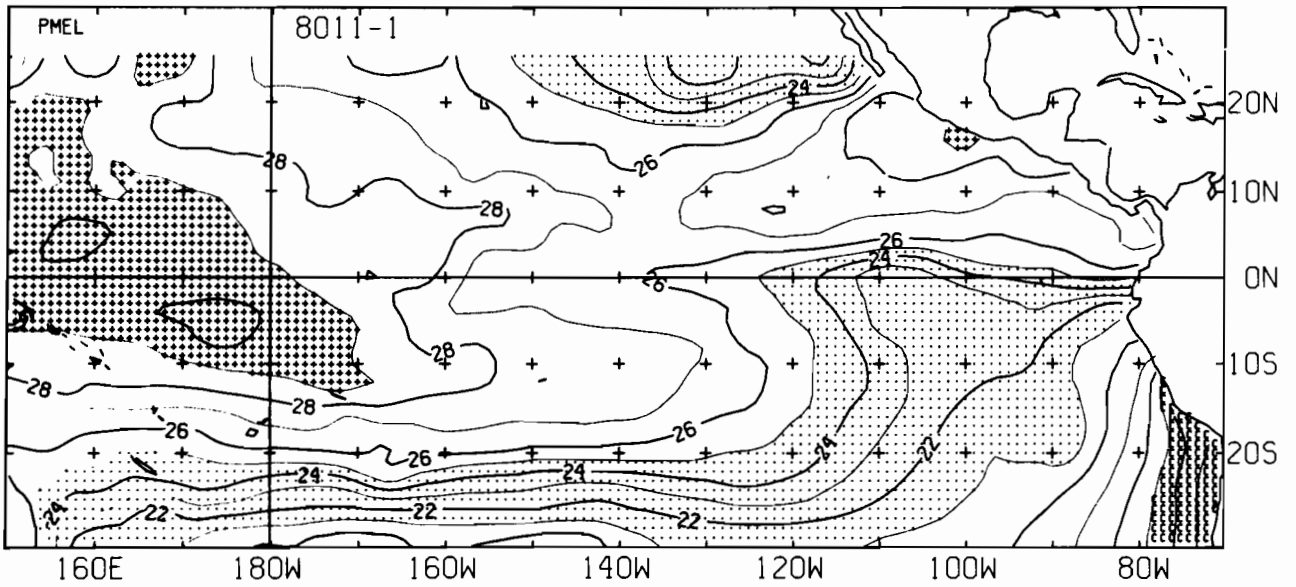

8011-1 SST. 207 E-BUØY. 0 BT. 0 XBT. 1033 SPØT DATA

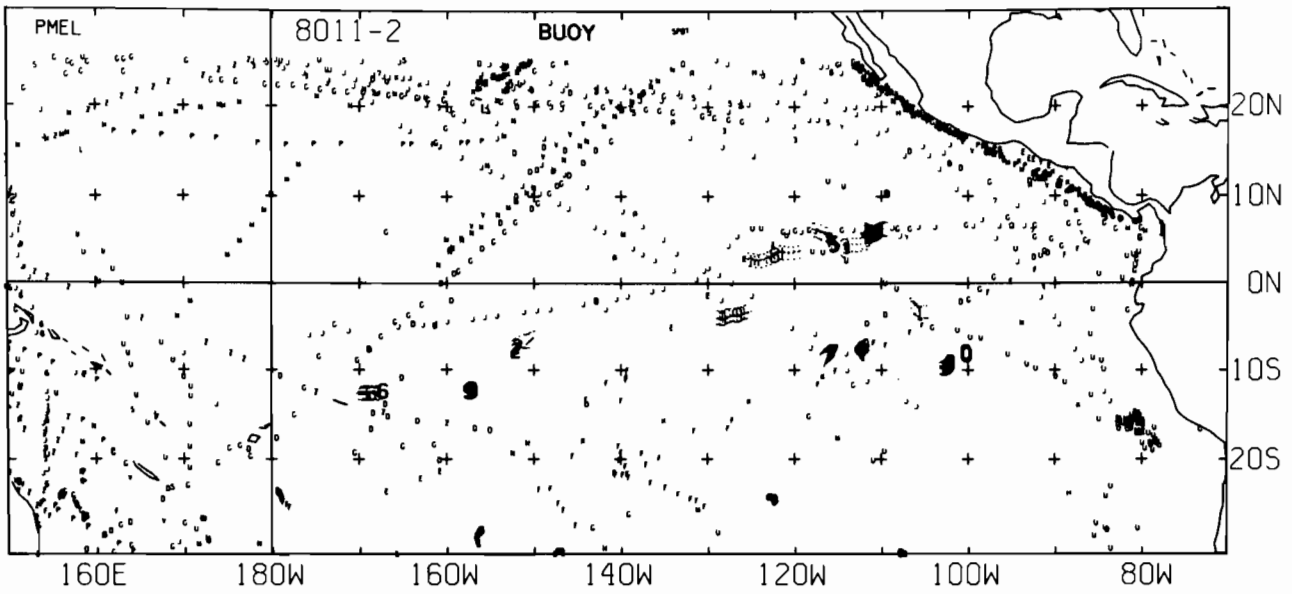

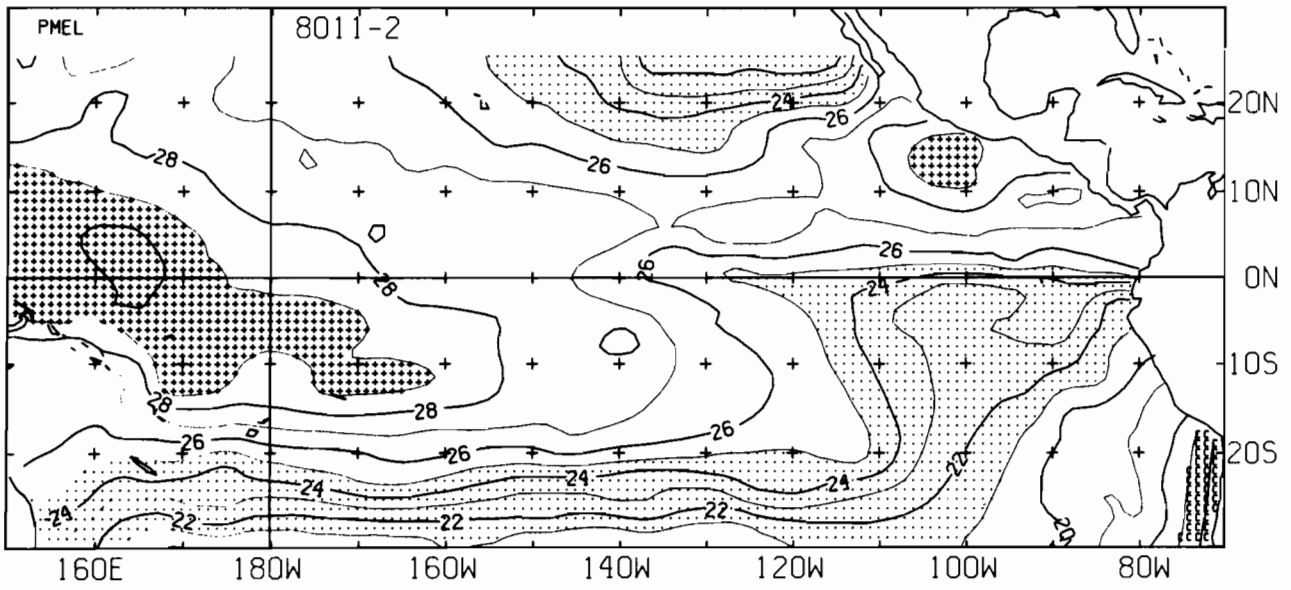

8011-2 SST. 201 E-BUØY. 0 BT. 0 XBT. 1166 SPØT DATA

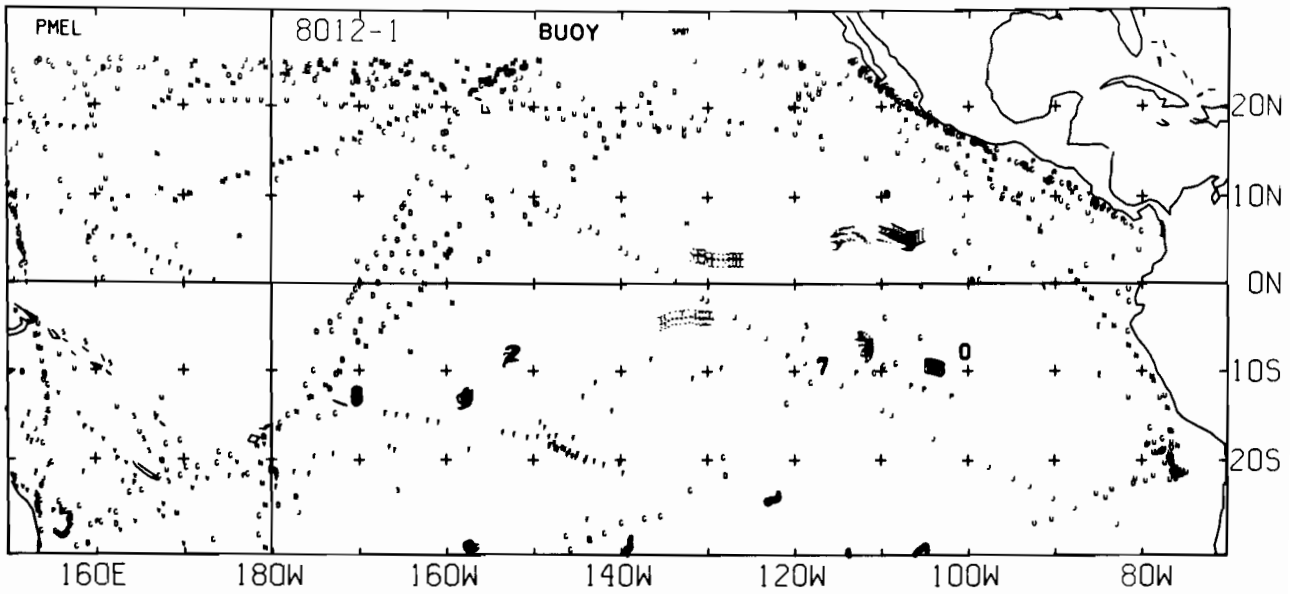

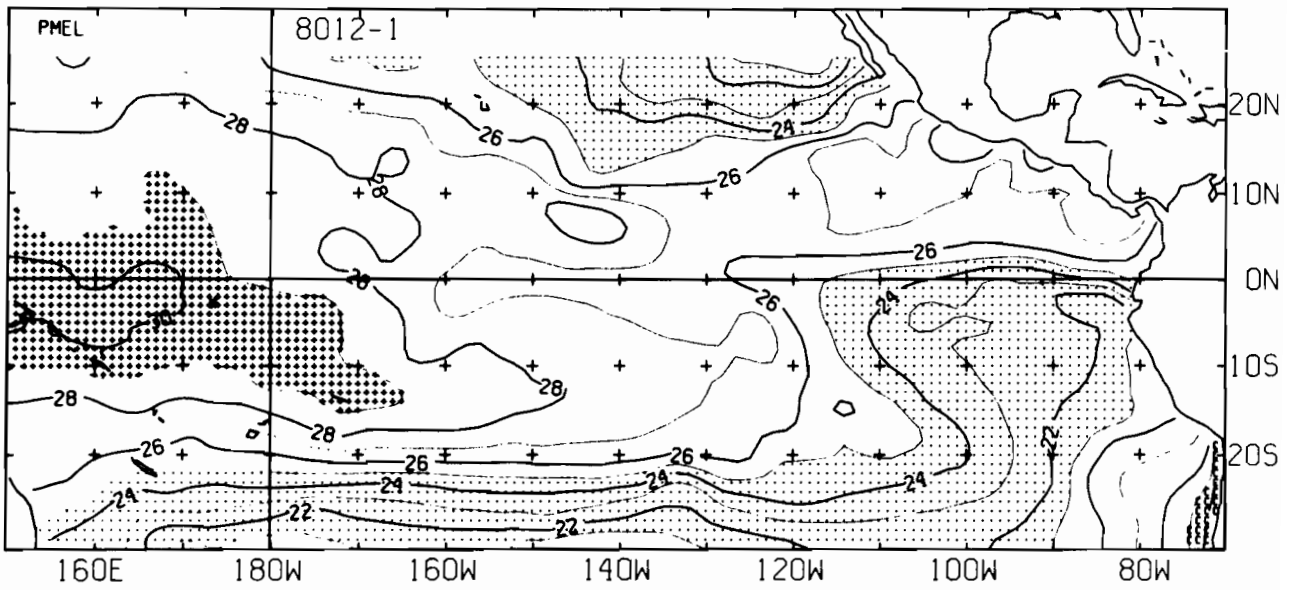

8012-1 SST. 193 E-BUØY. 0 BT. 0 XBT. 1029 SPØT DATA

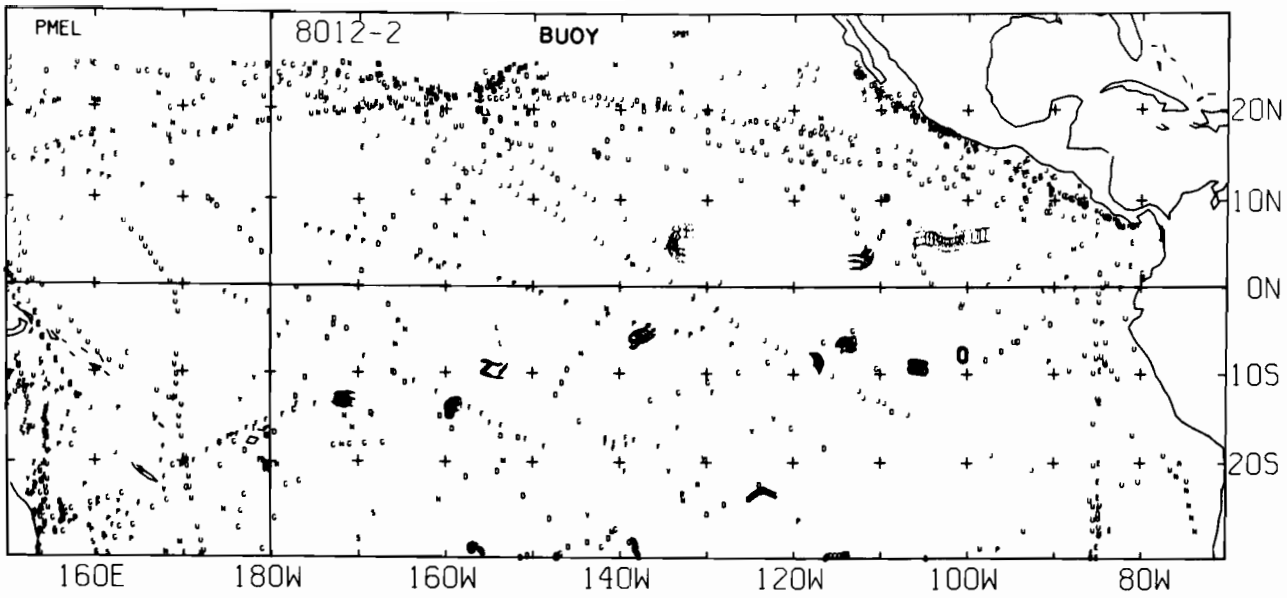

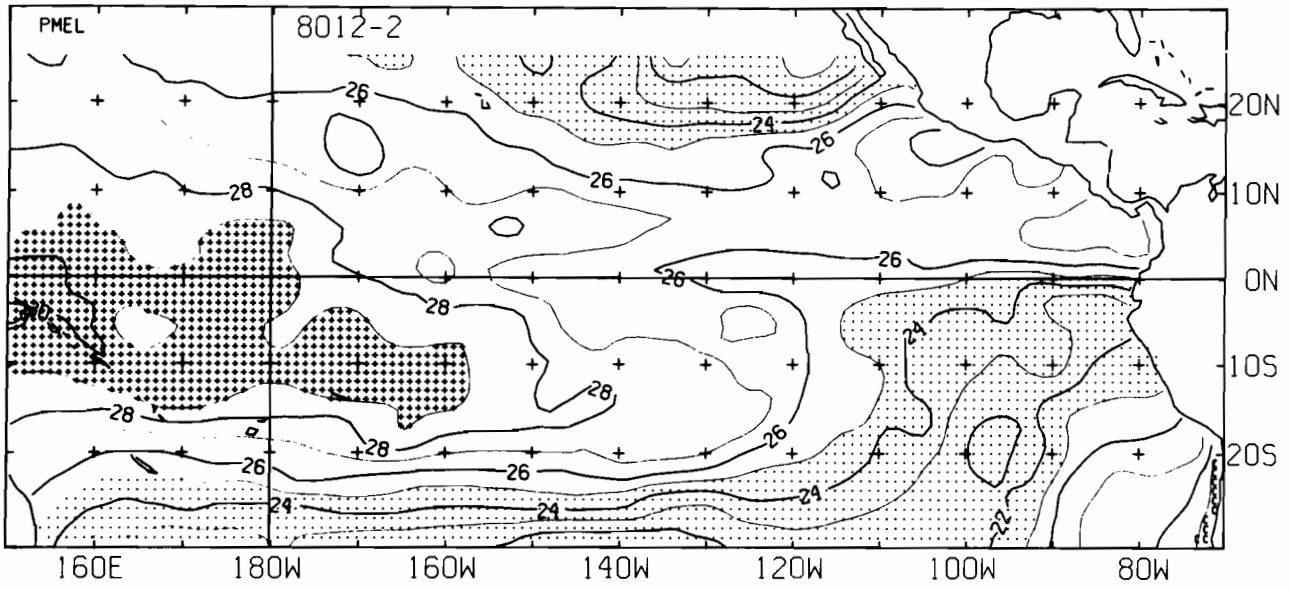

8012-2 SST. 206 E-BUØY. 0 BT. 0 XBT. 1227 SPØT DATA